53)

A STUDY OF THE LARGE SCALE CIRCULATION AND WATER MASS FORMATION IN THE NORDIC SEAS AND ARCTIC OCEAN

by

Cecilie Mauritzen

Cand. Mag. (B.S.), University of Bergen, Norway
(1985)

Cand. Scient. (M.S.), University of Bergen, Norway
(1987)

Submitted in partial fulfillment of the
requirements for the degree of

Doctor of Philosophy

at the

MASSACHUSETTS INSTITUTE OF TECHNOLOGY

and the

WOODS HOLE OCEANOGRAPHIC INSTITUTION

October 1993

Signature of Author ..... Cecilie Mauritzen .....
Joint Program in Physical Oceanography
Massachusetts Institute of Technology
Woods Hole Oceanographic Institution

Certified by ..... W. Brechner Owens .....
W. Brechner Owens
Thesis Supervisor

Accepted by ..... Lawrence J. Pratt .....
Lawrence J. Pratt
Chairman, Joint Committee for Physical Oceanography
Massachusetts Institute of Technology
Woods Hole Oceanographic Institution

A Study of the Large Scale Circulation and Water Mass Formation in the Nordic Seas and Arctic Ocean

by

Cecilie Mauritzen

Submitted to the Massachusetts Institute of Technology and the Woods Hole Oceanographic Institution Joint Program in Oceanography/Applied Ocean Science and Engineering on October 5, 1993, in partial fulfillment of the requirements for the degree of Doctor of Philosophy

ABSTRACT

In this thesis, production of dense water that feeds the dense overflows across the Greenland-Scotland Ridge has been considered. A new circulation scheme is developed which is consistent with the water masses, currents and air-sea fluxes in the region, and with the important observation that the dense overflows show little or no seasonal or interannual variability. An inverse box model has been constructed that shows that the new circulation scheme is consistent with conservation statements for mass, heat and salt as well.

According to the new circulation scheme the major buoyancy is lost in the North Atlantic Current, which enters the Norwegian Sea between Iceland and Scotland, and flows northward towards the Arctic Ocean and the Barents Sea. The transformation is due to a large net annual heat loss over the North Atlantic Current, combined with a long residence time (2-3 years) and a large surface area. After subduction, one branch of the North Atlantic Current enters the Arctic Ocean, is modified in hydrographic properties into those associated with the Denmark Strait Overflow Waters in the western North Atlantic, exits the Arctic Ocean in the western Fram Strait and flows with the East Greenland Current towards the Denmark Strait. Another branch of the North Atlantic Current recirculates directly in the Fram Strait and flows towards the Denmark Strait with the East Greenland Current. This branch will not sink to the bottom of the North Atlantic as it is less compressible than the Arctic branch. The third branch of the North Atlantic Current enters the Barents Sea, continues to lose buoyancy, and enters the Arctic Ocean at intermediate depth. This branch exits the Arctic Ocean in the western Fram Strait, circulates around the Greenland Sea, enters the Norwegian Sea, and flows towards the Færø-Shetland Channel.

The traditional view holds that the major sources of the dense overflows are the Iceland and Greenland gyres, west of the North Atlantic Current. Aside from the finding that the new circulation scheme is more likely in terms of water mass properties, currents etc., one fundamental problem with the old scheme lies with supplying a substantial overflow. There are indications that the production of dense water in the gyres is sensitive to the highly variable surface conditions and that indeed the production tends to shut on and

off. The reservoirs in the gyres are so small that they would be drained within a few years if they were to supply the overflows during a shutdown period.

Production of dense water within the North Atlantic Current is less sensitive to surface conditions. The density in the gyres is gained at a temperature around freezing, whereas in the North Atlantic Current the density is gained well above freezing. Therefore a freshwater anomaly in the two domains will have different consequences for vertical overturning: within the North Atlantic Current the freshening can be overcome by further cooling, whereas in the gyres freezing will occur and the vertical overturning will cease.

The observed lack of a significant seasonal signal associated with the dense overflows is consistent with the new circulations scheme. The net annual cooling dominates the seasonal oscillation in the atmospheric heat loss for time scales comparable with the residence time of the Atlantic Water within the domain. Thus winter formation of dense water within the North Atlantic Current does not induce a seasonal signal in the transport field of the dense water.

Thesis Supervisor: Dr. W. Brechner Owens
Title: Senior Scientist, Woods Hole Oceanographic Institution

Acknowledgements

I have had the good fortune to be surrounded by many incredibly nice people during my stay in the Joint Program, and I would like to thank you all!

I would especially like to express my gratitude towards my thesis advisor, Breck Owens, for his advice and guidance, and most importantly for always showing faith that I would find a solution to whatever problem I was up against. I thank him immensely for that. I thank my thesis committee - Nelson Hogg, Joseph Pedlosky, Paola Rizzoli and Carl Wunsch - for their valuable advice and encouragement.

A special thanks goes to Mike McCartney for all his advice on interpretation of ocean data, and also for reminding me (when needed) that "oceanography is fun!" I am grateful to Hugh Livingston, Bill Jenkins, Alison Macdonald, Jochem Marotzke, Glen Gawarkiewicz and Al Plueddemann for numerous conversations that were valuable to this work. I am indebted to Al Plueddemann and Birgit Klein for suffering through an early draft of this thesis.

Peter Koltermann, Jim Swift, Eberhardt Fahrbach and Gerhard Bönisch kindly gave me access to the data sets used in this thesis. I would also like to thank Charmaine King, Roger Goldsmith, Chris Wooding, Marg Zemanovic, B. L. Owens and Saralee Perel for all their good help. The support of Ileana Blade, Gary Jaroslow, Javier Escartin, Hege and Dan Lizzaralde and Susan Wijffels has been invaluable to me. And a million thanks to Molly Baringer, Sarah Gille and Becky Schudlich for amazing teamwork!

Lastly, I would like to thank my family for all their love and support during these years. They have always reminded me where I come from and encouraged me to never give up what I set out to do. And the one who made it possible for me to do so is my beloved Joseph LaCasce. The English language fails me in expressing my gratitude to him.

Funding for this work was partly provided by a NASA Global Change Fellowship.

Contents

Chapter 1

Introduction

The energy that the Earth receives from the sun is unevenly distributed, the lower latitudes receive much more energy than the higher latitudes. As a result the climate of the Earth is non-uniform, but to a lesser degree than one would expect from the uneven distribution of the incoming radiation. The difference is due to the ability of the atmosphere and oceans to redistribute energy by transporting heat. It has been suggested (see Gill, 1982) that the oceans may be responsible for as much as 50 % of this transport, which means that the oceans are very important for maintaining the earth's climate. One envisions a meridional overturning cell with warm water flowing poleward in the uppers layers and returning equatorward as cold deep water. Because the ocean basins are connected, this circulation - the thermohaline circulation - encompasses all the major world oceans. The conversion from light to dense water is the focus of this thesis. The stability of the thermohaline circulation hinges crucially on this conversion, which provides a direct link between the atmosphere and deep ocean.

The densest waters in the North Atlantic are formed north of the Greenland-Scotland Ridge. The conversion is thought to occur within the gyres of the Iceland and Greenland Seas. These gyres, especially the latter, have extremely low vertical stability, thus the conditions for convection are ideal. Warm water is expected to be drawn into the gyre, cool off and sink during winter, and exit as dense water (fig. 1.1). The concept that the gyres are the principal locations of water mass conversion for the thermohaline circulation - the pipelines connecting the atmosphere and the deep ocean - is challenged in this thesis. I propose that the dense water is formed to the east of the gyres, within the North Atlantic Current in the Norwegian Sea. The large heat flux over the North Atlantic

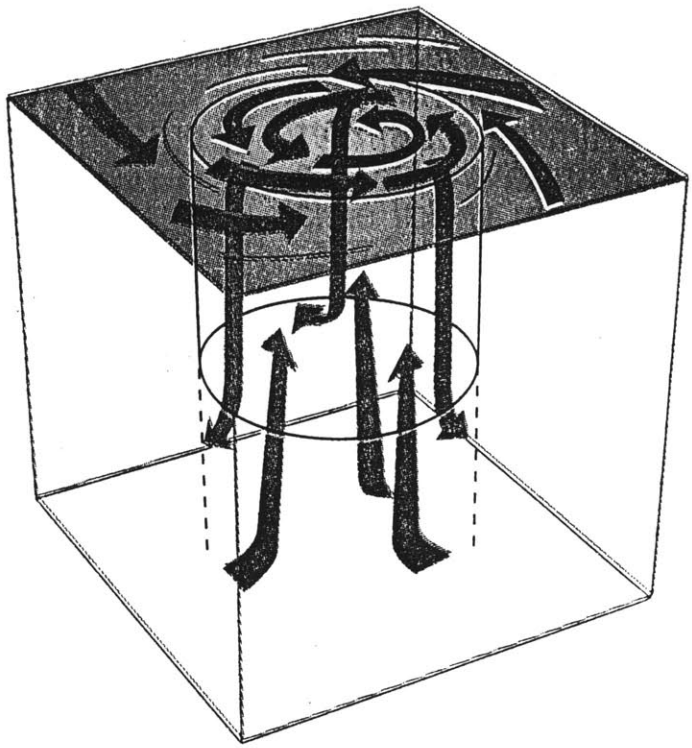

Fig. 1.1 Conceptual picture of an open-ocean gyre.

Current and the existence of even denser water over which the current flows makes it possible to increase the density of the North Atlantic Current so that by the time it subducts in the Fram Strait it is dense enough to sink to the bottom of the North Atlantic. One branch of the Atlantic Water is further modified in the Arctic Ocean and is carried to the Denmark Strait by the East Greenland Current. Another branch enters the East Greenland Current directly in the Fram Strait, and is similarly carried to the Denmark Strait, bypassing the gyres. There is a small contribution of dense waters from the gyres to the dense overflows at the Iceland-Scotland Ridge, but also for these waters most of the buoyancy has been removed within the North Atlantic Current before entering the gyres. So although there is ample evidence that vertical convection is occurring in the gyres, eg. that oxygen levels are larger than those of the surroundings at all depths, the results of this thesis research indicate that the net export of dense water from the gyres is small.

There are several important implications of these findings. The temperature of the surface waters of the gyres is close to freezing. Thus the density that may be acquired through cooling strongly depends upon salinity: given a small fresh-water anomaly the water will freeze before it gets dense enough to sink. It has been suggested (Bryan, 1986) that the formation of dense water is sensitive to such fresh-water anomalies, and that the thermohaline circulation might easily shut down, drastically altering the earth climate. It is observed that the ice cover in the Greenland and Iceland Seas is in fact highly variable from year to year. Formation of dense water within the North Atlantic Current, as proposed in this thesis, is less sensitive to such fresh-water anomalies, for two reasons. First of all, the area of formation is greatly increased, reducing the importance of any local anomaly. In fact, the density of the waters of the North Atlantic Current has been increased even before it enters the Nordic Seas, during its transit of the subpolar gyre. Secondly, the density is acquired at higher temperatures than in the Greenland and Iceland gyres. A fresh water anomaly may be overcome by further cooling, obtaining the "correct" density without freezing. Observations indicate that the domain of the North Atlantic Current is in fact

always ice-free. These findings are consistent with the climate of northern Europe not having changed dramatically since the last ice-age, and with the fact that all monitoring of the dense transport into the North Atlantic indicate a substantial flow (O(several Sverdrups)), despite the observed tendency of gyre convection to shut on and off.

The long-term monitoring programs mentioned above also indicate that there is no seasonal signal associated with the dense overflows. One might expect that the formation of dense water during winter would cause the dense water to spill into the North Atlantic in larger amount during that season. This lack of a seasonal signal is explainable, once the focus is shifted from the gyres to the North Atlantic Current. The residence time within this domain is 2-3 years. The net annual heat loss is extremely large, and even though there is a seasonal signal superimposed, with net heating during a few summer months, the seasonal signal becomes a small perturbation at the Fram Strait. By the time the North Atlantic Current subducts the water is uniformly dense.

1.1 Organization and Primary Results of the Thesis

To address these issues of dense water formation and seasonality the thesis is organized as follows: chapter 2 contains a literature review of the theories of formation of dense water, and raises the questions which will be examined in the thesis. It also contains a general description of the Nordic Seas and the Arctic Ocean. In chapter 3 a new circulation scheme is proposed. Section 3.1 contains a systematic search through the primary data set (data obtained during 11 cruises in the 1980's) for robust features that indicate circulation. This search was important because the literature on the Nordic Seas is very rich in definitions of water masses and water types; while the level of interannual variability is large, the actual range in temperature and salinity is small. Based on this analysis it was possible to formulate three hypotheses, each dealing with different aspects of the circulation, and each differing from the current understanding. The first hypothesis

suggests that the densest water in the western North Atlantic originates in the Arctic Ocean, rather than in the Greenland and Iceland Seas. This water flows straight towards the Denmark Strait as part of the East Greenland Current, and bypasses the gyres. The second hypothesis suggests that the primary production site of the dense water is the domain of the North Atlantic Current, and not the Greenland and Iceland Seas. As this water subducts in the Fram Strait a branch enters the Arctic Ocean. Without change in density the temperature and salinity, properties of this branch are gradually modified toward those of the source water discussed in hypothesis 1. Hypothesis 3 suggests that even the densest waters within the Nordic Seas are produced without much influence of the Greenland Gyre. In fact, this research suggests that the only water mass exported from the Greenland and Iceland Gyres is a water mass found at intermediate depths in a 100 m thin layer characterized by a salinity minimum. These hypotheses are supported with as many different kinds of data as possible. In chapter 4 a box model is formulated based on the proposed circulation scheme. It is confirmed that the proposed scheme conserves mass, heat and salt, and that the hypotheses are robust features of the model. Chapter 5 deals with some of the implications of the new circulation scheme. In particular, the processes responsible for the water mass formation in the North Atlantic Current are considered. The implications of an Arctic branch feeding the Denmark Strait overflows is examined, in particular the higher residence time of the water. Observations of oscillations in the hydrographic properties on a roughly 10 year time scale within the North Atlantic Current are discussed. It is suggested that these oscillations will propagate into the North Atlantic. Finally, the issue of the seasonality imposed by winter formation, as discussed above, is considered. A summary and concluding remarks are found in chapter 6.

Chapter 2

Background

The review of Warren (1981) describes the evolution of our present understanding of the ocean deep circulation. The accepted picture, that warm water is confined to a relatively thin layer near the surface in the tropics and the subtropics, and that the cold waters of the abyss originate at polar latitudes, dates back to the 18th. century. Thus the sinking of dense water at high latitudes has long been acknowledged as the source of renewal/ventilation of the World Ocean.

As early as 1899, Knudsen noted (Tait, 1967) that dense water spills over the Greenland-Scotland Ridge into the North Atlantic, after considering data from the Danish Ingolf-expedition in 1895-1898. In 1912, Nansen published sections across the Denmark Strait (fig. 2.1) and across the Iceland-Færø Ridge (fig. 2.2), clearly showing dense overflows into the North Atlantic. However, Nansen assumed that these overflows could not contribute in any substantial way to the enormous volume of the North Atlantic Deep Water (NADW), and rather suggested that most of the deep water was formed in an area southeast of Greenland (fig. 2.3).

Until the 1950's the area southeast of Greenland and the Labrador Sea were considered to be the production sites for the densest water in the North Atlantic (e.g. Wüst (1935), Sverdrup et. al. (1946)). Observations that the density of the upper layers of the Labrador Sea never exceeded $\sigma_t = 27.78$, as compared to the deep water which exceeded 27.9, led Worthington (1954) to suggest that North Atlantic Deep Water was not formed in the modern era. In Worthington's (1982) own words: "My error, which was common to many of us, from H. U. Sverdrup on down, was that of neglecting the Norwegian Sea overflows.". Cooper (1955) was responsible for suggesting that the

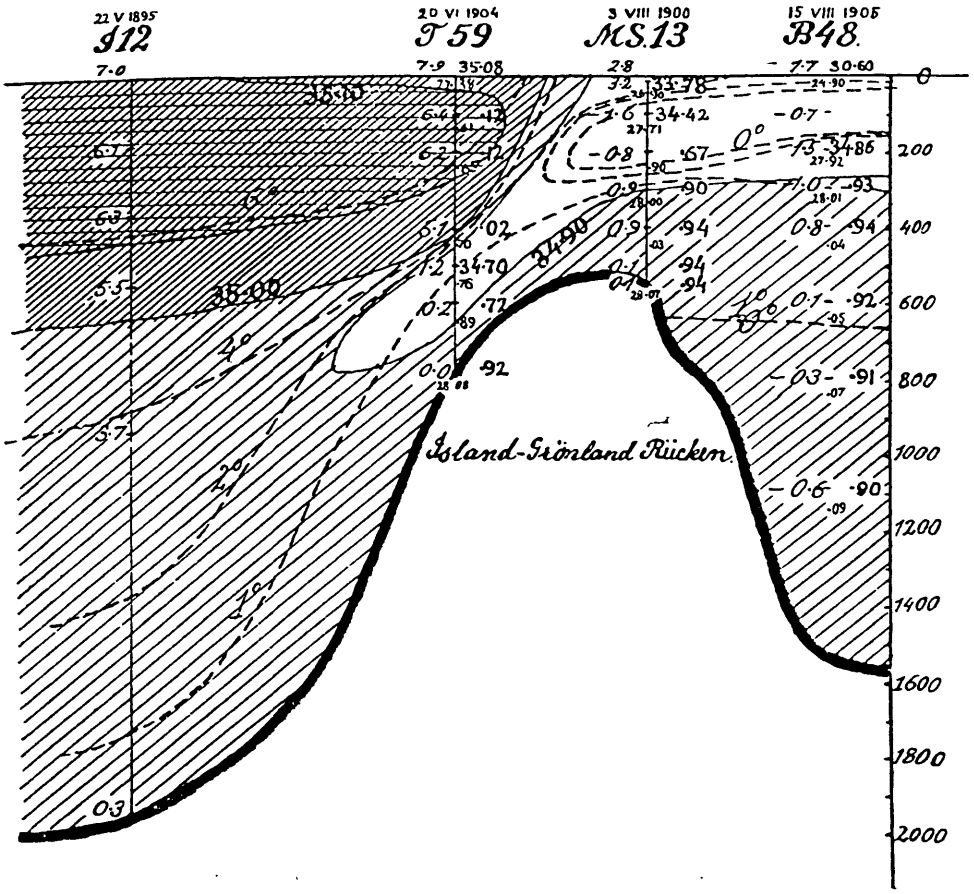

Fig. 2.1 Section along the Denmark Strait (from Nansen, 1912)

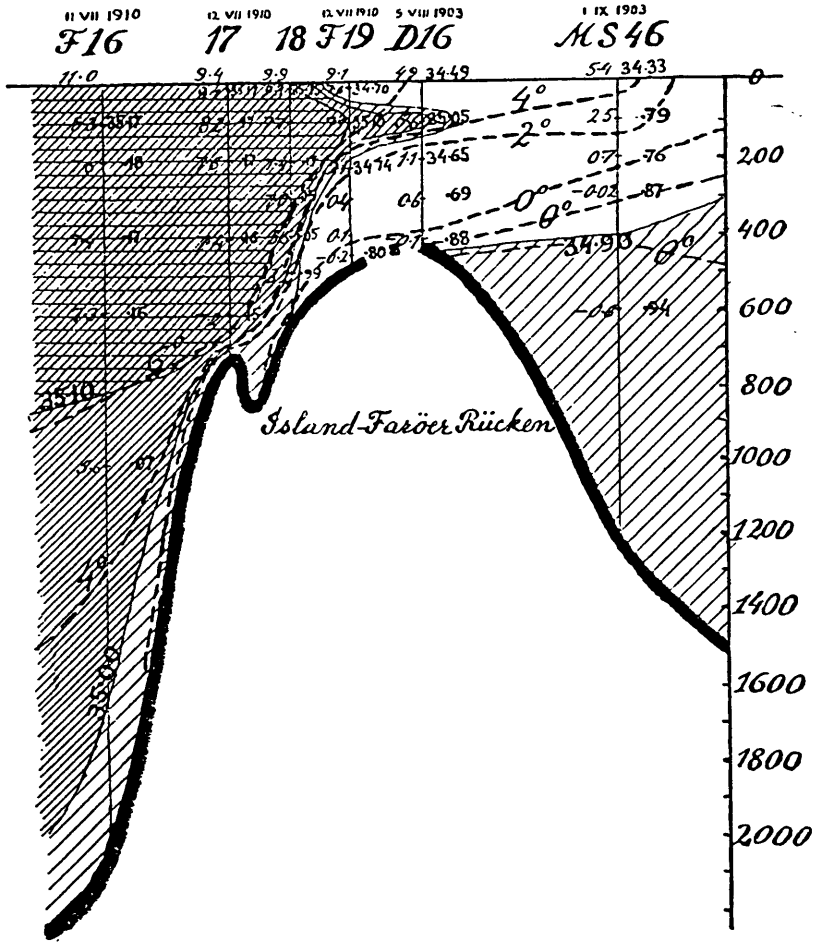

Fig. 2.2 Section across the Iceland-Færø Ridge (from Nansen, 1912).

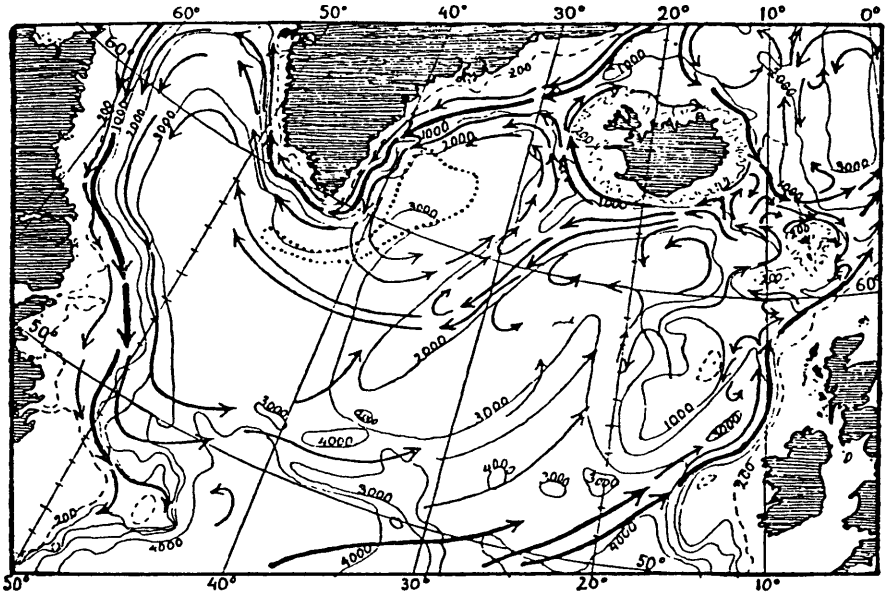

Fig. 2.3 Site of dense water formation (dotted lines) (from Nansen, 1912)

overflows were important for NADW replenishment. Motivated by the observed decline in nutrient levels in the English Channel and adjacent waters in the 1930's from higher values in the 1920's, he linked the upward motion of nutrients in the North Atlantic with the input of dense water at depth. He suggested that the dense water originated in the Nordic Seas, and entered the North Atlantic in intermittent boluses whose volume could vary greatly from year to year. Cooper's hypothesis spurred renewed interest in the Nordic Seas, and several multinational expeditions followed. The resulting observations confirmed his notion of a Nordic origin of the densest waters, both in the eastern and the western North Atlantic.

The remainder of this chapter is divided into four sections: A brief description of the general features of the Nordic Seas and Arctic Ocean, such as bathymetry, current systems and climate; a literature review of the nature of the velocity fields of the dense overflows; a similar review of the water masses constituting the dense overflows, and their sources; and, lastly, a discussion of the questions that are raised by the literature review.

2.1 General Features of the Nordic Seas and Arctic Ocean

2.1.1 Nomenclature and Bathymetry

When discussing the different seas north of the Greenland-Scotland Ridge (fig. 2.4a and 2.4b), some care must be taken as there is some variation in the naming conventions. The Norwegians have tended to denote the entire region between Norway, Spitsbergen, Greenland and Iceland "the Norwegian Sea". This nomenclature was used for example, by Worthington (1970).

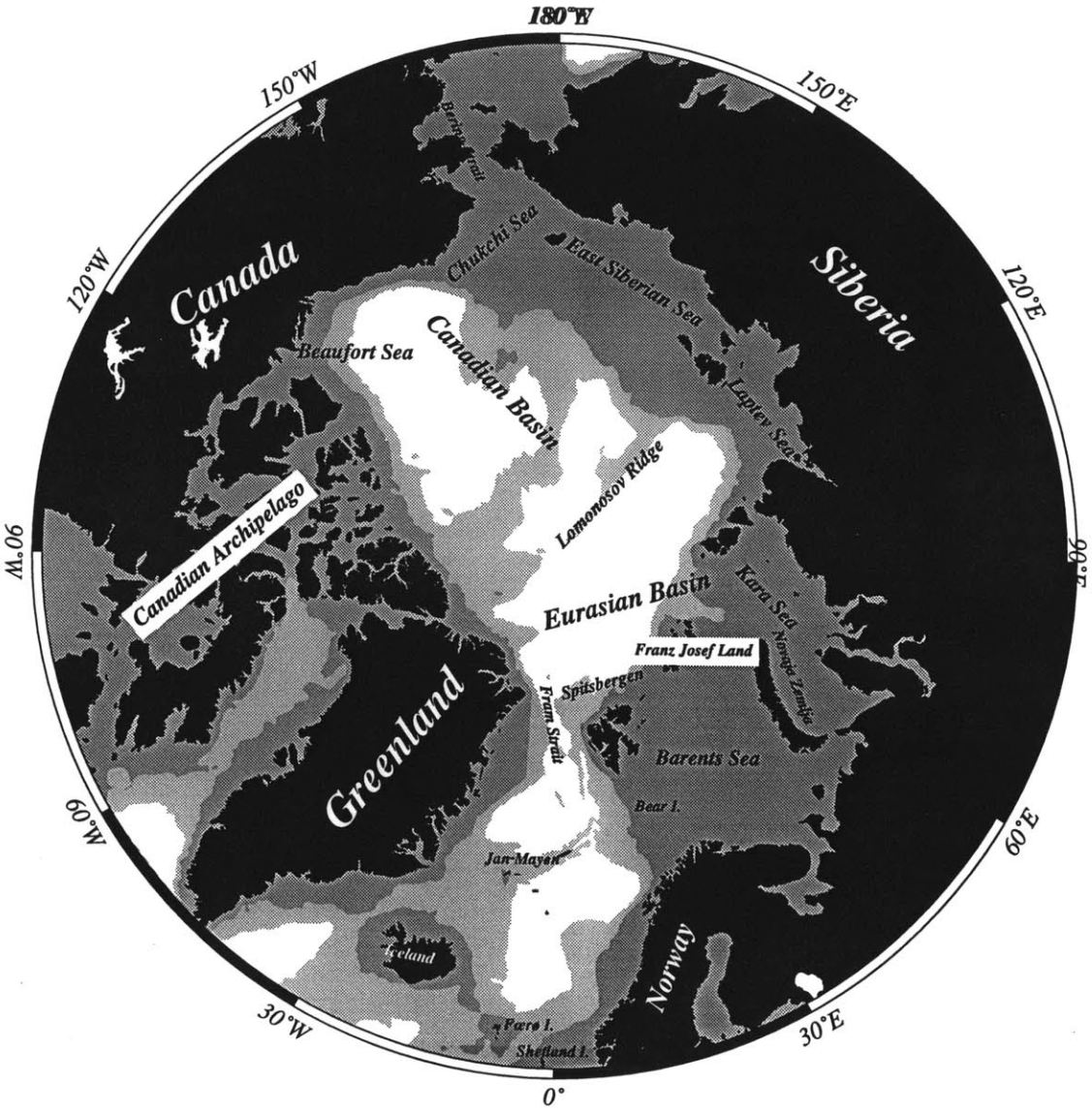

Fig. 2.4a Bathymetry and location of geographic features in the Nordic Seas and Arctic Ocean

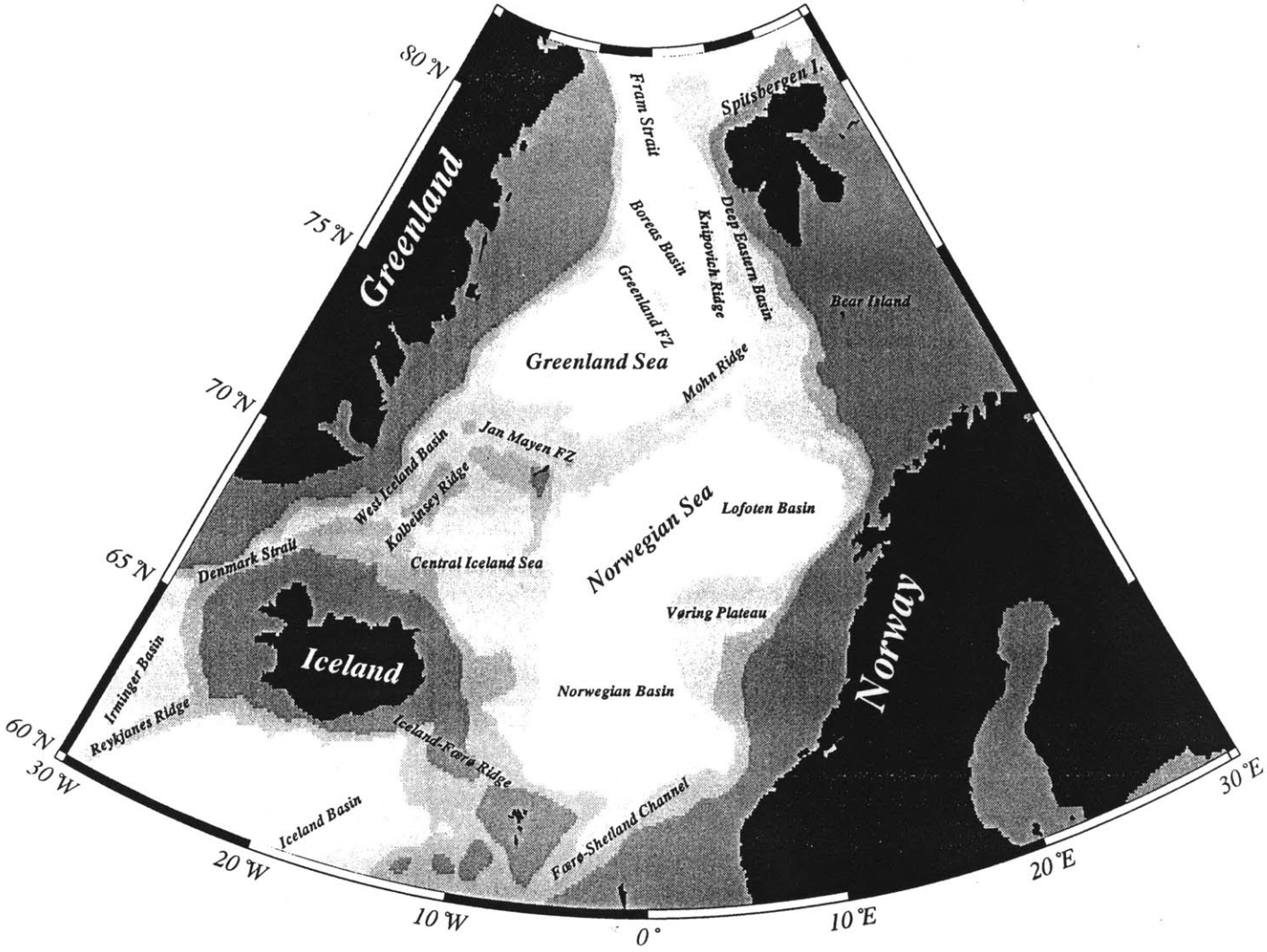

Fig. 2.4b Bathymetry and location of geographic features in the Greenland, Iceland and Norwegian Seas

This thesis will follow a more common convention of dividing the region into three seas: the Iceland Sea, the Norwegian Sea and the Greenland Sea. The Iceland Sea is defined as the area between Greenland, Iceland, and the island of Jan Mayen, and is divided by the Kolbeinsey Ridge into two basins: the West Iceland Basin and the Central Iceland Sea. The Iceland Sea is relatively shallow, around 2000 m deep, and is thus shallower than the Norwegian Basin, to its east. The Norwegian Sea contains the Norwegian Basin and the Lofoten Basin, both of which are deeper than 3000 m. Further north the Norwegian Sea extends east of the Knipovich Ridge towards the Fram Strait, in what will be called the Deep Eastern Basin. The Greenland Sea is separated from the Norwegian Sea by the Mohn/Knipovich Ridge, and from the Iceland Sea by the Jan Mayen Fracture Zone. This sea also contains more than one basin: the Greenland Basin and the Boreas Basin, both of which are also deeper than 3000 m. These basins are separated by the Greenland Fracture Zone. Furthermore, the shallow sea bounded by Scandinavia, Novaya Zemlya and Spitsbergen, is referred to as the Barents Sea. I will refer to the Barents Sea, the Norwegian Sea, the Greenland Sea and the Iceland Sea collectively as "the Nordic Seas".

The thesis will refer to the region north of the Fram Strait as the Arctic Ocean, as opposed to Nansen's (1906) label of "the North Polar Basin". The Arctic ocean comprises the Eurasian Basin and the Canadian Basin, separated by the Lomonosov Ridge, and all the shelf seas, except the Barents Sea. To summarize the definitions used in this work:

- The Nordic Seas - the Norwegian Sea, the Greenland Sea, the Iceland Sea and the Barents Sea.
- The Arctic Ocean - the Eurasian Basin, the Canadian Basin and the shelf seas, excluding the Barents Sea.

2.1.2 Connections with the World Ocean

The Arctic Ocean connects with the Pacific through the Bering Strait, which is less than 50 m deep. It connects with the North Atlantic through the Canadian Archipelago, which is approximately 200 m deep. The exchange with the Nordic Seas is topographically less restricted: the sill depth of the Fram Strait is 2600 m. The Nordic Seas join the North Atlantic across the Greenland-Scotland Ridge. South of the ridges the Reykjanes Ridge, part of the Mid-Atlantic Ridge, separates the Western North Atlantic from the Eastern North Atlantic (fig. 2.5). The Denmark Strait, which is around 600 m deep, connects with the Irminger Basin in the Western North Atlantic. The Iceland-Færø Ridge (around 500 m deep) and the Færø-Shetland Channel (850 m deep) connect with the Iceland Basin in the Eastern North Atlantic. Exchange of deep waters between these two basins of the North Atlantic is limited, the only passage being the Gibbs Fracture Zone. Therefore only the Denmark Strait overflows have direct access to the Deep Western Boundary Current.

2.1.3 Ice

Most of the Arctic Ocean is ice covered even in summer. In fig. 2.6 is shown the seasonal cycle of the ice cover, averaged over the years 1973-1977 (Parkinson et. al., 1987). In the Greenland and Iceland Seas there are large variations in the ice cover during the year, whereas the Norwegian Sea and large parts of the Barents Seas are ice free year round. The east-west difference in ice conditions within the Nordic Seas largely reflect the fact that in the east the North Atlantic Current is bringing warm water northwards, whereas in the west the East Greenland Current is bringing cold polar water southward from the Arctic.

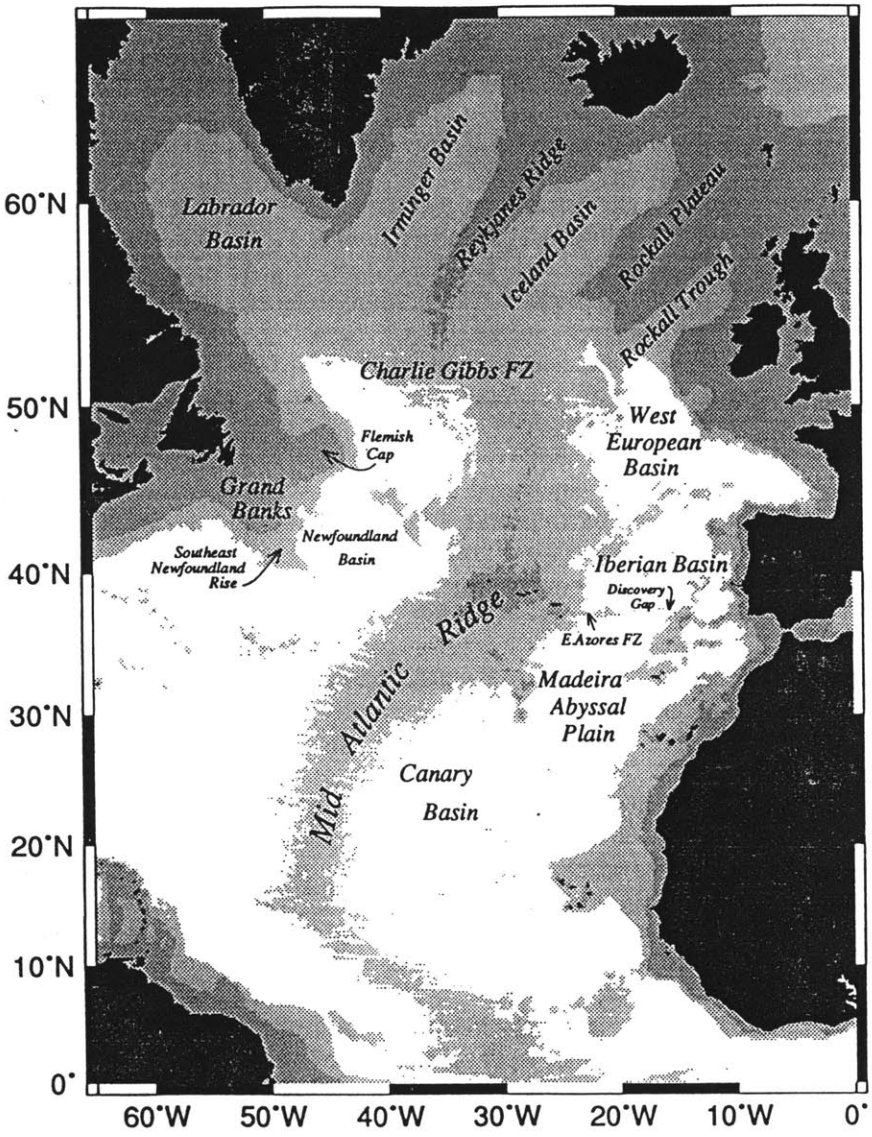

Fig. 2.5 Bathymetry and location of geographic features south of the Greenland-Scotland Ridge

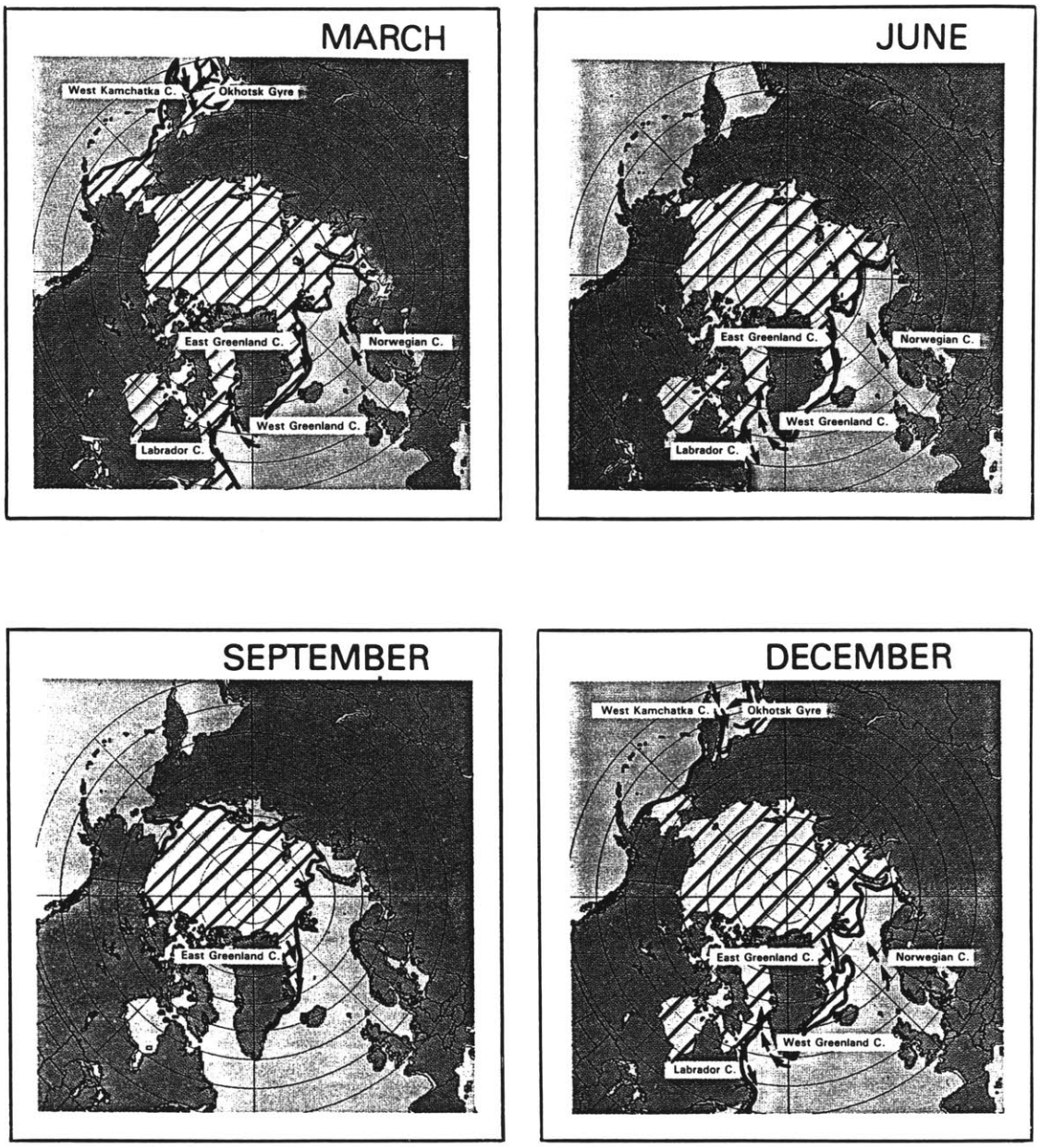

Fig. 2.6 Sea ice distribution for March, June, September and December, averaged over 4 years for the Arctic Ocean / Nordic Seas (from Parkinson et. al. 1987).

2.1.4 Atmospheric Conditions

Climatically, the Arctic Front separates the Norwegian Sea from the Greenland and Iceland Seas (fig. 2.7) (Hopkins, 1988). Northwest of the front polar easterlies prevail, with little seasonal variability, whereas to the southeast the winds are more variable, dominated by cyclonic storms which emanate from the Icelandic Low and travel towards the Barents Sea. The seasonal cycle here is strong, with a maximum in early winter and a minimum in early summer (op. cit.). Fig. 2.8 shows the mean wind stress curl, averaged over the years 1955-1987 (Jónsson, 1989). The values are positive over most of the area, with two separate maxima, one over the Greenland Basin and one over the Boreas Basin. There is also a strong seasonal signal associated with the wind stress curl, which is practically zero for the whole region during the summer months May through August.

2.1.5 Current Systems

The upper ocean currents are synthesized by Aagaard et. al. (1985b) in fig. 2.9. The major circulation features are the Bering Strait inflow (A), the Beaufort gyre (B), the Transpolar Drift (C), the East Greenland Current (D), the Norwegian Atlantic Current (E), the West Spitsbergen Current (F), the Greenland Gyre (G) and the Iceland Gyre (H). In addition, there is a flow of Atlantic Water into the Iceland Sea west of Iceland: the Irminger Current (I), and, lastly, the Norwegian Coastal Current (J).

2.2 Velocity Fields of the Dense Overflows

In the following sections I will consider the characteristics of the dense currents at the sills which join the Nordic Seas to the North Atlantic. The definition of

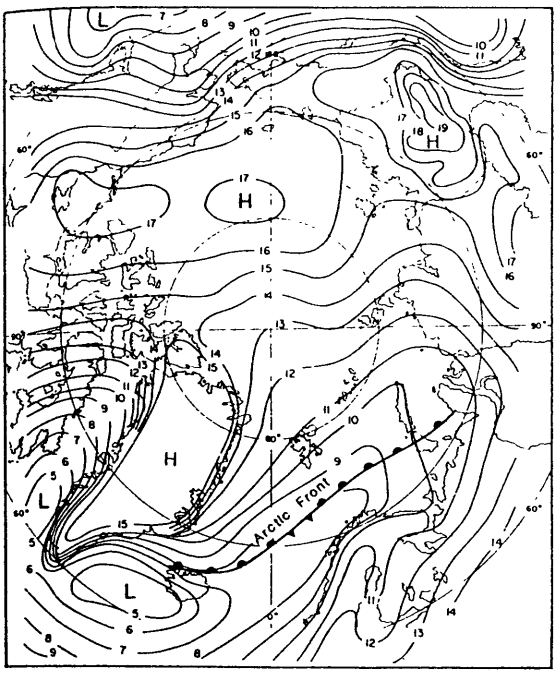

Fig. 2.7 Annual mean air pressure (from Hopkins, 1988).

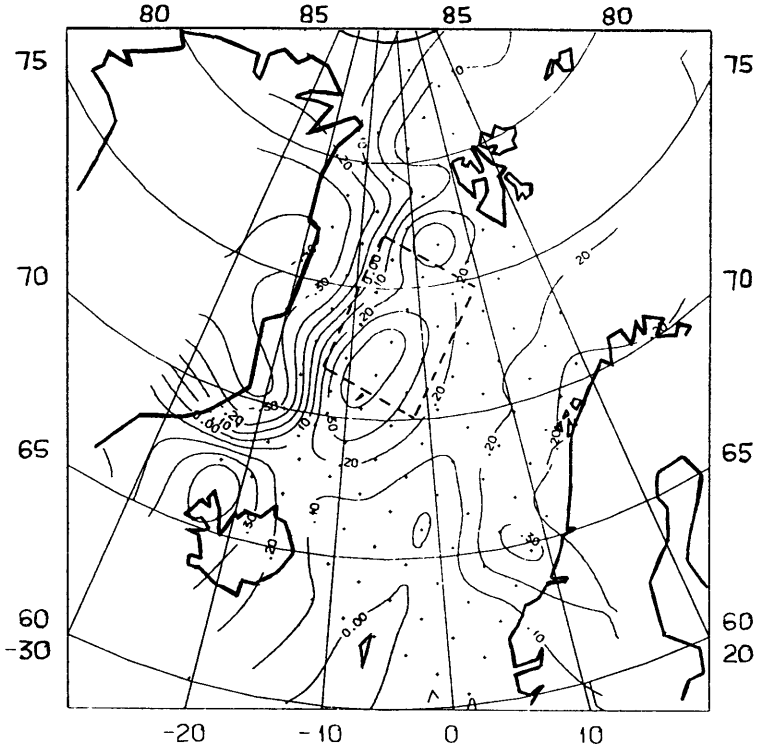

Fig. 2.8 Mean wind stress curl (from Jónsson, 1989).

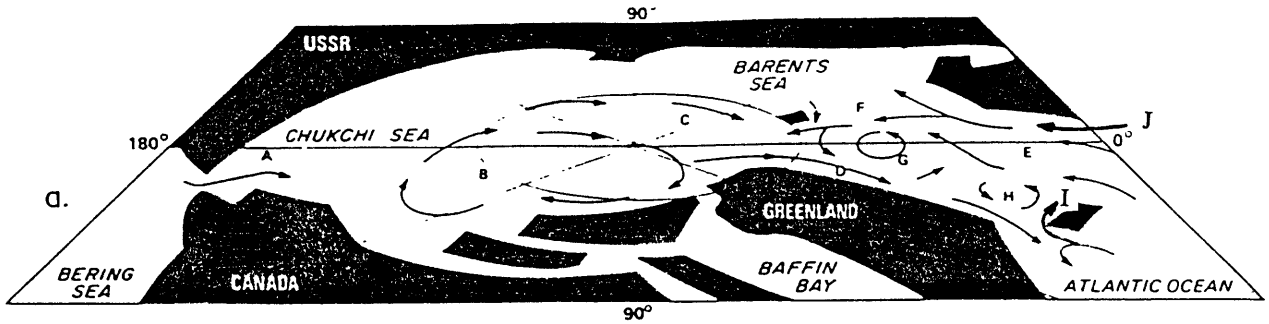

Fig. 2.9 Upper layer circulation in the Nordic Seas/Arctic Ocean (from Aagaard et. al., 1985b)

"dense water" varies from author to author (eg. $\theta < 2^0C$, or $\sigma_0 > 27.85$), but since there is a definite division of light and dense water near the sills, the actual definition is not crucial. The velocity fields will be discussed first, followed by a section on the water masses present at the sills and their origins. Previous work and our present understanding of both will be reviewed.

2.2.1 Denmark Strait

Numerous investigators have found the dense overflow at the Denmark Strait to be highly variable on a time scale of 2-3 days, but to be comparatively constant on longer time scales. The multinational Overflow '60 experiment, comprising a quasi-synoptic hydrography survey by nine ships and several deep current meters yielded information about this strait and the Iceland-Færø Ridge. Harvey (1961) showed two sections across the strait, separated in time by only 20 hours. Only the second section indicated the presence of dense water (fig. 2.10). A joint US-Canadian experiment was conducted in 1967, with repeated hydrographic surveys across the strait and the deployment of 30 current meters. Mann (1969) found similar short time scale variability, and noted that the overflow water masses tended to fall in a well-defined region of TS-space (fig. 2.11). From the two current meter records that performed properly, Worthington (1969) found irregular pulses of overflow water with a time scale of about three days. The speeds were substantial (up to 140 cm/s) and the fluctuations were uncorrelated with the wind.

The Overflow '73 experiment sampled the entire Greenland-Scotland Ridge over the period of one month and yielded a much larger data return than previous attempts. Ross (1975) found that although the flow is intense and highly variable, the dense outflow was always present, suggesting that the overflow was not intermittent in time as was previously believed. The first long term monitoring of the dense outflows

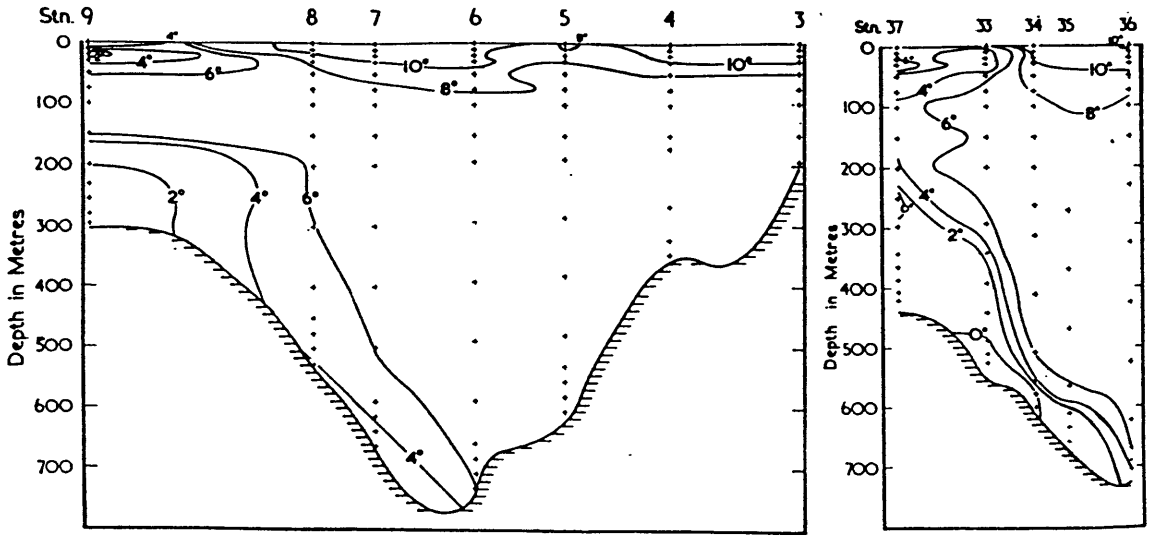

Fig. 2.10 Two sections across the Denmark Strait (from Harvey, 1961)

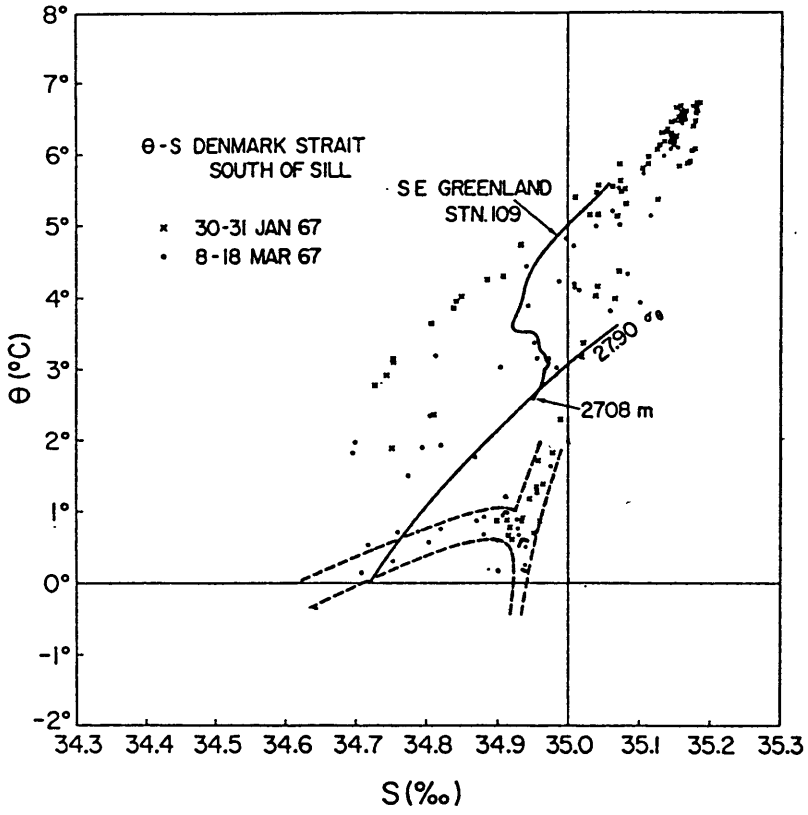

Fig. 2.11 TS diagram for stations near Denmark Strait. The dashed lines indicate the envelope of the dense overflow water (from Mann, 1969).

occurred in 1975 during the MONA (Monitoring the Overflow to the North Atlantic) experiment, where current meters were deployed in the region for more than one year. Aagaard and Malmberg (1978) found the dense overflows in the Denmark Strait to have large fluctuations in the period band 1.5 to 2.5 days, with amplitudes comparable to the mean. For longer time scales (weeks to months) the fluctuation amplitude did not exceed 20 % of the mean, and in particular they found no seasonal signal in the speed nor in the temperature of the overflow.

2.2.2 Iceland-Færø Ridge

This is the shallowest of the three sills, and the flow of dense water is apparently restricted here (fig. 2.12). Hermann (1967) identified four main paths of flow over the Ridge during the Overflow '60 experiment (fig. 2.13). Dietrich (1967), studied the record of ten short-term current meters from the same experiment and found bottom velocities which were relatively stable over the three day record and directed towards the North Atlantic. Based on the results of the Overflow '73 experiment and other data, Hansen and Meincke (1979) found the variability in the bottom flow to be most intense in the 3-24 day band, and suggested that there was significant eddy activity in the region. Willebrand and Meincke (1980) found that the variability as seen in the MONA records was strongest at a period of about ten days, and consequently suggested that conversion of available potential energy via baroclinic instability was a more potent influence than wind forcing. Longer term variability is apparently weaker, or unresolved.

2.2.3 Færø-Shetland Channel

This channel is the deepest of the three, and is the site of significant transport of dense water (fig. 2.14). Hermann (1959) found a thick layer of cold water in the deep

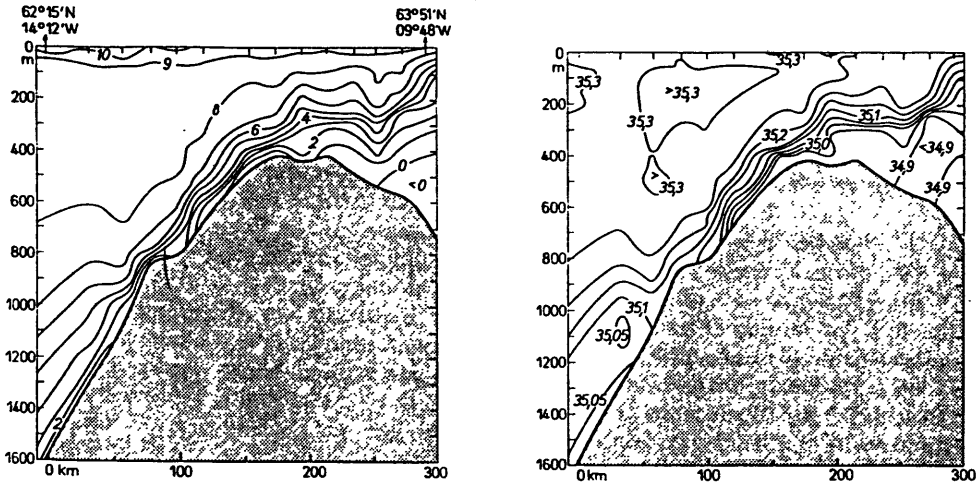

Fig. 2.12 Sections of T and S across the Iceland-Færø Ridge (from Dietrich, 1967)

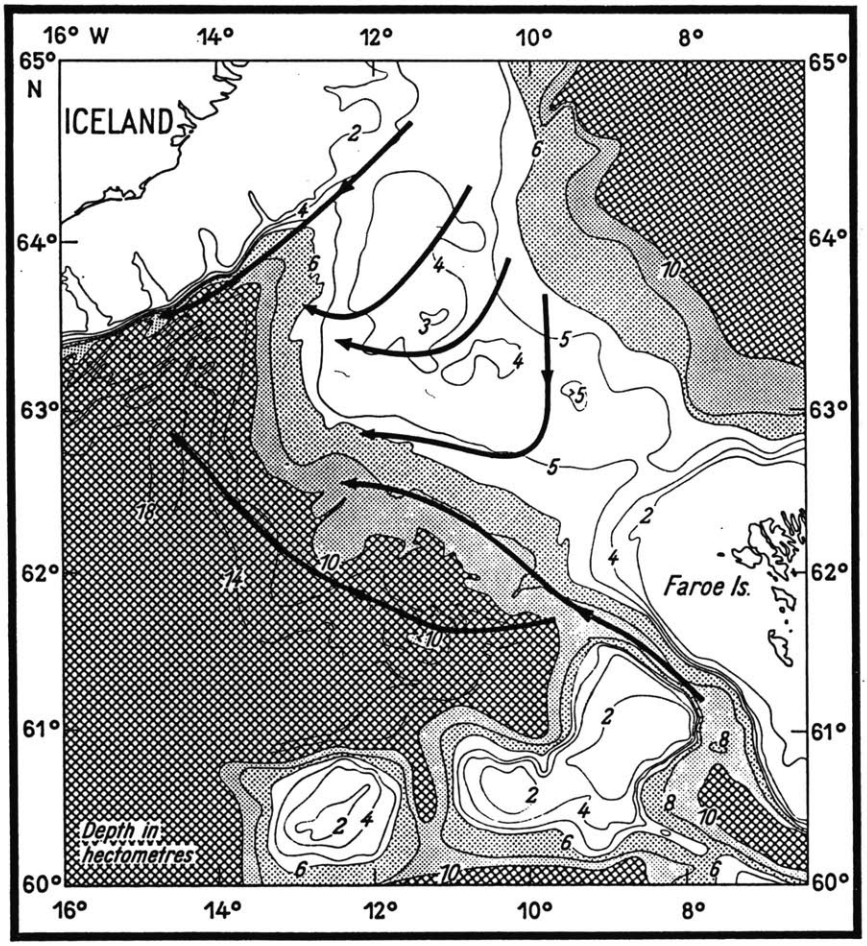

Fig. 2.13 Main overflow branches over the Iceland-Scotland Ridge (from Hermann (1967), redrawn by Dietrich (1967))

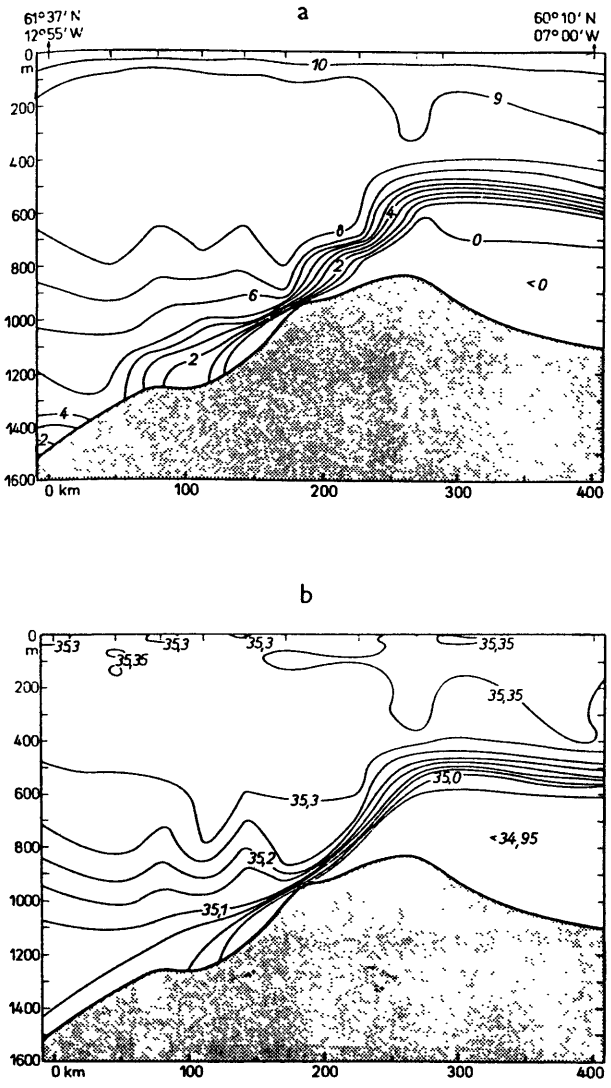

Fig. 2.14 Sections of T and S along the Færø-Bank Channel (from Dietrich, 1967)

Færø Bank Channel, and suggested that the overflow was much more constant than that over the Iceland-Færø Ridge. Crease (1965), based on hydrography and the few current meter observations that existed, suggested that the flow was fairly constant. Willebrand and Meincke (1980) found shorter term variability, peaked at about 10 days as over the Iceland-Færø Ridge. Saunders (1990), using CTD, ADCP and three long-term current meter mooring records, found the dense overflow in the Channel to be persistent and never reversing in direction. Fluctuations in strength were found to be much smaller than the mean. No seasonal signal was found to be associated with the dense overflow.

2.3 Dense Water Masses near the Sills

This section seeks to identify the dense water masses present at the Denmark Strait and Iceland-Scotland Ridge, and to compare those masses with adjacent water masses in the deep North Atlantic. It will further discuss the origins of these various water masses, as well as the evolution of theories regarding their circulation. Due to their geographic separation, I will discuss the Denmark Strait and the Iceland-Scotland Ridge separately, but due to the proximity of the Iceland-Færø Ridge and the Færø-Shetland Channel, I will group these together under the name "Iceland-Scotland Ridge".

2.3.1 Denmark Strait

There are three principal dense water masses which have been identified in the Denmark Strait: the upper and lower Arctic Intermediate Water masses (uAIW and lAIW hereafter) and the Norwegian Sea Deep Water (NSDW) (see table 2.1). The NSDW is the densest of the three, the uAIW is the freshest and the lAIW, marked by a salinity maxima in T-S space, lies in between the other two. This water was identified by

Helland-Hansen and Nansen (1909) as returning Atlantic Water that has entered the East Greenland Current near the Fram Strait.

The question of which of these water masses flows over the sill has been the subject of much study. In 1967, Lee and Ellett showed that the overflow is too fresh to be comprised solely of NSDW; they suggested instead that the overflow was NSDW mixed with AIW and slope waters. In the western North Atlantic the dense overflow water is typically characterized by salinities around 34.9, and potential temperatures around 1-1.5 ^{0}C, as seen on the westernmost slope in fig. 2.15 from the Hudson cruise in 1967 (Grant, 1968). High oxygen and low silicate values are also associated with the dense waters originating in the Denmark Strait (fig. 2.15). Petersson and Rooth (1976) used transient tracers to demonstrate that the dense overflows were younger than the NSDW. Swift et. al. (1980) suggested that only small amounts of NSDW and lAIW enter the North Atlantic, based on the salinities south of the sill. They proposed that uAIW is instead the major overflow component in the Denmark Strait. Furthermore, Ross (1984) performed a thorough investigation of the flow in TS-classes during the Overflow '73 experiment and found the overall transport for water with $\theta < 2^0$ (ie. all water dense enough to sink to the bottom of the North Atlantic) to be 2.9 Sv, with only 0.5 Sv for $\theta < 0^0$ (NSDW).

Swift et al. (1980) proposed a scheme to explain the origin of the uAIW and thus its counterpart in the North Atlantic, the Northwest Atlantic Bottom Water (NWABW). In their scheme, Atlantic water flows into the upper portion of the Iceland Sea from the Norwegian Sea, south of Jan Mayen. There the water is cooled and convects downward, eventually spreading horizontally along isopycnals to the Denmark Strait. By considering a winter minus summer volume census for the region, they estimated that 0.7 Sv of uAIW was formed during the winter. According to the scheme, the 0.7 Sv spreads westward and exits the region before summer warming commences.

Strass et al. (1993) suggested that an additional amount (0.6 Sv) of uAIW is formed by mixing between the lAIW in the East Greenland Current and winter-cooled

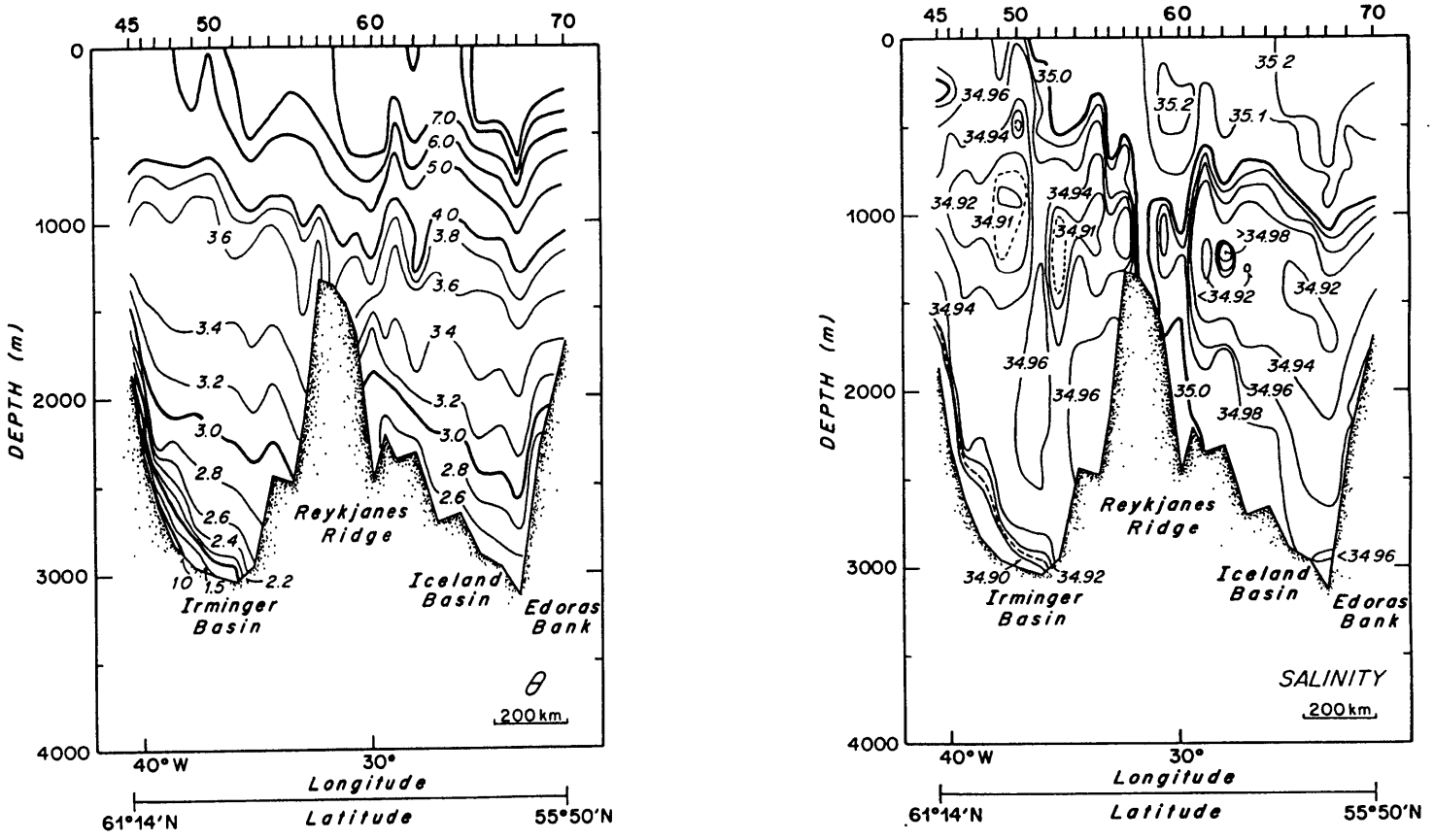

Fig. 2.15 Sections of potential temperature and salinity from the Hudson 57 N transect in 1967 (Grant 1968, redrawn by McCartney, 1992).

surface water in the Greenland Gyre. Such a contribution would obviously increase the available water for the deep overflow over that from the Swift et al. (1980) scenario alone.

2.3.2 Iceland-Scotland Ridge

As mentioned above, the Iceland-Færø Ridge and the Færø-Shetland Channel are physically quite different, but the water masses present are similar and hence the two are considered jointly. Note though that the greater depth of the Færø-Shetland channel permits flow of denser water. The principal water masses present in the region are the North Iceland Winter Water (NIWW), the Arctic Intermediate Water (AIW) and the Norwegian Sea Deep Water (NSDW) (see table 2.1). Though identical names are used for water masses in the Denmark Strait, it is not clear that they share the same source. Thus each should be discussed in relation to its location, at least until it is shown that they are actually the same water mass. Thus no distinction is made between different components of the AIW. Again, the NSDW is the densest water mass present. The AIW and NIWW are comparable in salinity, although the AIW tends to be associated with a weak salinity minimum. The NIWW is warmer and therefore lighter than AIW.

The densest waters in the eastern North Atlantic are much warmer and saltier than those in the western North Atlantic. Typically, the dense waters on the eastern side are characterized by salinities around 35.0, and potential temperature around 2-3 ^{0}C. This is seen in the Hudson section (fig. 2.15), where the dense overflows from the Iceland-Scotland Ridge are seen on the eastern slope of the Reykjanes Ridge. None of the water masses north of the Iceland-Scotland Ridge are similar to the densest water in the eastern North Atlantic so some modification of the water mass characteristics must occur across this ridge. This can be seen clearly in a series of TS-profiles in the Færø-Shetland Channel (fig. 2.16, from Saunders, 1990). Water similar to that of the deep Northeast

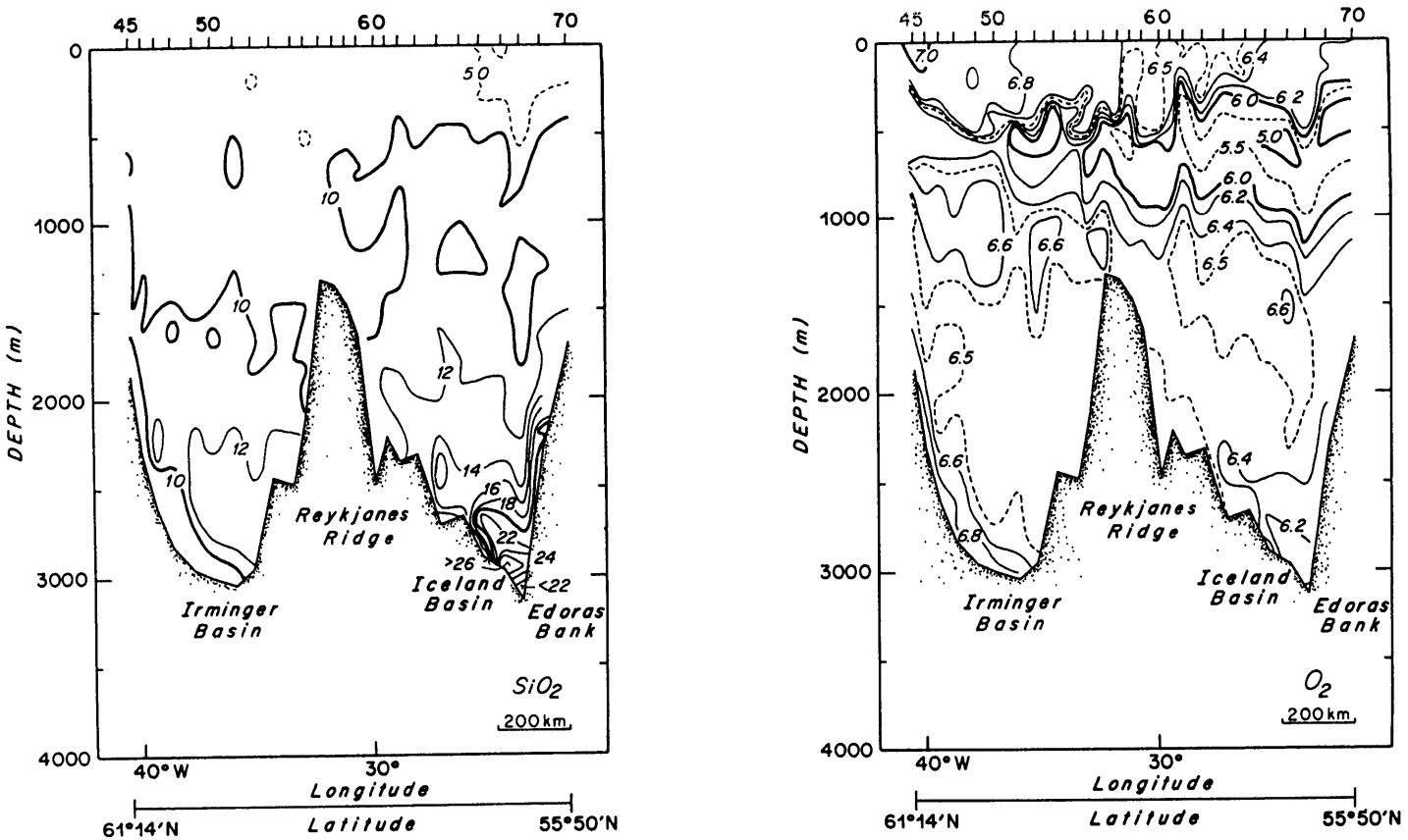

Fig. 2.15 continued. Sections of oxygen and silicate from the Hudson 57 N transect

Atlantic is only found downstream in the Channel, whereas other water masses are present on the Norwegian Sea side of the Channel . Thus one can see that the situation in this region is not as straightforward as is the Denmark Strait.

Transport estimates for the overflows in this region are uncertain, especially for the Iceland-Færø Ridge, as the flow field is most variable. Steele et. al. (1962) suggested that 1.4 Sv of "pure Norwegian Sea Water" (θ=0 ^{0}C, S=34.95) entraining 4 Sv of Atlantic Water to produce the overflow through the whole region. Hermann (1967) found that the transport of dense water over the Iceland-Færø Ridge is 1.1 Sv, very little of which has $\theta < 0^0$C, suggesting that NSDW is not a constituent. But in the deeper Færø-Shetland Channel, where Hermann estimated a 1.4 Sv transport, the contribution of NSDW water is ~ 90 %. Hermann's results were basically supported by Saunders (1990) who found the transport of water colder than 3 ^{0}C (ie. all the dense waters) in the Færø-Shetland Channel to be 1.9 $\pm$ 0.4 Sv.

As all three water masses may participate in the formation of the overflow at the Iceland-Scotland Ridge, it is worthwhile considering the origin of each. In the following I present a summary of the history of each.

1. Arctic Intermediate Water: Helland-Hansen and Nansen (1909) observed water with salinities in the range 34.86-34.9 and low temperatures (~ 0^{0}C) across the entire southern Norwegian Sea. They suggested that this water flows as a cyclonic tongue originating from lower levels of the East Icelandic Current, and proposed that it is formed by gradual mixing of waters in the Iceland Sea and by atmospheric cooling. This water, a salinity minimum in TS space, was also observed in the Overflow '60 experiment, but the anomaly was so small that Hermann (1967) chose to consider it a mixture of North Icelandic Winter Water and Norwegian Sea Deep Water. Renewed attention to the water mass was given by Blindheim (1986, 1990) who considered it a separate water mass, formed in the Iceland and Greenland Seas. He found it was present in most of the

Norwegian Sea, effectively insulating the Atlantic Water from the Deep Water (fig. 2.17), although he could not deduce the circulation pattern from the salinity distribution.

2. North Icelandic Winter Water: Stefansson (1962) defined NIWW as water formed in the North Icelandic coastal area during winter by vertical mixing of Atlantic Water (the Irminger current, with S > 35.0) with the surface waters in the Iceland Sea.

3. Norwegian Sea Deep Water: The NSDW is a thick, isohaline water mass which occupies the temperature range -1.05 to 0 degrees C. Only that portion in the range -.5 to 0 ^{0}C exits the Færø-Shetland Channel, the colder portions lying below the sill and further being too old to be consistent with transient tracer data in the overflow (Petersson and Rooth, 1976). Nevertheless I will discuss formation theories of the NSDW as a whole as there is no hydrography which can distinguish between the formation of the two portions.

Nansen (1906) proposed that the formation region of NSDW had to lie between 73 N and 76 N, 4 W and 4 E (the Greenland Gyre region), where he found surface waters with salinities around 34.9. As there is no vigorous horizontal circulation in the Gyre, he suggested that the warm surface waters could be cooled to -1.3 ^{0}C and sink. From there, it would spread along the bottom, perhaps generating isolated cyclonic circulation patterns in the process. The temperature of the water would rise as it propagated, heated by the adjacent waters.

Metcalf (1960) found that the deep waters of the Greenland Sea were separated from those of the Norwegian Sea, and that the former represent a gyre, surrounded by warmer water, separated by a front. Thus Nansen's deep water was distinct from the NSDW. Aagaard et. al. (1985b) presented evidence of a dense outflow from the Arctic in the western Fram Strait, flowing along the slope of Greenland (fig. 2.18), and bringing warmer and saltier water into the periphery of the Greenland Sea. They suggested that this Arctic Ocean Deep Water (AODW) mixes with the deep water

Table 2.1 Dense water masses near the Greenland-Scotland Ridge

Denmark Strait			Iceland-Scotland Ridge		
name	temperature	salinity	name	temperature	salinity
uAIW	$0 < \theta < 2^0C$	$34.7 < S < 34.9$	NIWW	2.5^0C	34.88
lAIW	$0 < \theta < 2^0C$	$34.9 < S < 35.0$	AIW	0^0C	34.86
NSDW	$\theta < 0^0C$	$S \sim 34.92$	NSDW	$\theta < 0^0C$	$S \sim 34.92$

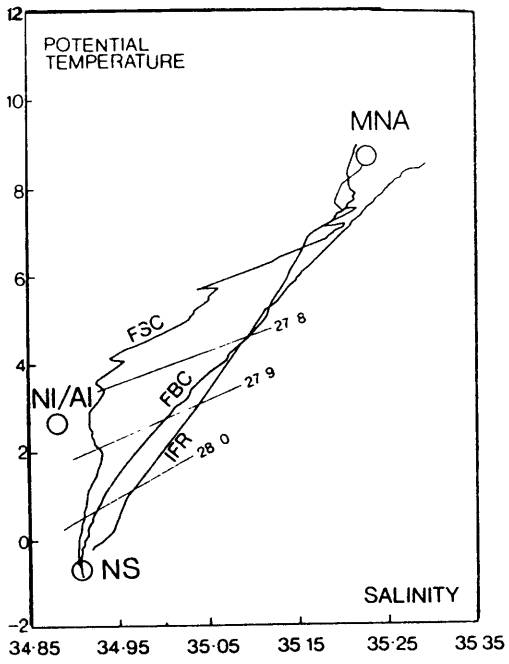

Fig. 2.16 TS-diagram for stations along the Færø-Bank Channel (from Saunders, 1990)

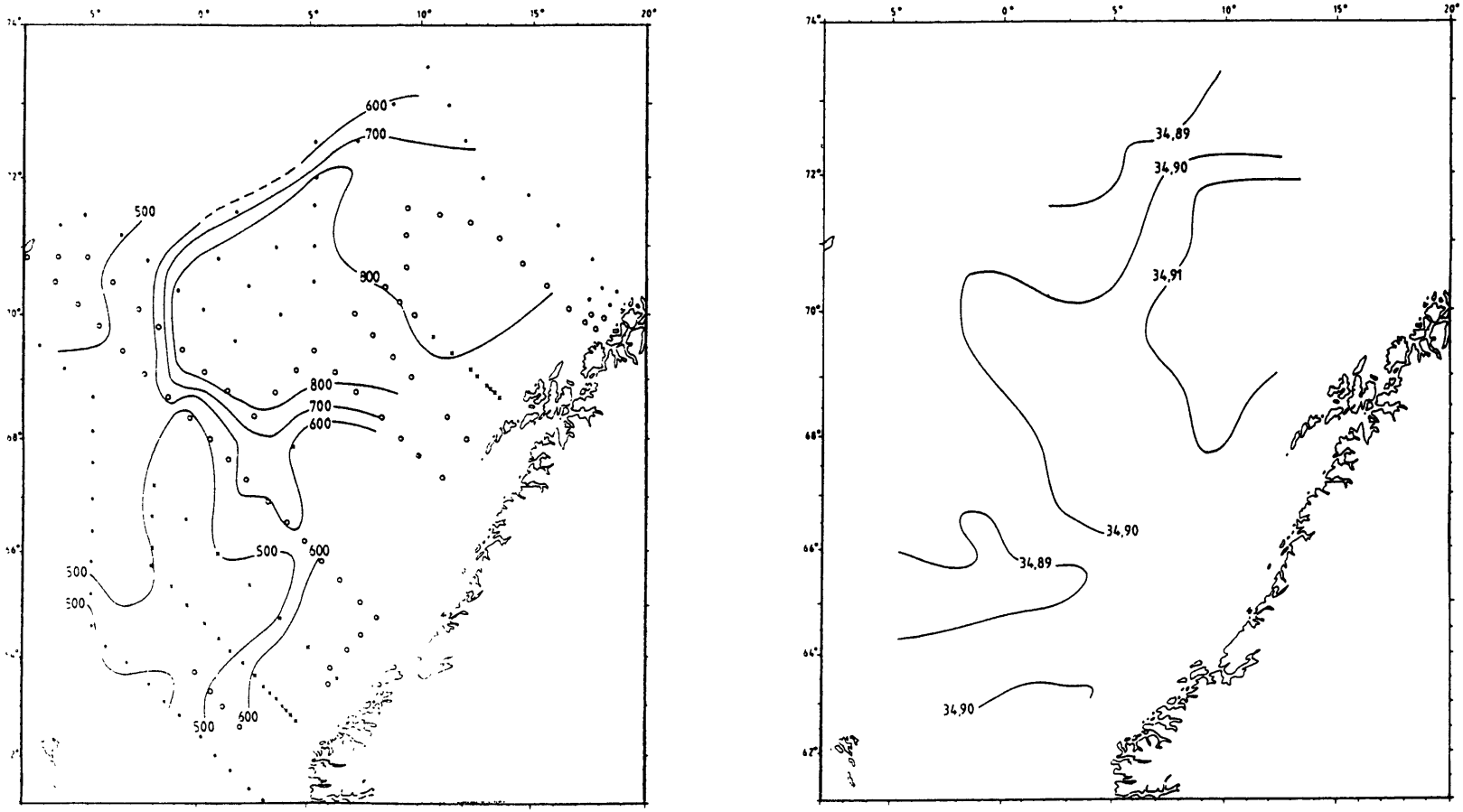

Fig. 2.17 Depth and value of minimum salinity in the AIW (from Blindheim, 1990)

of the Greenland Gyre (GSDW) to produce new NSDW (the NSDW is everywhere within the Nordic Seas overlaid by other water masses and hence has no direct contact with the atmosphere, so local production of NSDW is not possible). They suggested that the NSDW then entered the Norwegian Sea through the Jan Mayen Fracture Zone. Swift and Koltermann (1988), using current meter moorings, estimated this import of new NSDW to be 0.9 Sv. Smethie et al. (1988), using chlorofluoromethanes, found the import to be 0.8-0.93 Sv. They also deduced a net production of 0.5 Sv new GSDW, implying a 1:1 mixing ratio between AODW and GSDW.

4. Greenland Sea Deep Water: Although the exact mechanism for the formation of this water is still debated (see e.g. Clarke et. al. 1990), it is clear that it originates in the surface of the Greenland Sea. The GSDW is the coldest, densest, and freshest of the deep waters of the Nordic Seas and Arctic Ocean. The first assessment of the formation rate of this water was made by Carmack and Aagaard (1973). Using a summer minus winter volumetric census, they estimated that roughly 1 Sv was formed during the winter. The same order-of-magnitude production rate was found by Smethie et. al. (1988), as mentioned above.

5. Arctic Ocean Deep Water: Nansen (1906) observed higher temperatures and salinities in the Arctic Ocean than in the Norwegian / Greenland Seas. As he assumed that the deep waters of the Arctic Ocean were also of Greenland Sea origin, he went to great lengths to try to deduce that his salinity measurements in the Arctic Ocean were wrong (too high). He eventually accepted that the salinities were in fact correct, and that there thus could be no inflow of dense waters from the Greenland/Norwegian Seas into the Arctic Ocean through the Fram Strait. He hypothesized that there were a sill in the Fram Strait, preventing communication between the Nordic Seas and the Arctic Ocean. He then proceeded to address the question of the source of the dense waters in the Arctic

Ocean. Based on the assumption that the Arctic surface waters were very light due to river run-off and ice, he deduced that the formation of dense water in the Arctic Ocean had to occur in the Barents Sea and/or near Novaya Zemlya.

In the 1950's, Soviet bathymetric surveys revealed that instead of the presumed Nansen Sill a depression exists in the Fram Strait: the Lena Trough (e.g. Hopkins, 1988). Aagaard (1981) readdressed the question of the high salinities in the deep water in the Arctic, and suggested that the source of salt must either be the overlying Atlantic Water or production on the continental shelves. This view is modified by Aagaard et. al. (1985b) who conclude that the primary salt source is brine expulsion during freezing on the adjacent continental shelf seas.

2.4 Discussion

Fig. 2.19 synthesizes the current scheme for the sources of the overflow waters. The bulk of the overflow waters are intermediate waters formed in the Iceland Sea, together with (according to Aagaard et. al. 1985b) similar water from the Greenland Sea. The Norwegian Sea Deep Water is formed in a 1:1 ratio from GSDW and AODW. The upper layers of the NSDW comprises the densest overflows (in the Færø-Shetland Channel). The locations of water formation in this picture are: the shelves in the Arctic (brine rejection), the Greenland Gyre (open ocean convection), and the Iceland Sea (open ocean convection).

There are a few unclear aspects of the above scheme:

1. The surface conditions in the Iceland Sea can be highly variable, with ice in some years covering almost the entire area (fig. 2.20). It is reasonable to assume that this variability will affect the production of dense water, and yet there seems to be little variation in the flow of dense water through the Denmark Strait.

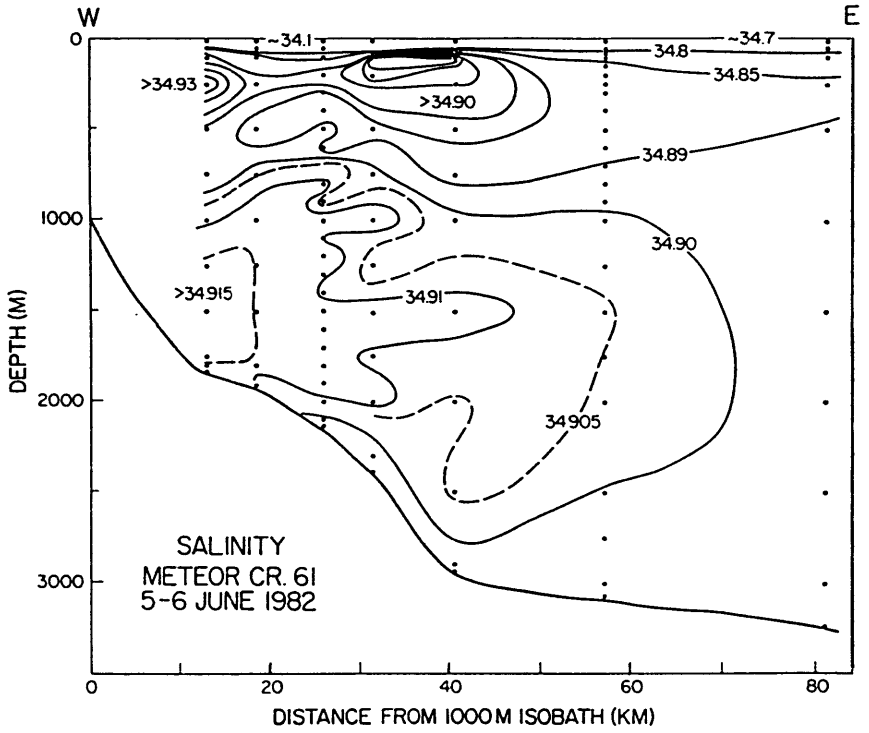

Fig. 2.18 Composite salinity section across the western Greenland Sea (from Aagaard et. al., 1985b)

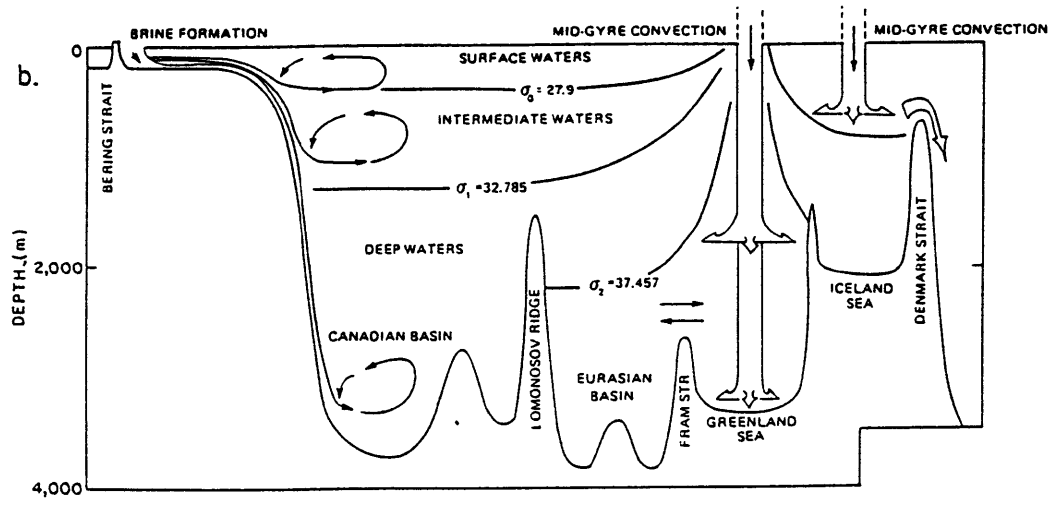

Fig. 2.19 Synthesis of current scenario (from Aagaard et. al., 1985b)

Fig. 2.20 Distribution of drift ice in Icelandic Waters in 1950-1971 (from Malmberg, 1972).

2. Recent observations suggest that during the 1980's the production of dense water in the Greenland Sea is much reduced (Clarke et. al. 1990, Rhein, 1991). Schlosser et. al. (1991) used a tracer box-model to suggest that the production was as low as 0.1 Sv for the 1980's. Yet the outflows even in the deep Færø-Shetland Channel remained 0(1 Sv) during these years (Saunders, 1990).

3. One might expect that the production of dense water during winter in the Nordic Seas forces the dense waters to spill over the ridges in larger volumes during the winter season than during the summer season. Yet no such seasonal signal is found in the Deep Western Boundary Current of the North Atlantic (Dickson et. al., 1990), and not near the sills themselves (Aagaard and Malmberg, 1978, Saunders, 1990). In particular, two volumetric censuses, one for the Greenland Sea (Carmack and Aagaard, 1973), and one for the Iceland Sea (Swift and Aagaard, 1981) find increased amounts of dense water between summer and winter surveys, and equate these amounts to net production of dense water during winter. Assuming that these seas stay in a relatively steady state from year to year the dense water needs to be removed from the area before the onset of summer to avoid getting warmed up to the summer situation of the year before. Such removal implies imposing a seasonal signal on the circulation.

It seems appropriate, therefore, at this point to take a fresh look at the circulation in the Arctic Ocean and the Nordic Seas with special emphasis on the watermasses and their pathways. The primary question is: How is a steady, substantial (O(several Sverdrups)) source of dense waters for the overflows to the North Atlantic maintained?

Chapter 3

Construction of the Circulation Scheme

3.1 Analysis of the Primary Data Set

The data set to be analyzed in this work was collected during eleven different cruises in the 1980's (table 3.1). A key advantage of using these modern data is that they provide greater accuracy in the salinity measurements. The primary data set consists of roughly 800 hydrographic stations, with temperature, salinity, oxygen and nutrients. The majority of the stations were collected between 70 N and 80 N in the Greenland Sea, the Lofoten Basin and the Fram Strait. This extensive data set will be referred to as the primary data set. The cruise tracks are shown in fig. 3.1. In addition, references will be made to older hydrographic data (especially in the areas where the primary data set gives little coverage) and also to numerous current meter observations made in the region.

In constructing a circulation scheme exact definitions of water masses, in terms of their temperature and salinity properties are avoided as much as possible. Such definitions are normally intended to categorize the water present in the volume of water under consideration, and each name is intended to indicate the source of that particular water mass. But such definitions of water masses can confuse the analysis, for several reasons: First of all, waters found in two separate locations with the same TS characteristics need not have the same source. To show that the water flows from one location to the other one needs to identify the connection. Secondly, as the Nordic Seas/Arctic Ocean is an area of intense water mass formation there is a close connection between the upper and the lower water masses. Therefore the variations in temperature and salinity within the domain are unusually small, compared to other parts of the World

Table 3.1 The cruises of the primary data set.

Research Vessel	Dates	Abbr.	no.stations	variables
Ymer	July-August 1980	Y80	38	T,S,O,Si,Ph,No
Knorr (TTO/NAS)	July-August 1981	TTO81	31	T,S,O,Si,Ph,No
Hudson	2/28-4/6 1982	H82	129	T,S,O,Si,Ph,No
Bjarni Sæmundsson	February 1982	BS82	34	T,S,O,Si,Ph,No
Meteor	5/19-7/6 1982	M82	115	T,S,O,Si,Ph,No
Polarstern	7/19-8/7 1984	P84	169	T,S,O,Si,Ph,No
Meteor	6/14-8/16 1985	M85	143	T,S,O,Si,Ph,No
Polarstern	6/8-7/3 1988	P88	64	T,S,O
Valdivia	6/1-6/17 1988	V88	50	T,S,O
Polarstern	5/18-6/6 1989	P89	34	T,S,O
Håkon Mosby	6/26-7/5 1989	M89	30	T,S,O

a) Ymer 1980

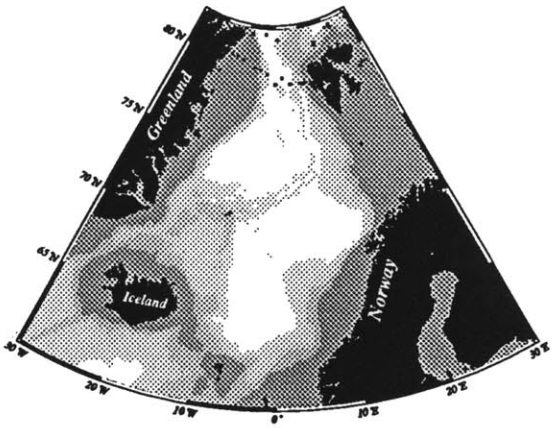

b) Knorr 1981

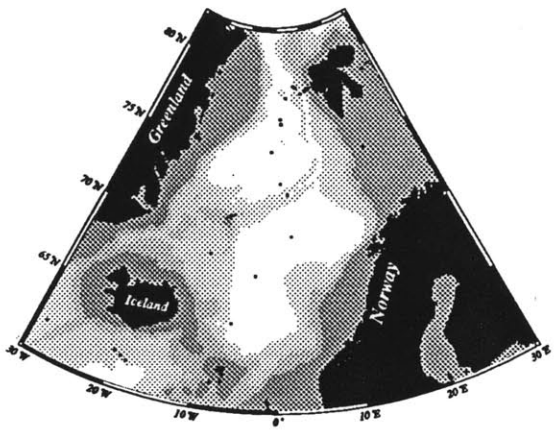

c) Hudson 1982

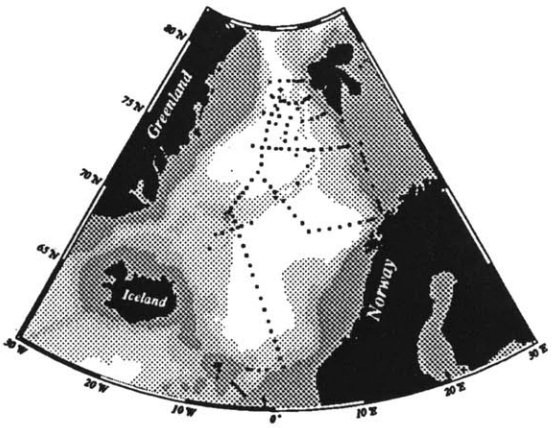

d) Bjarni Sœmundsson 1982

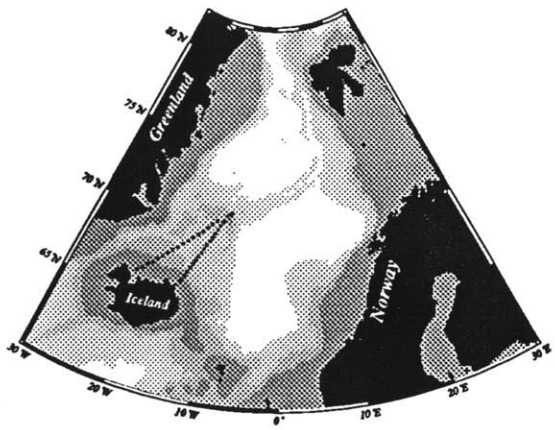

e) Meteor 1982

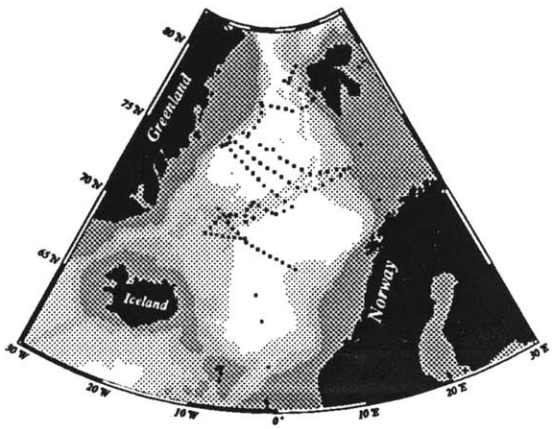

Fig. 3.1 Cruise tracks for the 11 cruises constituting the primary data set.

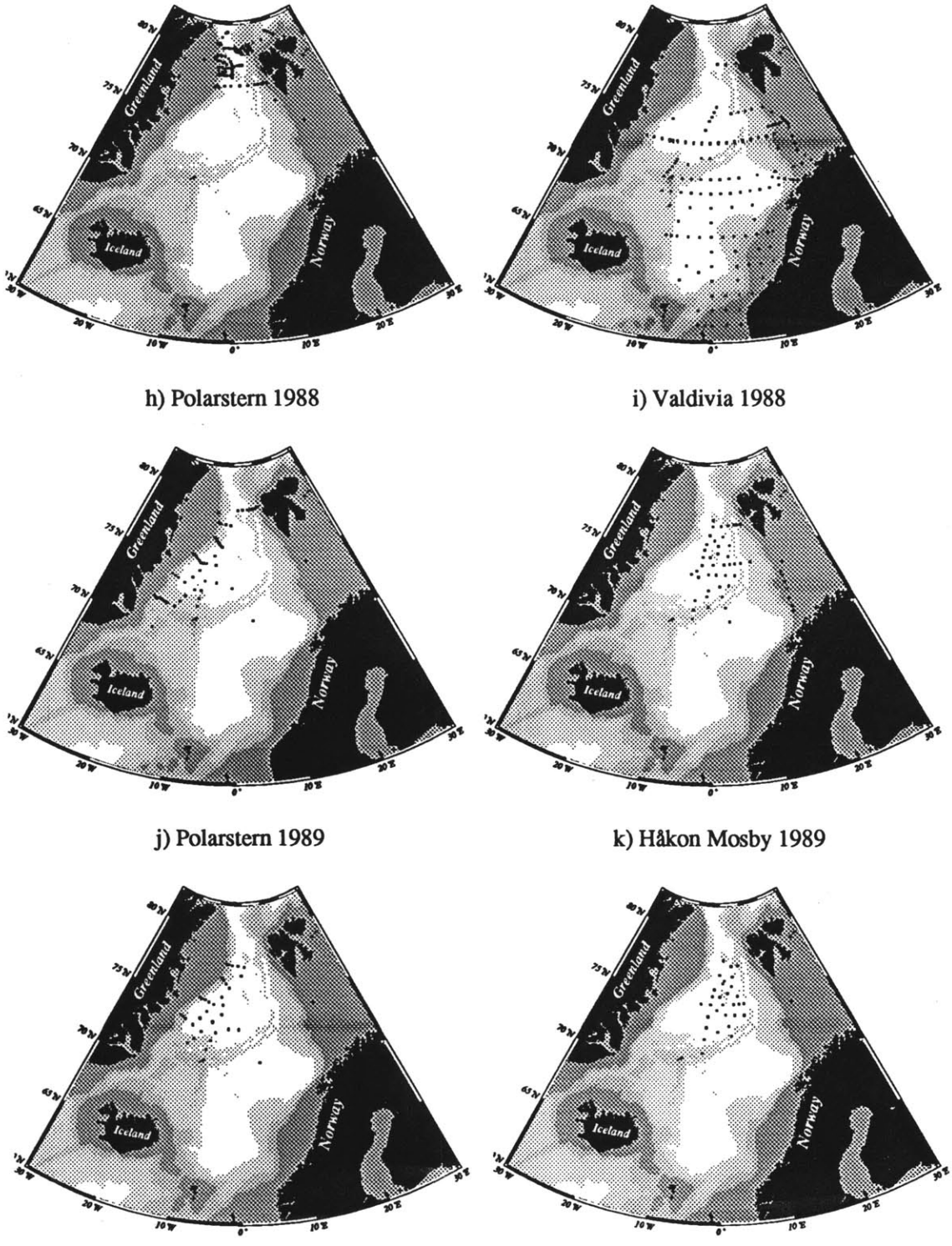

Fig. 3.1 cont. Cruise tracks for the 11 cruises constituting the primary data set.

Ocean, making it hard to differentiate water masses. Thirdly, waters from the same source need not have the same TS characteristics year after year. This type of interannual variability is a prominent feature of the water masses in the Nordic Seas. For example, Atlantic Water in the Nordic Seas is often defined as water with potential temperature higher than 3 ^{0}C. In some years there is no water with this characteristic in the Fram Strait. Based upon this observation one should not conclude that in this year the Atlantic Water took a different path, but rather that in this year the Atlantic Water was somewhat colder.

Instead, the water mass definitions are based on persistent extrema in the hydrographic profiles. For example, the Atlantic Water is always associated with a maximum in temperature and salinity. Similar extrema, or cores, that are found year after year in the same density range in different data sets are said to indicate"horizontal" advection, following Wüst (1935). Although the actual core value at each location may be hard to interpret, due to imperfect data resolution, interannual variability, or calibration biases, the existence of a core does imply circulation; if there were no advective supply the core would vanish, by diffusion. Note that basing the circulation on the existence of cores imposes an upper limit on how well one can resolve the circulation: if there are only two cores, one can identify only two paths of water masses.

3.1.1 Identification of Cores

The salinity and oxygen fields exhibit several extrema that are seen in all the data sets and that therefore are persistent from year to year. The temperature and nutrient fields tend to not have similar extrema. Rather, the temperature profiles decrease monotonically with depth, at least beneath the upper 500 m. The reason is that density is primarily a function of temperature at higher pressures in this region. One, therefore, tends to find increasingly colder water with depth. Likewise, the nutrient profiles tend to

increase monotonically with depth. The reason for this is that in the surface layer (the euphotic zone) the plankton deplete the nutrients. As the plankton sink below the euphotic zone nutrients are released, thus increasing the nutrient concentration with depth.

So it is primarily in the salinity and oxygen fields that one can identify pathways of circulation. There are four cores that appear in all the data sets and therefore can be considered robust:

Cores:	**Identified by:**
Atlantic Water (AW)	maximum in temperature and salinity.
(return Atlantic Water (rAtW), see item 3 below)	
Polar Water (PW)	minimum in salinity.
Intermediate Water (IW)	minimum in salinity and maximum in oxygen.
Deep Water (DW)	maximum in salinity and minimum in oxygen.

The presence of the different water masses is limited geographically. In all the data sets one can differentiate between three geographical regimes where different water masses are found (fig. 3.2a):

1. The Greenland Gyre Domain, limited to the abyssal plain between the Mohn/ Knipovich Ridge, the Greenland Fracture Zone, the continental slope of Greenland, and the Jan Mayen Fracture Zone, and also the southern Boreas Basin. Here only the Deep Water core is found.
2. The Atlantic Domain, limited to the Norwegian Sea, east of the Mohn/ Knipovich Ridge , and the northern part of the Boreas Basin. Here the Atlantic Water, the Intermediate Water and the Deep Water cores are found.

Distribution of Watermasses

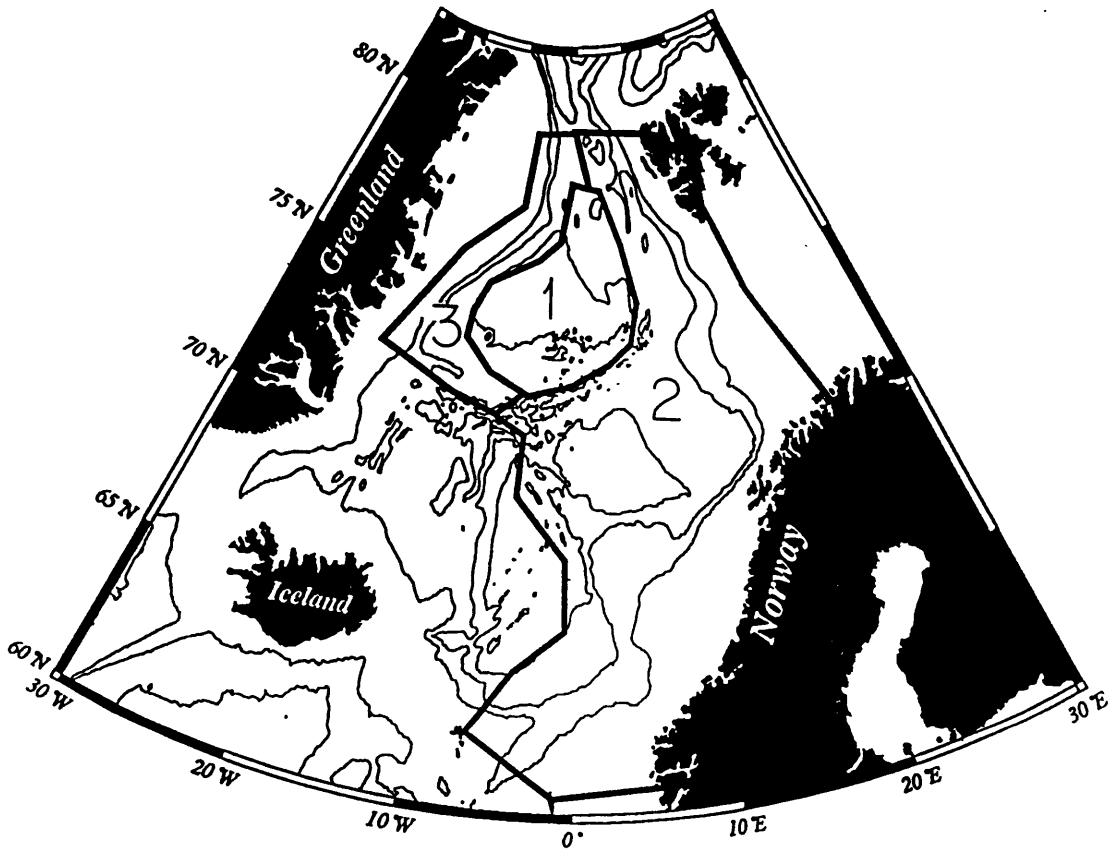

Fig. 3.2a Schematic of the geographical distribution of watermasses

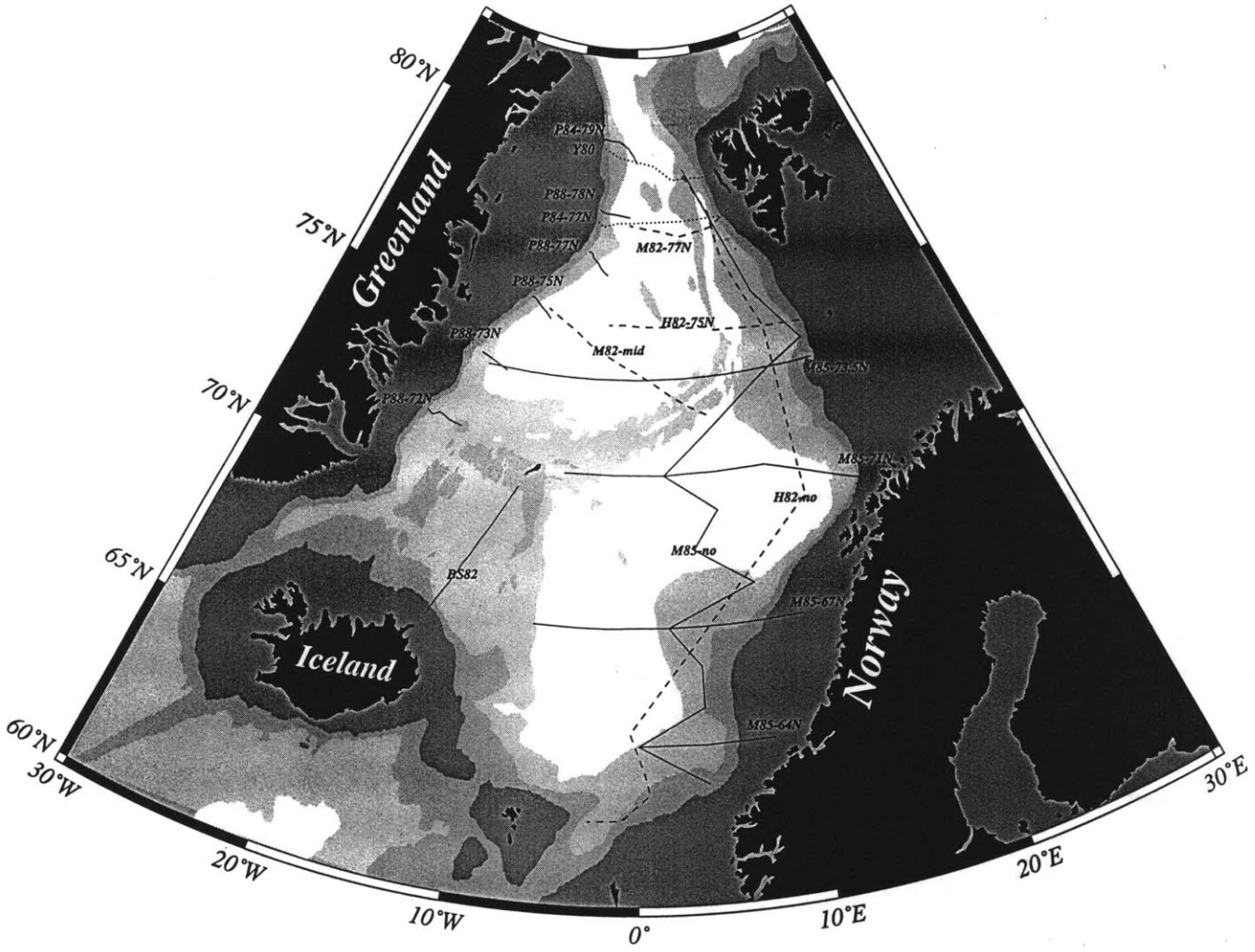

Fig. 3.2b Cruise tracks for the sections discussed in the text

3. The Greenland Continental Slope. Here the Polar Water, the Atlantic Water (which for practical reasons will be called return Atlantic Water when found along the coast of Greenland), the Intermediate Water and the Deep Water cores are found.

3.1.2 Description of Water Masses

The different water masses, and the geographical regimes, will be described next. The starting point is the Atlantic Water entering the Norwegian Sea. The cruise tracks of the sections to be described in the text are shown in fig. 3.2b.

1. Atlantic Water: This is a surface water mass, associated with a temperature and salinity maximum. Typically the salinity is higher than 35.0, the temperature higher than 3 ^{0}C, and the potential density is in the range 27.4 to 27.8. The Atlantic Water enters the Norwegian Sea across the Iceland-Scotland Ridge. A schematic of the flow pattern of the Atlantic Water is shown in fig. 3.3. In the Norwegian Basin the core of the Atlantic Water follows the eastern slope of the basin, as seen at 64 N (fig. 3.4). The layer is around 500-600 m thick in this basin. At 67 N the Atlantic Water has reached the Vøring Plateau, the extension of which marks the division between the Norwegian Basin and the Lofoten Basin. The Atlantic Water is steered westward by topography here (fig. 3.5), and as it enters the Lofoten Basin the Atlantic Water not only fills a larger portion of the water column (up to 900 m in 1985), but also fills the entire area of the basin (fig. 3.6), indicating that the water takes less of a straight path, but rather recirculates in the Lofoten Basin. The Mohn/ Knipovich Ridge limits the westward extension of the Atlantic Water.

Further north, a branch of the Atlantic Water enters the Barents Sea north of Norway (fig. 3.7) , whereas the rest flows northward in the Deep Eastern Basin

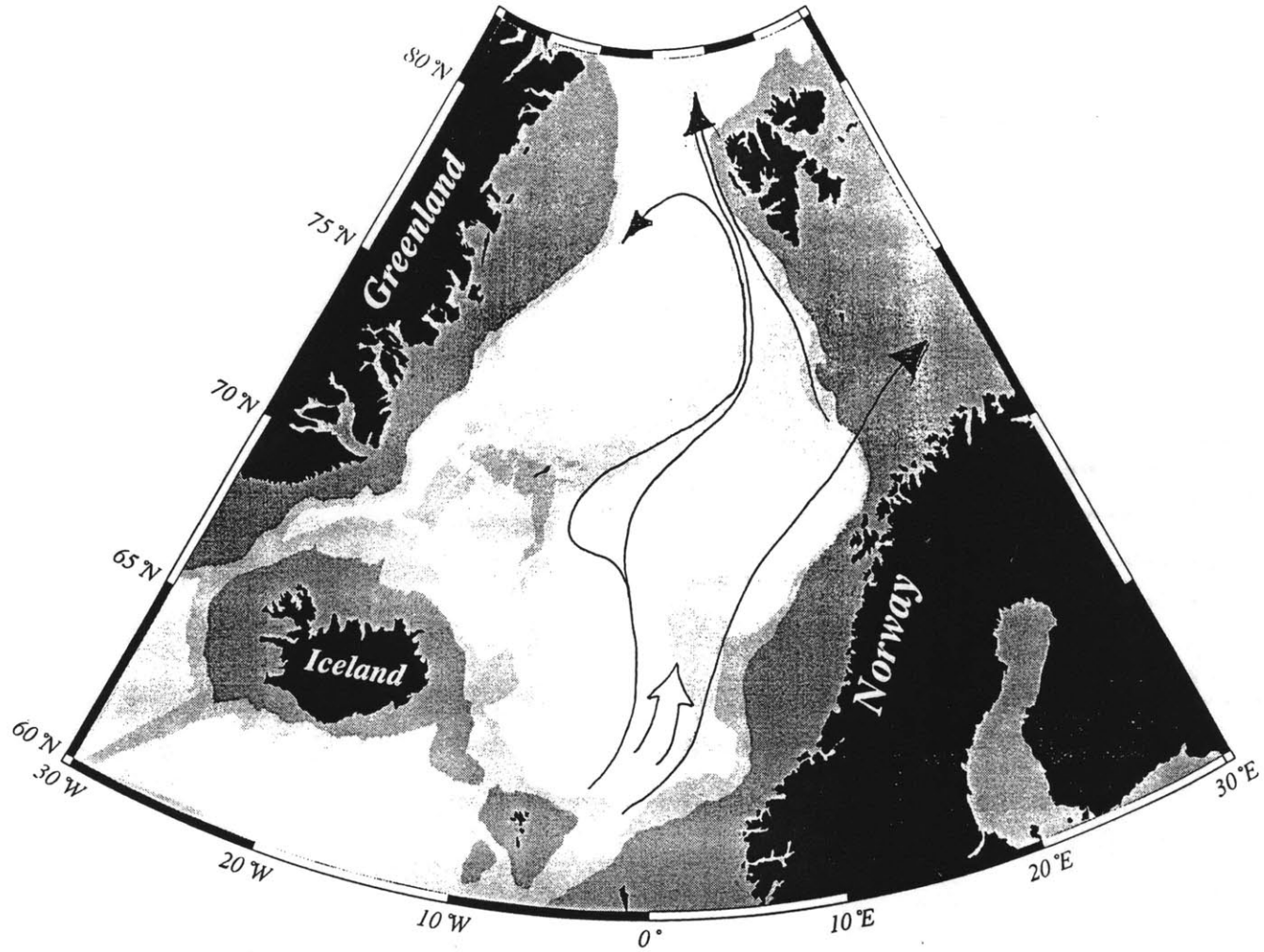

Fig. 3.3 Schematic of flow of Atlantic Water.

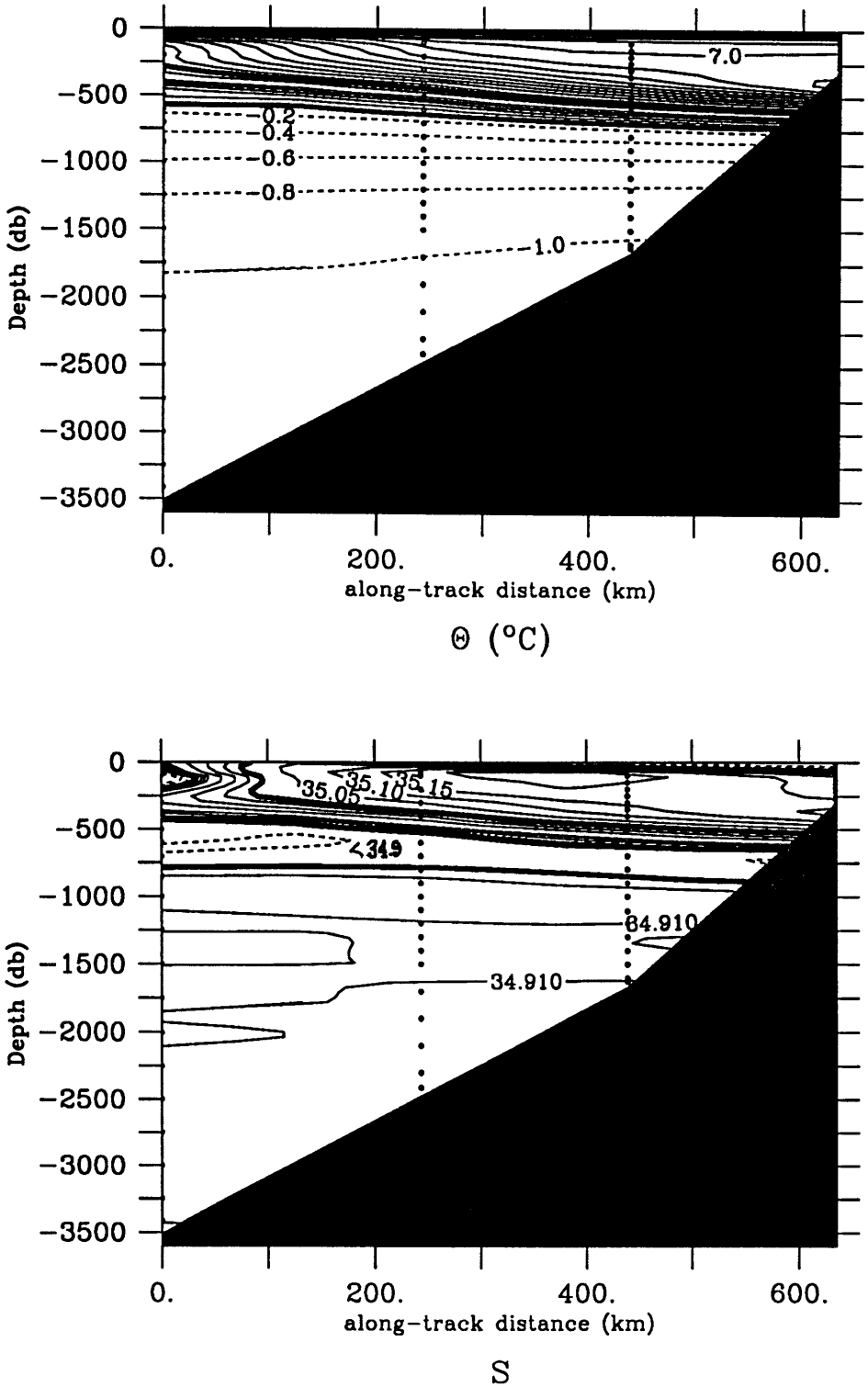

Fig. 3.4 Temperature and salinity section at 64 N. Meteor 1985 transect. Cruise track is shown in fig. 3.2b (M85-64).

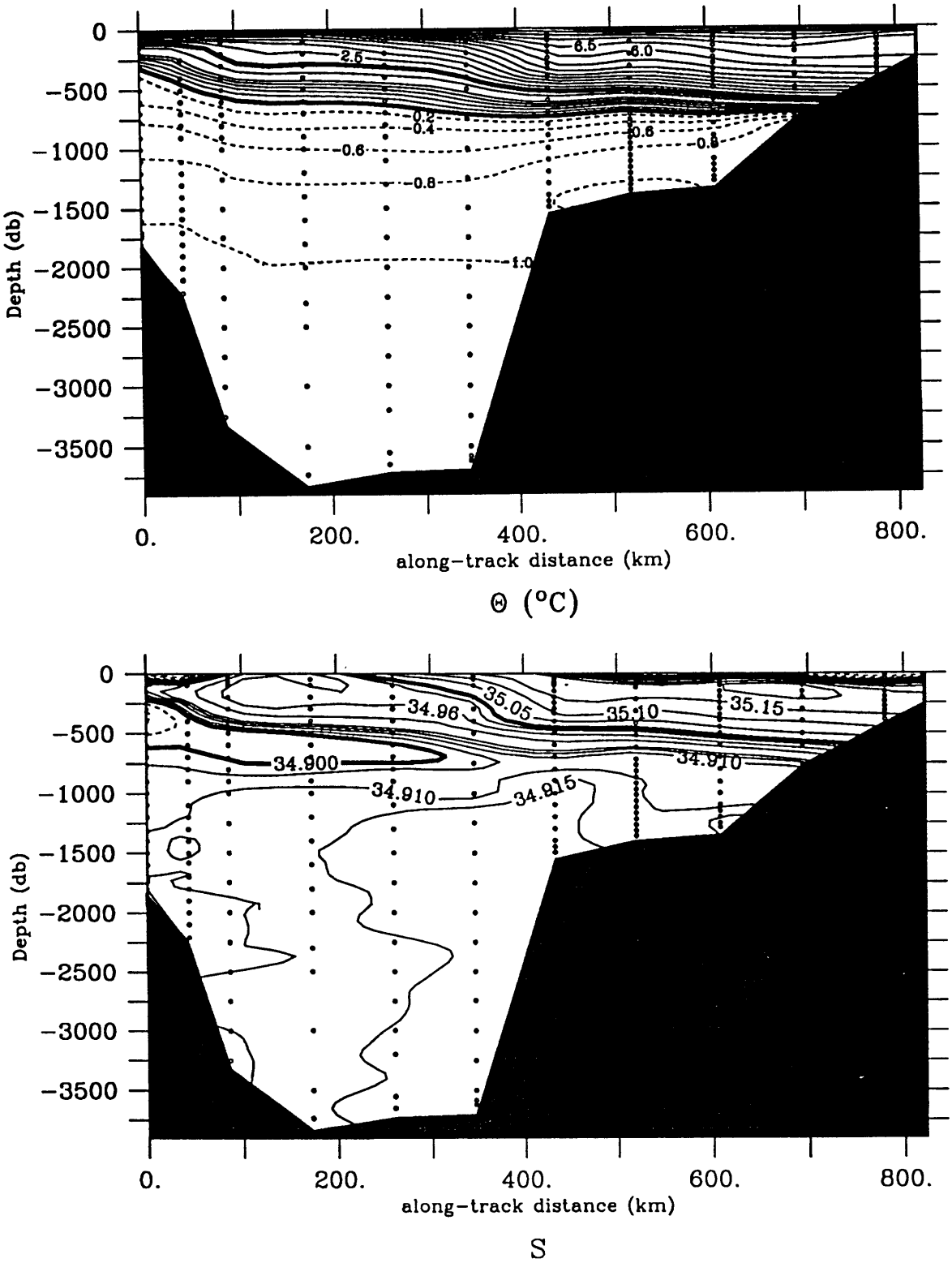

Fig. 3.5 Temperature and salinity section at 67 N. Meteor 1985 transect. Cruise track is shown in fig. 3.2b (M85-67).

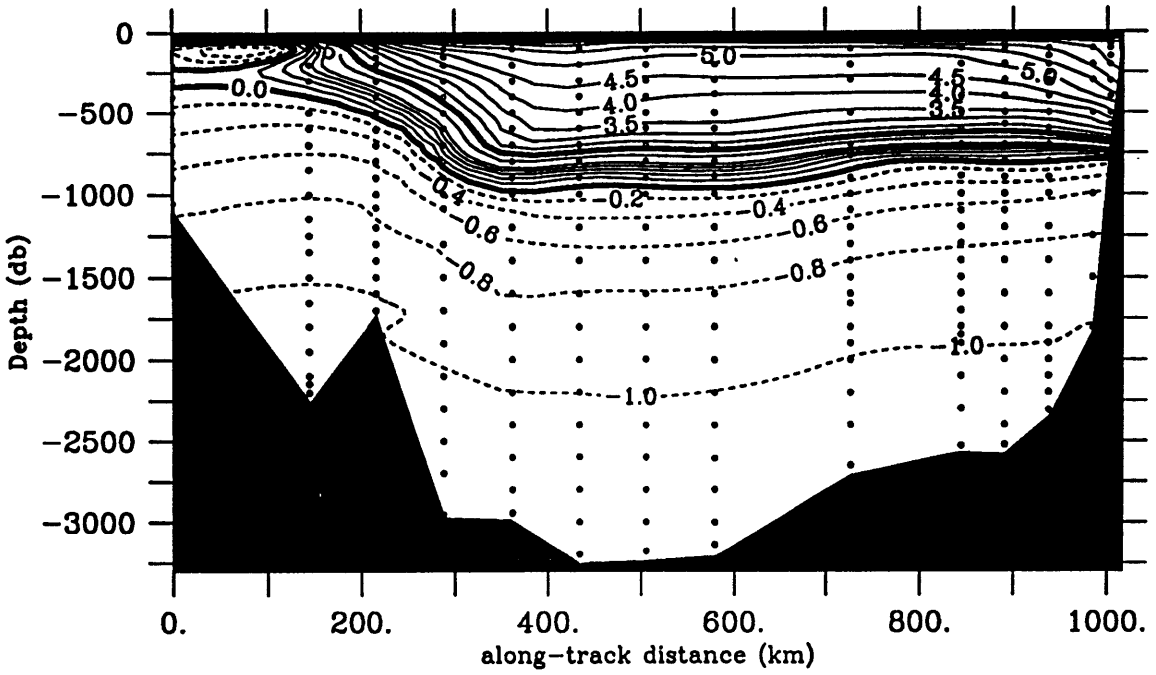

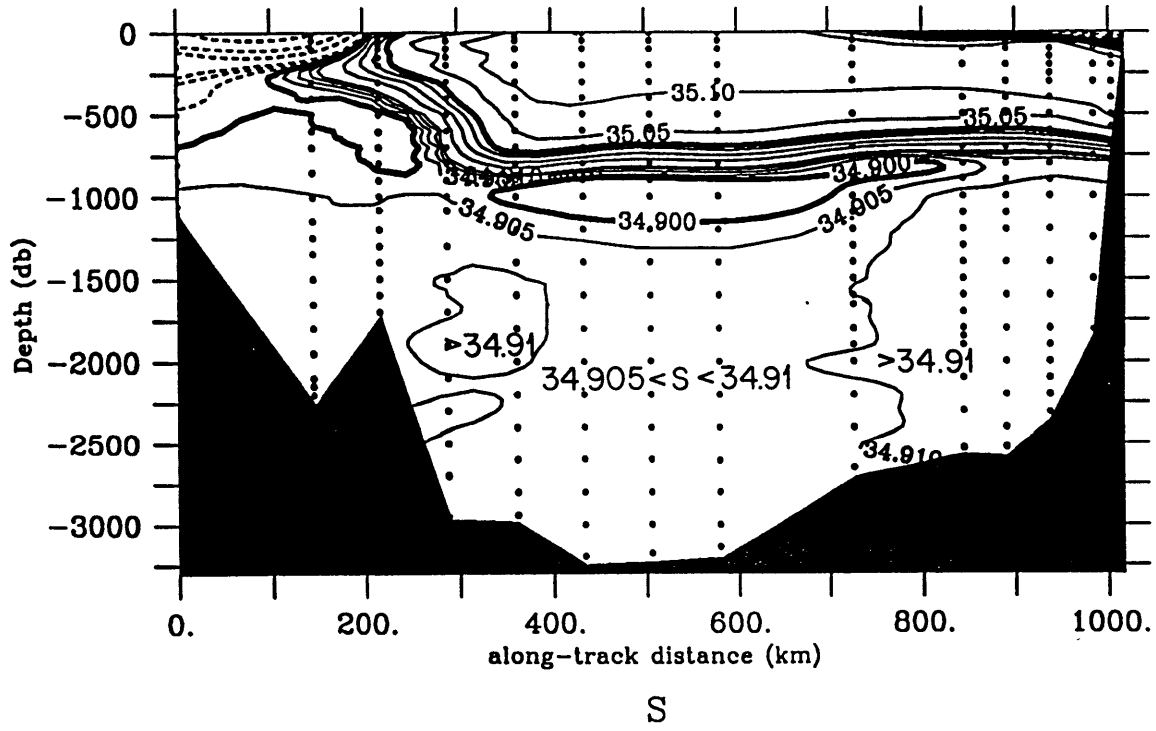

Fig. 3.6 Temperature and salinity section at 71 N. Meteor 1985 transect. Cruise track is shown in fig. 3.2b (M85-71).

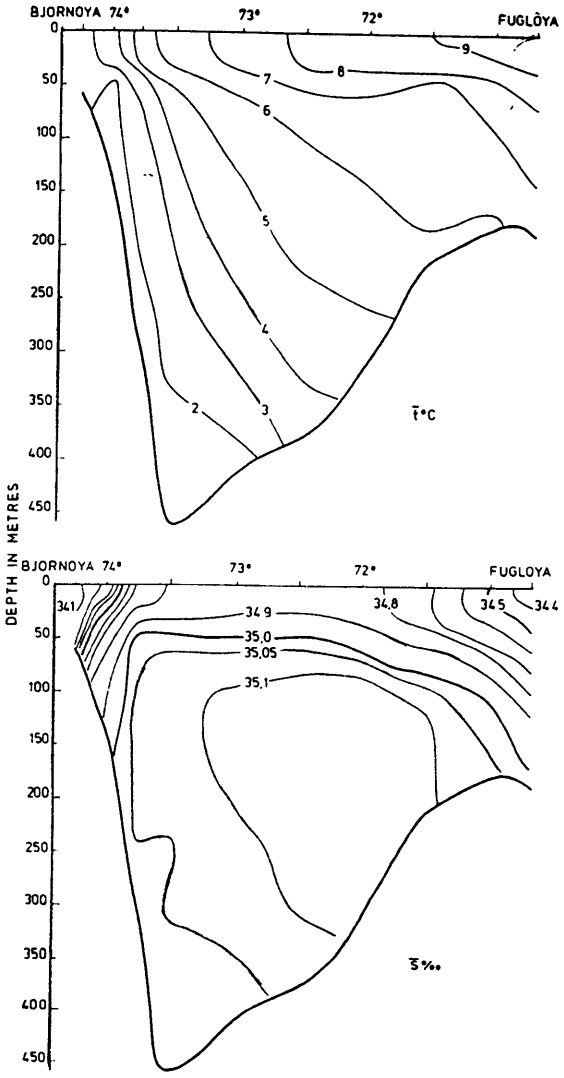

Fig. 3.7 Mean values (1953-1979) of temperature and salinity in the Barents Sea opening (Blindheim et. al., 1981).

towards the Fram Strait, as seen in fig. 3.8, a section at 77.7 N from the Polarstern 1984 cruise. Approaching the Fram Strait the Atlantic Water partly recirculates, as can be seen in fig. 3.8, where a second core of warm and salty water is found on the western end of the section.

The remaining Atlantic Water enters the Arctic Ocean in the swift West Spitsbergen Current, and subducts beneath the Polar Water (fig. 3.9). Recirculation is occurring also in these sections, and probably also further north along the narrow Strait.

2. *Greenland Continental Slope:* The most complex water mass structure is found along the slope of Greenland, where Polar Water, return Atlantic Water, Intermediate Water and Deep Water are present. This region is typically ice-covered year-round, and not many cruises have ventured this far west. The Polarstern 1988 and 1989 cruises were designed to study this area. Consider the five sections from the Polarstern 88 cruise, crossing the slope at 78 N, 77 N, 75.5 N, 73.5 N, and 72 N (fig. 3.10). The cores (which are labelled in fig. 3.10a, and will be discussed below) are found over the slope. To the east, on the abyssal plains, the Greenland Gyre Domain is found. The array of current meters at 75 N showed that on the slope there is a systematic southward flow along the isobaths, whereas on the abyssal plains there is no preferred direction in the velocity field (fig. 3.11). The concentration of cores over the slope, and the current meter observations, collectively suggests that on the Greenland Continental Slope there is a narrow boundary current, and that even the lower layers are moving with considerable speed.

3. *Polar Water:* This water originates in the Arctic Ocean, where large river runoff and ice melt give it a low salinity, typically $S < 34.5$. It is found in a 100-200 m thick surface layer most everywhere in the Arctic, and is assumed to exit the Arctic Ocean

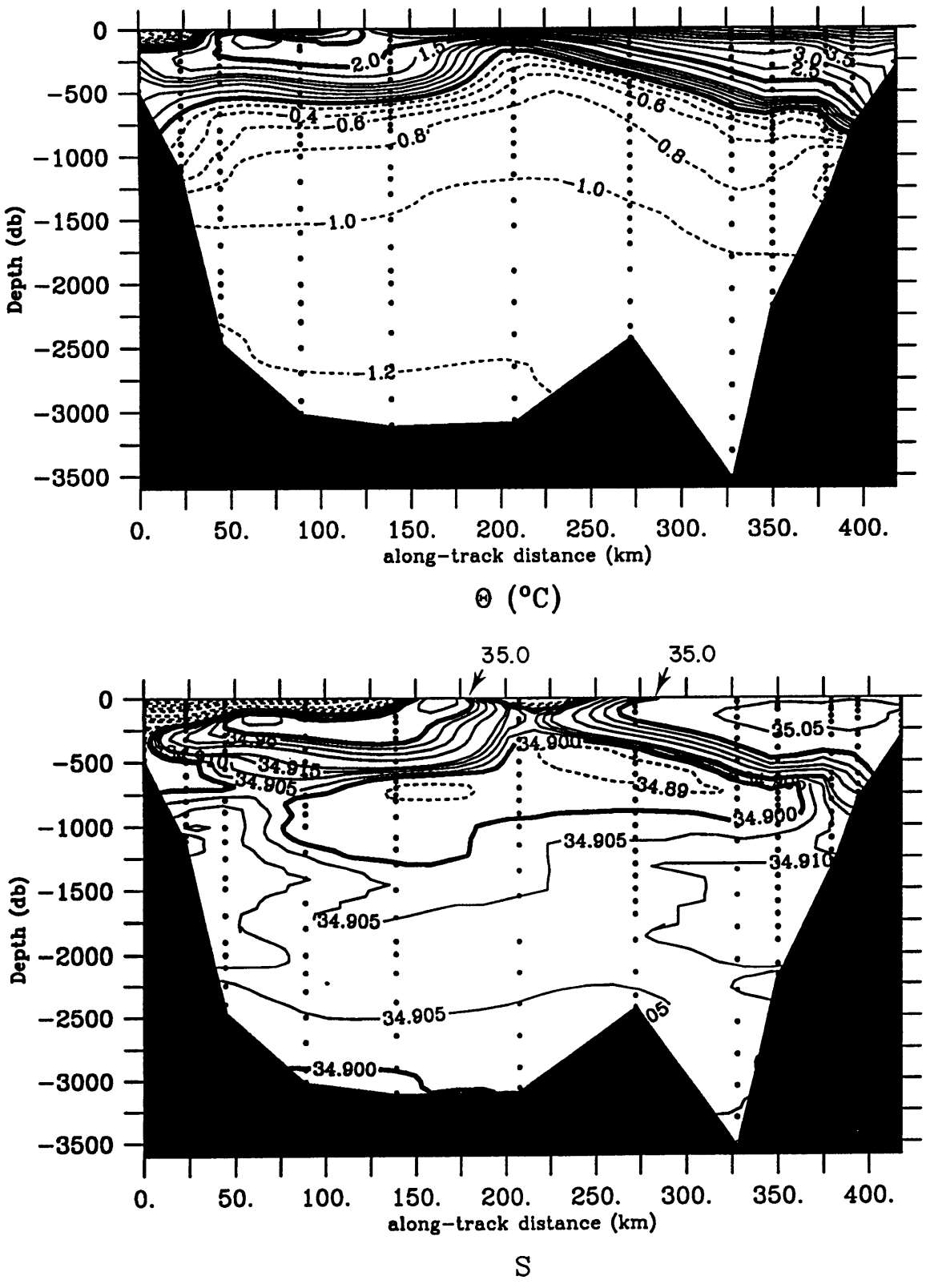

Fig. 3.8 Temperature and salinity at 77.7 N. Polarstern summer 1984 transect. Cruise track is shown in fig. 3.2b (P84-77).

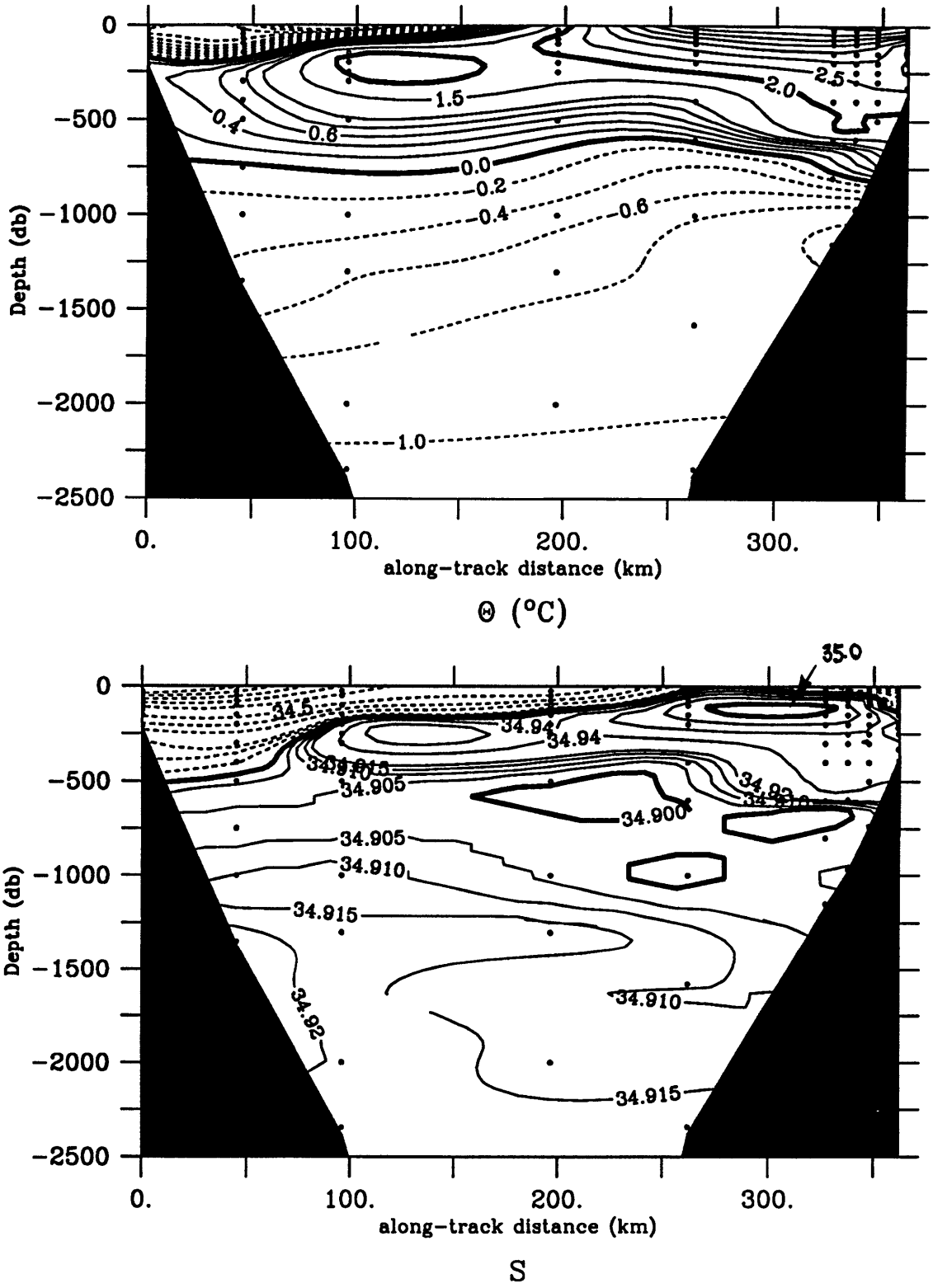

Fig. 3.9 Temperature and salinity in the Fram Strait. Ymer 1980 transect. Cruise track is shown in fig. 3.2b (Y80).

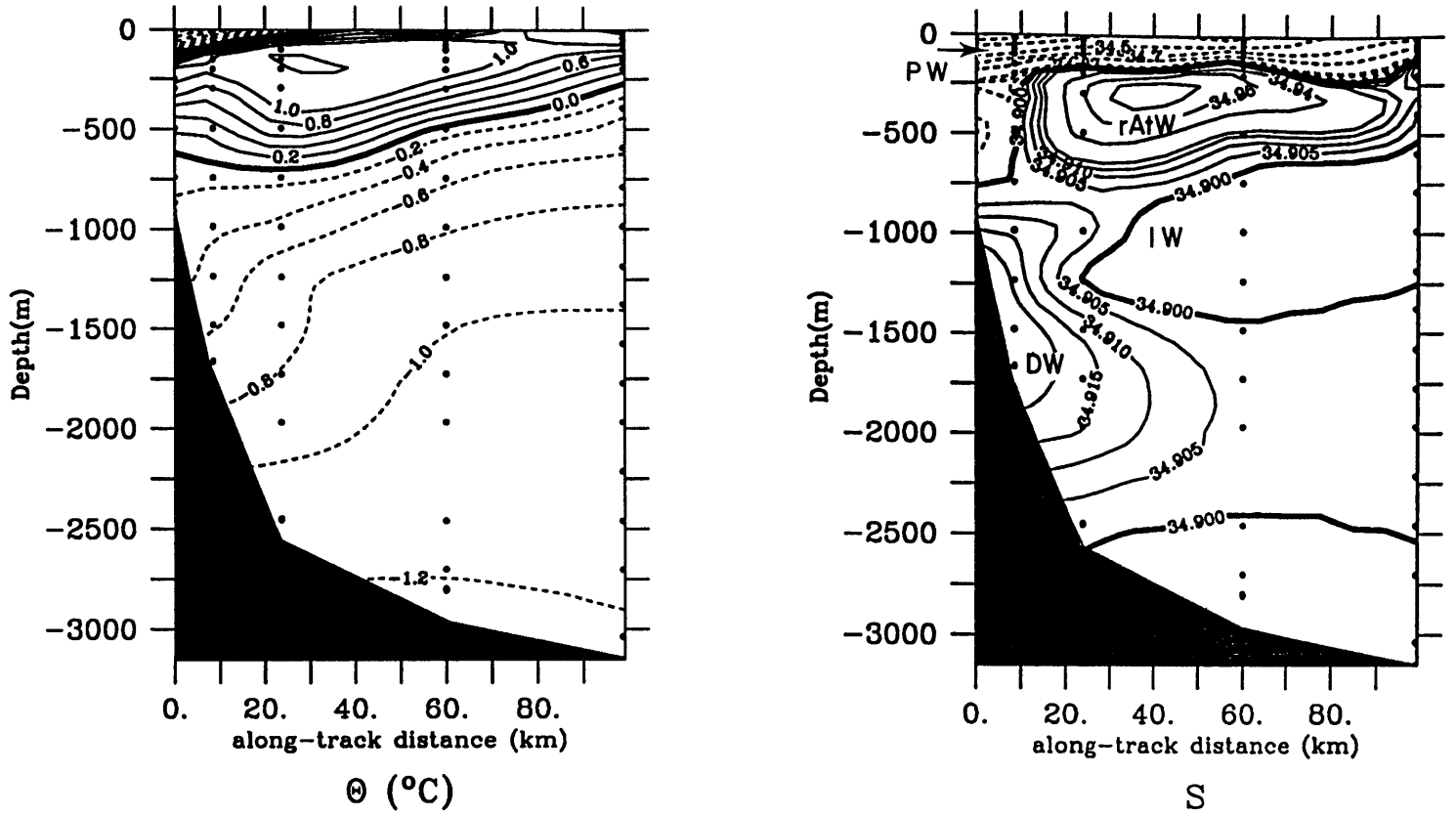

Fig. 3.10a Temperature and salinity across the Greenland Slope at 78 N. Polarstern 1988 transect. Cruise track is shown in fig. 3.2b (P88-78)

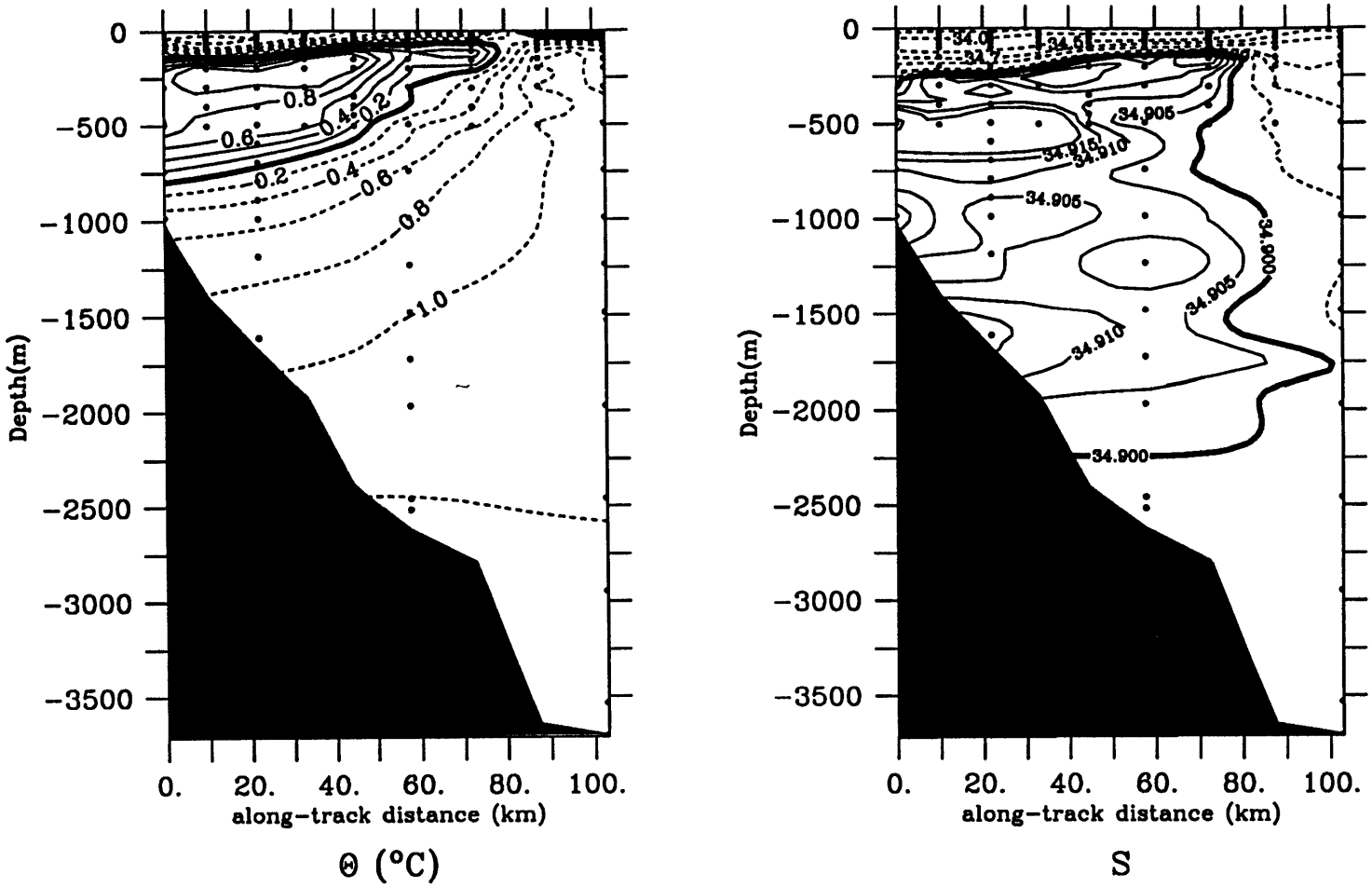

Fig. 3.10b Temperature and salinity across the Greenland Slope at 77 N. Polarstern 1988 transect. Cruise track is shown in fig. 3.2b (P88-77)

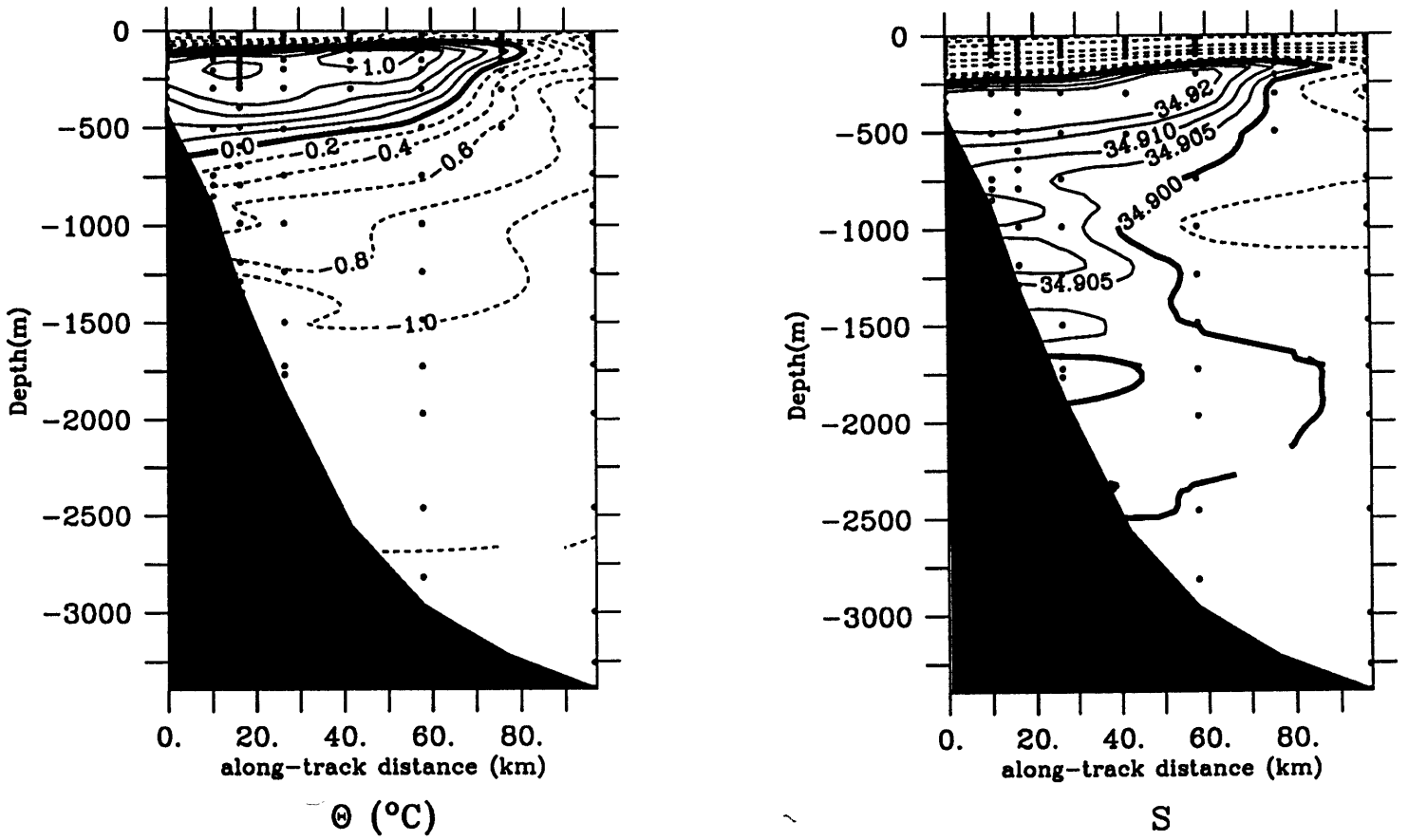

Fig. 3.10c Temperature and salinity across the Greenland Slope at 75.5 N. Polarstern 1988 transect. Cruise track is shown in fig. 3.2b (P88-75)

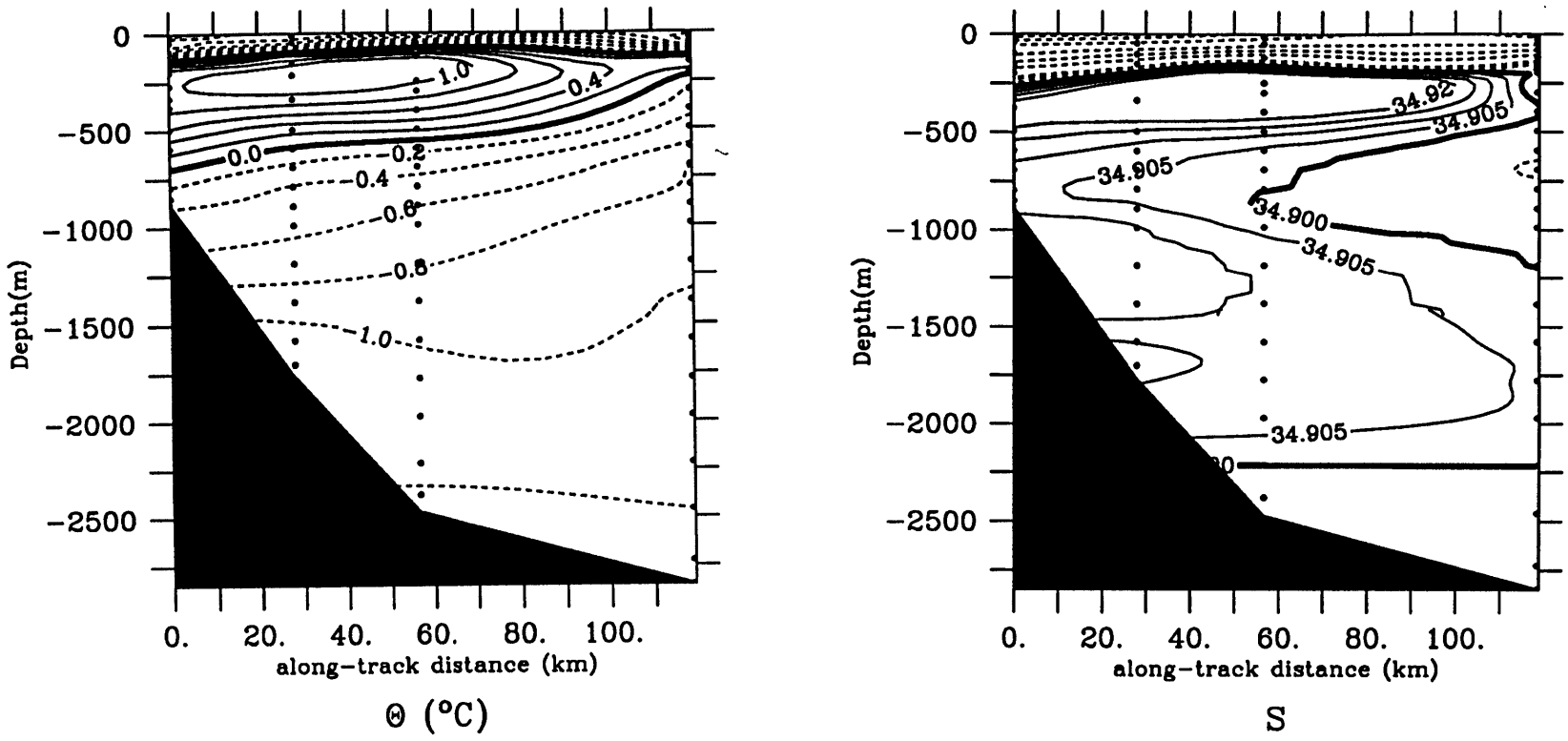

Fig 3.10d Temperature and salinity across the Greenland Slope at 73.5 N. Polarstern 1988 transect. Cruise track is shown in fig. 3.2b (P88-73)

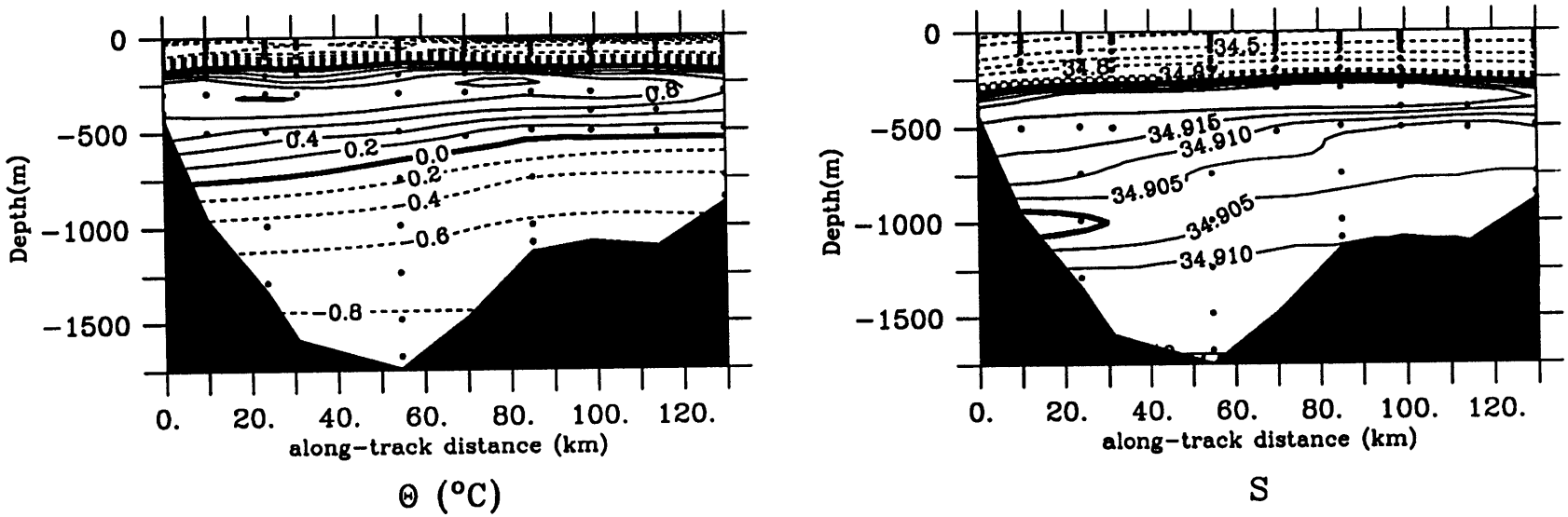

Fig. 3.10e Temperature and salinity across the Greenland Slope at 72 N. Polarstern 1988 transect. Cruise track is shown in fig. 3.2b (P88-72)

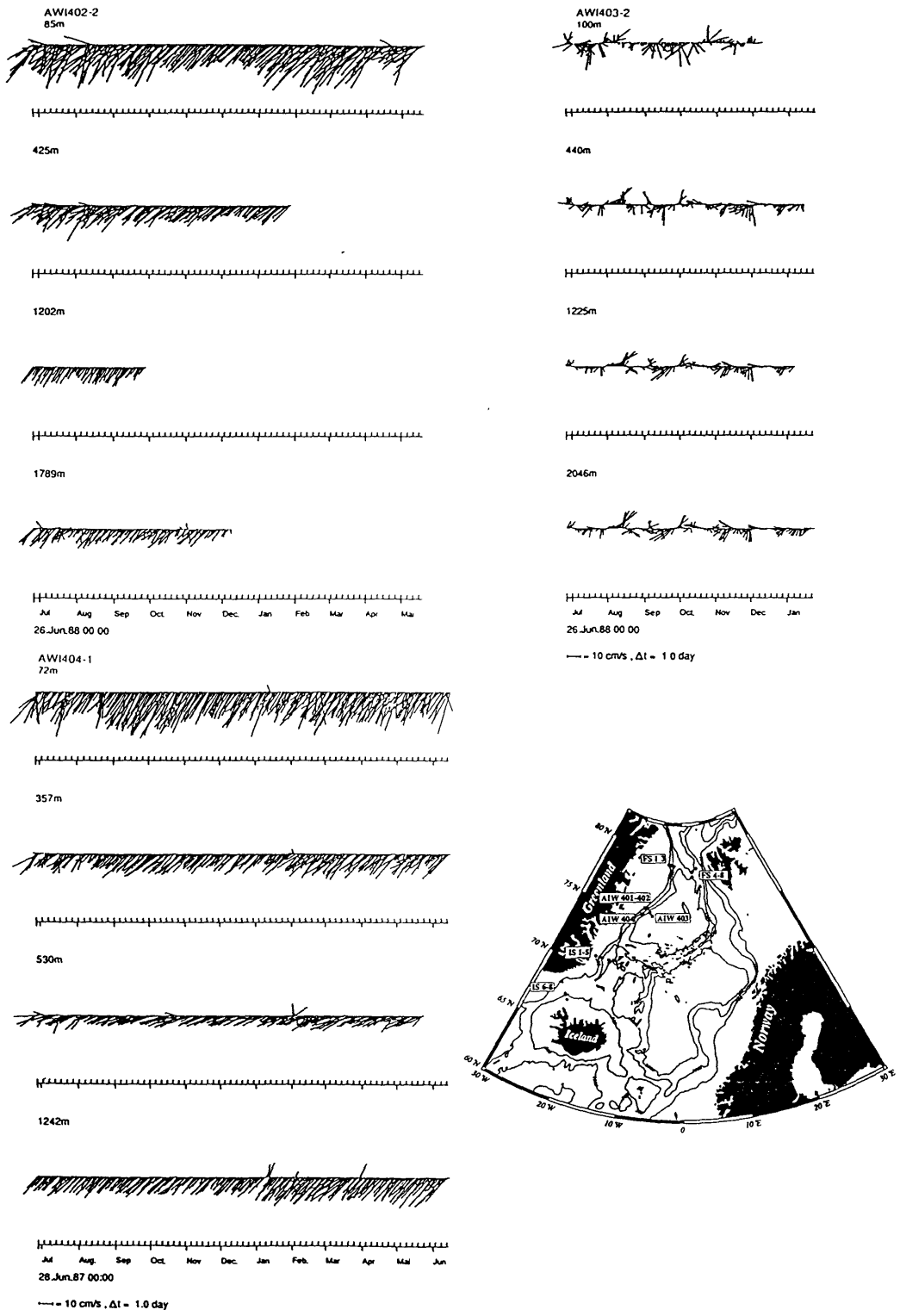

Fig. 3.11 Current meter array at 75 N (from Sellmann et. al. 1992). Moorings 402 and 404 are positioned on the slope, no. 403 on the abyssal plain.

in the same manner as the ice: following the path of the Transpolar drift (anticyclonically). The water is found in the upper 50-100 m all along the coast of Greenland (see fig. 3.10), associated with high oxygen , and potential density typically less than 27.8.

4. *Return Atlantic Water:* The return Atlantic Water flows southwards, associated with a temperature and salinity maximum at intermediate depth, and is found all along the coast of Greenland (see fig. 3.10). Near 73 N, in the southwestern corner of the Greenland Sea, part of the rAtW continues eastward.

5. *Intermediate Water* With a salinity just below 34.9, and potential temperature around 0 ^{0}C, this water is similar to the Arctic Intermediate Water found by Helland-Hansen and Nansen (1909) and Blindheim (1986) in the southern Norwegian Sea, as discussed in chapter 2. In the primary data set this layer is found along the Greenland Continental Slope beneath the return Atlantic Water, typically at 500-800 m (fig. 3.10), associated with a salinity minimum and an oxygen maximum, suggesting fairly recent contact with the atmosphere. This layer is found not only on the Greenland continental slope, but everywhere around the Greenland Gyre, although it is not always associated with an oxygen maximum. In the Norwegian Sea it is found beneath the Atlantic Water (fig. 3.6) as a very thin layer, usually around 100 m. The Intermediate Water is completely unmappable; low salinities are found as isolated "islands" in the middle of the basins, and some of the lowest salinities are found in the Deep Eastern Basin, far from any potential source.

6. *Deep Water:* This layer is found beneath the Intermediate Water all along the Greenland Continental Slope, represented by a salinity maximum and an oxygen minimum (fig. 3.10). The salinity is typically 34.91. This is the core that Aagaard

et. al. (1985b) suggested represents an outflow of water from the Arctic in the western Fram Strait, as discussed in chapter 2. The Deep Water is the only core that is found everywhere within the domain of this study. It is more mappable than the Intermediate Water, in the sense that within the Greenland Gyre the salinities are always less than 34.9, whereas outside the gyre the values are always above 34.9, indicating that the Deep Water intrudes into the Greenland Gyre from the sides. There are variations from year to year, but the highest values certainly seem to be found near the western Fram Strait, supporting the idea of a source there (fig. 3.9).

A schematic of the flow of Deep Water is shown in fig. 3.12. The core values are well maintained along the path around the Greenland Gyre towards the Jan Mayen Fracture Zone. It is likely that some of this water leaves the Greenland Sea through the Jan Mayen Fracture Zone, as there is an abrupt change in core properties downstream of this channel, ie. in the eastern Greenland Sea, north of the fracture zone. This pathway has been suggested to be the major pathway for source waters for the NSDW (Aagaard et. al. 1985b). The property values of the Deep Water in the Norwegian Basin are as high as anywhere along the coast of Greenland (fig. 3.6). In the Lofoten Basin it is hard to identify which way this deep core flows. In some sections there are indications of a concentration of the core on the slopes, suggesting that it continues as a boundary current, whereas in other sections the values are equally high all across the Deep Water. There are not many current meter data available to resolve this problem. A record in the southwestern Lofoten Basin at 70 N, 0 longitude (Sellmann et. al., 1992) displays fairly random motion (both at 500 m and 3000 m), suggesting that the core, as it exits the Jan Mayen Fracture Zone, might not choose a cyclonic path, but rather flows northeastward in an anticyclonic fashion in the Lofoten Basin. This is speculative, but is somewhat supported by the section at 71 N (fig. 3.6).

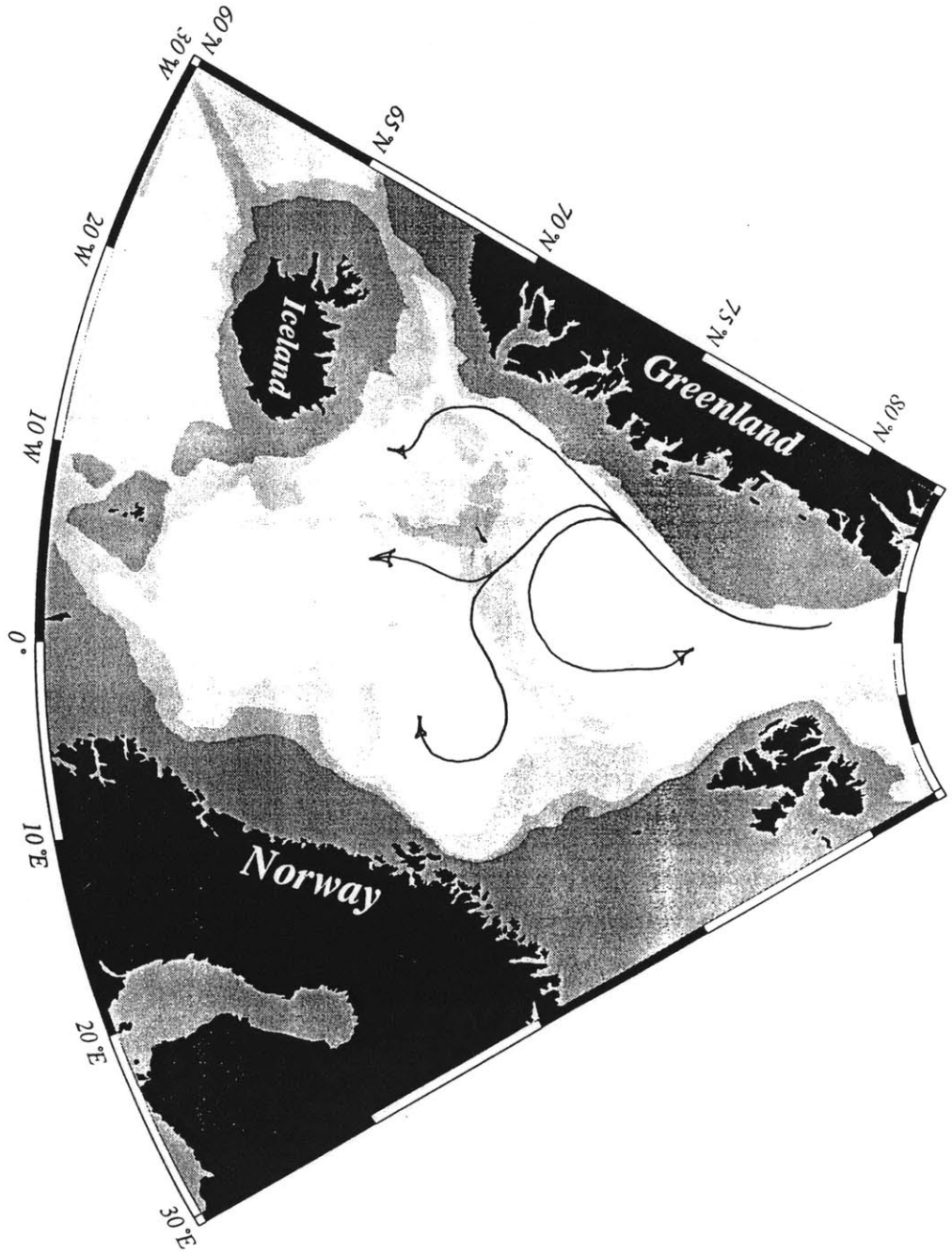

Fig. 3.12 Schematic of flow of Deep Water.

Likewise in the Norwegian Basin the flow path of the deep water is unclear. Sælen (1986) suggests that the water exiting the Jan Mayen Fracture Zone flows in a cyclonic manner in this basin. The part of the core that does not enter the Norwegian Basin, but rather continues past the Jan Mayen Fracture Zone into the Greenland Sea does so as a boundary current northward along the western slope of the Knipovich Ridge. It can be followed until the Boreas Basin, at which point it becomes so narrow that it cannot be tracked.

7. *Greenland Gyre:* The sharp boundary between the Greenland Gyre and the surroundings has been mentioned several times. Almost at all depth - or density - levels one finds lower temperatures; lower salinities, higher densities, higher oxygen and lower nutrient levels in the Greenland Gyre than in the surrounding waters, as seen in the Meteor 82 section across the Greenland Sea (fig. 3.13a and b), and in the horizontal maps of oxygen (fig. 3.14) and silicate (fig. 3.15) at 2000 m (Koltermann, 1989). The bottom waters of the Greenland Gyre are the densest water in the entire Nordic Seas / Arctic Ocean, with salinities around 34.89 and potential temperatures around -1.2 ^{0}C (Greenland Sea Deep Water). Potential density as high as 28.0 is found almost to the surface even during summer, so the vertical stability is lower inside the gyre than outside.

   A salinity maximum (the Deep Water) is found all across the gyre - nominally at 1750 m (fig. 3.13a) - with extreme values towards the edges. An oxygen minimum is found above the salinity minimum.

These cores do not explain the properties of all the water masses in the region, in particular one may question the source of the waters beneath the Deep Water core in the Norwegian Sea. These are waters with the lowest temperatures in the Norwegian Sea, as the temperature decrease monotonically with depth. It is possible that the source of the

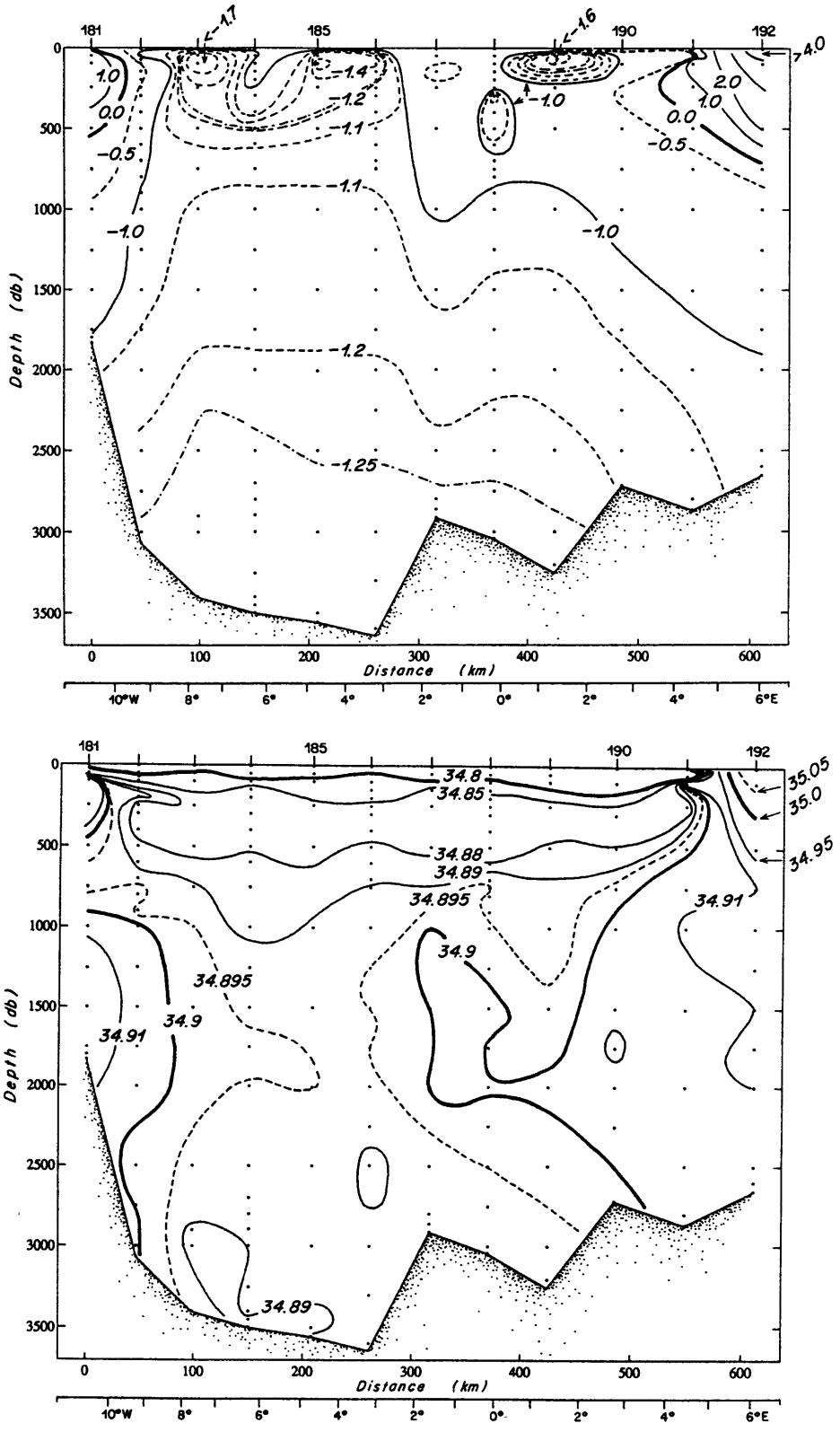

Fig. 3.13a Temperature and salinity crossing the Greenland Sea. Meteor 1982 transect. Cruise track is shown in fig. 3.2b (M82-mid).

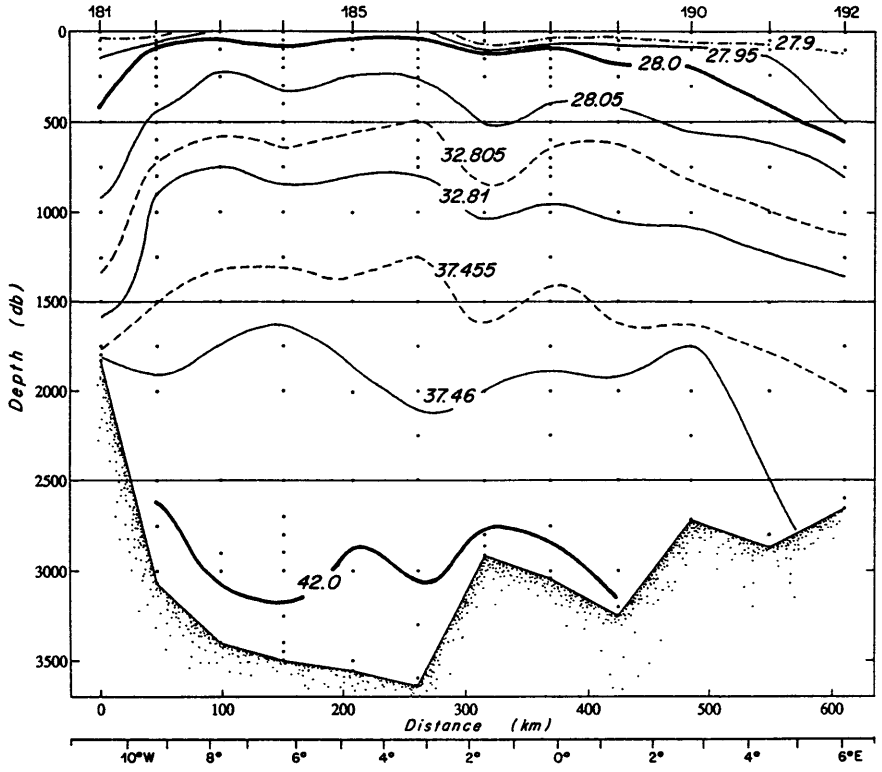

Fig. 3.13b Density section the Greenland Sea. Meteor 1982 transect.

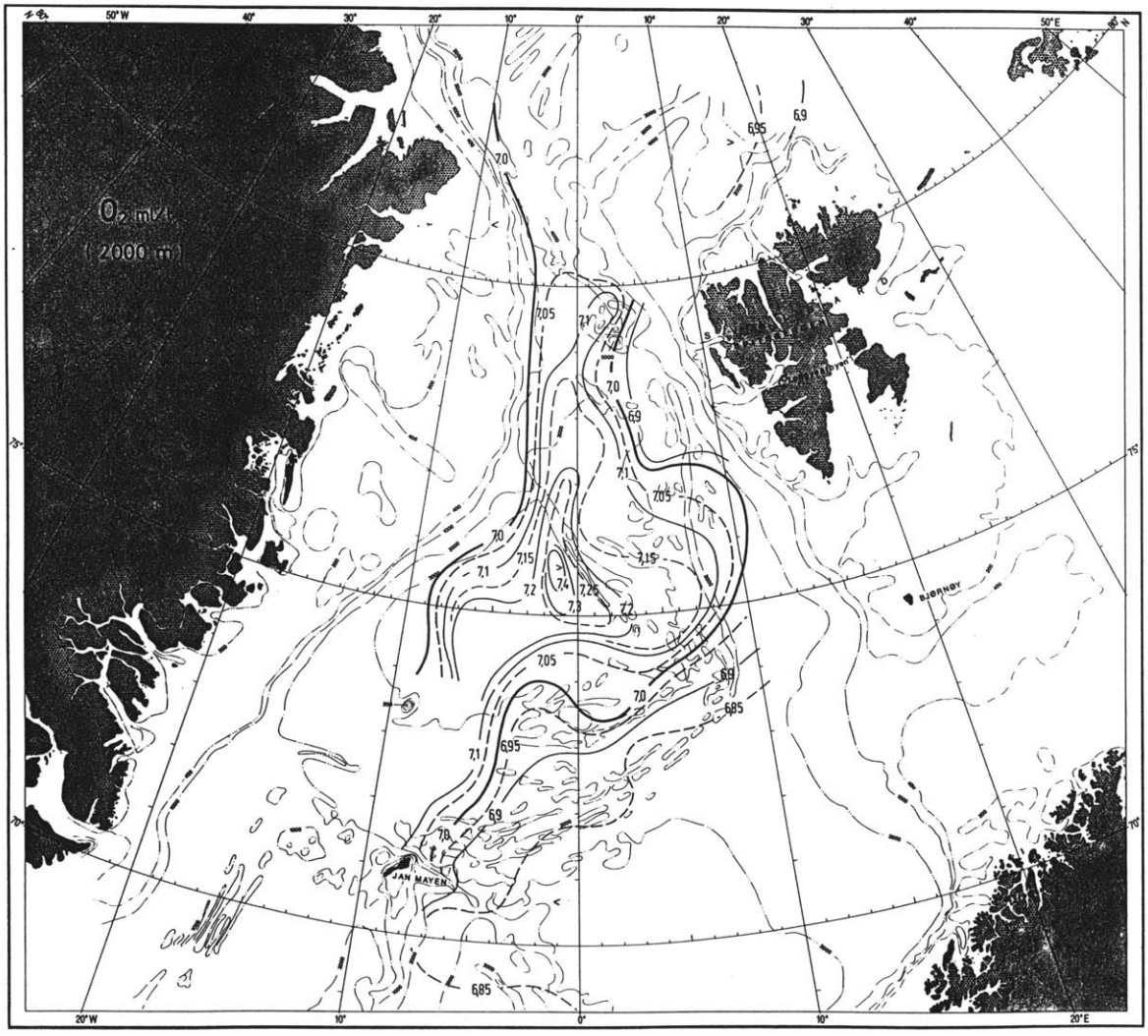

Fig. 3.14 Oxygen at 2000 m (from Koltermann et. al., 1989)

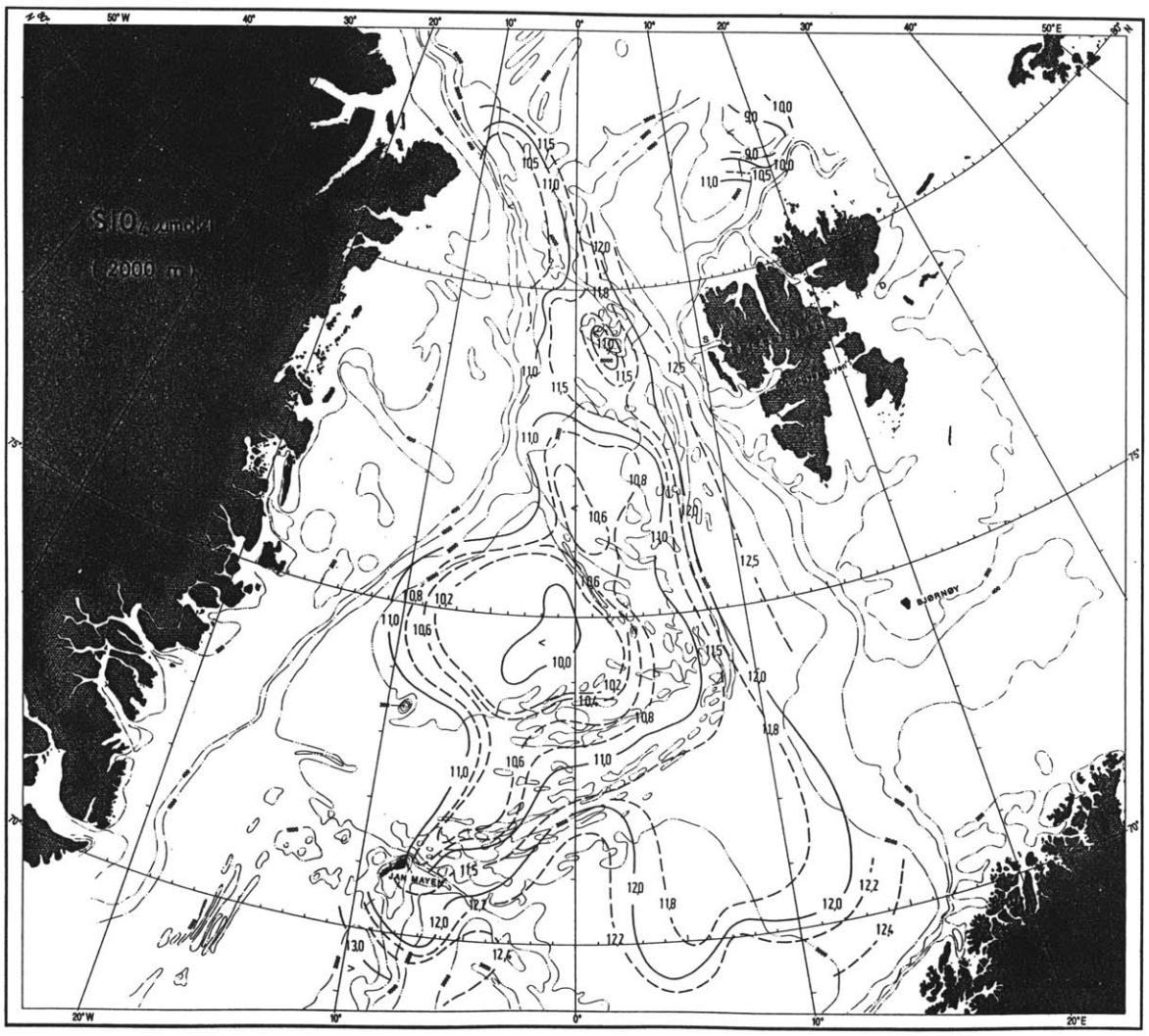

Fig. 3.15 Silicate at 2000 m (from Koltermann et. al., 1989)

Deep Water produces a range in TS properties, differing somewhat from year to year. When such a flow enters a basin the coldest water will tend to sink to the bottom, as cold water is more compressible than warm water at elevated pressure. It is also possible that the cold waters observed near the bottom of the Norwegian Sea are more influenced by the Greenland Gyre - along the Gyre one can observe Gyre waters penetrating outwards beneath the Deep Water core.

For completeness, one section from the Iceland Sea, and one from the Arctic Ocean, are included, although the modern data coverage is less there. The section from the Iceland Sea is shown in fig. 3.16. This is a section from the winter of 1982, and it shows that the salinity decreases monotonically with depth, except for a core of high salinities (34.91) in the upper 200 meters in the northeastern Iceland Sea. These high salinities are probably associated with Atlantic Water from the Norwegian Sea, as has been noted by Stefánsson (1962). The corresponding temperatures are between 0 and 1°C. These temperatures and salinities are so much smaller than those of the Atlantic Water to the east that the influence must be weak. In the rest of the Iceland Sea the temperatures are generally below zero, and there are indication of vertical overturning in the upper 200 m.

The section in the Arctic Ocean is from a Polarstern cruise in 1987, and is shown in fig. 3. 25 (courtesy G. Bönisch, see also Anderson et. al. 1989). The section crosses the Nansen Basin, and the core of the Atlantic Water (temperature and salinity maximum at 300 m) is seen on the southern slope. In general the salinities increase monotonically with depth. There is a maximum in temperature across most of the section at around 300 m, and a minimum at 3000 m.

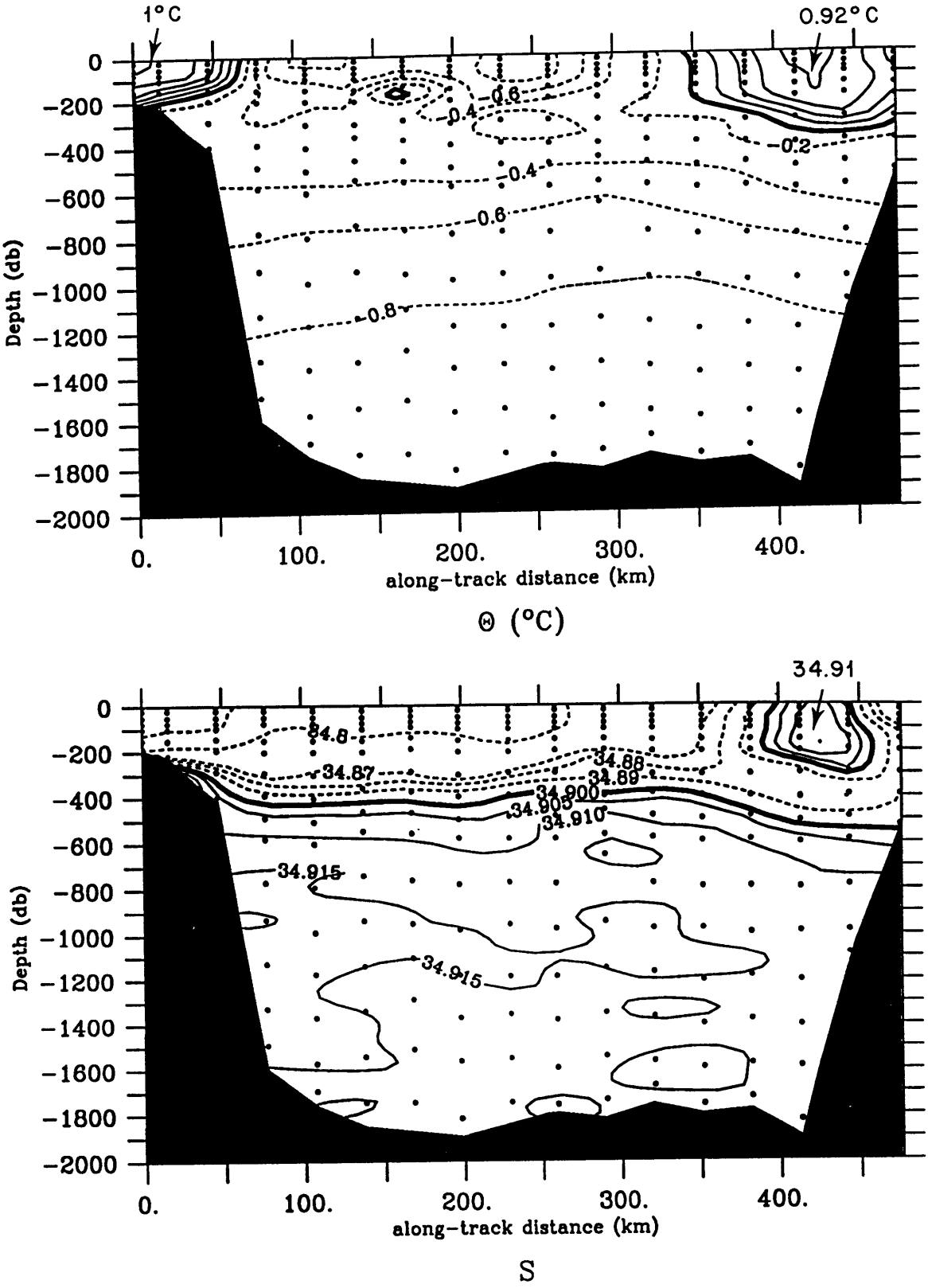

Fig. 3.16 Temperature and salinity crossing the Central Iceland Sea. Bjarni Sæmundsson 1982 transect. Cruise track is shown in fig. 3.2b (BS82).

3.1.3 Interannual Variability

The difficulty in inferring circulation of the Intermediate and Deep Water, as discussed above, is an indication of the variability of the system: the water properties do not remain constant from year to year.

To investigate these variations an extensive time series is available; the weather station Mike, positioned nominally at 66N, 2E. This weather ship has made weekly hydrographical observations since 1948, and although there are some gaps, this is one of the longest and most complete deep ocean time series. Gammelsrød et. al. (1984) present monthly averages of the temperatures and salinities from 1948-1981 (fig. 3.17). There is a recurrent oscillation in temperature and salinity with time scales of (very roughly) ten years. These oscillations are in phase down to at least 300 m, and presumably throughout the Atlantic Water. The amplitudes are equally large (0.5 ^{0}C, 0.1 per mille) at each depth within the Atlantic Water, an observation that led Gammelsrød et. al. (1984) to conclude that the signal is advected, as the influence of local surface heating and cooling tends to decrease with depth (the latest salinity minimum - around 1977 - is part of what is called the "Great Salinity Anomaly" by Dickson et. al. (1988)). Such interannual variability, present not only in the Atlantic Water, influences the analysis of hydrographic data: mapping of a property becomes less useful, even if the cruise is more or less synoptic, because some parts of the survey region may correspond to the oscillation in a certain phase, whereas other parts may correspond to the situation a few years earlier. Only if the property change along the path is much larger than the oscillation - as is the case for the Atlantic Water - or if the current is so swift that all positions along the path correspond to the same phase of the oscillation will the mapping be useful.

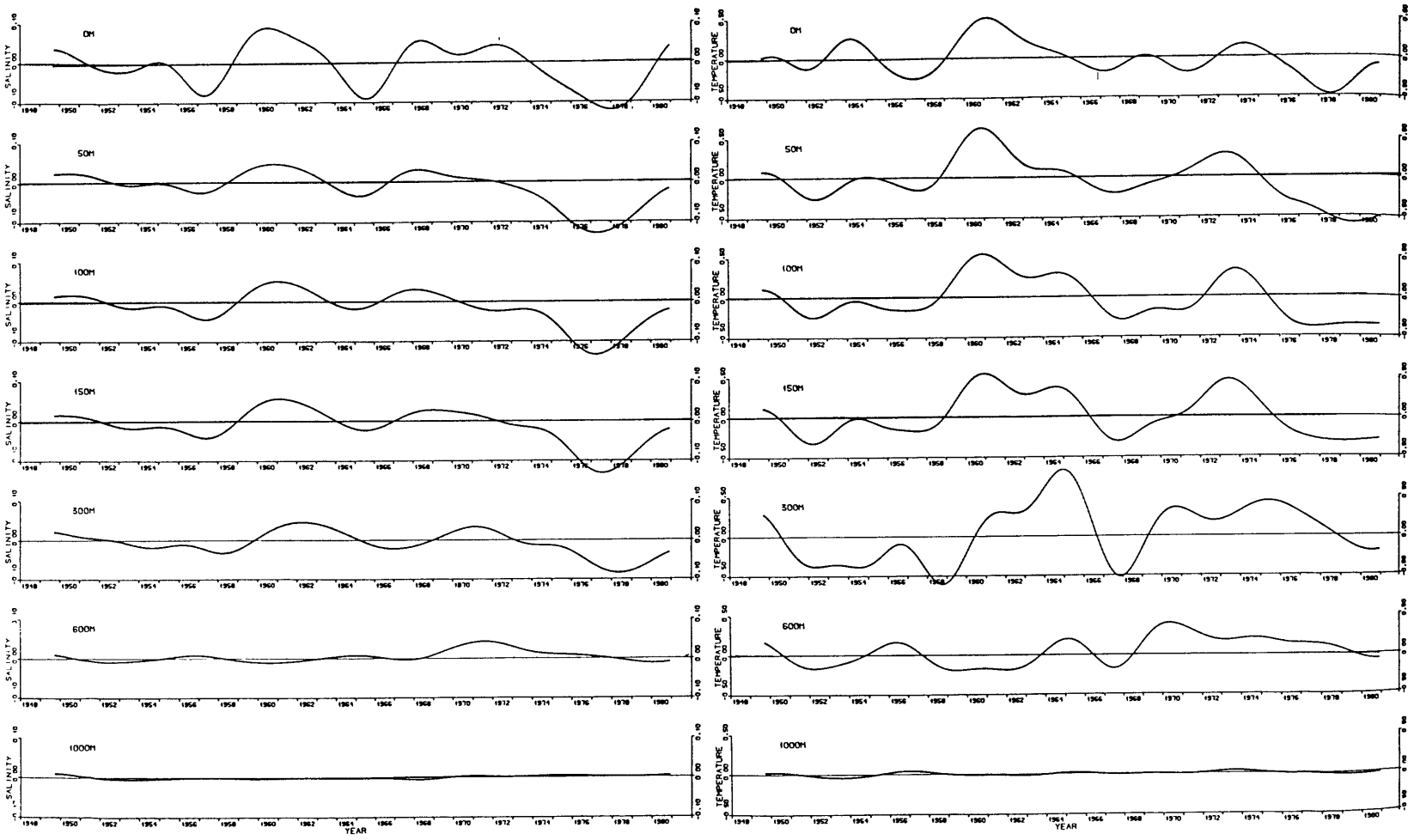

Fig. 3.17 Monthly means of temperature and salinity anomalies at Weather Station Mike (1948-1981) (Gammelsrød et. al., 1984)

3.1.4 Discussion

The picture of the circulation that emerges from the above analysis is consistent with what was previously known about the circulation, indicating that the hydrographic situation during the 1980's is not atypical. The importance of topography in steering the flow is clear. The generally weak stratification and the steep slopes allow the topographic beta-effect to influence the whole water column. This has been noted earlier by Eggvin (1961) who writes: "we see that the Mohn's Transverse Ridge, which in this section rises to about 1700 m, influences the flow of Atlantic Water, even up to the surface". Additional detailed resolution is provided in the deeper layers by this modern data set. The presence of the intermediate and deep water cores over such a large area at all times has not been previously noticed.

The high level of interannual variability of the hydrography within the Nordic Seas has been discussed. This variability makes it difficult to infer the circulation of the two deepest layers, except over the slopes surrounding the Greenland Sea.

3.2 Circulation Hypotheses

The above analysis has led to the formulation of three hypotheses. Each addresses a different part of the circulation, and differs from the current understanding of the circulation in the Arctic Ocean and Nordic Seas. By inference the circulation scheme is extended into the parts of the Arctic Ocean/ Nordic Seas where the modern hydrographic data coverage is less extensive. Together, the above analysis and the three hypotheses constitute the new circulation scheme.

3.2.1 The Direct Path from the Arctic to the Denmark Strait

Hypothesis: The dense overflow in the Denmark Strait is fed by sources in the Arctic and in the Atlantic Domain, flowing relatively uninterrupted along the coast of Greenland, with little interaction with the gyres in the Greenland Sea and the Iceland Sea.

This hypothesis suggests a different source for the upper Arctic Intermediate Water overflowing the Denmark Strait than is suggested in the much-quoted scenario of Swift et. al. (1980), or in the more recent scenario of Strass et. al. (1993) (see chapter 2). It also suggests that lower Arctic Intermediate Water does enters the North Atlantic, contrary to the claim of Swift et. al. (1980).

The topographic steering of flow over the Greenland Continental slope was commented upon in section 3.1. The shallower isobaths of this slope (1500 m and shallower) continue unperturbed through the West Iceland basin towards the Denmark Strait (fig. 3.18), so one would expect that at least the outer streamlines of the current would continue through the basin along the shallow isobaths. A hydrographic section at 71 N (fig. 3.19), just south of the entrance to the West Iceland Basin, corroborates this idea: the Polar Water and the return Atlantic Water cores are seen over the western slope. A section at 65 N (fig 3.20), and several sections from the Overflow '73 experiment (fig. 3.21) show the cores of the East Greenland Current over the slope in the West Iceland Basin. Aagaard and Coachman (1968, part 2), based on drifter float "Arlis" data, also find a part of the East Greenland Current which continues into the West Iceland Basin, containing not only the Polar Water, but also the return Atlantic Water ("Atlantic Intermediate Water", in their nomenclature).

Bathymetry

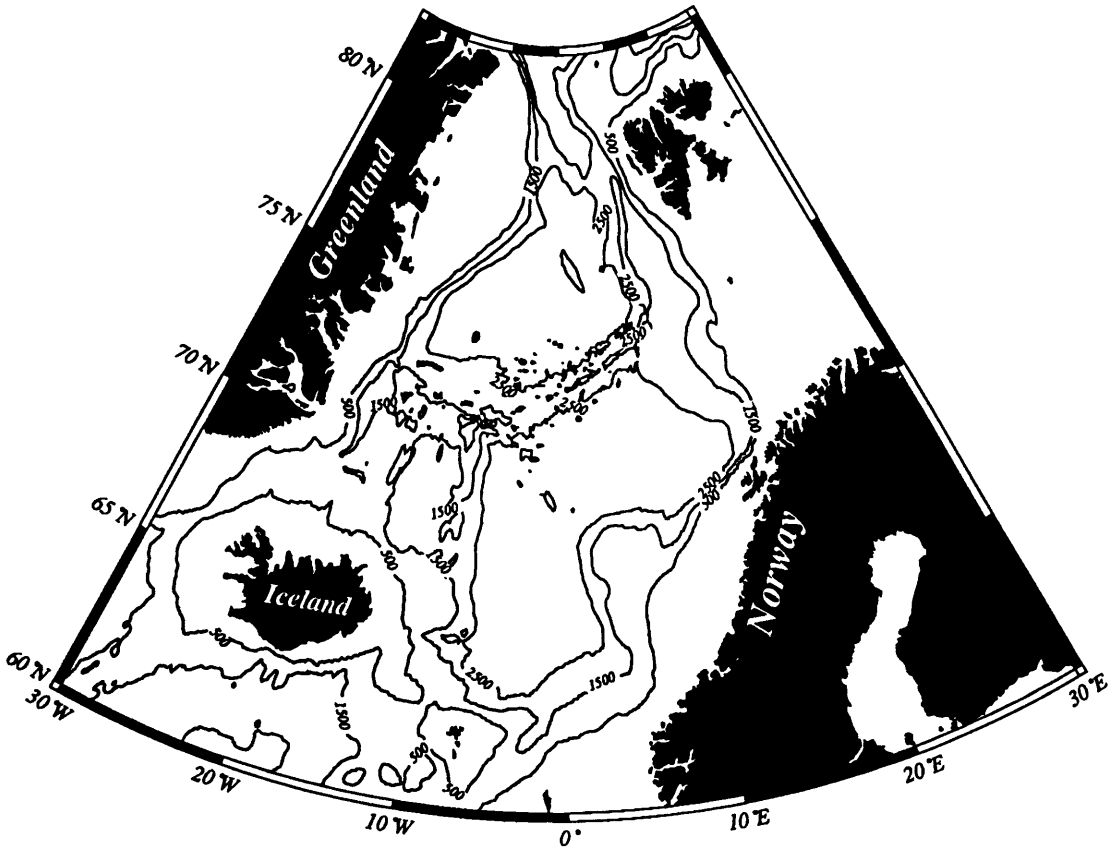

Fig. 3.18 Bathymetry in the Nordic Seas

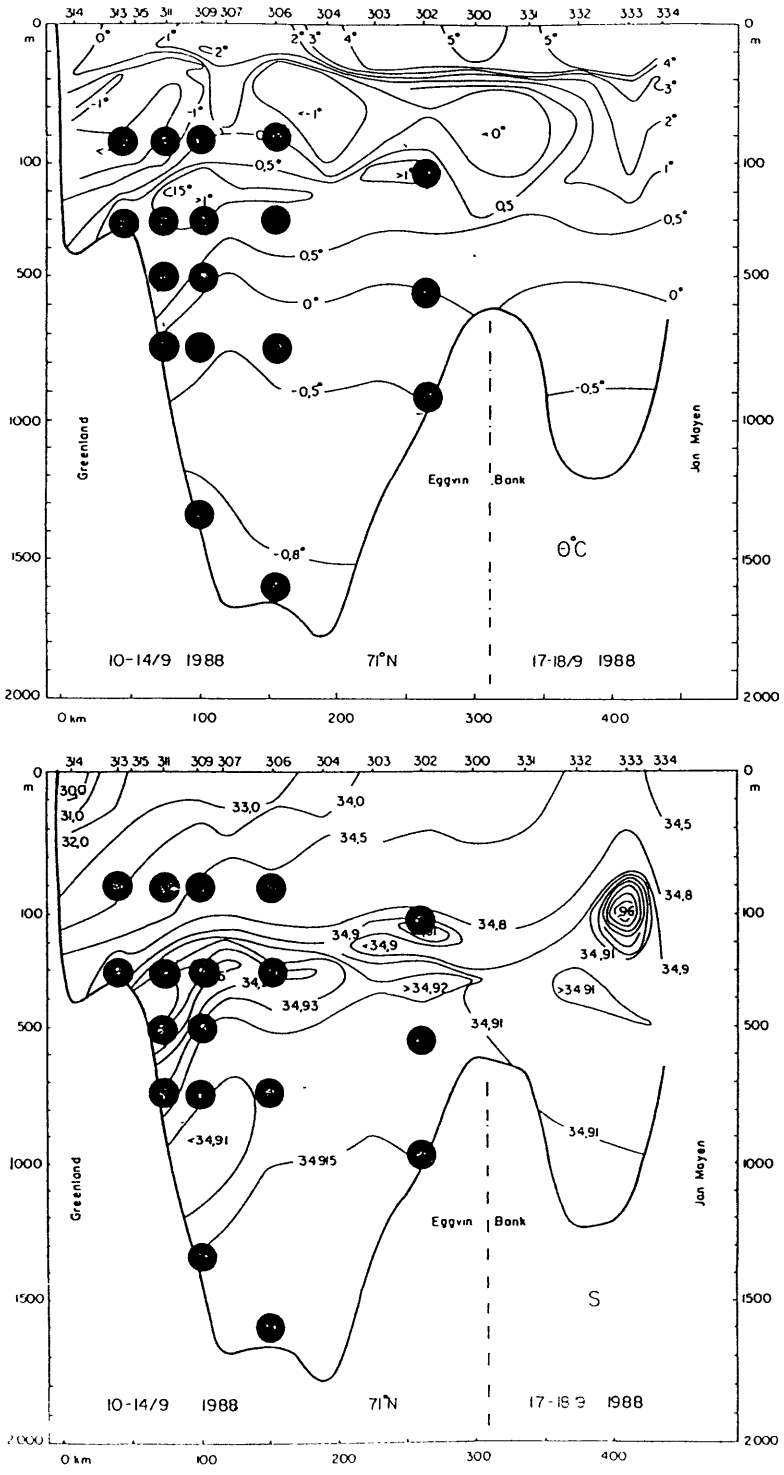

Fig. 3.19 Potential temperature and salinity section at 71 N in the West Iceland Basin in 1988 (Aken et. al., 1992).

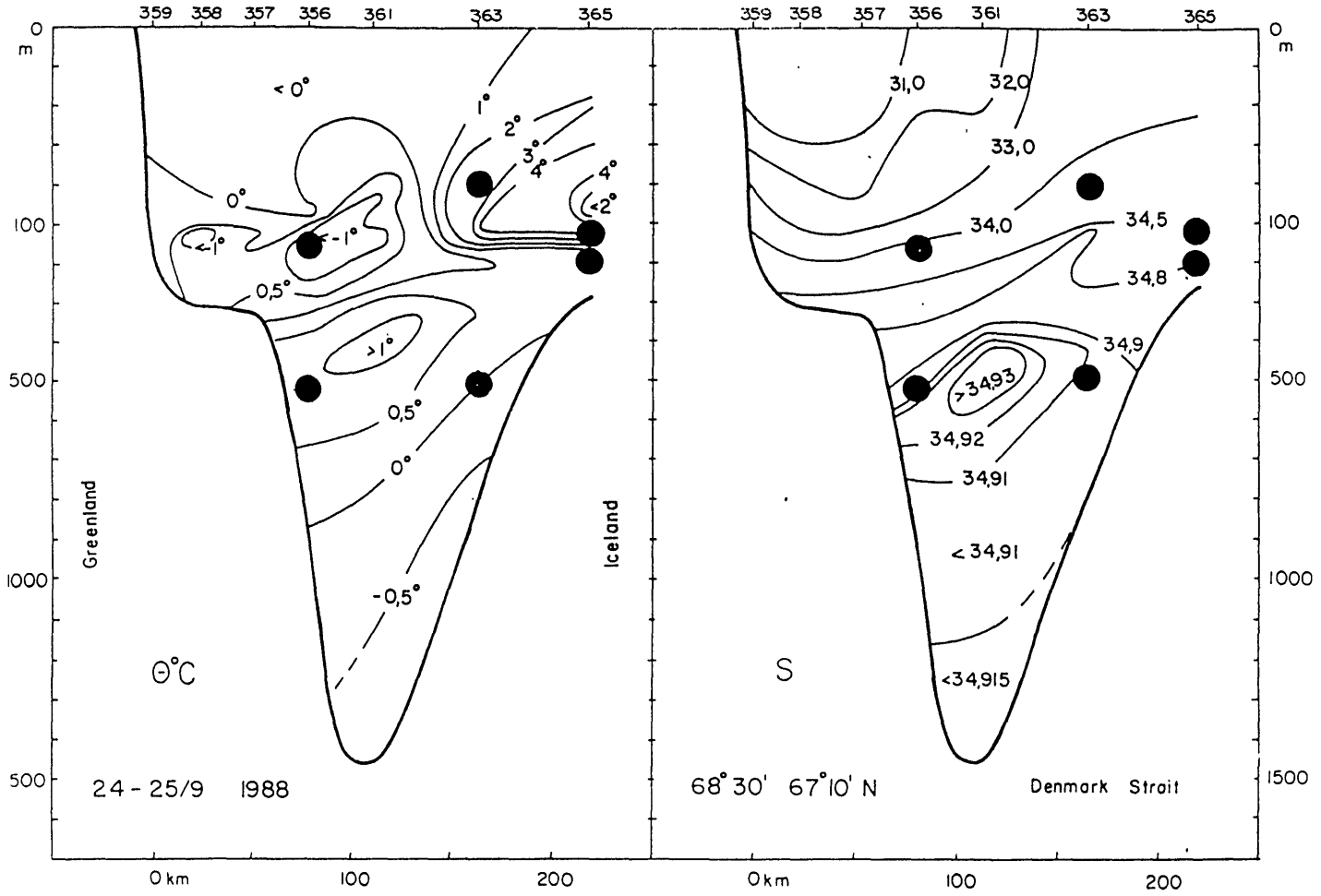

Fig. 3.20 Potential temperature and salinity sections near the Denmark Strait in 1988 (Aken et. al., 1992)

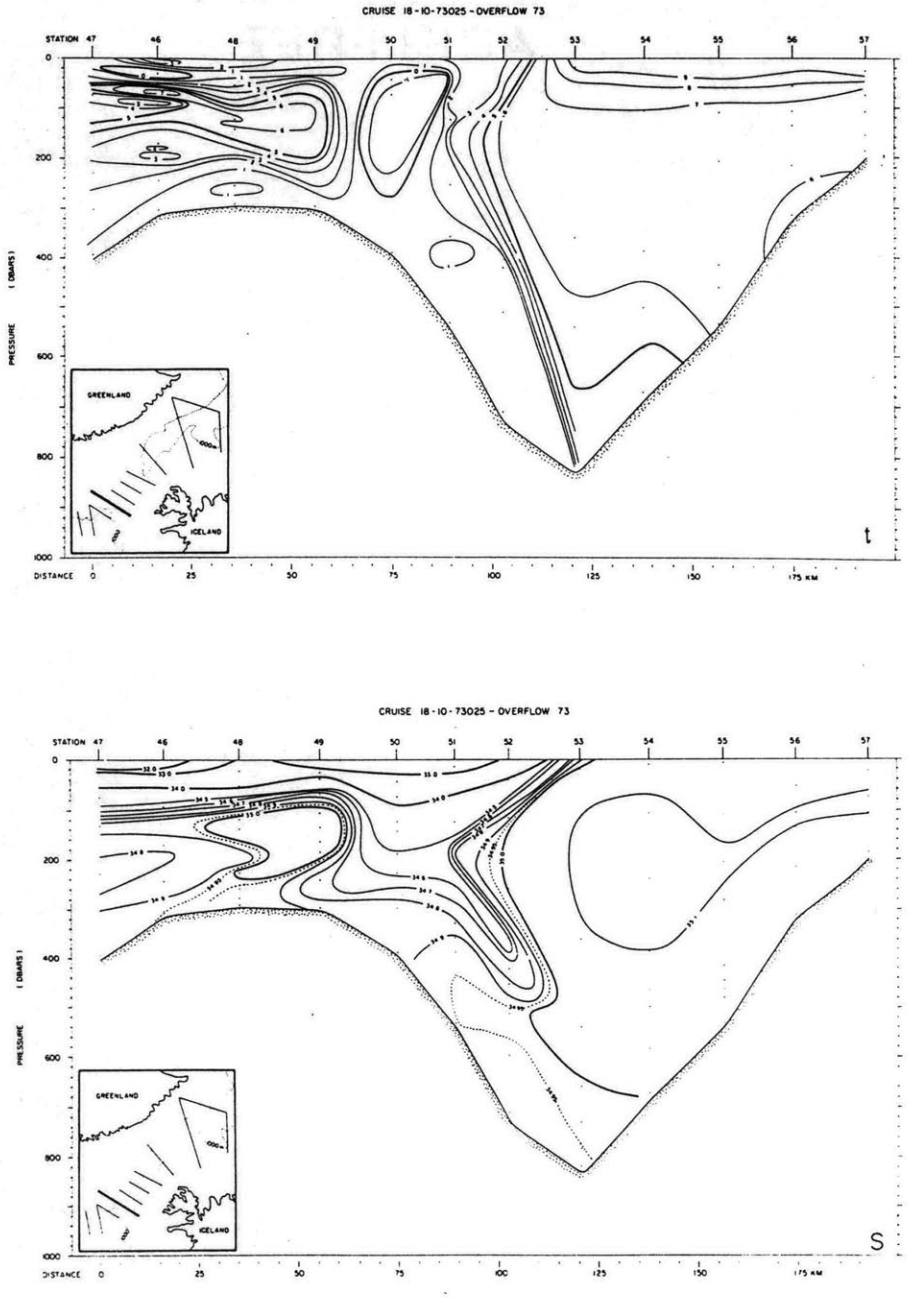

Fig. 3.21 Potential temperature and salinity sections near the Denmark Strait from the Overflow '73 experiment (Ross 1982)

The water with the properties of the dense overflows in the Denmark Strait lies between the Polar Water and the return Atlantic Water in TS-space. Typical properties for the dense overflows are shown in table 3.2. There is a reservoir of water in the Arctic Ocean with properties comparable with those in the Denmark Strait. The Polar Water is typically found in the upper 100 m in the Arctic. Beneath the Polar Water there is a thick layer (typically 600-700 m thick) of water characterized by a temperature maximum (0-0.5 ^{0}C) and salinities around 34.8-34.9. This water is generally called Arctic Intermediate Water. Aricticc Intermediate Water is a very broad definition that includes most of the intermediate water in the Greenland and Iceland Seas as well, so for clarity, water stemming from intermediate depths in the Arctic will in this work be called Arctic Atlantic Water (AAW). Typical values and ranges for the AAW are given in table 3.2, for stations north of Greenland.

The Arctic Atlantic Water flows out of the Arctic Ocean in the East Greenland Current. The East Greenland Current is often characterized as a shallow current bringing fresh and cold Polar Water from the Arctic into the North Atlantic (see e.g. Worthington, 1969). Nevertheless, the three existing sets of long-term current meter moorings along the slope; at 79 N, at 75 N and at 71 N (positions shown in fig. 3.11) indicate that the East Greenland Current has a strong barotropic component. At 79 N three moorings, with three instruments each, recorded the currents over the Greenland Continental Slope in the Fram Strait for 1 year (Aagaard et. al. 1985a). At all levels, except at the easternmost bottom instrument, there is persistent southward flow (see table 3.3). At the intermediate level, which is at roughly 400 m, the mean speed is O(5 cm/s), and towards the bottom the speeds are O(2.5 cm/s).

At 75 N there are four moorings from 1987 to 1989; three over the slope, and one further east in the Greenland Basin (Sellmann et. al. 1992). A persistent flow is found over the slope at all depths (table 3.3 and fig. 3.11), mean speeds ranging between 9 and

Table 3.2 Properties of the Denmark Strait Overflow Water, and its potential sources

	θ [^{0}C]	Salinity	O_2 [ml/l]	PO_4 [µmol/l]	SiO_4 [µmol/l]	NO_3 [µmol/l]
Denmark Strait[1]	0.4 - 2	34.8 - 34.9	6.9 - 7.1	0.9 - 0.99	6.7 - 8.5	13.4 - 14.7
Arctic Ocean[2]	0.2 - 0.6	34.8 - 34.9	6.7 - 7	0.8 - 0.95	5.6 - 8	10.8 - 13.7
Iceland Sea[3]	-0.5 - 0	34.7 - 34.9	7.5 - 8	0.78 - 0.84	4.9 - 5.9	8.8 - 12.3

[1] Data from: Erika Dan 1962 (Worthington and Wright, 1970)
Hudson 1967 (Grant, 1968)
Knorr 1981 (TTO/NAS)
Knorr 1983 (McCartney, 1992)

[2] Data from: Ymer 1980
Polarstern 1984

[3] Data from: Bjarni Sæmundsson 1971 (Malmberg, 1983)
Knorr 1981 (TTO/NAS)
Bjarni Sæmundsson 1982

Table 3.3 Current Meter Statistics

Station	Latitude	Longitude	Bottom [m]	Start	Length [days]	Depth [m]	U [cm/s]		V [cm/s]		T [^{0}C]	
							mean	st.dev.	mean	st. dev.	mean	st. dev.
FS-1[1]	78^{0}59'N	5^{0}16'W	1094	06/17/84	394	94	0.0	7.4	-6.2	9.5		
					394	374	-0.1	2.8	-1.4	3.7		
					394	1069	0.6	2.0	-2.5	3.0		
FS-2[1]	79^{0}00'N	4^{0}26'W	1678	06/18/84	393	78	-2.1	7.0	-8.8	8.6		
					393	378	0.0	3.0	-3.8	4.3		
					271	1378	0.1	1.3	-2.3	3.4		
FS-3[1]	78^{0}55'N	3^{0}18'W	2359	06/18/84	392	109	-4.1	6.4	-8.6	8.7		
					392	409	-2.2	4.2	-5.6	6.0		
					392	2334	0.2	4.6	-0.4	8.2		
AWI 402-2[2]	75^{0}26'N	10^{0}50'W	1994	06/20/88	341	85	-16.5	5.3	-15.4	7.4	-0.28	0.95
					227	425	-12.3	3.7	-9.3	3.9	0.78	0.31
					105	1202	-5.2	2.1	-8.0	3.1	-0.62	0.09
					176	1789	-5.0	4.4	-6.2	4.2	-0.94	0.11
AWI 403-2[2]	75^{0}00'N	9^{0}06'W	3309	06/20/88	171	100	0.1	5.2	-1.9	5.4		
					213	440	-2.2	5.3	-1.5	4.8	-0.59	0.23
					207	1225	-1.2	5.3	-1.2	4.2	-1.01	0.04
					224	2046	-1.7	5.4	-1.1	4.2	-1.05	0.02
IS1[3]	70^{0}59'N	20^{0}26'W	327	09/14/88	415	85	1.6	5.5	-9.6	8.7	-1.71	0.11
					368	307	2.2	4.2	-5.6	5.8	0.04	0.66
IS2[3]	70^{0}59'N	19^{0}28'W	822	09/14/88	200	80	-1.7	2.3	-12.3	4.6	-1.60	0.14
					162	300	-2.5	2.4	-5.0	4.3	1.06	0.15
					229	500	-0.5	4.2	-3.9	5.1	0.75	0.12
					143	750	-3.1	2.6	-4.4	3.7	0.12	0.29
IS3[3]	70^{0}59'N	18^{0}50'W	1423	09/13/88	192	80	-1.9	2.8	-14.2	5.7	-1.32	0.61
					159	300	-2.7	2.5	-9.9	5.4	0.76	0.12
					206	500	-1.5	1.5	-10.2	4.6	0.58	0.19
					265	750	-1.6	1.5	-7.6	3.6	-0.10	0.13
					180	1350	-1.2	1.5	-4.8	4.2	-0.60	0.11

[1] From Aagaard et. al., 1985a, and Jónsson, 1989
[2] From Sellmann et. al., 1992
[3] From van Aken et. al., 1992

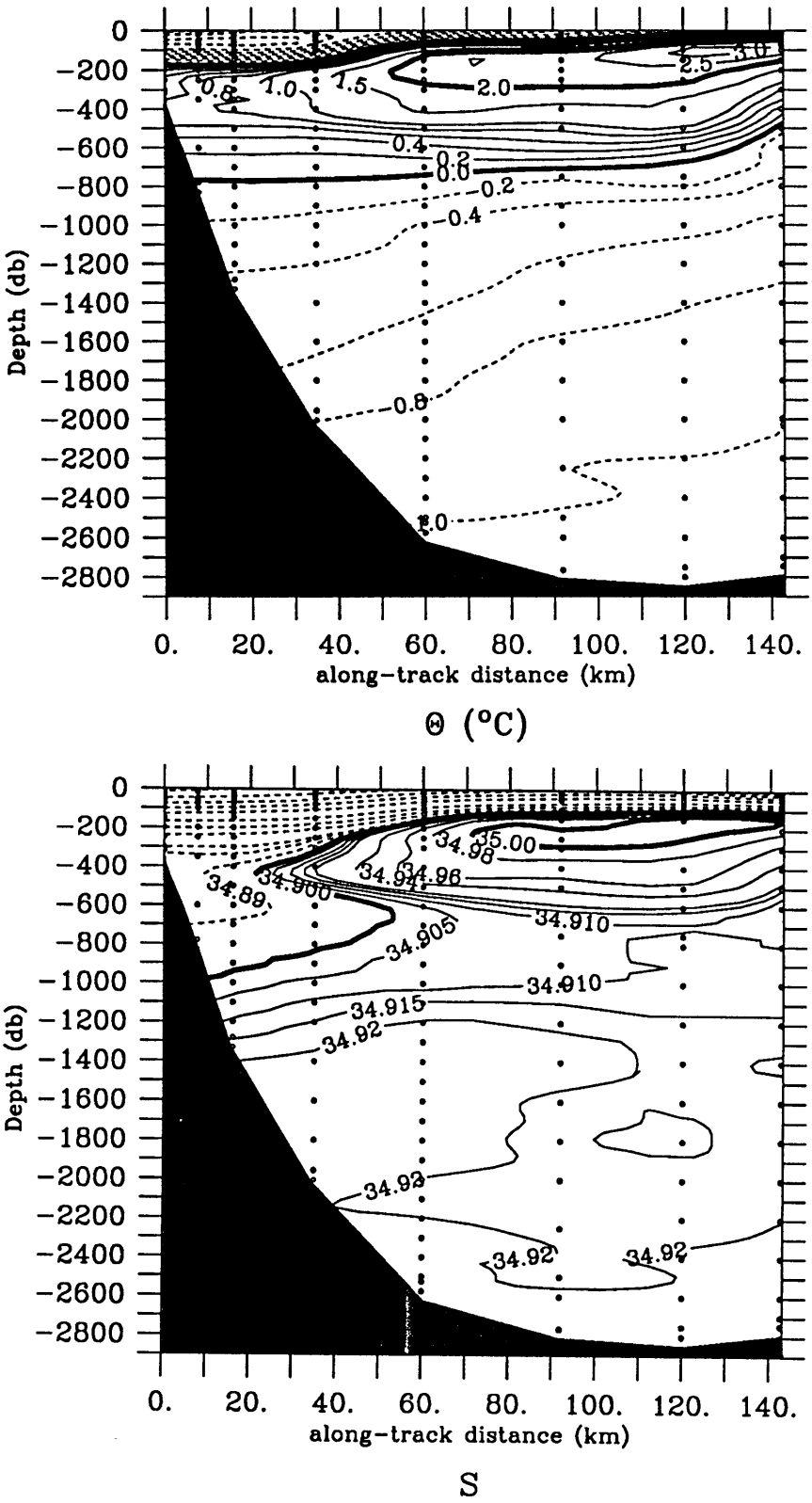

Fig. 3.22 Potential temperature and salinity in the western Fram Strait. Polarstern 1984 transect. Cruise track is shown in fig. 3.2b (P84-79).

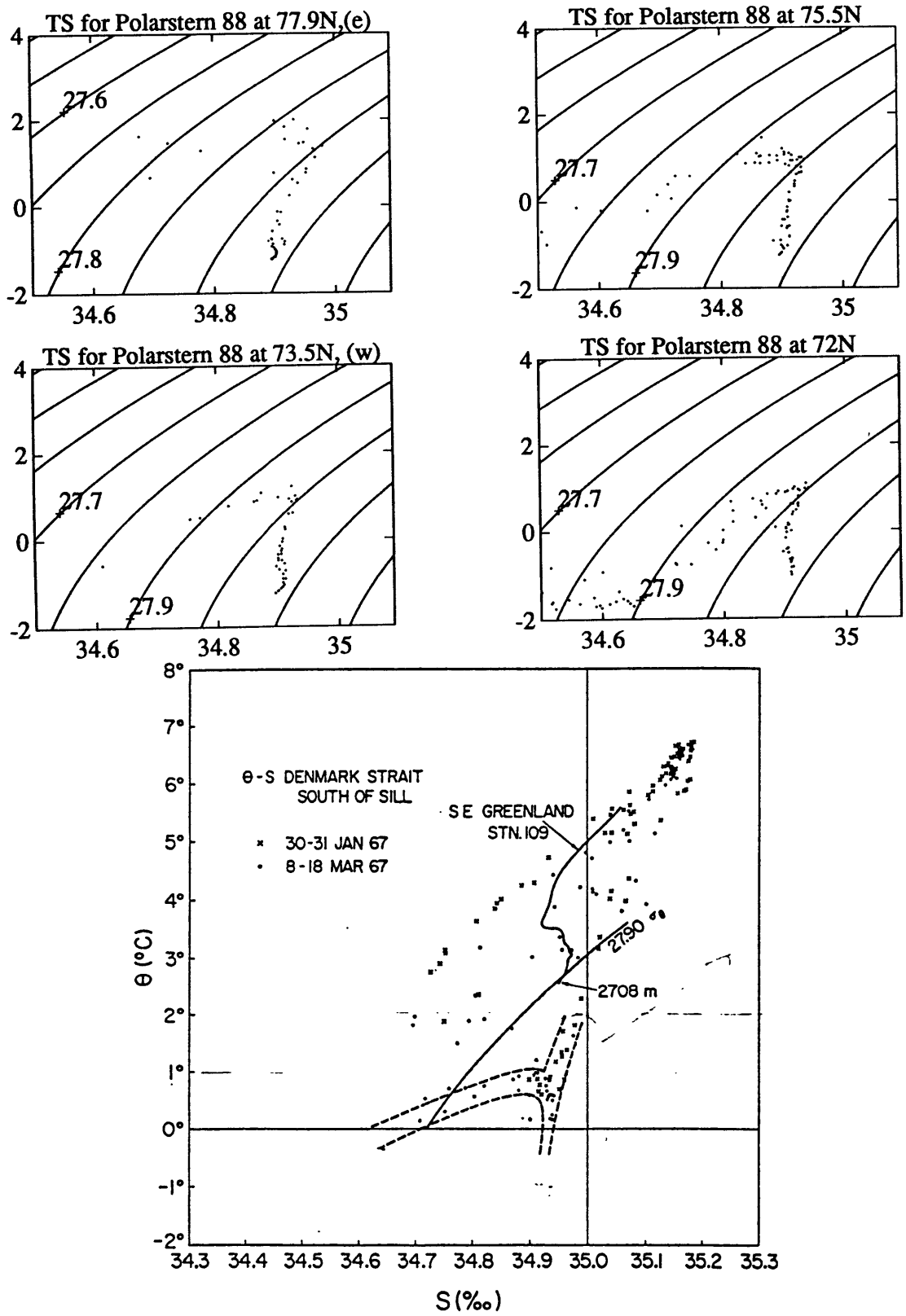

Fig. 3.23 TS diagrams along coast of Greenland for the P88 cruise. Also shown is Mann (1969)'s TS diagram for the Denmark Strait.

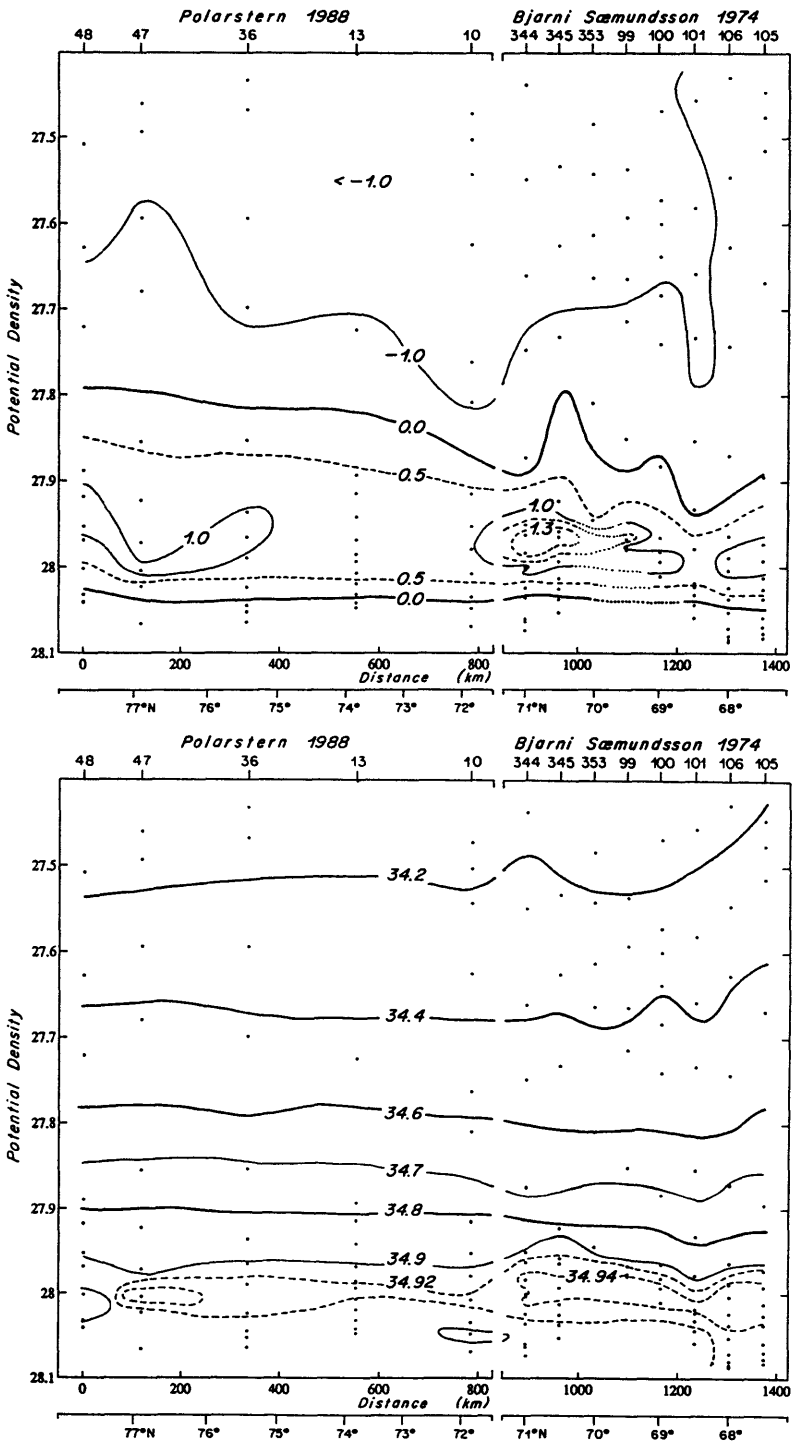

Fig. 3.24 Potential temperature and salinity sections along the path of the East Greenland Current, nominally at 900 m. Polarstern 1988 and Bjarni Sæmundsson 1974.

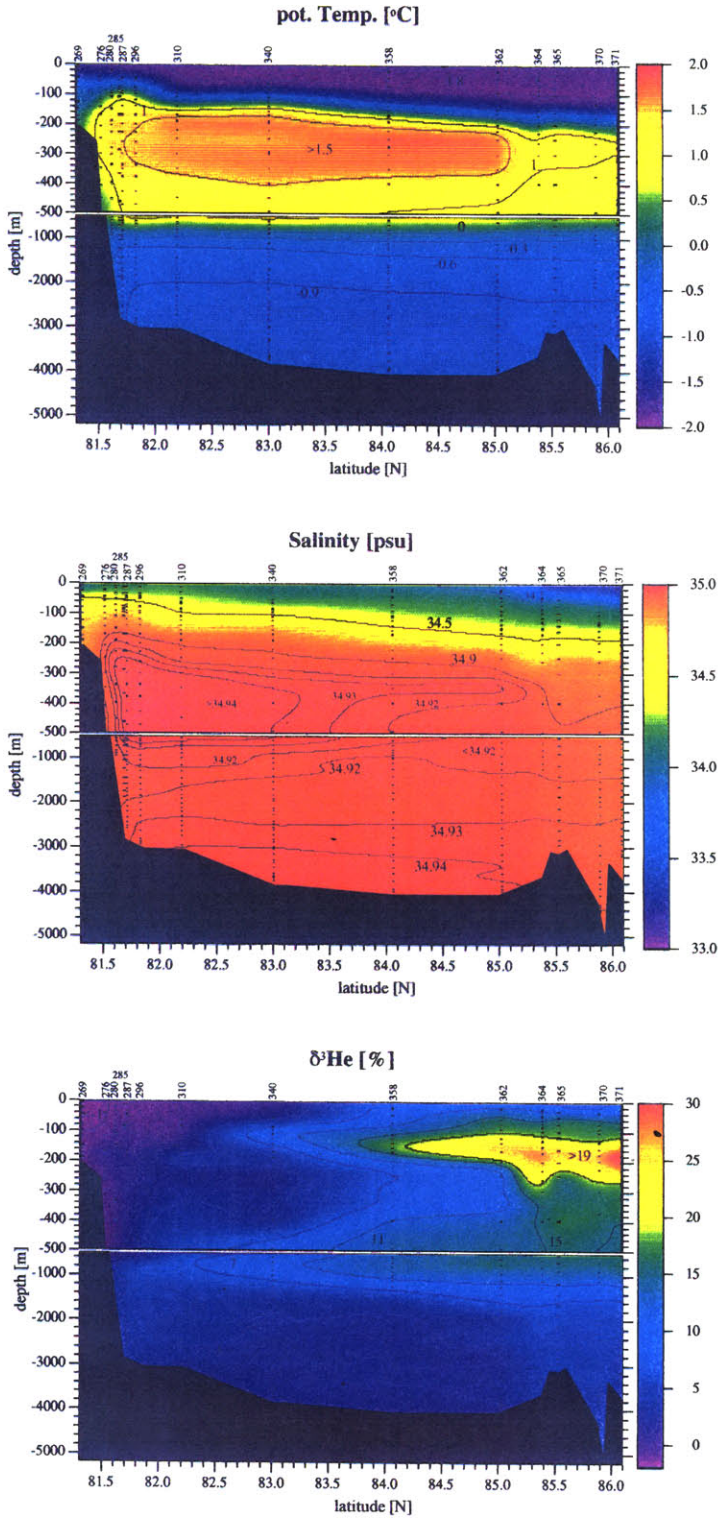

Fig. 3.25 Sections of potential temperature (°C), salinity and δ^3He (%) in the Nansen Basin, nominally at 30E. Polarstern 1987 transect (by courtesy of Gerhard Bönisch).

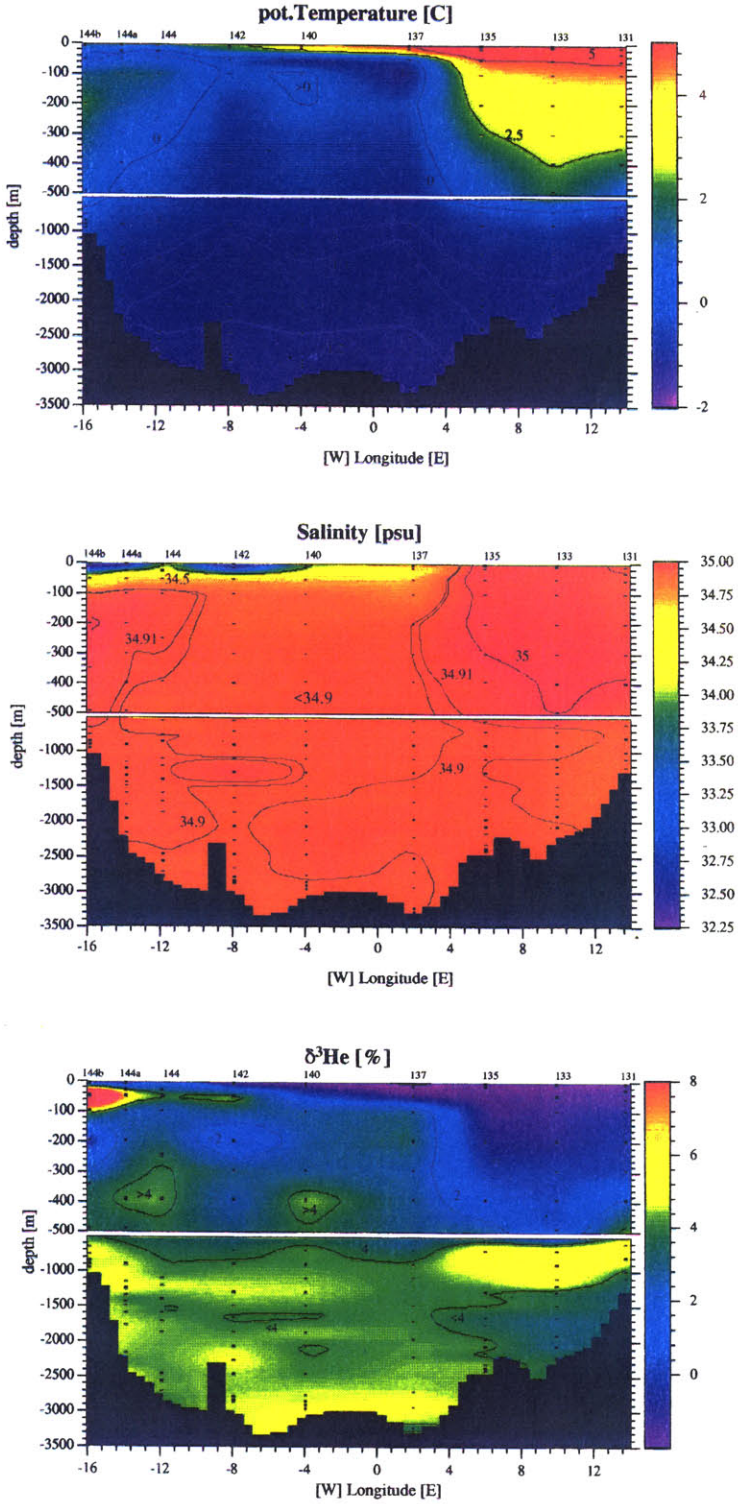

Fig. 3.26 Potential temperature (°C), salinity and δ^3He (%) along 73°30'N in the Greenland Sea and Lofoten Basin. Meteor 1985 transect (courtesy Gerhard Bönisch).

18 cm/s. The mean speeds of the easternmost mooring are, on the other hand, not statistically distinguishable from zero. The moorings at 71 N, south of the Greenland Sea; in the West Iceland Basin, were in operation between 9/1988 and 8/1989 (Aken et. al. 1992). Persistent southwestward flow is found over the slope, with mean speeds ranging between 4 and 14 cm/s, whereas further east the flow is less unidirectional. Since the East Greenland Current has a barotropic component it is capable of transporting not only Polar Water, but also Arctic Atlantic Water out of the Arctic Ocean.

Arctic Atlantic Water exiting the Arctic Ocean via the East Greenland Current can be seen in three sections in the Fram Strait (Y80 at 79N; fig 3.9, P84 at 79 N; fig. 3.22, and P88 at 78 N; fig. 3.10a) where the presence of AAW is evident beneath the Polar Water to the west of the return Atlantic Water. In the sections along the coast of Greenland the AAW is seen flowing along with the return Atlantic Water beneath the PW (see fig. 3.10), intermediate in TS properties between the Polar Water and the return Atlantic Water.

Within the swift East Greenland Current the areal coverage of the AAW is quite small (it is not clear that the AAW is as well resolved as it could be if the sections were extended further up the slope). Nevertheless, one can see that the TS relationships found along the coast in the Greenland Sea are comparable to the characteristic TS diagram of the overflow waters in the Denmark Strait described by Mann (1969) (fig. 3.23). The cores are identifiable all along the coast and there is no smoothing along the path. This is reasonable; the current is swift, giving little time to mix.

An artificial section over the 900 m isobath, intending to follow approximate streamlines of the East Greenland Current from the Fram Strait to the Denmark Strait, is shown in fig. 3.24. The extension into the West Iceland Basin towards the Denmark Strait is made with data from the Bjarni Sæmundsson 1974/75 cruises. Using these data

is not ideal, because if one compares data from the central Iceland Sea from this data set to data from the 1982 Bjarni Sæmundsson cruise one finds that the central Iceland Sea was in a different state in the mid-seventies than in the 1980's; in the former there is a large density jump at middepth, whereas in 1982 the stratification is more stable. Nevertheless, the data in the West Iceland Basin show (except for the higher temperatures of the rAtW in the mid-seventies) uninterrupted flow towards the Denmark Strait. It also shows that most of the water column within the East Greenland Current is denser than 27.9, which is dense enough to sink to the bottom of the North Atlantic. Most of the return Atlantic Water is above sill level (600 m) and is therefore expected to exit through the Denmark Strait as well.

Transient tracers are harder to compare descriptively than the steady tracers that have been considered so far. The time history of their sources, the flow path and mixing, and the decay time scale need to be taken into account, and this is better done with a time-dependent model. Only if the observations are made closely in time and if little mixing occurs along the way does one expect the values to be comparable. The Ymer cruise in 1980 measured tritium in the Arctic, and this can be compared with the TTO/NAS measurements in the Denmark Strait in 1981, assuming the hypothesized flow along the coast of Greenland (that Arctic Atlantic Water follows the East Greenland Current). The values are comparable: typical values for the Arctic are 2-4.5 TU81N, and for the Denmark Strait 2.7-4 TU81N (Østlund and Grall, 1993).

The daughter product of tritium is helium. The Ymer cruise in 1980 did not measure helium, so one cannot compare helium values in the Arctic directly to those in the Denmark Strait (as measured on the Knorr 1981 expedition). Nevertheless, the Arctic Atlantic Water in the Arctic Ocean is associated with high helium values, attributed to the long residence time in this large ocean. This can be seen in fig. 3.25, which shows helium, temperature and salinity from the Polarstern 1987 section crossing the Nansen

Basin (the hydrography of this section was discussed in section 3.1). The high helium values of the AAW are seen in the northern end of the section, at 200-300 m.

Consider now the helium section at 73.5 N from the Meteor 1985 cruise (fig. 3.26) (the hydrography of this section was discussed in section 3.1 as well). On the slope of Greenland, between the Polar Water in the surface and the return Atlantic Water at 200-300 m, there is a large peak in helium concentration, as expected. It is appealing that the Arctic Atlantic Water in this way is associated with a property extremum: it is apparent that the Arctic Atlantic Water represents a distinct water mass. So although the temperature and salinity properties are intermediate in value between those of the Polar Water and the return Atlantic Water it is clear that the AAW does not represent mixing of PW and rAtW.

Although one cannot directly compare the helium values in these sections with those in the Denmark Strait (because of the time separation of the cruises), there still exists some information about the values in the Denmark Strait: Doney (1991) ran a multi-tracer model for the ventilation of the abyssal North Atlantic, assuming that the formation site of upper Arctic Intermediate Water was the Iceland Sea. He found that although most of the properties in the dense overflows in the Denmark Strait can be explained by the Iceland Sea source, such was not the case for helium: these values were too high in the Denmark Strait.

Formation of Denmark Strait Overflow Water in the Iceland Sea, as suggested by Swift et. al. (1980), is therefore a less likely scenario than the above hypothesis. The Arctic Atlantic Water flows with the East Greenland Current towards the overflows on an advective time scale. The upper Arctic Intermediate Water of the Iceland Sea requires mixing - especially in temperature and oxygen, and in helium, as mentioned above - to become the overflow water. The properties of the uAIW in the Iceland Sea are shown in table 3.2. There is no water mass available that would shift the properties in the right

direction (unless maybe if one invoked a multi-endpoint mixing scheme). Furthermore, there is no current flowing from the Iceland Sea to the Denmark Strait. The dynamic height field shows cyclonic circulation in the Iceland Sea (fig. 3.27). The analysis presented above demonstrates that the East Greenland Current flows along isobaths, with a significant barotropic component, suggesting that the dynamic height streamlines represent mean streamlines of the total velocity field as well. It is expected, based on the importance of topographic steering found in the primary data set, that the Kolbeinsey Ridge, which separates the central Iceland Sea from the West Iceland Basin (fig. 3.18) further separates the cyclonic movement of the central Iceland Sea from the streamlines of the East Greenland Current. Therefore the time scale on which the water can flow from the Iceland Sea to the Denmark Strait is likely to be a mixing time scale, slower than the time scale of the flow of the Arctic Atlantic Water.

Likewise, Strass et. al. (1993)'s scenario of forming uAIW in the Greenland Sea implies crossing of streamlines (fig. 3.28). They argue that this is due to baroclinic instability: the return Atlantic Water of the East Greenland Current mixes with the surface waters of the Greenland Gyre. But such a scenario of baroclinic instability, for which - as they found - the conditions are not always met, is hard to reconcile with the observed persistent overflows such a short distance downstream.

The Denmark Strait Overflow Water that has been discussed thus far is not the densest water found at the sill: in Mann (1969)'s TS-diagram one finds return Atlantic Water beneath. Swift et. al. (1980) show along-path sections of θ and S exiting the Denmark Strait and note that water with $S > 34.9$ is only found less that 200 km downstream of the strait (fig. 3.29). Since the water in the deep western North Atlantic gets progressively fresher towards the bottom, Swift et. al. (1980) concluded that no rAtW (his lAIW) actually exits the Denmark Strait. But such a conclusion is not

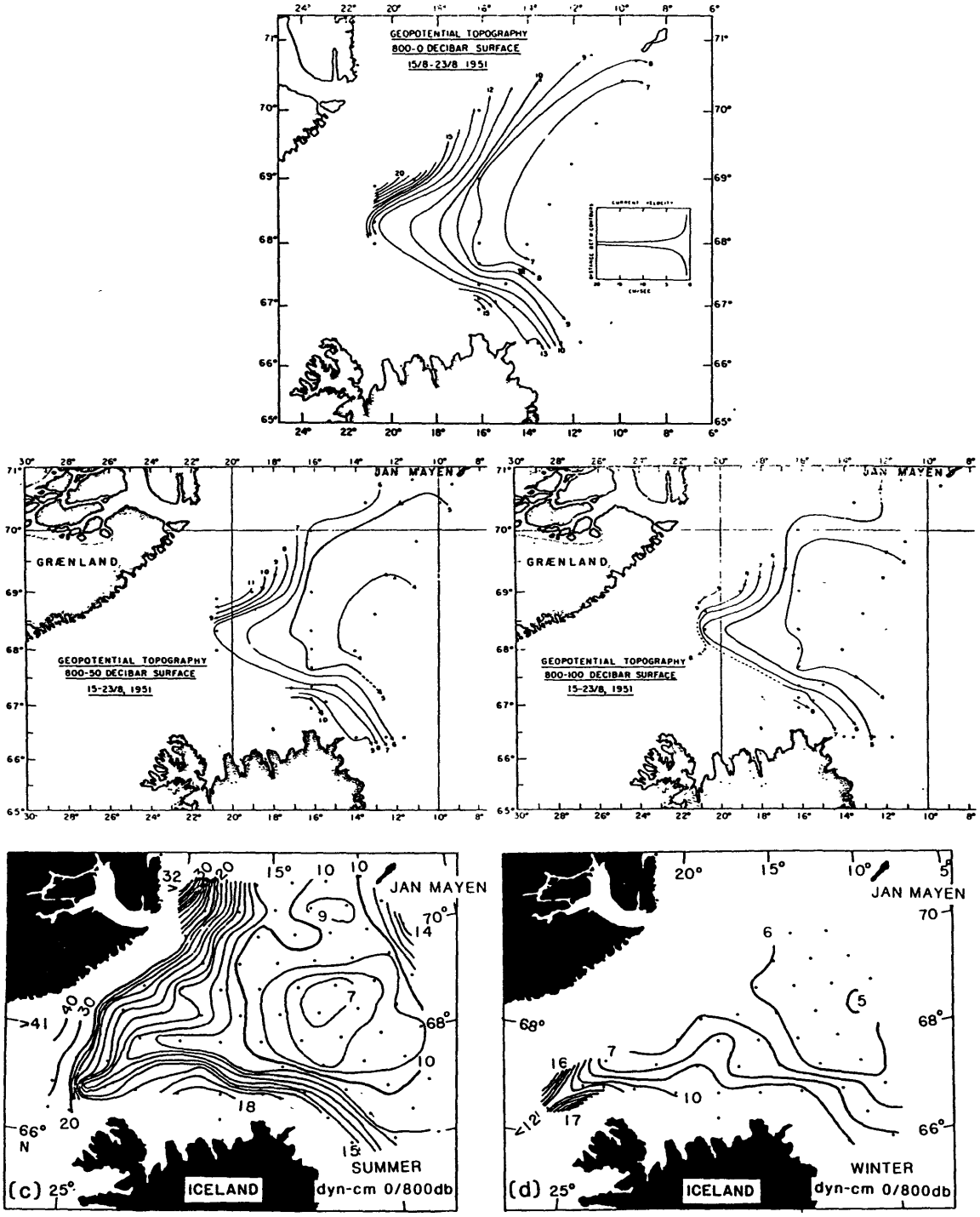

Fig. 3.27 Dynamic topography for Iceland Sea (Hopkins (1988) and Stefánsson (1962))

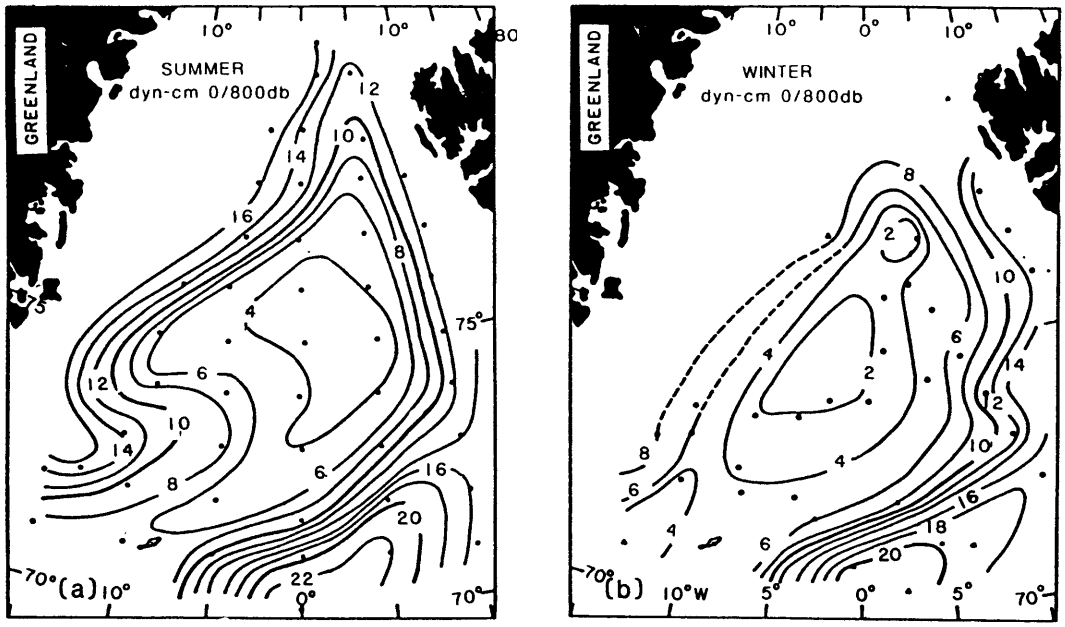

Fig. 3.28 Dynamic topography for Greenland Sea (from Hopkins, 1988)

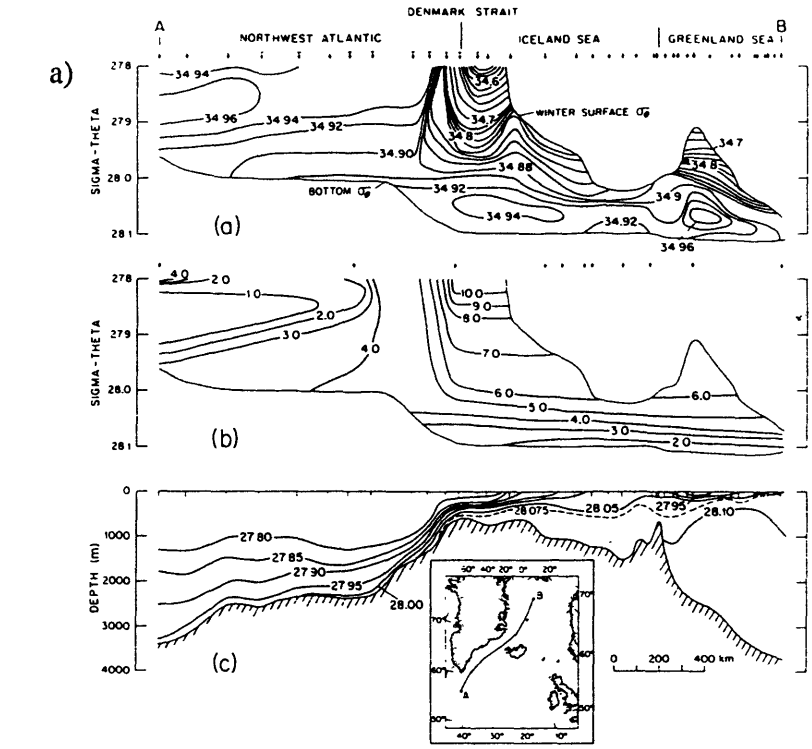

TS diagram, sigma-3 contours

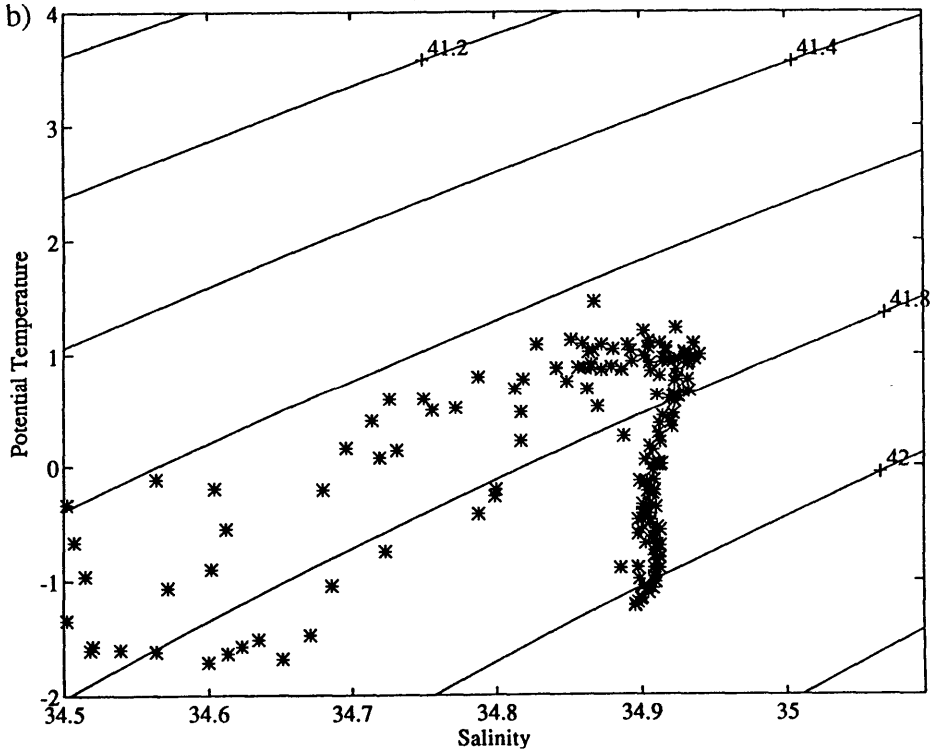

Fig. 3.29 a) θ, S and σ_0 along path in the Denmark Strait (Swift et. al., 1980)
b) θS relations in the East Greenland Current. Polarstern 1988 cruise.

warranted: as the overflowing water sinks and the pressure increases the coldest water will get denser relative to the other (warmer) water mass. One can overlay σ_2 or σ_3 isopycnals on the TS diagrams from the coast of Greenland, and find that at higher pressure the AAW is denser than the rAtW (also shown in fig. 3.29). It is therefore likely that rAtW exits in the Denmark Strait and contributes to the dense overflows. This water will be found above, and not at, the bottom in the North Atlantic.

3.2.2 Formation of Denmark Strait Overflow Water

Hypothesis: The density for the Denmark Strait Overflow Water has been acquired in the Atlantic Domain, by interaction with the atmosphere. Further modifications occur in the Arctic, without change in density.

The Atlantic Water becomes progressively denser and more homogeneous in TS properties as it flows northward in the Norwegian Sea. Two artificial along-path sections, one for the H82 cruise (fig. 3.30) and one for the M85 cruise (fig. 3.31), show the development in T and S: from having a large scatter (σ_0=27.4-27.8) near the Færø-Shetland Channel and in the southern Norwegian Sea, the Atlantic Water becomes progressively denser and more homogeneous in T and S.

As the Atlantic Water flows northward it becomes progressively colder (compare figs. 3.5, 3.6, 3.32, 3.33, 3.34). This happens throughout the entire Atlantic Water, ie. not only on the edges; the along-path variations in temperature are much larger than the across-path variations. The development in TS space is seen in fig. 3.35, where the Atlantic Water becomes progressively denser. The range in density within the Atlantic Water becomes less; a progressively larger portion of the part of the water column belonging to the Atlantic Water acquires the same density (just less than σ_0=28.0),

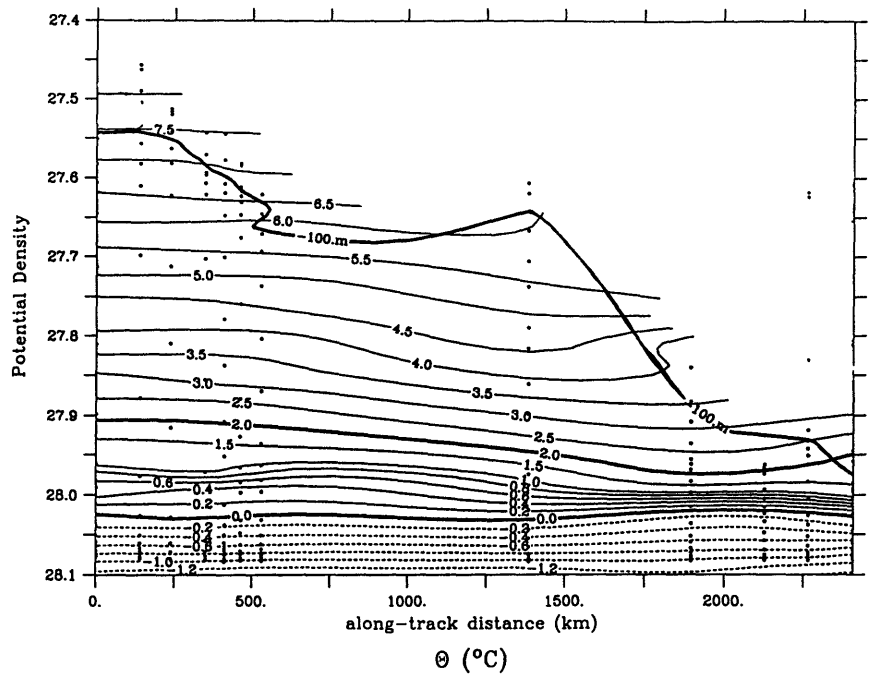

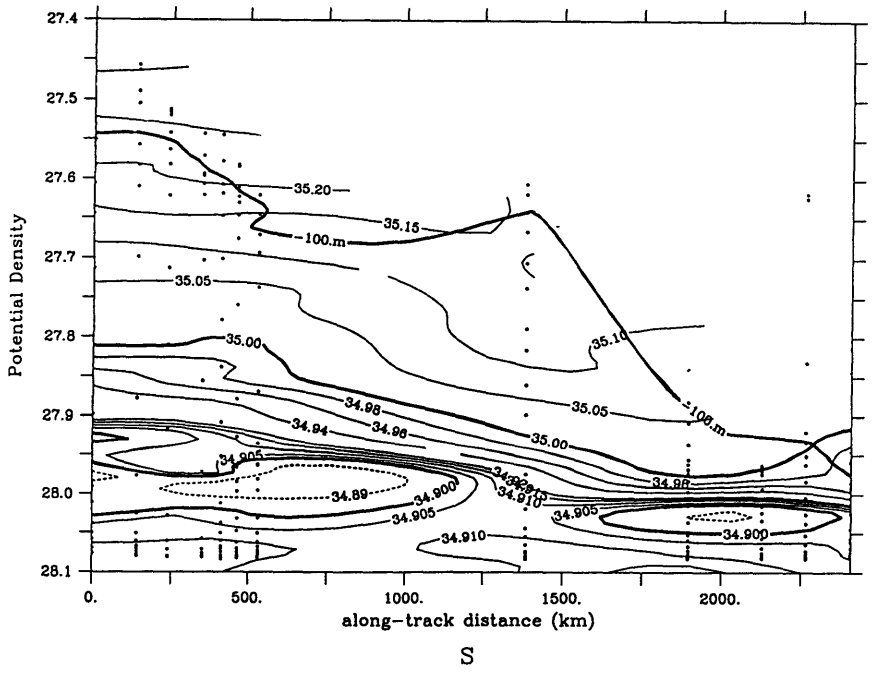

Fig. 3.30 θ and S vs. potential density along path of Atlantic Water for H82 cruise. Cruise track is shown in fig. 3.2b (H82-no).

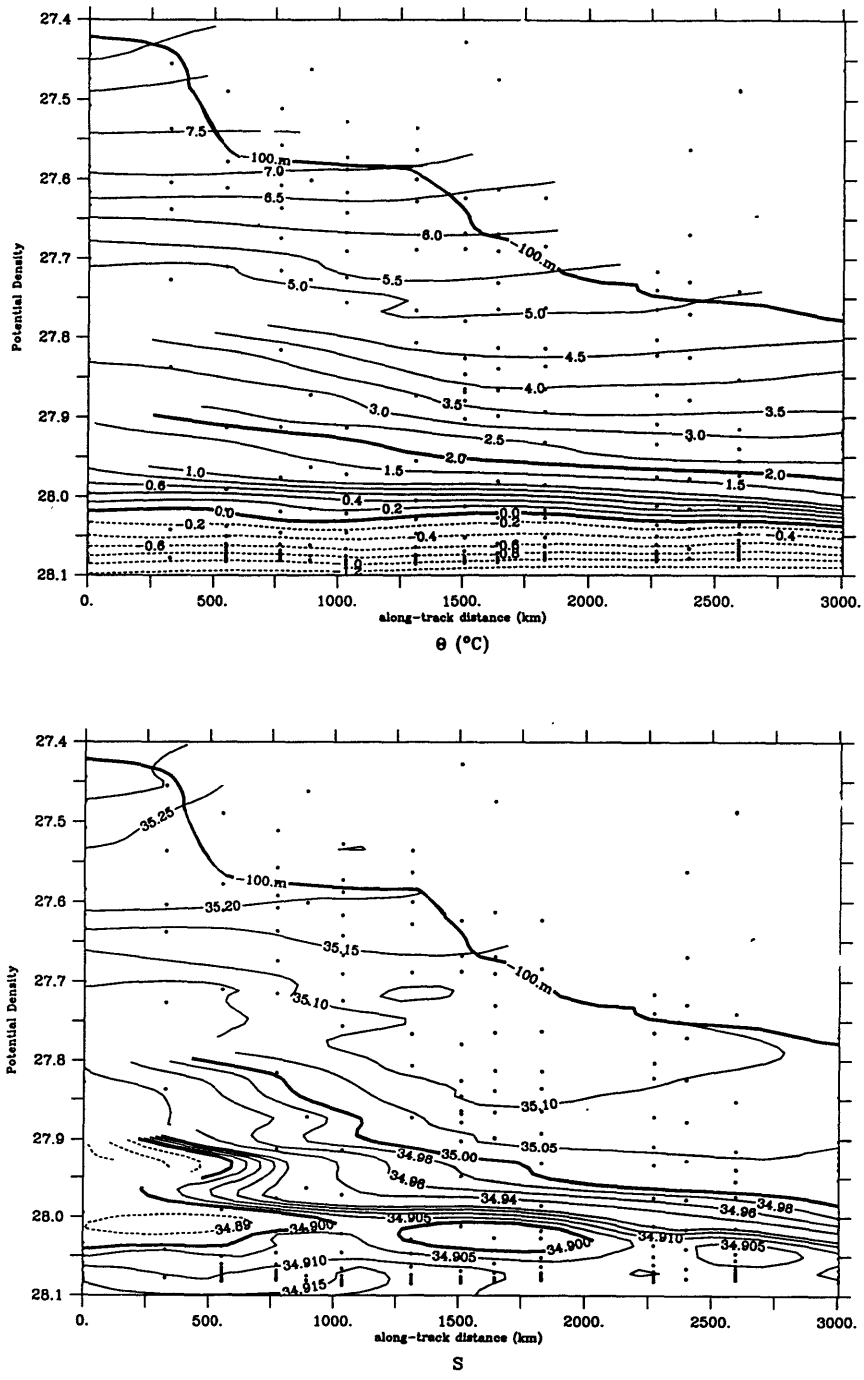

Fig. 3.31 θ and S vs. potential density along path of Atlantic Water for M85 cruise. Cruise track is shown in fig. 3.2b (M85-no).

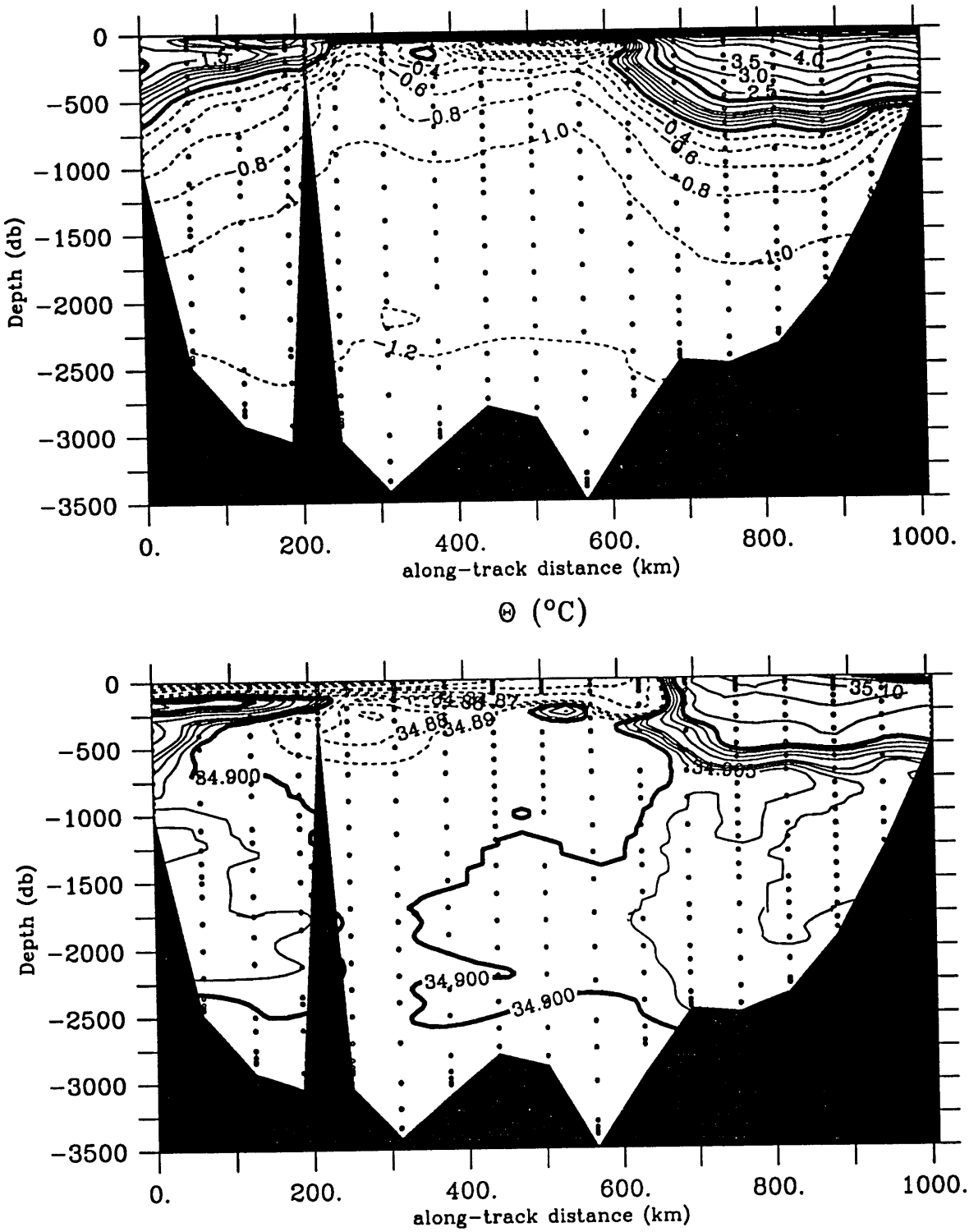

Fig. 3.32 Temperature and salinity crossing southern Greenland Sea at 73.5N. Meteor 1985 transect. Cruise track is shown in fig. 3.2b (M85-73).

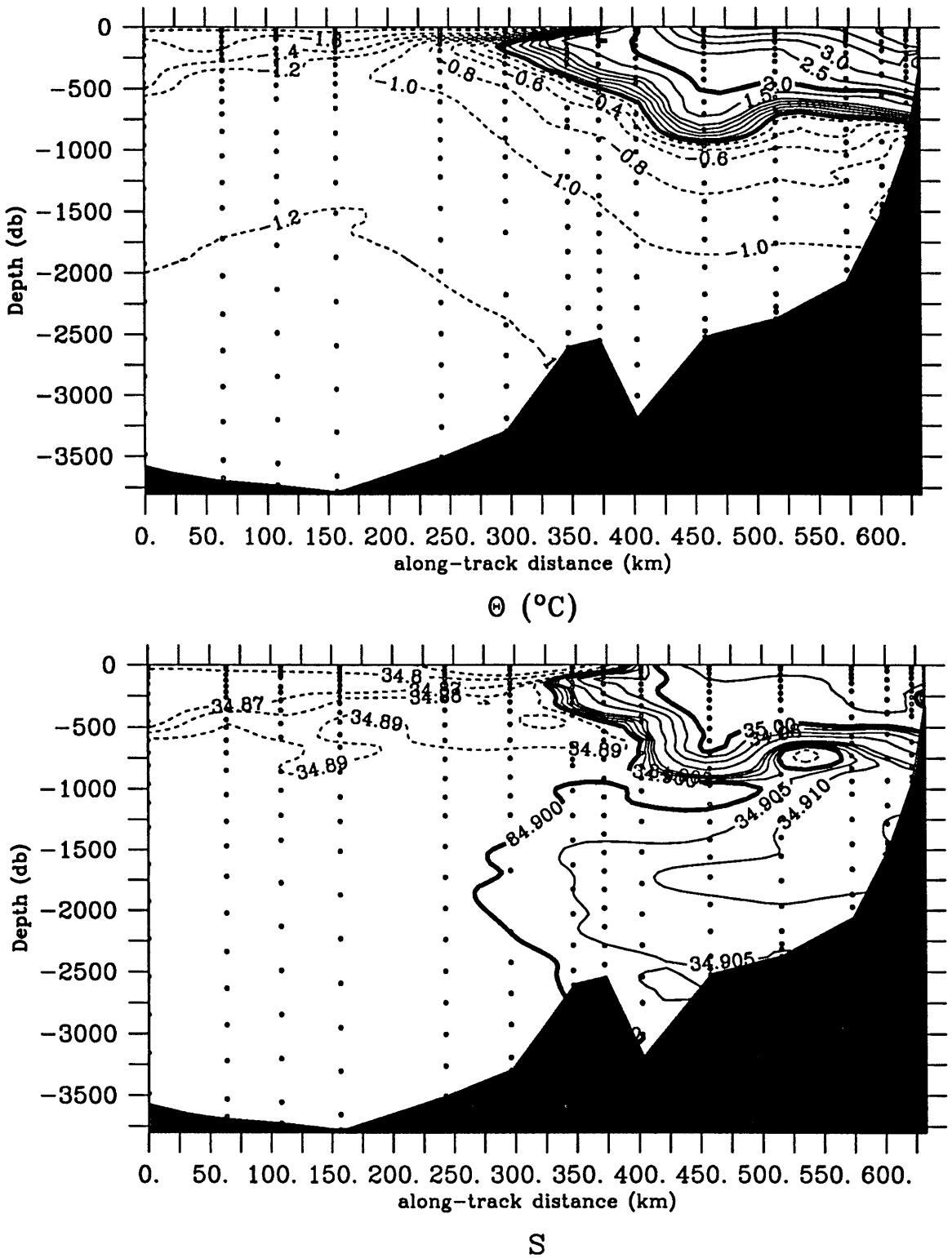

Fig. 3.33 Temperature and salinity crossing eastern Greenland Sea and northern Lofoten Basin at 75N. Hudson 1982 transect. Cruise track is shown in fig. 3.2b (H82-75).

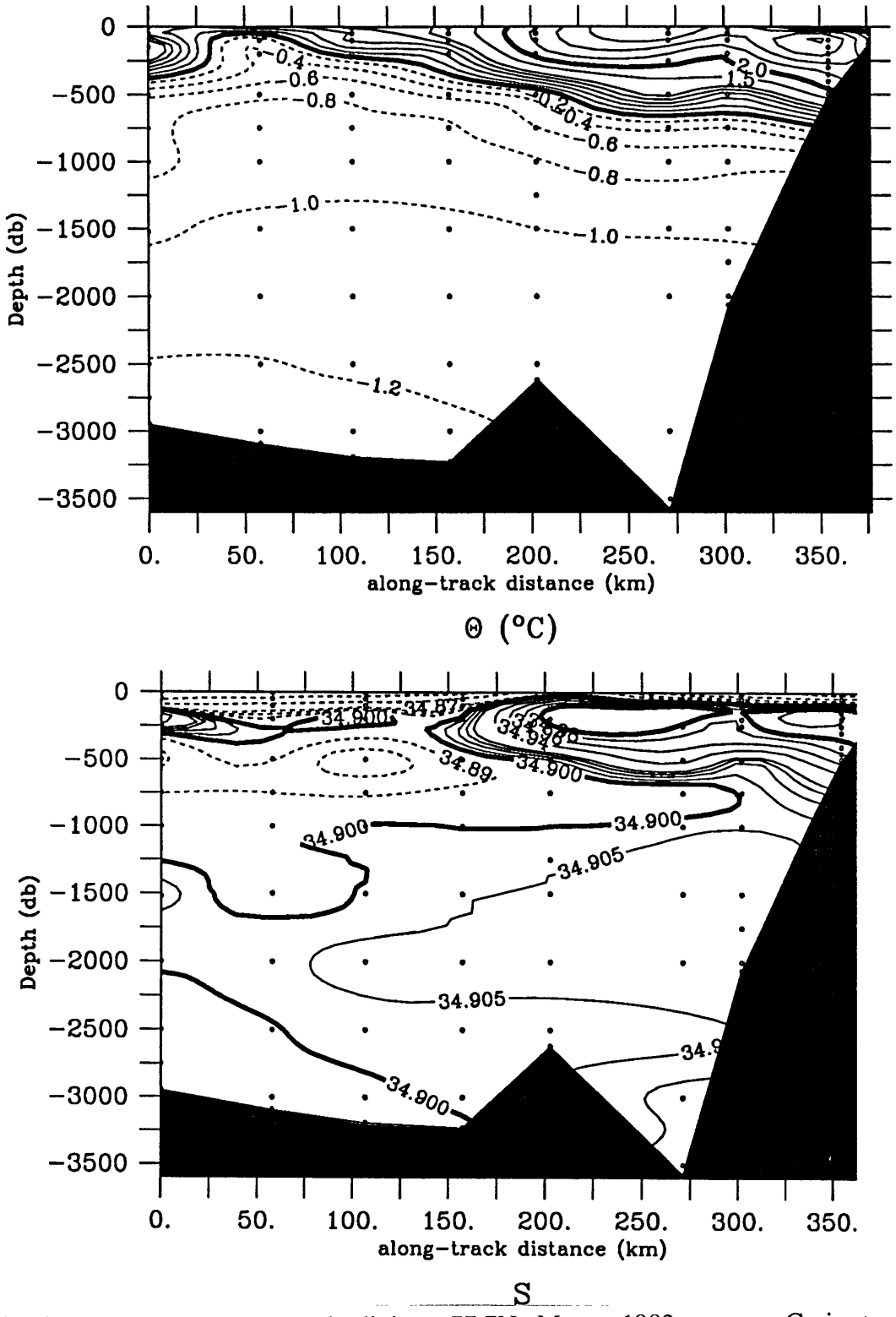

Fig. 3.34 Temperature and salinity at 77.7N. Meteor 1982 transect. Cruise track is shown in fig. 3.2b (M82-77).

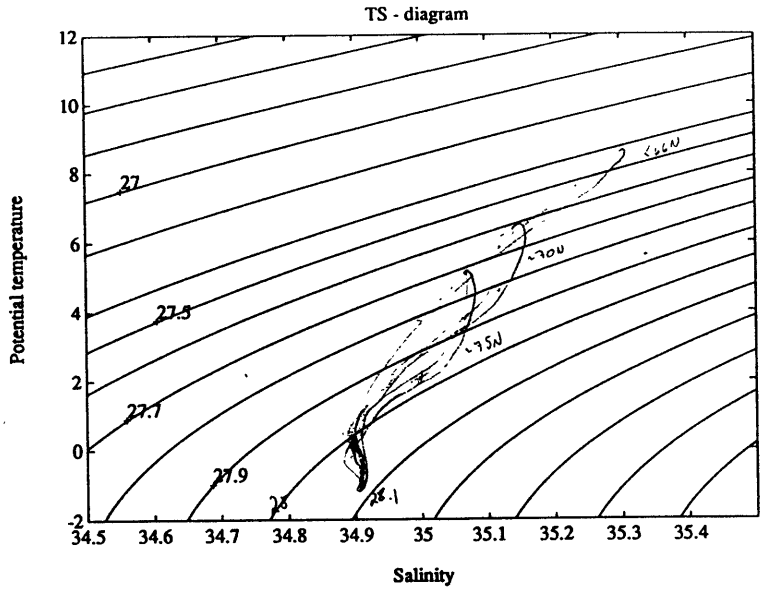

Fig. 3.35 TS diagram for stations in the Norwegian Sea, H82.

indicating that there is a level beneath the Atlantic Water through which the cooling does not reach. This finding indicates that the heat is lost through the air-sea interface, rather than by mixing with neighboring water masses . A similar decrease in salinity is seen in the Atlantic Water as it flows north, indicating that freshwater is gained through the sea surface. However, this change in salinity cannot be explained by precipitation alone, and this freshening of the Atlantic Water will be further discussed in chapter 5.

At the point of subduction in the Fram Strait the density of the Atlantic Water is higher than 27.9, as can be seen in fig. 3.36, which shows typical TS-diagrams for stations in the Fram Strait. The water is dense enough to sink to the bottom of the North Atlantic.

The directly recirculating return Atlantic Water already has its properties determined in the Atlantic Domain. The return Atlantic Water continues unperturbed towards the Denmark Strait in the East Greenland Current as described in the previous section. The core of the return Atlantic Water, as defined by the salinity maximum, is found at more or less the same density level here, and the spread in density remains constant.

In the Arctic Ocean the Atlantic Water is gradually modified to Arctic Atlantic Water. Numerous investigators suggest that within the Arctic Ocean the Atlantic Water propagates cyclonically around the basins. Coachman and Barnes (1963) follow the core of the Atlantic water and infer a circulation scheme based on the gradual reduction in core properties. The circulation is basically cyclonic within the entire Arctic Ocean, with several shortcuts (fig. 3.37). More recent data (Aagaard, 1989) suggest that rather than broad interior movement, the flow is concentrated in narrow boundary currents. Current meter data on the slope north of the Barents Sea at 45 E from 1980 show persistent

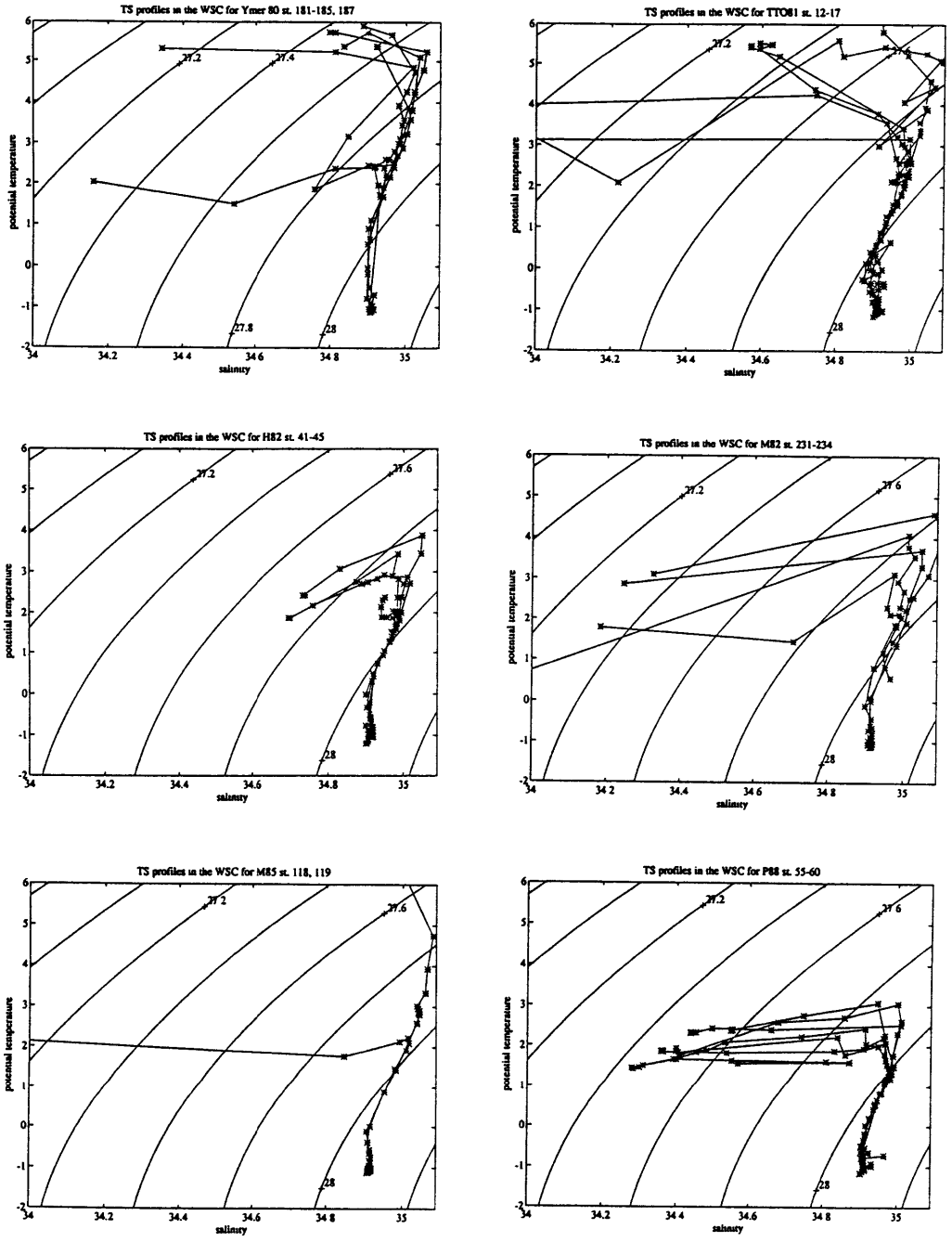

Fig. 3.36 TS profiles for stations near the Fram Strait.

a)

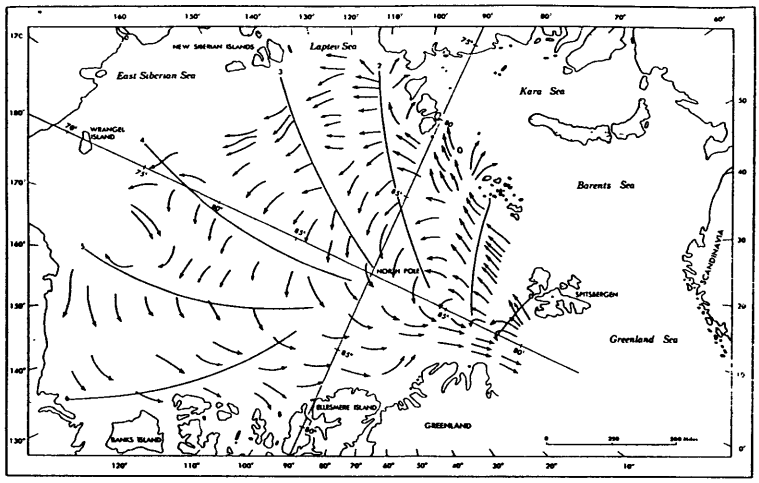

b)

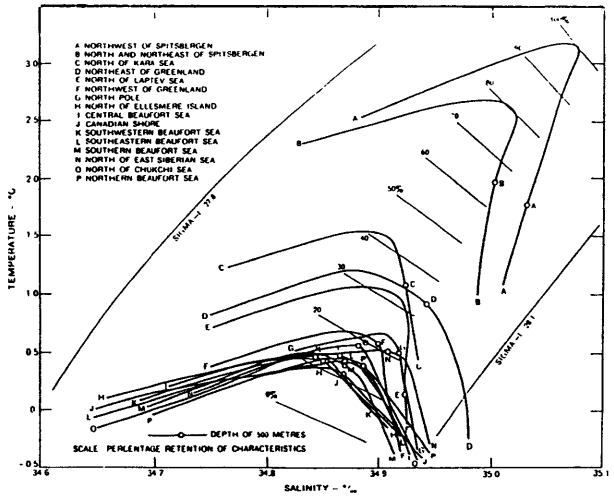

Fig. 3.37 a) circulation in the Arctic (Coachman and Barnes, 1963)
b) Progressive TS diagrams along path in the Arctic (Coachman and Barnes, 1963).

eastward flow along the isobaths (fig 3.38). The section across the Nansen Basin near 30E also shows the core of the Atlantic Water concentrated on the slope (fig 3.25). The gradual decrease in core properties of Coachman and Barnes (1963) is supported in the newer data. Y80 data near 45 E indicate that the salinity maximum has mostly vanished at this point, and that the core temperature is reduced to 1.5 ^{0}C. Data from the LOREX ice station on the Lomonosov Ridge, close to the North Pole, indicate that the core temperature is reduced to 0.5 ^{0}C (fig. 3.39). This is representative of most of the Arctic Ocean; one finds a thick layer with potential temperatures between 0 and 0.5 ^{0}C, situated below the Polar Water, and above the deep waters, both of which has temperatures less than zero. Most of the TS profiles in fig. 3.37 fall into this category. This is the water typically identified Arctic Intermediate Water, renamed above to Arctic Atlantic Water, and found at the stations north of Greenland (fig. 3.40 and table 3.2).

The modification of the Atlantic Water into Arctic Atlantic Water in the Arctic occurs along isopycnals (fig 3.37); the water becomes progressively colder and fresher, but it does not change its density. This can also be seen in fig 3.41 which shows schematically the position of the Atlantic Water in the TS diagram as it enters the Norwegian Sea, as it enters the Arctic Ocean, and as it exits the Arctic (which corresponds to the properties of the Denmark Strait Overflow Water).

a)

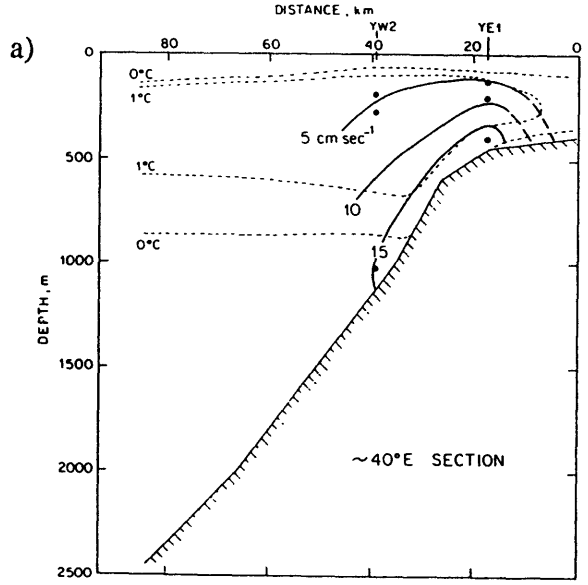

b)

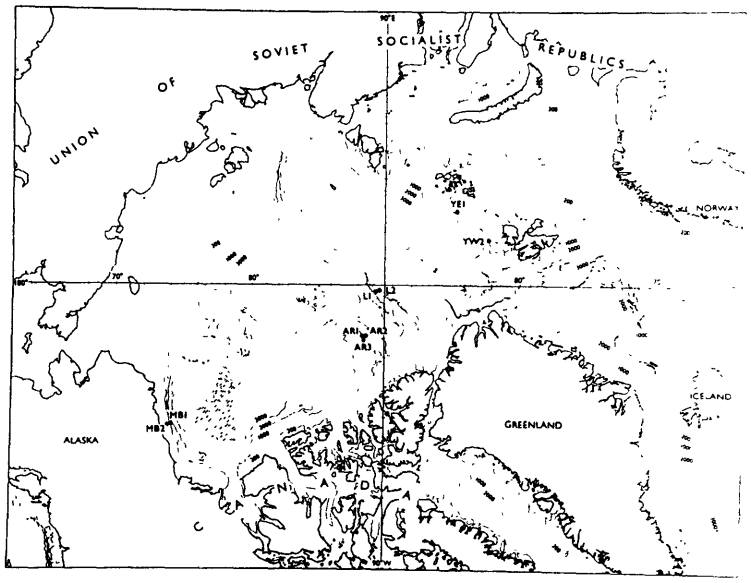

Fig. 3.38 a) current meter observations at 45 E (from Aagaard, 1989)
b) location of current meter moorings (from Aagaard, 1989)

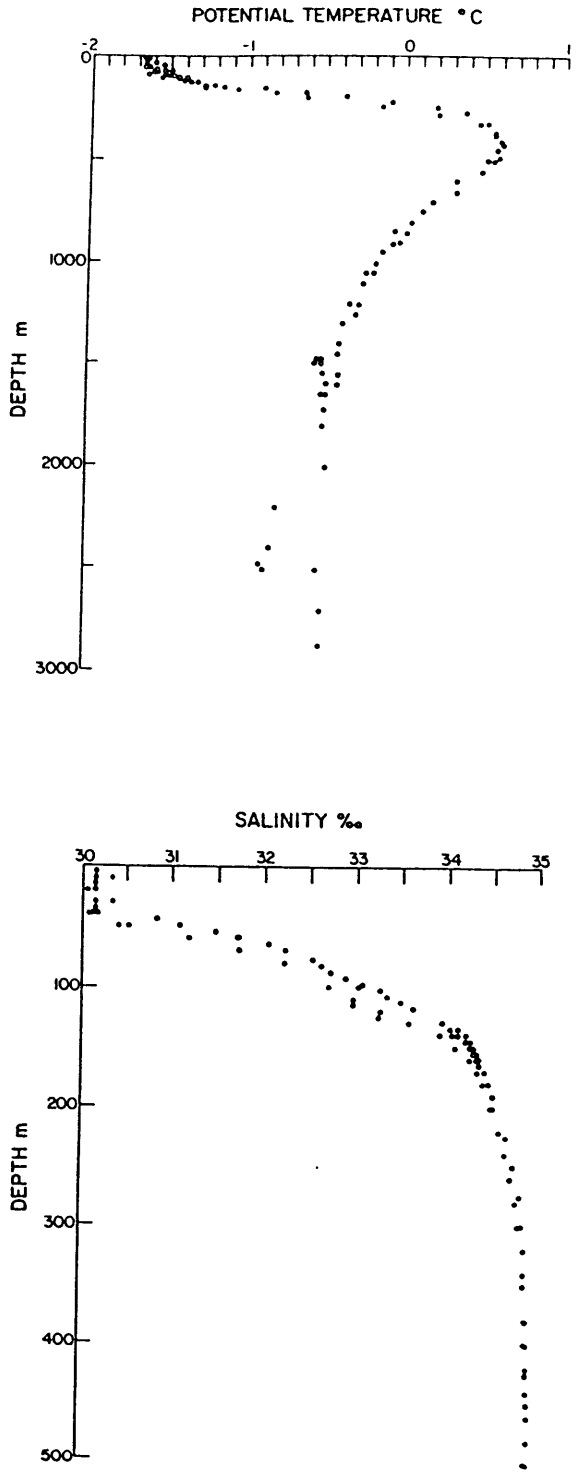

Fig. 3.39 θ and S profiles from the LOREX ice station.

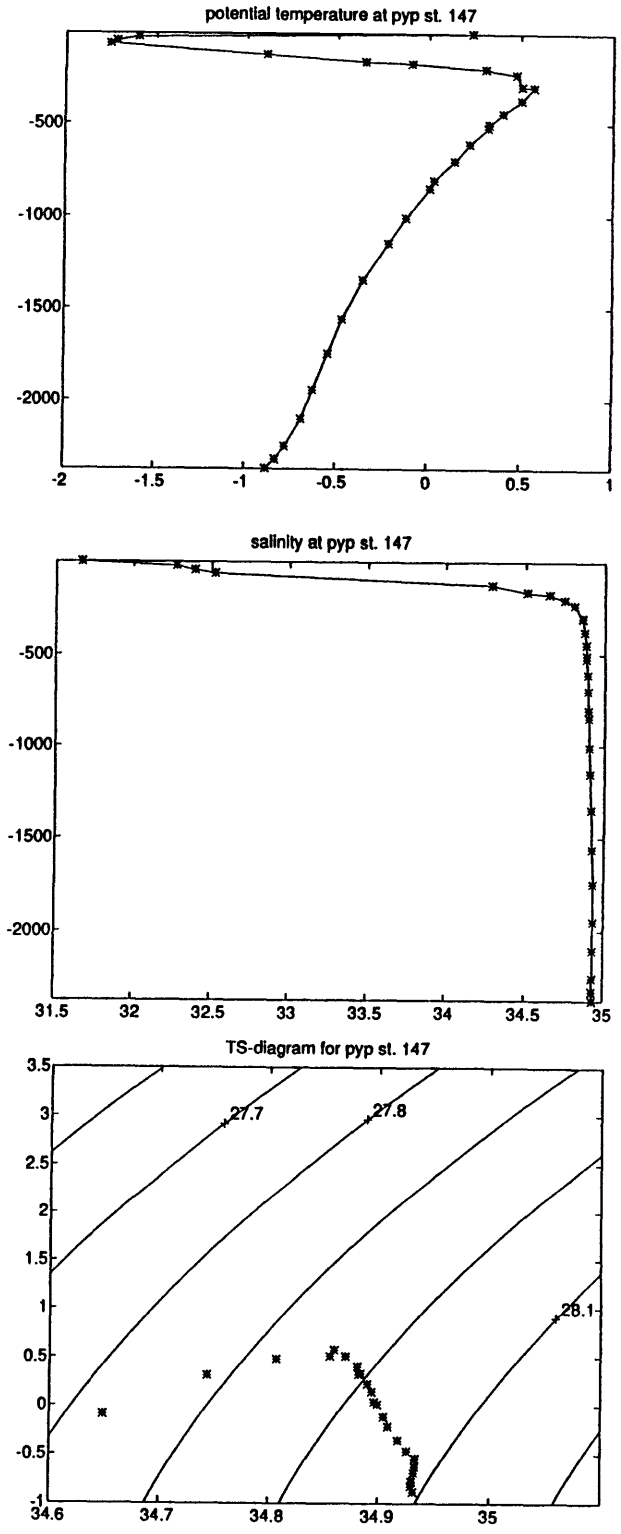

Fig. 3.40 Representative θ and S profile north of Greenland in the Arctic Ocean (Polarstern 1984)

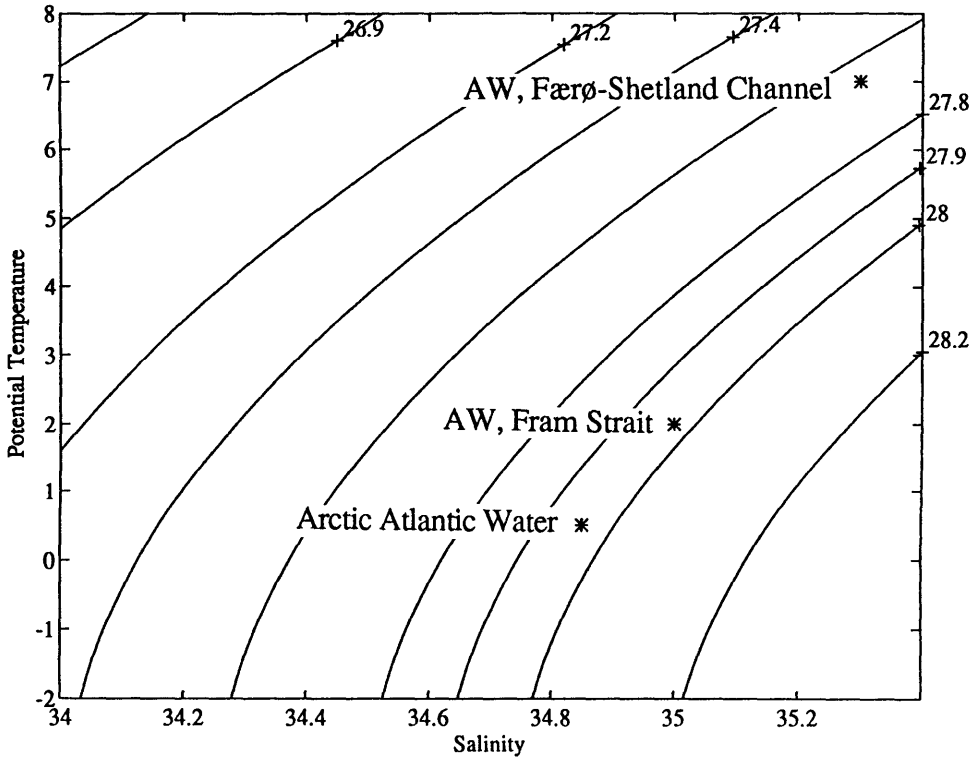

Fig. 3.41 Positions of water masses in the TS diagram: Atlantic water at 60N, at 80N entering the Arctic Ocean, and Arctic Atlantic Water (schematic).

3.2.3 Formation and Propagation of Iceland-Scotland Overflow Water

Hypothesis: The intermediate waters found in the Færø-Shetland Channel are formed not only in the Iceland Sea, but also in the Greenland Gyre, this water mass being the major contribution from the Greenland Gyre. The source of the densest water in the Channel is found in the Arctic, probably formed by surface cooling in the Barents Sea.

The Arctic Intermediate Water near the Iceland-Scotland Ridge is similar to the Intermediate Water core described in section 3.1. The Arctic Intermediate Water was discussed in chapter 2 as one of the water masses constituting the dense overflows over the Iceland-Scotland Ridge.

In chapter 2 it was pointed out that the source of this water traditionally is ascribed to the Iceland Sea, but that Blindheim (1990) suggested that the Greenland Sea could be another source. The salinity sections crossing the Greenland Sea (eg. fig. 3.32) show that the Intermediate Water is spreading from the Greenland Gyre. Although it follows an isopycnal (σ_0=28.0), the water cannot flow out radially as the circulation in the Greenland Sea is cyclonic (fig. 3.28). The current meter mooring at 75 N shows that at the level of the Intermediate Water in the East Greenland Current the velocity field has a small outward component compared to the levels above and below (see table 3.3 and fig. 3.11), suggesting that the Intermediate Water spirals out of the Gyre. The high oxygen content of the Intermediate Water suggests that the Greenland Gyre is a source of this water, as the oxygen level within the Greenland Gyre is high due to the recent contact with the atmosphere. As mentioned above, the Intermediate Water is completely unmappable - hardly surprising given the thinness of the layer and the potential for interannual variability - so one cannot predict the path this water will take towards the

Channel, but in the primary data set it is found everywhere in the Norwegian Sea, providing a path for it to flow to the Iceland-Scotland Ridge.

Except for the spreading of the Intermediate Water there are sharp hydrographic boundaries between the Greenland Gyre and the surroundings, indicating that the Intermediate Water is the only major water mass exported from the Gyre.

Clarke et. al. (1990) show a time series of the temperatures of the deep water (below 2000 m) in the Greenland Gyre from 1955 to 1981. This time series shows that the deep water became progressively colder during the 1960's, and then started warming up. I have extended this time series through to 1989 using the primary data set (fig. 3.42). The temperature of the deep water increased from -1.27 ^{0}C to -1.20 ^{0}C during the eighties. Uncertainties, estimated from the scatter over several stations in the deep water; typically 0.005-0.01 ^{0}C, suggest that an increase of 0.07 ^{0}C is significant. The corresponding time series for salinity indicates that S increases from 34.891 to 34.895, a change barely above the instrument error. Except for the decrease in salinity between the Hudson and the Meteor 82 cruises the salinities have been increasing during the 1980's.

The deep water in the Greenland Gyre can be renewed by vertical convection only if the new water has an equal or higher density (lighter water would not be able to penetrate the denser deep water). To maintain a constant density in the deep water of the Greenland Gyre during the 1980's, with the increasing temperatures, the salinity would have to be increased to 34.9. The average deep salinity has only increased by half that amount. The deep water has therefore become less dense, indicating that the vertical convection has been reduced if not shut off during the 1980's. Such a termination of deep water formation in the Greenland Gyre in the 1980's has been found by Schlosser et. al. (1991), using transient tracers. The warming of the deep water can be attributed to a lateral intrusion of the Deep Water-boundary current, as discussed in section 3.1.

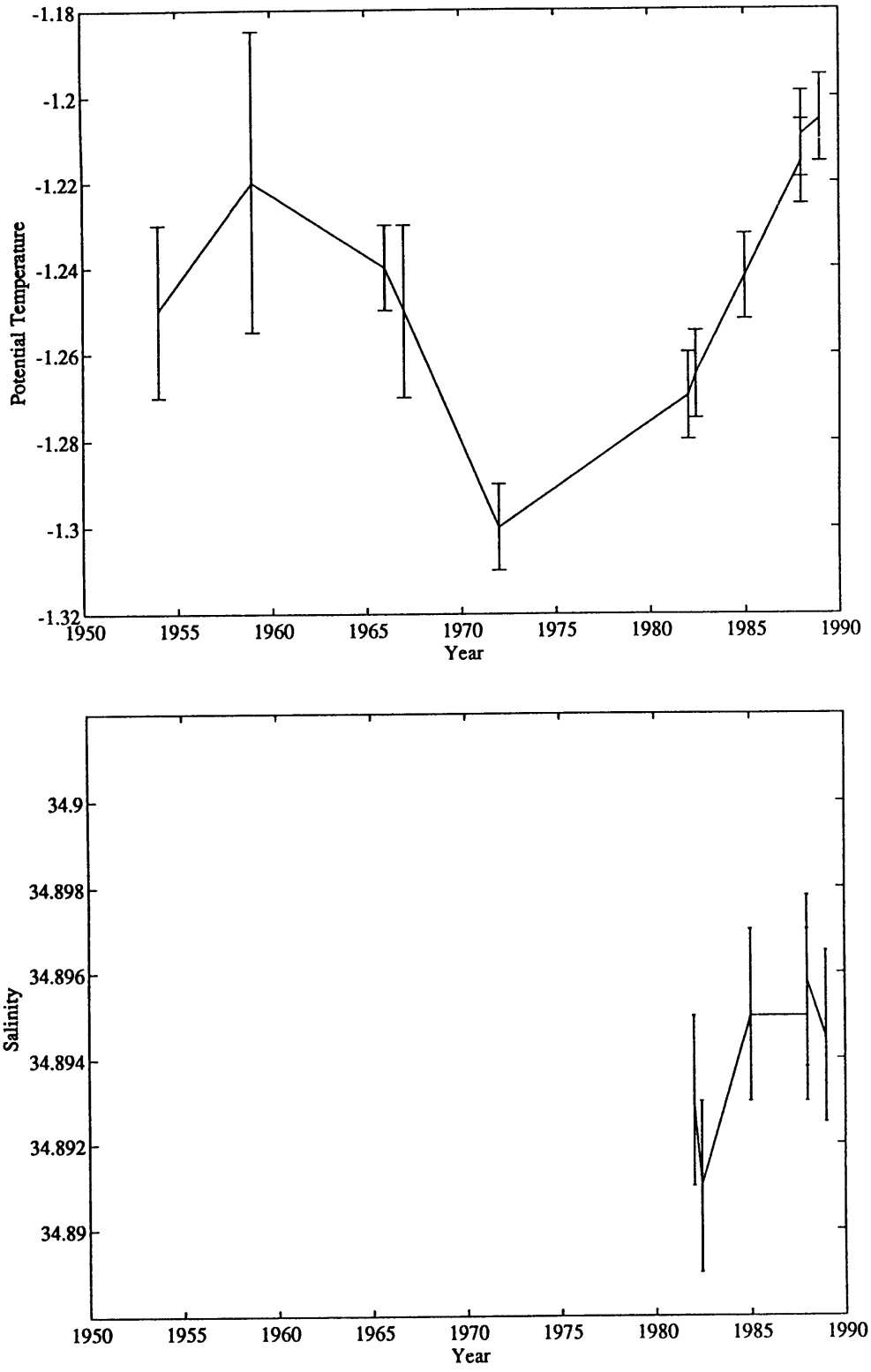

Fig. 3.42 Time series of potential temperature and salinity in the deep water of the Greenland Gyre (data point up to 1980 evaluated by Clarke et. al., 1990)

Substantial transport of the lightest NSDW (-0.5 to 0 ^{0}C) through the Færø-Shetland Channel occurred during the 1980's (Saunders 1990). Since there was no significant contribution from the GSDW, the NSDW must have formed primarily from sources in the Arctic Ocean.

The branch of the Atlantic Water that enters the Barents Sea must , by mass conservation, continue into the Arctic Ocean. As it enters, the Atlantic Water is already fairly dense. Within the Barents Sea it is exposed to ice-free conditions and extreme surface cooling (see fig. 2.6 and 4.6). It is therefore likely that this water continues to increase its density during its transit through the Barents Sea, so that bwhen it enters the Arctic Ocean it is as dense as the deep water there. The flow is substantial - O(1-2 Sv), large enough to feed the overflow through the Færø-Shetland Channel. This process is largely overlooked in the literature (except for a brief mention by Aagaard et. al. (1985b)). Instead, the focus has been on dense water formation by brine rejection, as discussed in chapter 2. However, the findings of Martin and Cavalieri (1989) indicate that the Arctic shelves might not be able to produce enough dense water to supply the Arctic Ocean . The character of the throughflow of Atlantic Water in the Barents Sea will presumably become better known in the future, as recently collected data become available.

3.3 New Circulation Scheme

The new circulation scheme is presented in fig. 3.43. The emphasis has shifted from mid-gyre convection to cooling of the Atlantic Water within the Norwegian Sea. The gyres are still producing dense overflow water for the Iceland-Scotland Ridge, especially the Intermediate Water and the North Icelandic Winter Water, but the waters entering the gyres to produce the denser water have already been cooled in the Atlantic Domain ("preconditioned" before entering the gyres). For the dense overflows in the

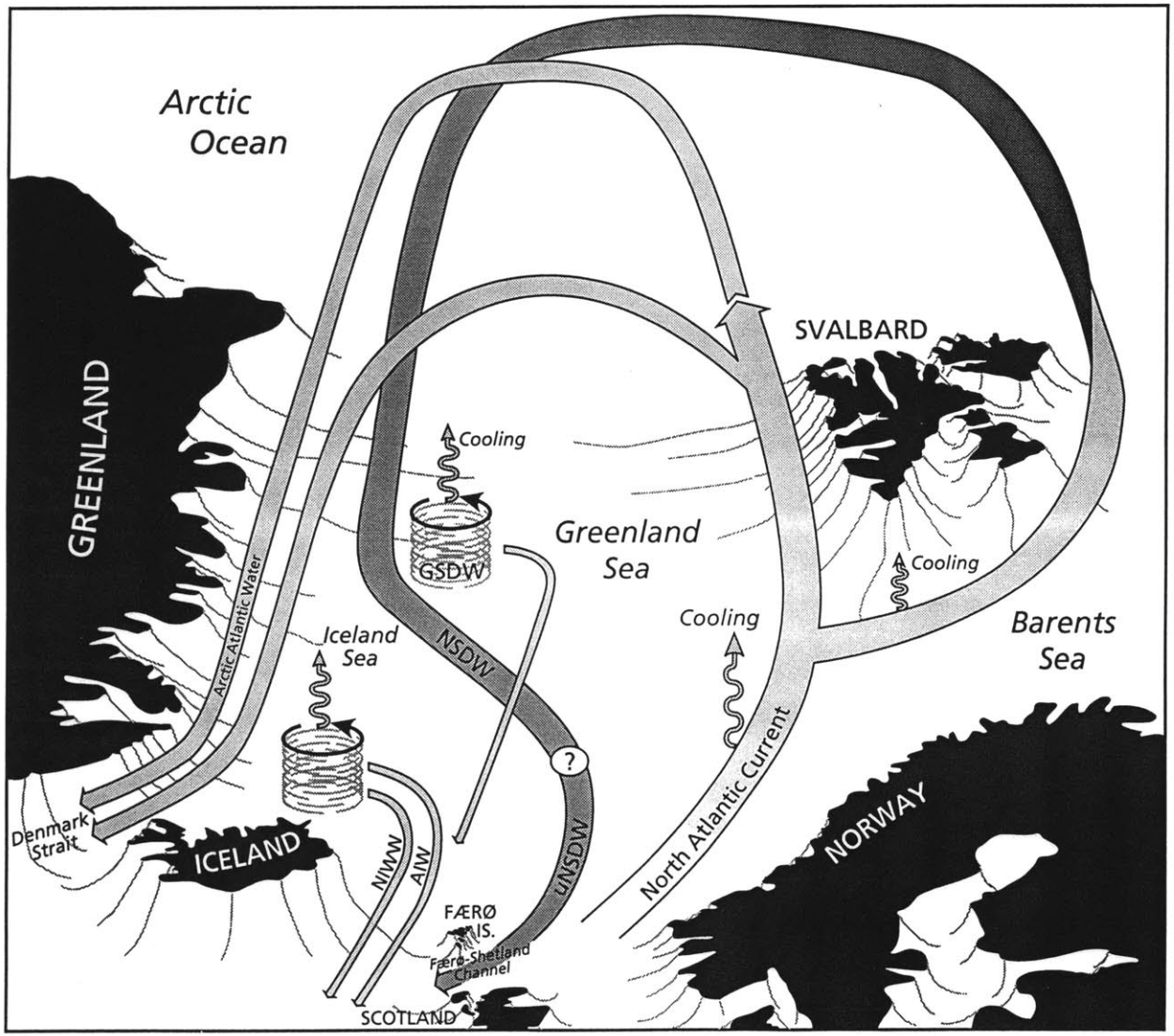

Fig. 3.43 New circulation scheme

Denmark Strait the gyres are of no importance: the freshest part of the dense water in the Denmark Strait comes from the reservoir of Arctic Atlantic Water in the Arctic Ocean, flowing directly to the Denmark Strait within the East Greenland Current. In addition, recirculating Atlantic Water in the East Greenland Current exits in the Denmark Strait. The densest water within the Nordic Seas, except for the Greenland Sea Deep Water in the Greenland Sea, are also produced without any influence of the gyres, at least during the 1980's.

Chapter 4

Box Model

To ensure that the circulation scheme formulated in chapter 3 satisfies simple conservation statements for heat, mass and salt, and to test the scheme, a box model has been constructed. The model includes all the basins of the Arctic Ocean/ Nordic Seas, divided into six general areas: the Norwegian Sea, the Barents Sea, the Arctic Ocean, the Greenland Sea, the Iceland Sea, and an elongated area along the coast of Greenland from the Fram Strait to the Denmark Strait, here designated as East Greenland (fig. 4.1). Within these areas each major water mass, as defined in chapter 3, defines one box in the vertical. For the regions which have no layering of watermasses, a division is made between an upper and a lower box. As illustrated in fig. 4.2, the vertical resolution is largest in the East Greenland area (5 boxes) and in the Norwegian Sea (3 boxes), is less in the Greenland Sea, the Arctic Ocean and the Iceland Sea, where only an upper and a lower box are defined, and is least in the shallow Barents Sea (see also table 4.1). A box interacts with other boxes through interfaces on which temperature and salinity are prescribed (fig. 4.3a). All boxes that are in physical contact are allowed to interact, and the temperature and salinity properties on the interfaces are determined from the data. The connections are shown in fig. 4.3b, and listed in table 4.1.

Within each box conservation statements for mass, heat and salt are written. The surface boxes include the effects of air-sea fluxes, river runoff, ice freezing and ice melting. The governing equations are:

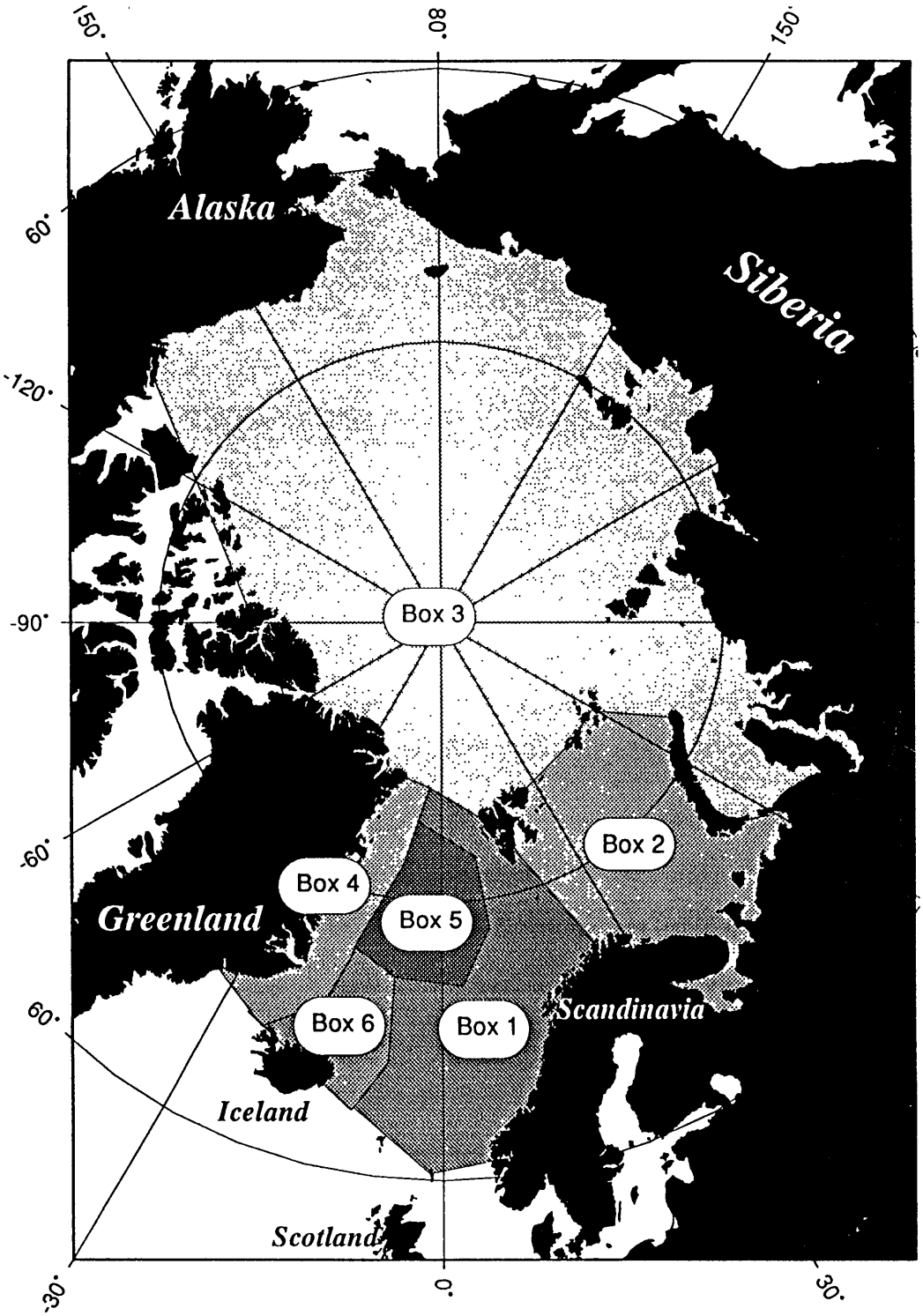

Fig. 4.1 The six areas of the box model.

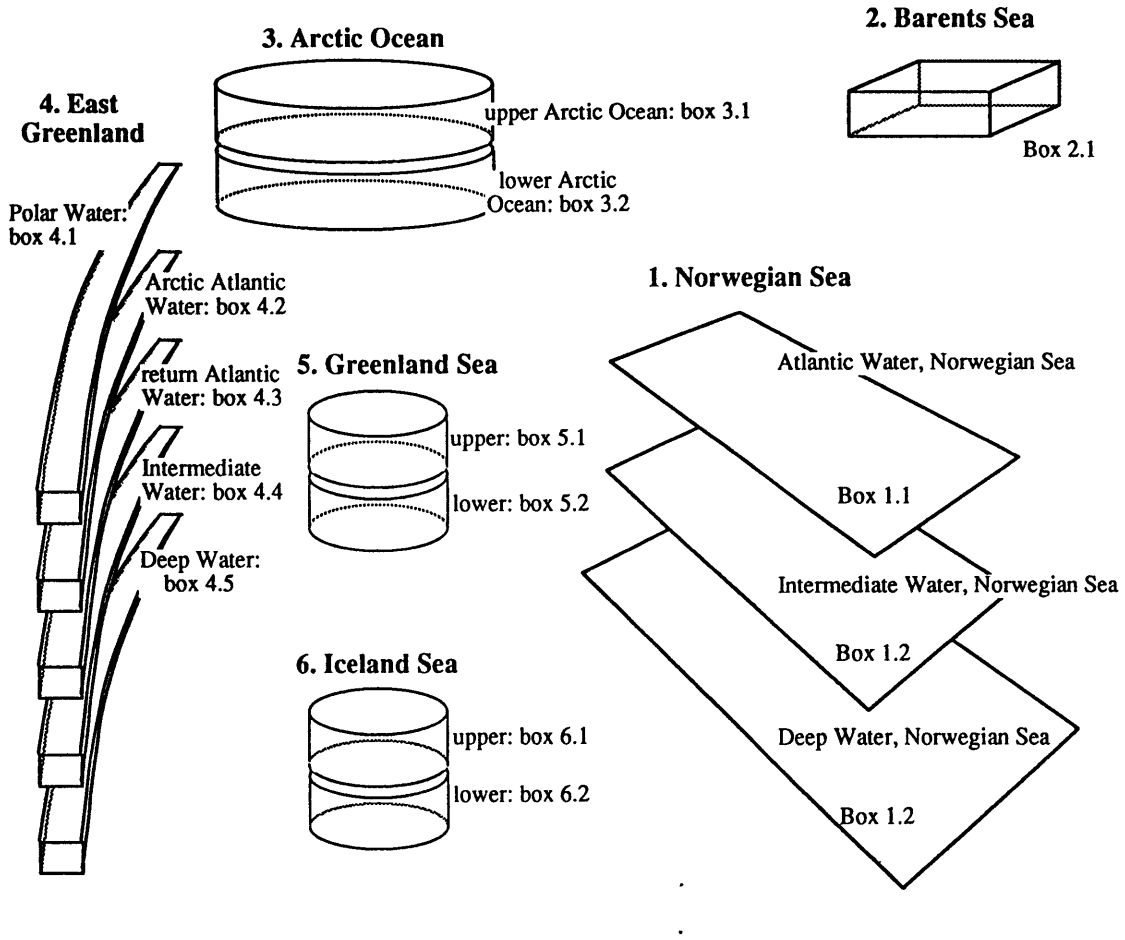

Fig. 4.2 The distribution of boxes in the model.

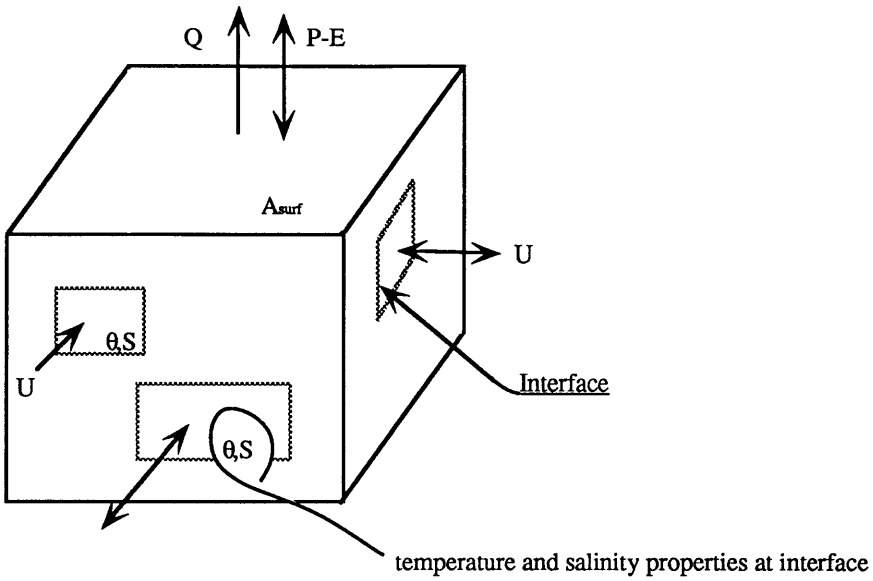

Fig. 4.3a Description of a box

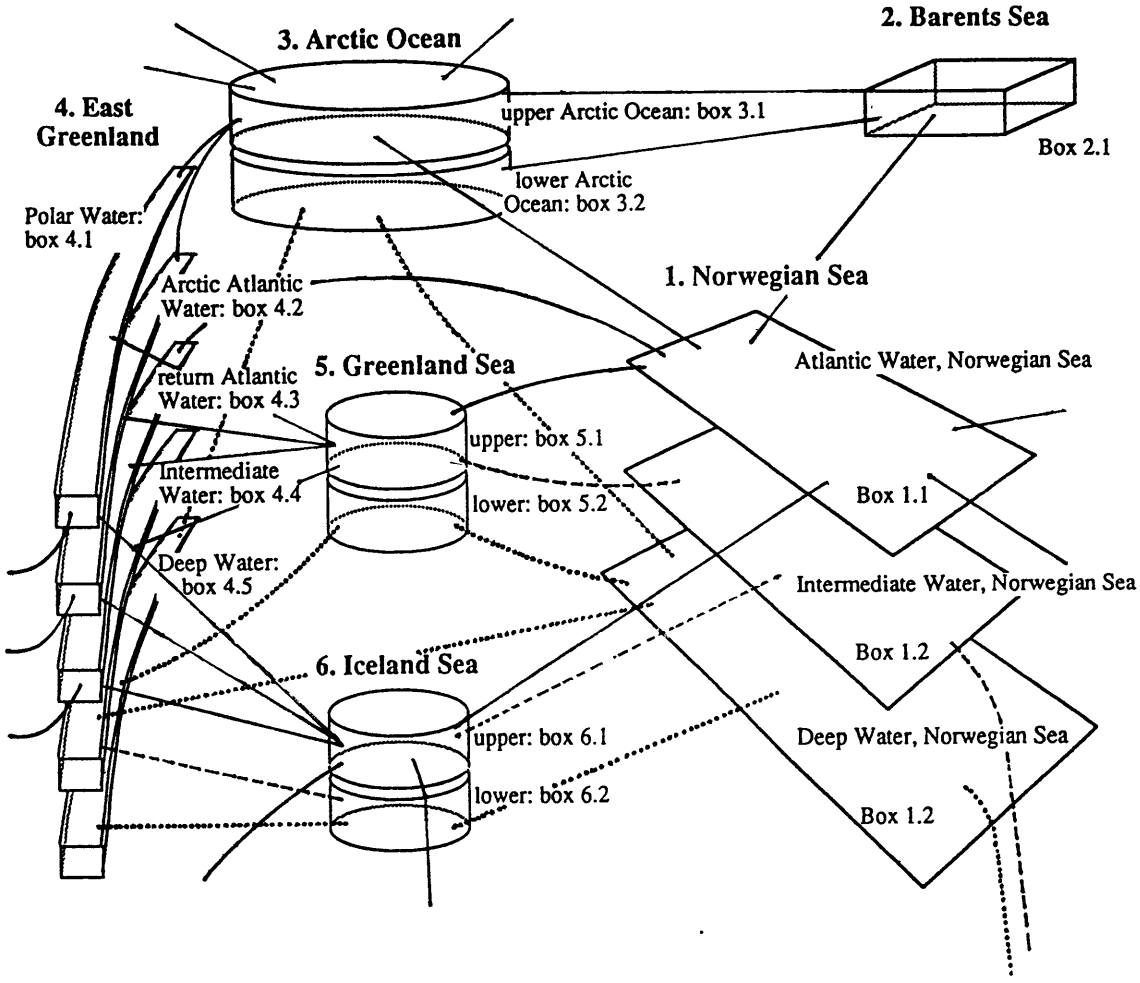

Fig. 4.3b Connections between boxes in box model

Table 4.1 Description of the boxes and their interfaces

1.1 Atlantic, Norwegian Sea
Inflow from Atlantic
NCC + runoff
Iceland Sea, upper, eastward, 6.1
Iceland Sea, upper, westward, 6.1
Greenland Sea, upper, 5.1
return Atlantic, 4.3
Arctic, upper, 3.1
Barents Sea, 2.1
Intermediate Water, vertical, 1.2
Air-Sea, salt

1.2 Intermediate Water, NS
Iceland Sea, upper, 6.1
Greenland Sea, upper, 5.1
Arctic, upper, 3.1
Færø-Shetland Channel
Atlantic, vertical, 1.1
Deep Water, vertical, 1.3

1.3 Deep Water, NS
Iceland Sea, lower, 6.2
Greenland Gyre, lower, 5.2
Deep Water, East Greenland, 4.5
Arctic, lower, 3.2
Færø-Shetland Channel
Intermediate Water, vertical, 1.2

2.1 Barents Sea
Atlantic, NS, 1.1
runoff
Arctic, upper, 3.1
Arctic, lower, 3.2
Air-Sea Interface, heat
Air-Sea Interface, salt

3.1 Arctic, upper
Atlantic, NS, 1.1
Intermediate Water, NS, 1.2
Barents Sea, 2.1
Bering Sea
Canadian Archipelago
Polar Water, EG, 4.1
Arctic Atlantic Water, EG, 4.2
Intermediate Water, EG, 4.4
runoff
Arctic, lower, vertical, 3.2
Air-Sea Interface, heat
Air-Sea Interface, salt

3.2 Arctic, lower
Barents Sea, 2.1
Deep Water, NS, 1.3
Deep Water, EG, 4.5
Arctic, upper, vertical, 3.1

4.1 Polar Water, East Greenland
Arctic, upper, 3.1
Greenland Gyre, 5.1
Iceland Gyre, upper, 6.1
Denmark Strait
runoff
Arctic Atlantic Water, vertical, 4.2
Air-Sea Interface, heat
Air-Sea Interface, salt

4.2 Arctic Atlantic Water, EG
Arctic, upper, 3.1
Greenland Gyre, upper, 5.1
Iceland Gyre, upper, 6.1
Denmark Strait
Polar Water, vertical, 4.1
rAtW, vertical, 4.3

4.3 return Atlantic Water, EG
Atlantic Water, NS, 1.1
Greenland Gyre, upper, 5.1
Iceland Sea, upper, 6.1
Iceland Sea, lower, 6.2
Denmark Strait
Arctic Atlantic Water, vertical, 4.2
Intermediate Water, vertical, 4.4

4.4 Intermediate Water, EG
Arctic, upper, 3.1
Greenland Gyre, upper, 5.1
Iceland Sea, lower, 6.2
rAtW, vertical, 4.3
Deep Water, vertical, 4.5

4.5 Deep Water, East Greenland
Arctic, lower, 3.2
Greenland Gyre, lower, 5.2
Deep Water, Norwegian Sea, 1.3
Iceland Sea, lower, 6.2
Intermediate Water, vertical, 4.4

5.1 Greenland Gyre, upper
Atlantic Water, NS, 1.1
Intermediate Water, NS, 1.2
Intermediate Water, East Greenland, 4.4
Polar Water, EG, 4.1
Arctic Atlantic Water, EG, 4.2
return At;lantic Water, EG, 4.3
Greenland Gyre, lower, vertical
Air-Sea Interface, heat
Air-Sea Interface, salt

5.2 Greenland Gyre, lower
Deep Water, NS, 1.3
Deep Water, EG, 4.5
Greenland Gyre, upper, vertical, 5.1

6.1 Iceland Sea, upper
Atlantic Water, NS, 1.1
Intermediate Water, NS, 1.2

Polar Water, EG, 4.1
Arctic Atlantic Water, EG, 4.2
return Atlantic Water, EG, 4.3
Atlantic, Irminger
North Atlantic Winter Water
Iceland Sea, lower, vertical, 6.2
Air-Sea Interface, heat
Air-Sea Interface, salt

6.2 Iceland Sea, lower

Deep Water, NS, 1.3
return Atlantic Water, EG, 4.3
Intermediate Water, EG, 4.4
Deep Water, EG, 4.5
Iceland Sea, upper, vertical, 6.1

Total Arctic Mediterranean

Atlantic, NS
North Icelandic Winter Water
Atlantic, Irminger
Polar Water, Denmark Strait
AAW, Denmark Strait
rAtW, Denmark Strait
Canadian Archipelago
Bering Strait
IW, Færø-Shetland Channel
DW, Færø-Shetland Channel
runoff, Norwegian Sea
runoff, Barents Sea
runoff, Arctic
runoff, West Greenland
Air-Sea, heat, NS
Air-Sea, salt, NS
Air-Sea,, heat, Barents Sea
Air-Sea, salt, Barents Sea
Air-Sea, heat, Arctic
Air-Sea, salt, Arctic
Air-Sea, heat, East Greenland
Air-Sea, salt, East Greenland
Air-Sea, heat, Greenland Gyre
Air-Sea, salt, Greenland Gyre
Air-Sea, heat, Iceland Sea
Air-Sea, salt, Iceland Sea

Conservation of mass:

$$\frac{\partial \rho}{\partial t} + \nabla \cdot \rho \vec{u} = 0 \tag{4.1}$$

Conservation of heat:

$$\frac{\partial \rho \theta}{\partial t} + \nabla \cdot \rho \theta \vec{u} = 0 \tag{4.2}$$

Conservation of salt:

$$\frac{\partial \rho S}{\partial t} + \nabla \cdot \rho S \vec{u} = 0 \tag{4.3}$$

Assuming the system to be in a steady state, and integrating over the volume under consideration, one obtains, in finite difference form:

$$\sum^{V} \rho U sgn + \sum^{H} \rho w A_H sgn + \sum^{V} \rho_{ice} U_{ice} sgn = 0 \tag{4.4}$$

$$\sum^{V} \rho \theta U sgn + \sum^{H} \rho \theta w A_H sgn - \sum^{V} \rho_{ice} L U_{ice} sgn/c_p - \frac{Q}{c_p} A_{surf} sgn = 0 \tag{4.5}$$

$$\sum^{V} \rho S U sgn + \sum^{H} \rho S w A_H sgn - \rho (P-E) S A_{surf} sgn = 0 \tag{4.6}$$

where:

sgn direction of inward normal: positive for east, north, and up.

U horizontal transport through a vertical section [10^6 m^3/s]

U_{ice} horizontal transport of ice through a vertical section [10^6 m^3/s]

w vertical velocity across horizontal interface [m/s]

Q total heat flux across the air-sea interface [W/m^2] (positive = oceanic heat loss)

P-E precipitation less evaporation across air-sea interface [mm/year]

Σ summation over all vertical (V) or horizontal (H) (excluding sea surface) interfaces in box

A_H area of horizontal interface(excluding sea surface)

A_{surf} area of air-sea interface

ρ *in situ* density of water

ρ_{ice} *in situ* density of ice

θ potential temperature at interface

S salinity at interface

L heat of fusion for sea ice ($3.35 \cdot 10^5$ J/kg)

c_p heat capacity of water ($3.99 \cdot 10^3$ J/^{0}Ckg)

4.1 Inverse Solution

The system of equations can be cast in matrix form and solved by the method of singular value decomposition (svd), a method that was first used for oceanographic data by Wunsch (1978). In this case the model is a kinematic inverse model, with unknowns U, w, Q and P-E[1]. The svd allows for both overdetermined and underdetermined systems, and seeks the solution that has minimum length and satisfies the system of equations with minimum residuals (Menke, 1984). If all the terms in the equations are unknown the system can be written:

$$Ab=0 \tag{4.7}$$

[1]The more traditional inverse model - using geostrophic shear and solving for reference level velocities (Wunsch, 1978) is not feasible, due to the uneven data coverage: in particular, transects are not available for several of the straits, and the station spacing is in general too wide to properly resolve the boundary currents.

where A is the data matrix and b is the solution vector. To obtain a heterogeneous system it was chosen to make initial estimates of the unknowns. These initial estimates are based on direct current estimates, estimated air-sea fluxes, and the core analysis of chapter 3:

let:

$$U=U_0 + U_b$$

$$w=w_0+w_b \qquad \text{etc.}$$

where the subscript zero refers to the initial estimate and the subscript b refers to the corresponding solution element from the svd. The sum of these: U/w/Q/P-E, will be denoted "total" transport/vertical velocity etc. These are the values that will be referred to when the results are discussed in later sections. In matrix form the system now becomes:

$$A \cdot b + n = \Gamma \tag{4.8}$$

where:

A is the data matrix of equation coefficients, containing such terms as $\rho\theta$.

b is the solution vector, containing such terms as horizontal transports (U_b), ie. deviation from the initial estimates.

n represents the noise in the system

Γ is the right hand side of the equations, containing such terms as $\rho\theta U_0$ and known imbalances in the equations.

Since the svd tends to yield solution elements that are proportional to the magnitude of the columns of the A-matrix, and residuals that are proportional to the magnitude of the rows of the A-matrix, the A matrix is weighted (Wunsch, 1978):

$$A' = S^{-1/2} A W^{1/2}, \quad b' = W^{-1/2} b, \quad \Gamma' = S^{-1/2} \Gamma \tag{4.9}$$

where, formally, S^{-1} is the covariance matrix of the observations, and W^{-1} is the covariance matrix of the solution.

The singular value decomposition of A yields:

$$A' = U\Lambda V^T \tag{4.10}$$

The singular values of the svd - the λ_i's - are the square roots of the eigenvalues of the system $A'A'^TU=\lambda^2U$. Using the svd, the solution to the problem (4.8) becomes:

$$b' = V_k \Lambda_k^{-1} U_k^T \Gamma \tag{4.11}$$

where k is the rank of the system. Often small non-zero λ's need to be excluded, as they represent noise in the system rather than independent information. If one includes these small singular values the solution will grow rapidly since the solution is inversely proportional to the singular values. Therefore one needs to determine how many λ's to keep in the summation, which determines the rank of the system. A discussion of the choice of rank will be given later.

4.2 Initial model: Interfaces and Initial Estimates

There are 15 boxes involved in the model. Each box has between 3 and 11 interfaces through which it interacts with the surroundings. The properties of the boxes and the interfaces will be discussed in the following, each interface being mentioned in

the box where it first appears. The T and S properties represent average core properties of the water mass at each interface. The initial estimates of the horizontal transports are based on direct estimates (from current meter moorings etc.) where such exist. If direct estimates do not exist, but the core analysis has indicated a direction of flow, an estimate of O(0.5-1 Sv) is used in the upper layers, and an estimate of O(0.1-0.2 Sv) is used in the lower layers. If no information of the direction of flow is known (as is the case for example for the vertical velocities) the initial estimate is set to zero. The boxes and interfaces are listed in table 4.1, and the properties on the interfaces are synthesized in table 4.2.

Air-Sea Heat Fluxes: The three atlases of net annual heat flux; Budyko (1974) (fig. 4.4), Bunker (1976) (fig. 4.5), and Gorshkov (1983) (fig 4.6) all show a tendency towards high heat fluxes in the Norwegian / Barents Sea (over the North Atlantic Current, as Bunker (1976) points out). Further east, over the Greenland and Iceland Seas the heat fluxes are smaller. But the uncertainties are large, and the initial estimates of the heat fluxes are therefore set to 70 W/m^2 over the Norwegian Sea, the Barents Sea, the Greenland Sea and the Iceland Sea, and 0 W/m^2 over the ice-covered areas: the East Greenland Box and the Arctic Ocean.

Air-Sea Freshwater Fluxes: The three atlases of net annual water flux; Baumgartner and Reichel (1975) (fig. 4.7), Gorshkov (1983) (fig. 4.8), and Schmitt et. al. (1989) (fig. 4.9) all display a change in sign through the domain, with precipitation exceeding evaporation in the south (O(500 mm/year)), and evaporation exceeding precipitation in the north (O(100 mm/year)). The P-E estimates are more uncertain than the heat fluxes, due to the lack of spatial correlation for precipitation measurements. The initial estimates of the P-E fluxes in all the six areas are therefore set to zero.

Table 4.2 The data setup and initial estimates.

Comments:	nsec	ρ [kg/m³]	θ [°C]	S [psu]	Area [km²]	init est
1) Atlantic, NS						
1) Inflow from Atlantic	1	1027.	7	35.3	-	7 Sv
2) NCC + runoff	2	1000.	5	0	-	-0.03 Sv
3) Iceland Sea, upper,east	3	1027.	1	34.85	-	0.1Sv
4) Iceland Sea, upper, west	4	1027.	4.5	35.1	-	-0.1 Sv
5) Greenland Sea, upper	5	1027.	3	35.1	-	-0.1 Sv
6) return Atlantic	6	1028.	1.5	34.95	-	-1 Sv
7) Arctic, upper	7	1028.	2	35.0	-	3.0 Sv
8) Barents Sea	8	1028.	4	35.05	-	1.5 Sv
9) IW, vertical	9	1028.	0	34.9	1.5×10^6	0 m/s
10) Air-Sea, heat	10	1026.	-	-	1.5×10^6	70 W/m²
11) Air-Sea, salt	11	1026.	-	35.0	1.5×10^6	0 mm/yr
2) IW, NS						
1) Iceland Sea, upper	12	1028.	0	34.89	-	0.2 Sv
2) Greenland Sea, upper	13	1028.	0	34.89	-	0.2 Sv
3) Arctic, upper	14	1028.	0	34.89	-	0 Sv
4) Færø-Shetland Channel	15	1028.	0	34.89	-	-0.5 Sv
6) DW, vertical	16	1028.	0	34.9	6×10^5	0 m/s
3) DW, NS						
1) Iceland Sea, lower	17	1028.	-0.9	34.915	-	0.1 Sv
2) Greenland Gyre, lower	18	1028.	-1.2	34.89	-	0 Sv
3) DW, East Greenland	19	1028.	-1	34.91	-	0.3 Sv
4) Arctic, lower	20	1028.	-1	34.91	-	0.1 Sv
5) Færø-Shetland Channel	21	1028.	-1	34.915	-	-1 Sv
4) Barents Sea						
2) runoff	22	1000.	5	0	-	0.03 Sv
3) Arctic, upper	23	1027.	-1	34.75	-	0 Sv
4) Arctic, lower	24	1028.	-0.85	34.95	-	1.5 Sv
5) Air-Sea Interface, heat	25	1026.	-	-	1.3×10^6	70 W/m²
6) Air-Sea Interface, salt	26	1026.	-	34.9	1.3×10^6	0 mm/yr
5) Arctic, upper						
4) Bering Sea	27	1027.	1	32.5	-	0.8 Sv
5) Canadian Archipelago	28	1027.	0	34.2	-	-1.5 Sv
6) Polar Water, EG	29	1027.	-1	34.3	-	-1.5 Sv
7) AAW, EG	30	1028.	0.5	34.85	-	-1.5 Sv
8) IW, EG	31	1028.	0	34.89	-	0 Sv
9) runoff	32	1000.	5	0	-	0.1 Sv
10) Arctic, lower, vertical	33	1028.	0	34.9	4.2×10^6	0 m/s
11) Air-Sea Interface, heat	34	1026.	-	-	7.5×10^6	0 W/m²
12) Air-Sea Interface, salt	35	1026.	-	34.0	7.5×10^6	0 mm/yr
6) Arctic, lower						
4) DW, EG	36	1028.			-	
7) Polar Water, EG						
2) Greenland Gyre	37	1027.	-1	34.3	-	0.1 Sv

3) Iceland Gyre, upper	38	1027.	-1	34.3	-	0.1 Sv
4) Denmark Strait	39	1027.	-1	34.3	-	-1.5 Sv
5) runoff	40	1000.	5	0	-	0 Sv
6) AAW, vertical	41	1027.	0	34.7	1.7×10^5	0 m/s
7) Air-Sea Interface, heat	42	1026.	-	-	1.7×10^5	0 W/m^2
8) Air-Sea Interface, salt	43	1026.	-	34.0	1.7×10^5	0 mm/yr
8) AAW, EG						
2) Greenland Gyre, upper	44	1028.	0.5	34.85	-	0 Sv
3) Iceland Gyre, upper	45	1028.	0.5	34.85	-	0 Sv
4) Denmark Strait	46	1028.	0.5	34.85	-	-2 Sv
6) rAtW, vertical	47	1028.	0.7	34.9	1.7×10^5	0 m/s
9) rAtW, EG						
2) Greenland Gyre, upper	48	1028.	1.5	34.95	-	0 Sv
3) Iceland Sea, upper	49	1028.	1.5	34.95	-	0.1 Sv
4) Iceland Sea, lower	50	1028.	1.5	34.95	-	0.5 Sv
5) Denmark Strait	51	1028.	1.0	34.92	-	-1 Sv
7) IW, vertical	52	1028.	0	34.9	1.7×10^5	0 m/s
10) IW, EG						
2) Greenland Gyre, upper	53	1028.	0	34.89	-	-0.2 Sv
3) Iceland Sea, lower	54	1028.	0	34.89	-	0.1 Sv
5) DW, vertical	55	1028.	-0.5	34.91	1.7×10^5	0 m/s
11) DW, EG						
2) Greenland Gyre, lower	56	1028.	-1.2	34.89	-	-0.1 Sv
5) Iceland Sea, lower	57	1028.	-0.9	34.915	-	0.1 Sv
12) Gr. Gyre, upper						
7) GG, lower, vertical	58	1028.	-1.1	34.89	2.2×10^5	0 m/s
8) Air-Sea Interface, heat	59	1026.	-	-	2.2×10^5	70 W/m^2
9) Air-Sea Interface, salt	60	1026.	-	34.7	2.2×10^5	0 mm/yr
14) Iceland Sea, upper						
6) Atlantic, Irminger	61	1027.	4	35.0	-	1 Sv
7) East of Iceland	62	1028.	2.5	34.9	-	-0.5 Sv
8) IS, lower, vertical	63	1027.	-0.5	34.9	2.0×10^5	0 m/s
9) Air-Sea Interface, heat	64	1026.	-	-	2.7×10^5	70 W/m^2
10) Air-Sea Interface, salt	65	1026.	-	34.7	2.7×10^5	0 mm/yr

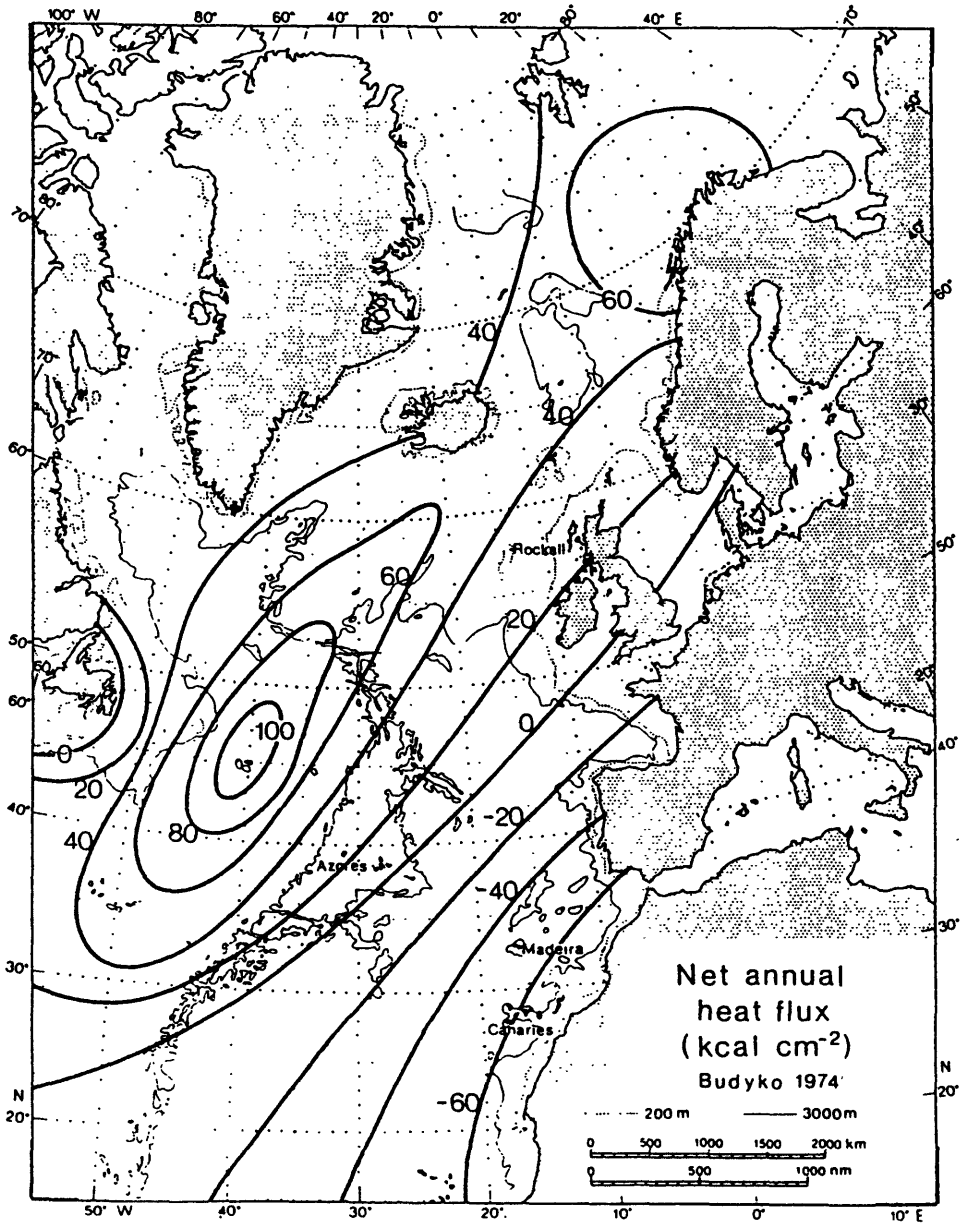

Fig. 4.4 Net annual heat flux (Budyko, 1974)

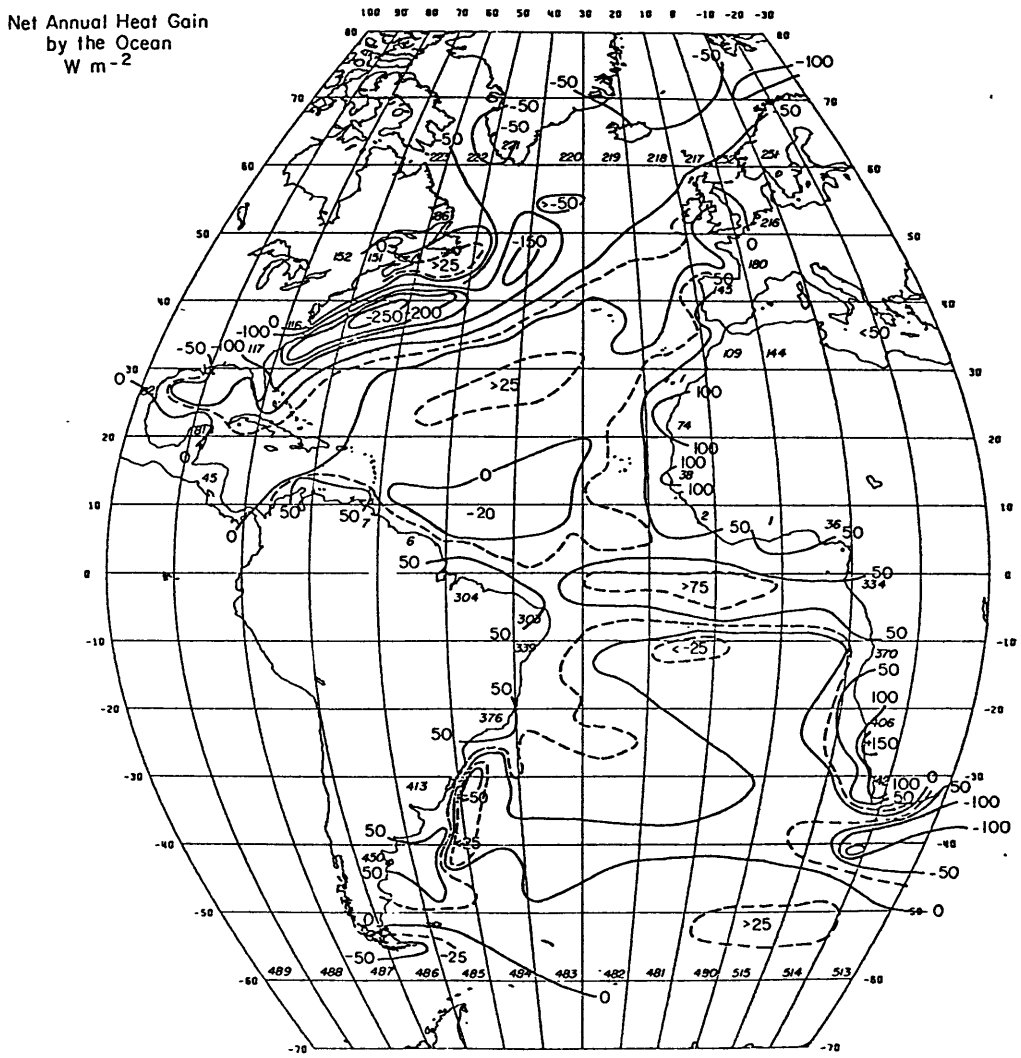

Fig. 4.5 Net annual heat flux (Bunker, 1976)

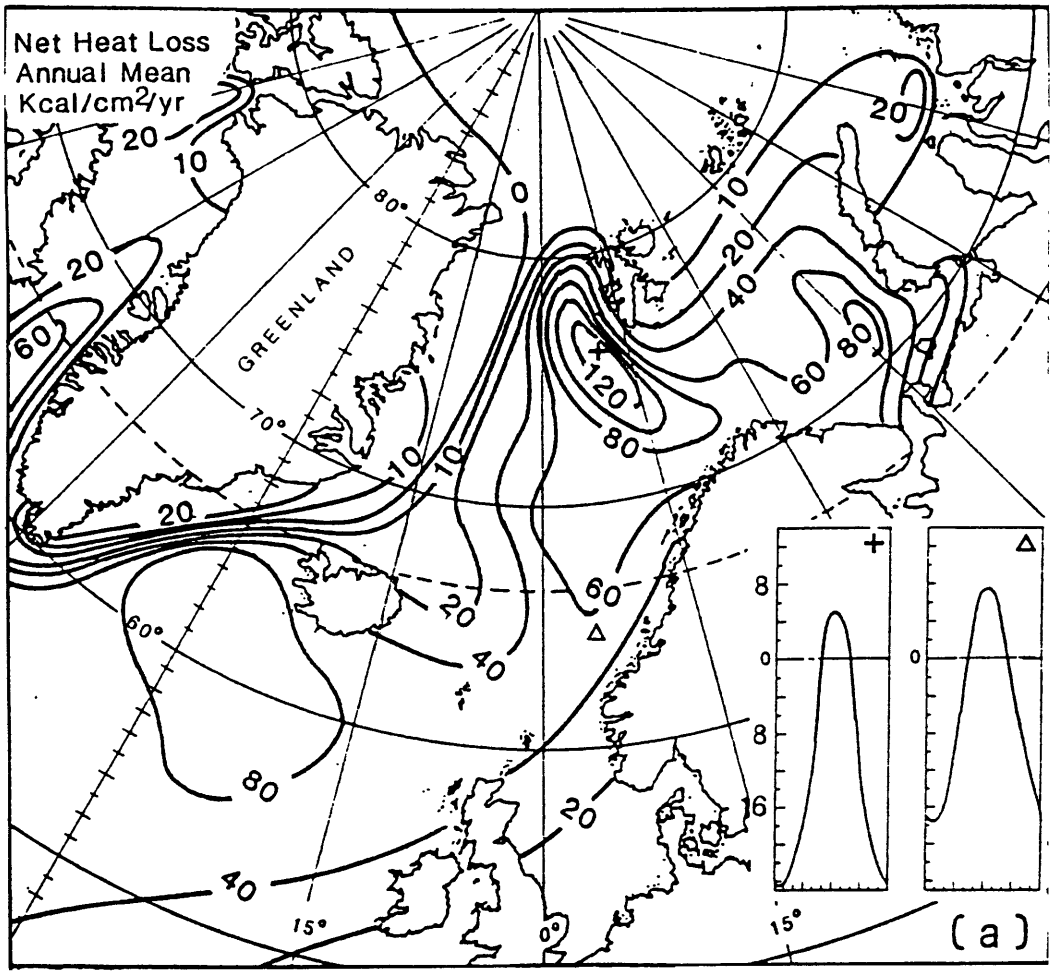

Fig. 4.6 Net annual heat flux (Gorshkov, 1983)

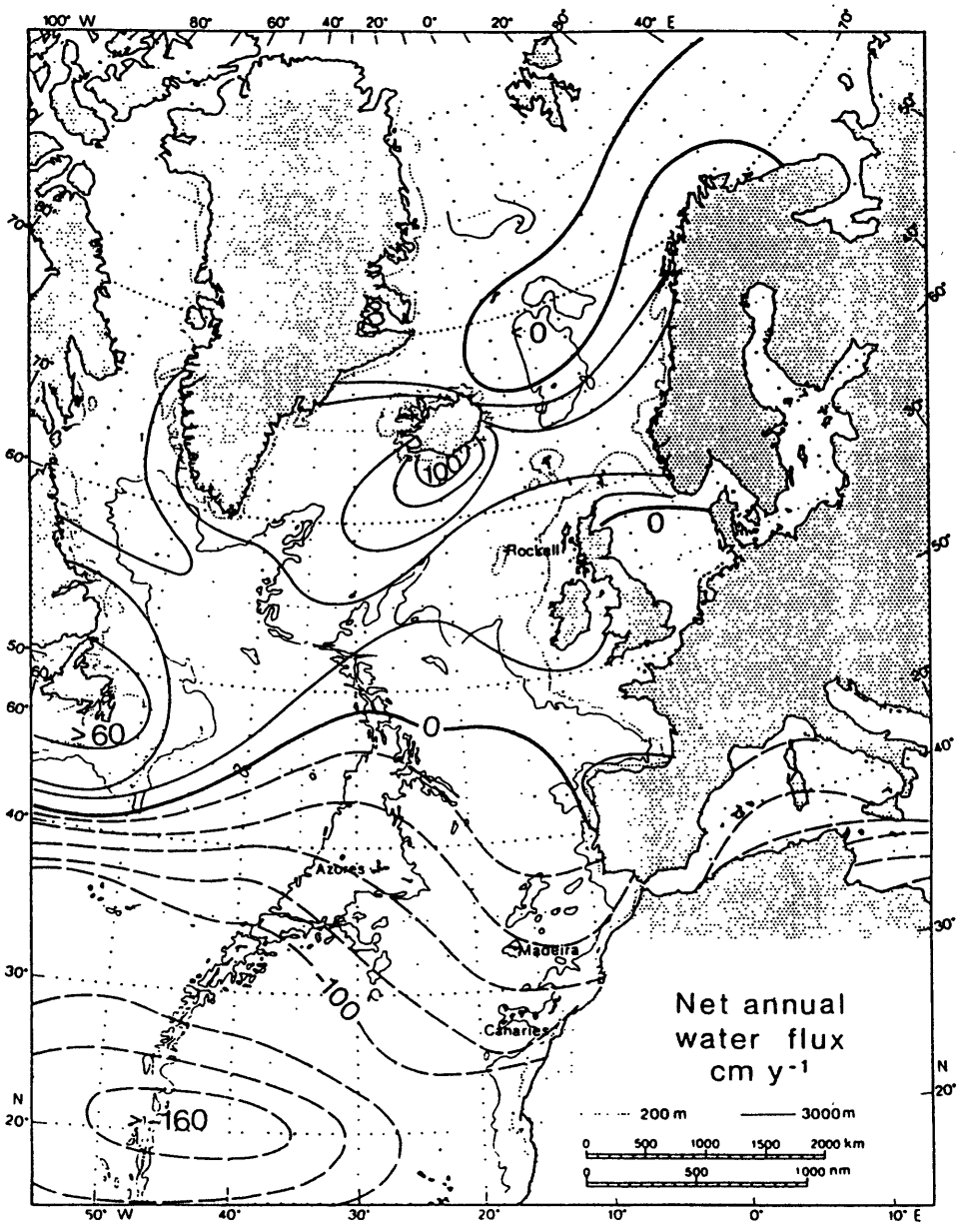

Fig. 4.7 Net annual water flux (Baumgartner and Reichel, 1975)

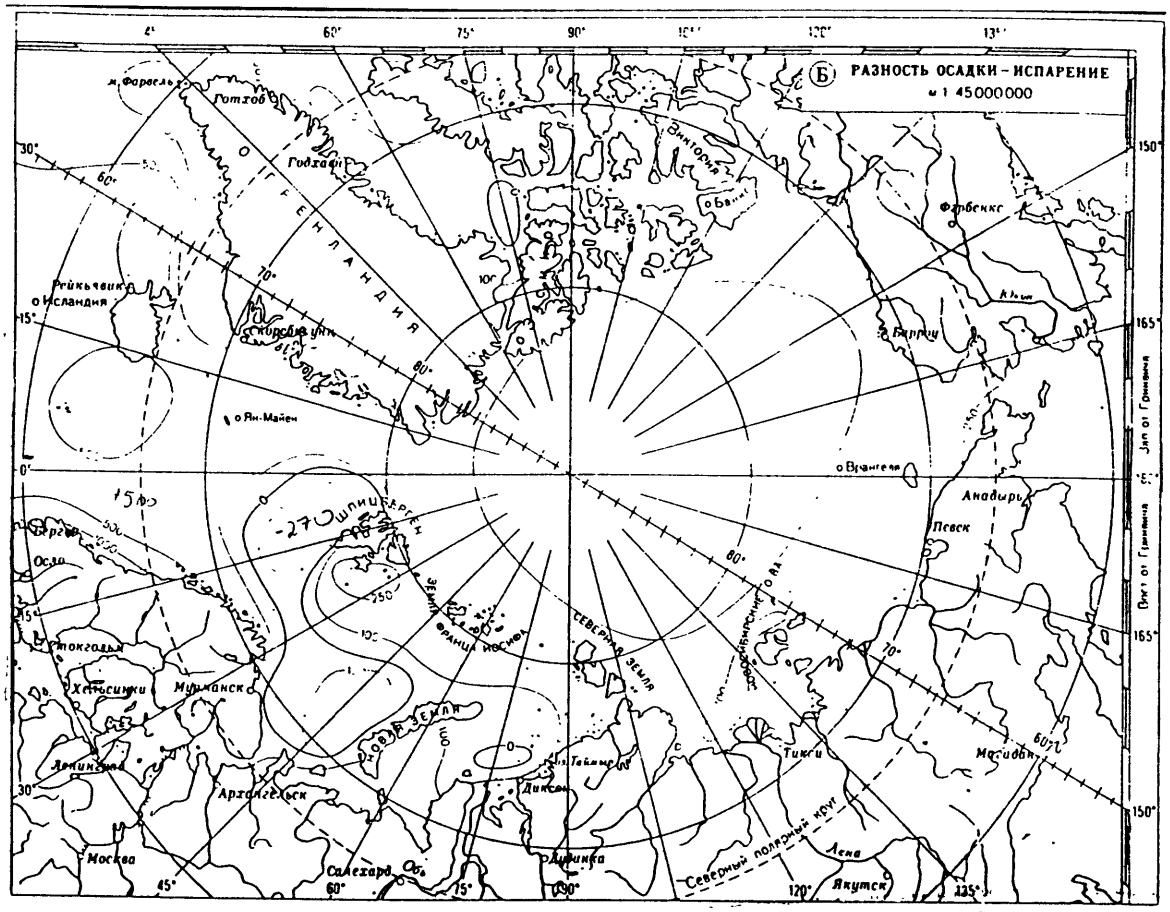

Fig. 4.8 Net annual water flux (Gorshkov, 1983)

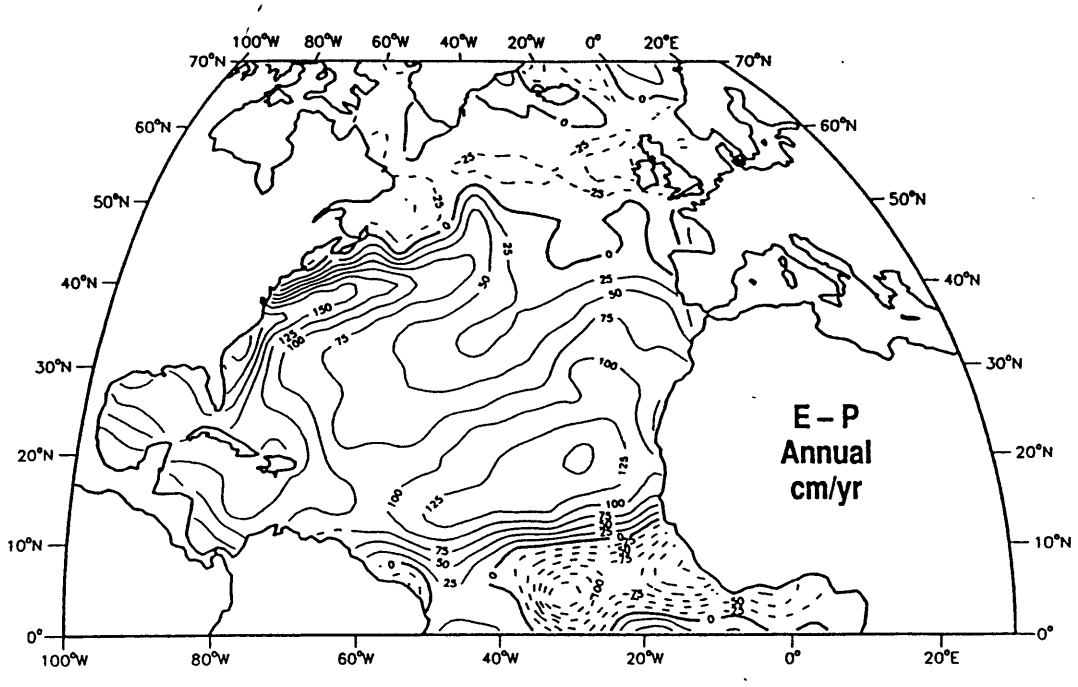

Fig. 4.9 Net annual water flux (Schmitt et. al., 1989)

River Runoff: Baumgartner and Reichel (1975) estimate a river runoff for the Arctic Ocean of 0.1 Sv, and for the Barents Sea / coast of Norway 0.03 Sv.

Ice: Vinje and Finnekåsa (1986) estimate that the average annual export of ice from the Arctic Ocean is 5000 km^3 (0.16 Sv). Untersteiner (1988) estimates that a good fraction of this ice (2/5) melts in the Fram Strait, where it encounters the warm Atlantic Water. Schlosser et. al. (subm. D-S. R 11/20/92) finds that the freshwater northeast of the Fram Strait consists primarily of meltwater, whereas further into the Arctic Ocean the freshwater consists primarily of river runoff. As an initial guess it is therefore assumed that the meltwater reenters the Arctic Ocean with the West Spitsbergen Current, and that the net export of ice from the Arctic Ocean is 0.1 Sv, which corresponds to $9 \cdot 10^7$ kg/s (using $\rho_{ice} = 900$ kg/m^3). Similar long-term monitoring of the ice-export through the Denmark Strait does not exist. It is assumed that only a fraction ($1.8\ 10^7$ kg/s) of the ice export from the Arctic Ocean enters the North Atlantic. Likewise, it is not known where within the Nordic Seas the remaining ice is melted. It is assumed that it all melts in the Atlantic Domain, because the warmest water is found there. The ice exits the Arctic via the East Greenland Current, and may enter the Atlantic Domain both north and south of the Greenland Gyre. South of the gyre one finds the "Odden", which is an eastward extension of ice, known to fishermen for centuries. The Odden may be the pathway by which ice is transported into the Atlantic Domain.

Box 1.1: Atlantic Water, Norwegian Sea: This box has eight vertical interfaces, and two horizontal ones; the sea surface plus the interface with the Intermediate Water beneath. The Atlantic Water, entering over the Iceland-Shetland Ridge, is assumed to have a core temperature of 7 ^{0}C, with S=35.3. Transport estimates of this inflow are uncertain, as the flow is broad, and may have seasonal variations. The estimate of Gould et. al. (1985) of

7.5 ±2.5 Sv was based on current meter moorings in the Færø-Shetland Channel. The initial estimate is set at 7 Sv.

A branch of the Atlantic inflow makes a detour into the North Sea, and reenters the Norwegian Coastal Current (Furnes et. al. 1986). It is not expected that the volume will have changed, but the return flow is fresher, due to the influence of the Baltic Sea. This process does not enter explicitly in the model, but is parameterized as river runoff. Baumgartner and Reichel (1975)'s estimate, which included both the Barents Sea and the Norwegian Sea, was 0.03 Sv. Here the initial estimate of the runoff into the Norwegian Sea alone, is set at 0.03 Sv.

There may be a two-way interaction between the Norwegian and Iceland Seas: The Atlantic Water influences the Iceland Sea in the north, where the waters are warmer and saltier than in the rest of the Iceland Sea. The Iceland Sea water influences the Atlantic Domain in the southern Norwegian Sea, where the waters are colder and fresher than in the rest of the Norwegian Sea, and where the core of the Atlantic inflow is found in the eastern portion of the basin. Therefore two interfaces are assumed, but since neither of these flows appear to be of substantial magnitude (the cores do not extend very far), the initial estimates are set at 0.1 Sv. Likewise, the inflow of Atlantic Water to the Greenland Sea is largely limited by the topographic steering of the Mohn / Knipovich Ridge, and the initial estimate is therefore 0.1 Sv. North of the Greenland Gyre there is a tendency for substantial recirculation of the Atlantic Water, and the initial estimate is a westward flow of 1 Sv.

The flow of Atlantic Water into the Arctic via the West Spitsbergen Current (WSC) is hard to estimate, due to the banded structure and bifurcation of the current. Hanzlick (1983) estimates the transport at 79 N to be 5.6 Sv, whereas Jónsson (1989) estimates this transport to be 3 ±1 Sv, with the possibility of further reduction due to recirculation further north. Aagaard and Carmack (1989) raise the possibility that the actual throughflow of Atlantic Water to the Arctic may be as low as 0.7 Sv. But during

1984, the year of the deployment of the current meter mooring used by Jónsson (1989), a substantial recirculation was found to occur south of 79 N. Because of this, and as there is sufficient evidence of a substantial core of Atlantic Water entering the Arctic, an initial estimate of 3.0 Sv is made.

Timofeyev (1963) estimated a 2 Sv flow of Atlantic Water into the Barents Sea, and a return flow of 0.9 Sv (with θ=1 ^{0}C) yielding a net throughflow to the Arctic Ocean of 1 Sv. Blindheim (1989) calculates a throughflow of 1.9 Sv, with 3.1 Sv entering and 1.2 Sv returning as denser water (with S> 35.0, so it still belongs to the Atlantic Water). The initial estimate of the net throughflow is set at 1.5 Sv, with θ=4 ^{0}C and S=35.05. There is also an exchange north of the Bear Island; Quadfasel et. al. (1988) observed outflow of dense water from this opening. This effect is ignored in the model, as the volume involved is small.

Box 1.2: Intermediate Water, Norwegian Sea. This layer is very thin, and expected to originate in the Iceland and Greenland Seas (initial estimate set at 0.2 Sv for each). The estimates for the dense overflows across the Iceland-Scotland Ridge lie around 2 - 2.5 Sv, as discussed in chapter 2. The initial estimates for these overflows are set to 2 Sv, divided into Intermediate Water (0.5 Sv), Deep Water (1 Sv, box 1.3) and North Iceland Winter Water (0.5 Sv, box 6.1).

Box 1.3: Deep Water, Norwegian Sea. This water is expected to enter the Norwegian Sea from the Arctic Ocean, via the Jan Mayen Fracture Zone (from the Deep Water in the East Greenland box), and via the Iceland Sea. The dense water of the Greenland Sea is expected to reduce the salinities of the Deep Water from the properties it has in the Arctic Ocean. No exchange is expected in the eastern Fram Strait. The sink in the Færø-Shetland Channel is set at 1 Sv (see box 1.2).

Box 2.1: Barents Sea. Little is known about the properties of the throughflow of Atlantic Water as it enters the Arctic Ocean. Two interfaces are defined: one with properties similar to those of light water in the Arctic Ocean, and one with properties similar to those of the dense water in the Arctic Ocean. Initially it is assumed that all the water is dense when it enters the Arctic. A river runoff of 0.03 Sv is expected also for this box, again parameterizing the effect of the Norwegian Coastal Current which enters the Barents Sea along with the Atlantic Water.

Box 3.1: upper Arctic Ocean. Many estimates exist for the flow of Pacific Water through the Bering Strait, all around 1 Sv: Maksimov (1944): 0.96 Sv, Sverdrup et. al. (1946): 0.3 Sv, Bloom (1961): 0.7 Sv, Coachman and Barnes (1961): 1 Sv, Vowinckel and Orvig (1962): 1.03 Sv, and Coachman and Aagaard (1988): 0.8 Sv. The most recent result is chosen as the initial estimate, with θ=1 ^{0}C (Vowinckel and Orvig (1962)), and S=32.5 (Aagaard and Greisman (1975)). The transport estimates for the Canadian Archipelago typically range between 1 Sv (Timofeyev (1956), Collin (1963), Vowinckel and Orvig (1970)) and 2 Sv (Muench (1971)). An intermediate value of 1.5 Sv is used as the initial estimate, with θ=0 ^{0}C (Vowinckel and Orvig (1962)) and S=34.2 (Aagaard and Greisman (1975)). Foldvik et. al. (1988) estimate a flow of 3 Sv above 700 m in the East Greenland Current at 79 N, 1 Sv of which is considered Polar Water, and 2 Sv of which is considered Arctic Intermediate Water ($0 < \theta < 3$ ^{0}C), with an 8 % contribution of Atlantic Water with $\theta > 3$ ^{0}C. As mentioned above, in the year of these measurements (1984) a substantial recirculation existed south of 79 N, and the initial estimate of the exit from the Arctic Ocean via the East Greenland Current is therefore 3 Sv, evenly distributed between the Polar Water and the Arctic Atlantic Water. An exchange with the Intermediate Water is also allowed for, as this water is found all across the Fram Strait, but the initial estimate is set to zero. The initial estimate of river runoff is taken from Baumgartner and Reichel (1975): 0.1 Sv.

Box 3.2: lower Arctic Ocean. The Barents Sea is expected to be the source of dense water to the Arctic Ocean. This box is connected to the deep waters both in the East Greenland Box and in the Norwegian Sea. As a substantial source for the densest overflow in the Færø-Shetland Channel is needed, the initial estimate of the export of Deep Water in the western Fram Strait is set to 1 Sv.

Box 4.1: Polar Water, East Greenland. It is expected that the Polar Water provides a fresh water supply for the Greenland and Iceland Seas, therefore initial estimates of 0.1 Sv are made for both Seas. But primarily the Polar Water is expected to flow straight to the Denmark Strait. Malmberg et. al. (1972) estimate the transport of Polar Water through the Denmark Strait to be 1.6 Sv. The initial estimate for the model is 1.5 Sv.

Box 4.2: Arctic Atlantic Water, East Greenland. Exchange is allowed with the Greenland and Iceland Seas, but most of the AAW is expected to flow straight to the Denmark Strait, where it constitutes part of the dense overflow. Ross (1984) estimates 2.9 Sv for this overflow. The initial estimate for the dense overflows in the Denmark Strait is 3 Sv (based on the discussion in chapter 2). This is divided into Arctic Atlantic Water (2 Sv) and return Atlantic Water (1 Sv, box 4.3).

Box 4.3: return Atlantic Water, East Greenland. The rAtW flows at a level in the water column where part of it may not be able to exit over the Denmark Strait sill, but rather continue into the Central Iceland Sea. The initial estimate assumes 1 Sv to exit in the Denmark Strait (see box 4.2), 0.1 Sv to enter the upper Iceland Sea, and 0.5 Sv to enter the lower Iceland Sea.

Box 4.4: Intermediate Water, East Greenland. The source is expected to be the Greenland Gyre, with an initial estimate of 0.2 Sv. This water is expected to flow southward into the West Iceland Basin, and - as it flows at a level too deep to exit into the North Atlantic - it enters the lower Iceland Sea.

Box 4.5: Deep Water, East Greenland. This water, whose source has been described above to be in the Arctic Ocean, is expected to receive a contribution from the deep Greenland Sea, and to continue into the Norwegian Sea, partly through the JMFZ and partly through the deep Iceland Sea.

Box 5.1: upper Greenland Sea. These interfaces have already been described.

Box 5.2: lower Greenland Sea. These interfaces have already been described.

Box 6.1: upper Iceland Sea. Atlantic Water from the Irminger Current enters the Iceland Sea in the eastern Denmark Strait. Part of this water will recirculate in the Strait, where boluses of warm water sometimes are found even on the western side. Stefansson (1962) estimates the inflow to the Iceland Sea to be 0.5 Sv, whereas the estimate of Kristmannson et. al. (1987) is higher: 1-2 Sv. An intermediate value of 1 Sv is chosen for the initial estimate. East of Iceland there is an outflow of North Icelandic Winter Water into the North Atlantic. The initial estimate is here set to 0.5 Sv (see box 1.2 for an explanation).

Box 6.2: lower Iceland Sea. These interfaces have already been described.

This completes the description of the boxes. There are a total of 65 unknowns: 44 horizontal transports, 9 vertical velocities, and 12 air-sea fluxes. The mass, heat and salt

conservation statements result in 48 equations (15 individual boxes plus the total Arctic Ocean and Nordic Seas). Additional constraints contribute through additional equations, as will be discussed below.

For the initial model, mass is well balanced, to within the uncertainties that will be discussed below. The largest imbalance is found in the Atlantic box (1 Sv), and in the Deep Waters in the Norwegian Sea and the East Greenland Box (0.7 Sv). Likewise, the salinity imbalances are all in the range 10^6 - 10^7 kg_s/s, which is acceptable. Based on these imbalances alone one might accept the initial model, and not go on with the inversion. However, in the heat budget there are unacceptably large imbalances, especially in the surface boxes (O(10^{10} kg^0C/s)), compared to the *a priori* expected uncertainties. The initial imbalances are therefore not acceptable, and an inverse solution is sought.

All rows are weighted by the average property concentration of the box to remove artifacts of different equations having different units. The columns are weighted by the length of the column to give the different terms in the equations equal footing, and by the expected order of magnitude of the solution, as discussed below.

The *a priori* uncertainties in the total solutions, which are the same as the expected magnitude of the solution elements, will be discussed next. The uncertainty for the Atlantic inflow to the Norwegian Sea and to the Arctic Ocean is 2 Sv, because the range in direct estimates is large. The total dense overflows in the Denmark Strait (boxes 4.2 and 4.3) and over the Iceland-Scotland Ridge (boxes 1.2, 1.3 and 6.1) are not expected to be in error by more than 1 Sv. 0.1 to 1 Sv is the range in expected magnitude of the transports that are determined by the core analysis.

The expected uncertainty of the interior flow fields is 0.5 to 1 Sv. For the vertical velocities the expected magnitude is $O(10^{-8}\text{-}10^{-6}$ m/s). The heat fluxes may vary by ±30 W/m^2 for ice-free conditions and otherwise ± 10 W/m^2 as the ice acts as an insulator. The P-E fluxes may vary by as much as ±500 mm/year.

4.3 The Standard Model

The standard model will be discussed next. This model is my best estimate of the circulation in the Nordic Seas and Arctic Ocean, based on the new circulation scheme constructed in chapter 3, based on the direct estimates of transports, and based on observational knowledge of the heatfluxes in the region. All later model runs will be compared to this model. The standard model has, in addition to the conservation statements, a number of further constraints imposed:

- the vertical velocity between the Atlantic Layer and the Intermediate Water beneath it is minimized. This assumption is of no importance to the Atlantic Water and thus on the issues that are to be tested with the model, but it produces a more reasonable flow field for the Intermediate Water. Also the data indicate little interaction between these layers (see chapter 3).
- ice is assumed formed in the Arctic and exported through the Fram Strait. Most of the ice is assumed to melt in the Atlantic Domain, with a fraction exiting through the Denmark Strait, following the initial model. As will be discussed below the confidence in the salinity budget is small. Therefore I have chosen not to test this parameter.

The rank of the best estimate model is determined to be k=30. The solution norm does not start growing rapidly with increasing rank before rank 44 (see discussion in

section 4.1), but individual solution elements become rather unstable from rank to rank above k=30. This instability occurs as the model attempts to better satisfy the salinity equations - by utilizing the P-E fluxes. As the knowledge of the oceanic P-E fluxes is so poor in the Polar regions, I have chosen to retain the lower rank of 30. This implies that P-E fluxes are not utilized, the benefit being that unnecessary noise is not included in the solution. The residuals in the salinity equations are in any case acceptable, as they were from the start. At and below rank 30 the solution is quite stable, so the exact choice of rank is not particularly important. However, one finds that the ranks with the smallest error norm are k=28 and k=30, and the rank with the smallest solution norm is k=30. Lastly, the norm of the residuals is reduced by 1/3 between ranks 29 and 30, thus the choice k=30.

The columns of the data resolution matrix UU^T show the information content in each equation. A diagonal element of 1 indicates that the corresponding constraint is completely independent of the other constraints. At rank 30 the diagonal elements of UU^T indicate that the heat conservation constraints generally contribute independent information, whereas the mass and salinity equations depend upon each other (diagonal elements ~ 0.45) (fig. 4.10). Linear dependency between the mass and salinity equations is typical of oceanic systems, and could probably be avoided if one used salinity anomaly instead of absolute salinity. Since I have little confidence in the salinity budget I have nevertheless chosen to work with absolute salinities.

If all the solution elements were perfectly resolved the diagonal of the model resolution matrix VV^T would be unity. With 65 unknowns and 30 pieces of independent information (rank 30) each solution element is on the average roughly 50 % determined. This can be seen in fig. 4.11, where the diagonal of the resolution matrix is plotted, the

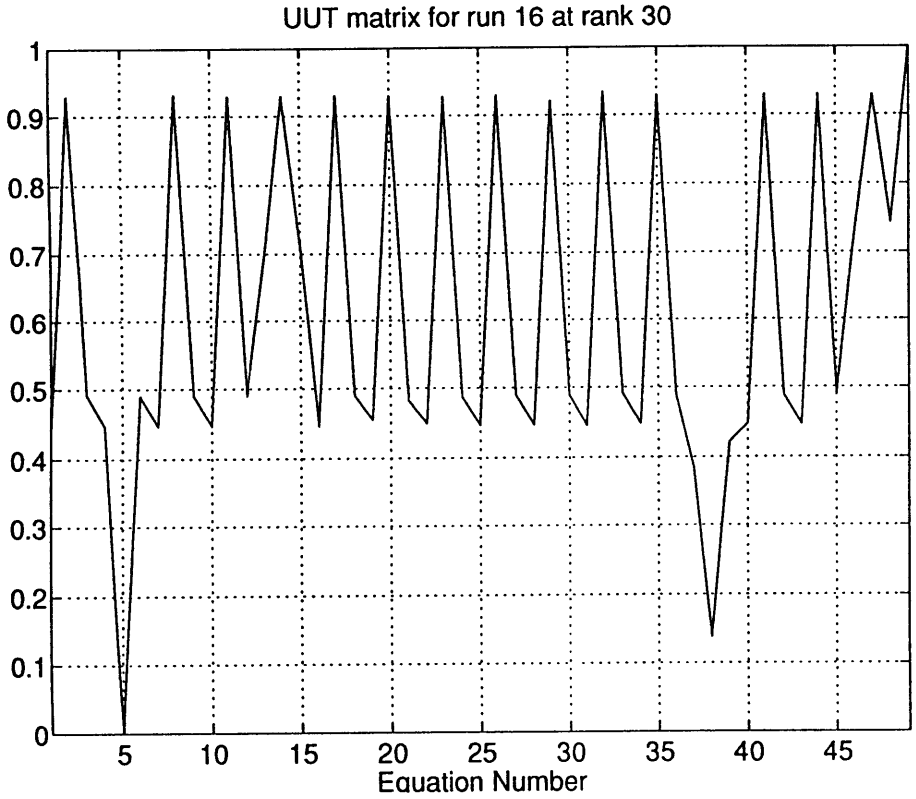

Fig. 4.10 Diagonal of the data resolution matrix for the standard model

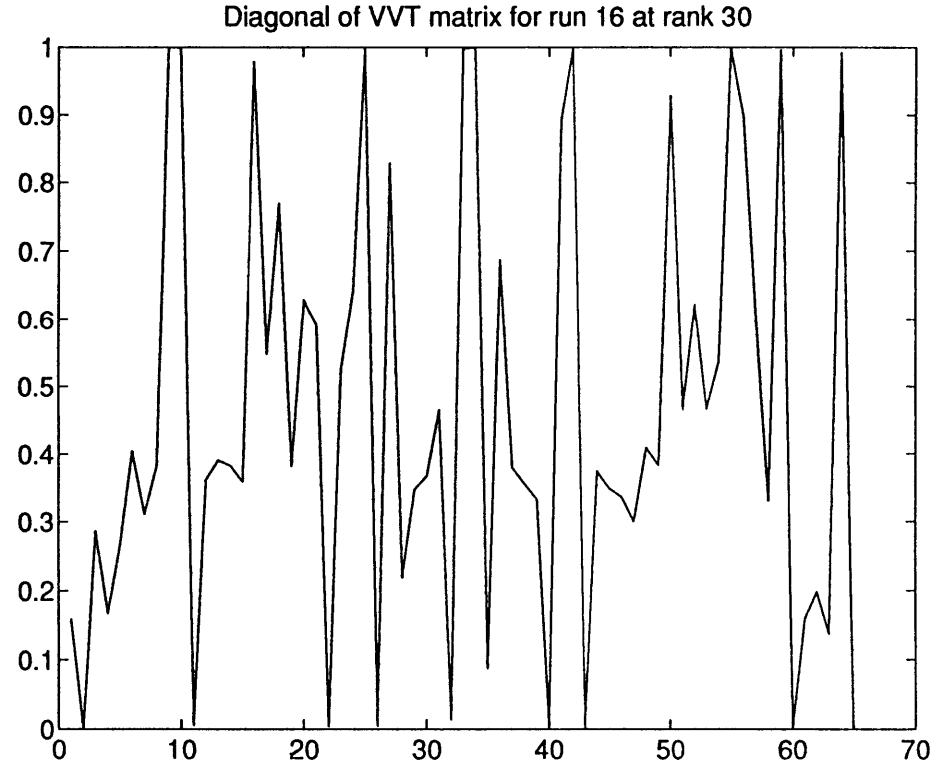

Fig. 4.11 Diagonal of the model resolution matrix for the standard model

average value being 0.46. The resolution is compact (Rintoul, 1988); fig. 4.12 shows that the off-diagonal entries are much smaller than the ones on the diagonal, i.e. there is no significant covariance between solution elements.

At rank 30 the weighted residuals are typically $O(10^6)$ (fig. 4.13). The only exceptions are the surface boxes of the Atlantic Domain, the Barents Sea, the Arctic, and therefore also the total Arctic Mediterranean. In these boxes the mass and salinity equations are not as well balanced as the other equations. These are the imbalances that the svd attempts to reduce at ranks higher than 30, by utilizing the P-E fluxes, as discussed above. The ice formation/ melting processes, and also the river runoff, are of great importance to the salinity balances in these boxes, and the peaks in the residuals probably indicate that these processes are not successfully dealt with in the model. I have chosen to accept these residuals, awaiting better observational control.

The formal estimate of the uncertainty in the solution b due to noise in the system is given by:

$$\left\langle b_j^2 \right\rangle = \sigma^2 \sum_{i=1}^{k} \frac{V_{ij}^2}{\lambda_i^2}$$

σ^2 is often calculated as:

$$\sigma^2 = \sum_{i=1}^{M} \frac{(Ab - \Gamma)_i^2}{M-k}$$

(M is the number of equations in the matrix) The calculated σ^2 ($6 \cdot 10^{13}$) give very small bounds: they are O(0.1 Sv) for most of the horizontal transports. This is in consonance with the finding that the solution is consistent with the equations of the model (the residuals are small). I consider these uncertainties to be unrealistically small, and have

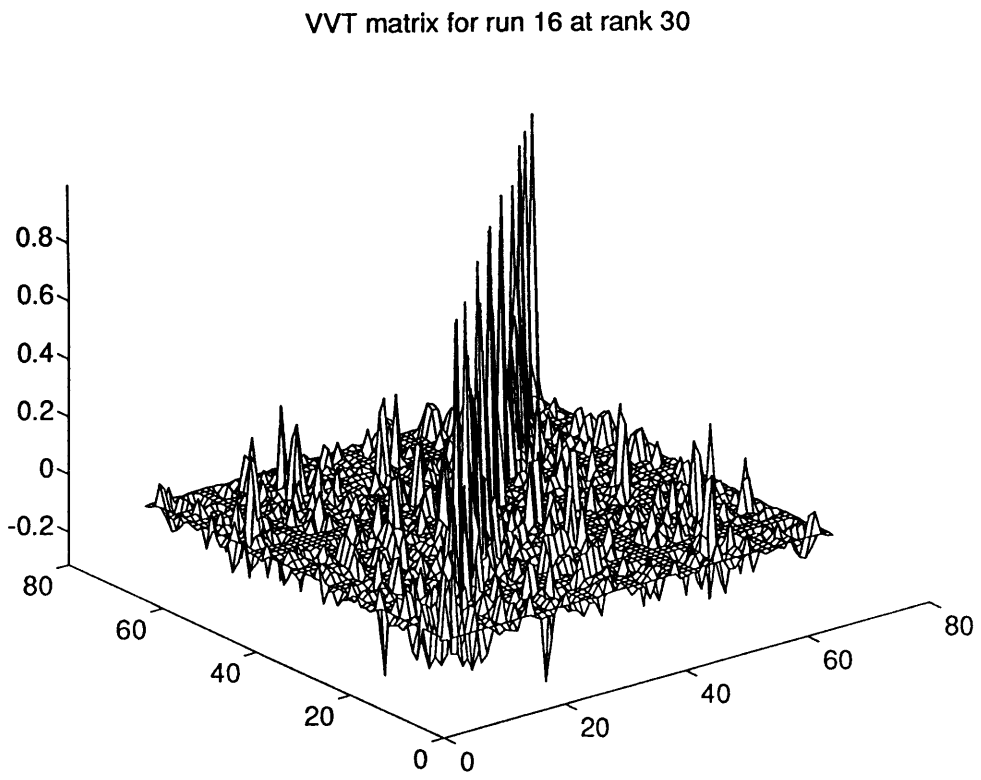

Fig. 4.12 Model resolution matrix for the standard model.

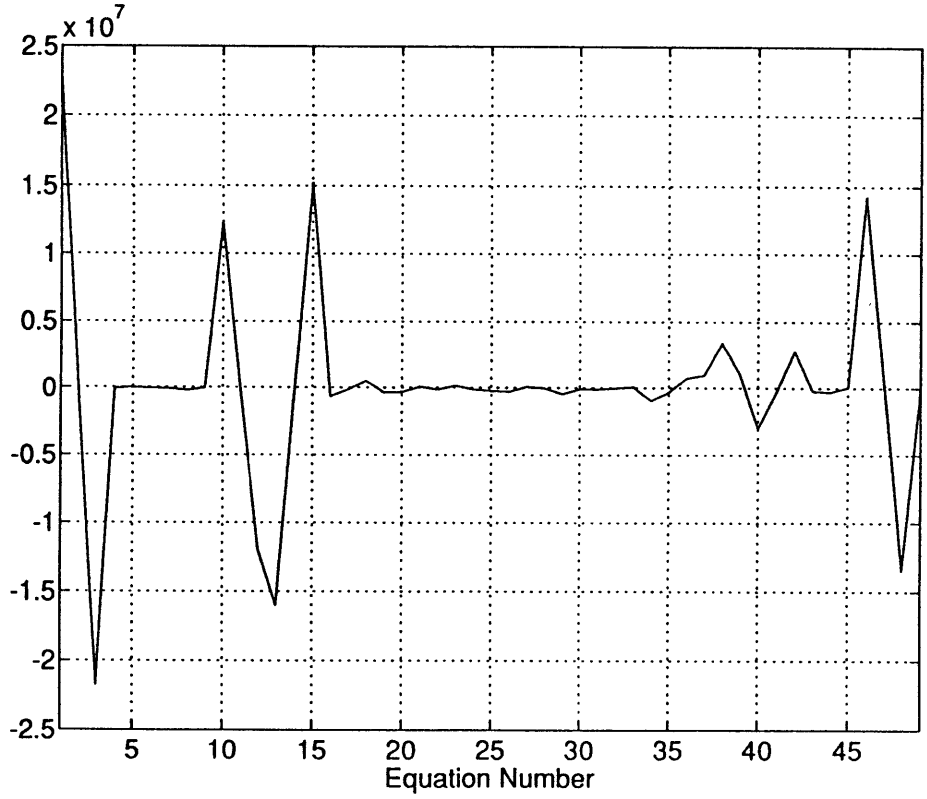

Fig. 4.13 Weighted residuals for the standard model.

adjusted σ^2 to $1 \cdot 10^{17}$ to obtain more realistic uncertainties. This is in accordance with some test runs (listed in the appendix) that were used to evaluate the uncertainties from a more experimental point of view.

Since the solution is not fully determined there is a part that is associated with the null space. One can write the full svd solution as:

$$b_{full} = b + b_{nullspace} \sum_{i=1}^{k} \alpha_i V_i + \sum_{i=k+1}^{N} \alpha_i Q_i$$

The variance associated with the nullspace is given by:

$$|b_{nullspace}|^2 = \left(\sum_{i=k+1}^{N} \alpha_i^2 \right) QQ^T$$

where $QQ^T + VV^T = I$. A plot of QQ^T is shown in fig. 4.14. There are no important covariances between the nullspace solution elements; most of the off-diagonal elements are less than 0.1. The nullspace uncertainty associated with each solution element is listed in table 4.3. The largest uncertainties are associated with the surface P-E fluxes, as expected, since these are not determined in the model (only the relative values are relevant as the multiplying factor α is not known).

The total solution (initial estimate + svd solution) at rank 30 - the standard model - is shown in fig. 4.15 and listed in table 4.3 with the formal and nullspace uncertainties. A simpler figure, with the most important parameters is shown in fig. 4.16. The transport of the North Atlantic Current is 6.8 ± 0.5 Sv into the Norwegian Sea. The NAC interacts only marginally with the Iceland Sea and the Greenland Gyre: 6.1 ± 0.8 Sv continues straight to the Barents Sea and the Fram Strait. This is consistent with hypothesis 2 of chapter 3 - that the Atlantic Water interacts mostly with the atmosphere. There is an

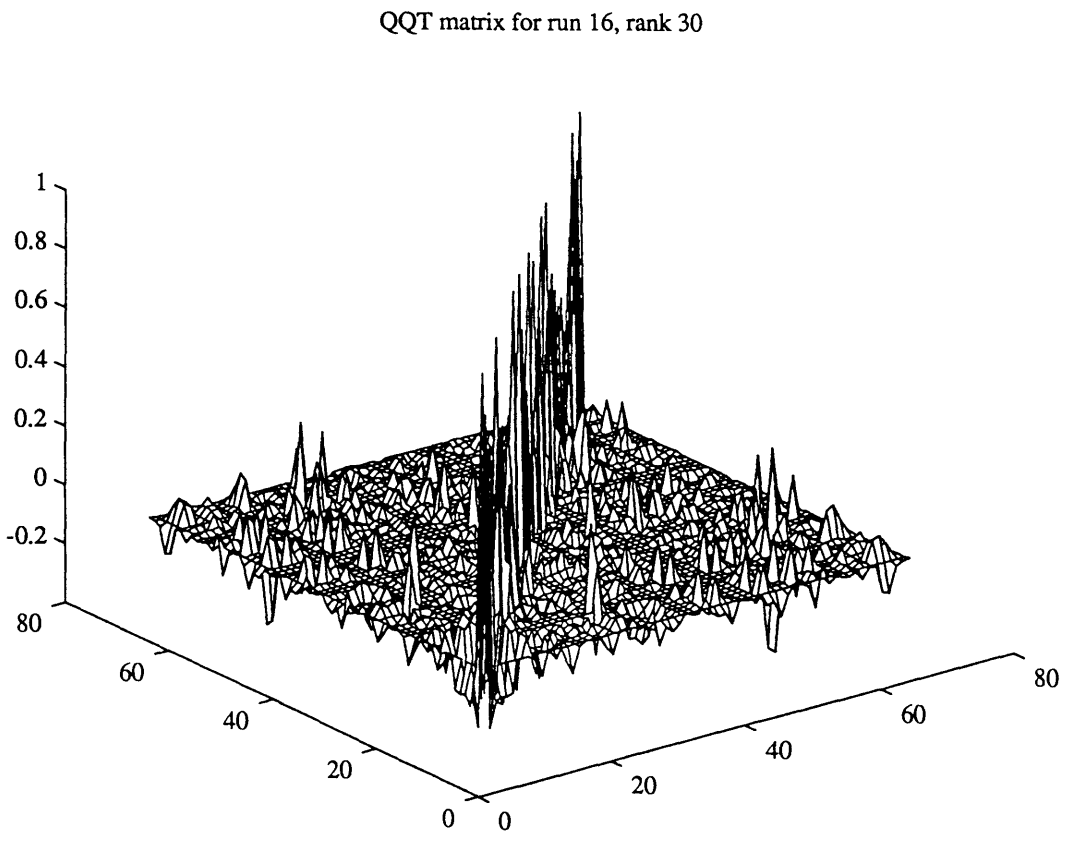

Fig. 4.14 QQ^T matrix for standard model

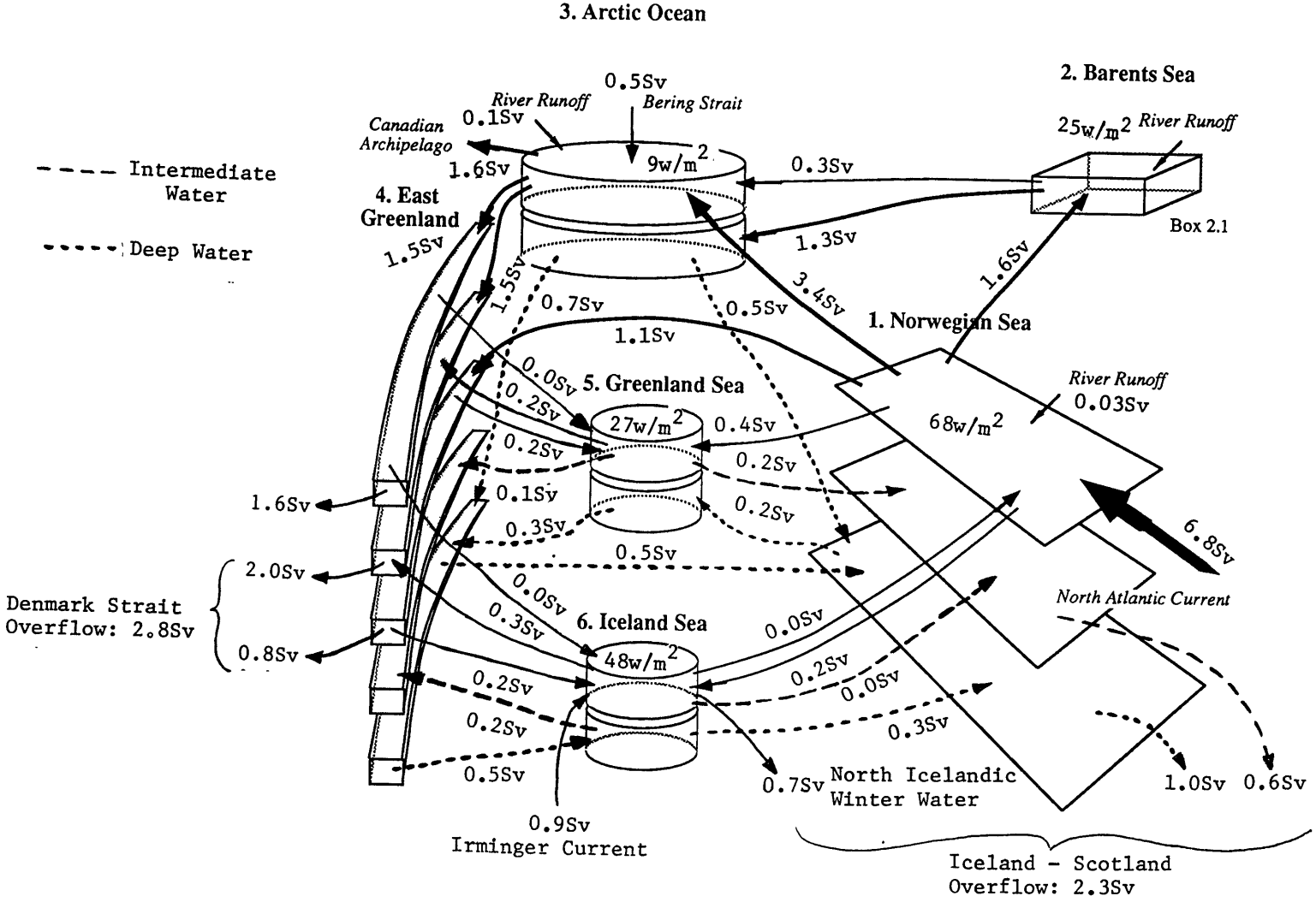

Fig. 4.15 Results of the standard model

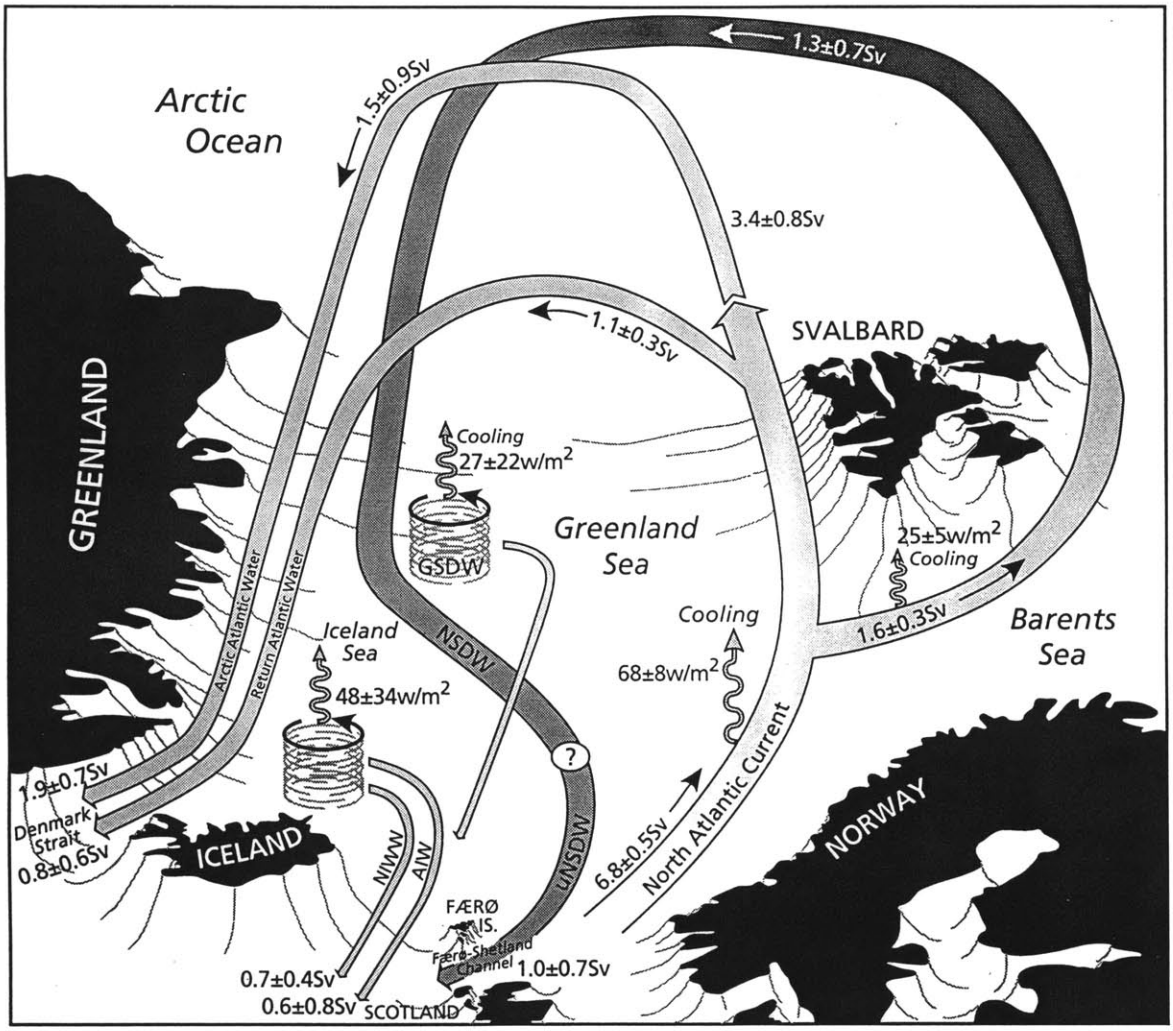

Fig. 4.16 Results of the standard model

Table 4.3 The Standard Model.

Unknowns:		Initial Estimate	Total Solution	Formal Uncertainty	Nullspace Uncertainty
1) Atlantic, NS					
1) Inflow from Atlantic	1	7 Sv	6.8	0.5	0.4
2) NCC + runoff	2	-0.03 Sv	-0.03	2.3e-05	5e-04
3) Iceland Sea, upper,east	3	0.1Sv	-0.14	0.2	0.6
4) Iceland Sea, upper, west	4	-0.1 Sv	-0.24	0.1	0.5
5) Greenland Sea, upper	5	-0.1 Sv	-0.37	0.1	0.5
6) return Atlantic	6	-1 Sv	-1.1	0.3	0.5
7) Arctic, upper	7	3.0 Sv	3.4	0.8	0.5
8) Barents Sea	8	1.5 Sv	1.6	0.3	0.4
9) IW, vertical	9	0 m/s	-1.5e-10	3.2e-07	2.8e-11
10) Air-Sea, heat	10	70 W/m^2	67.5	7.5	6.7
11) Air-Sea, salt	11	0 mm/yr	-3.6	59.1	116.4
2) IW, NS					
1) Iceland Sea, upper	12	0.2 Sv	0.37	0.27	0.6
2) Greenland Sea, upper	13	0.2 Sv	0.23	0.31	0.5
3) Arctic, upper	14	0 Sv	0.1	0.90	0.54
4) Færø-Shetland Channel	15	-0.5 Sv	-0.58	0.78	0.55
6) DW, vertical	16	0 m/s	1.3e-07	1.3e-06	1.3e-07
3) DW, NS					
1) Iceland Sea, lower	17	0.1 Sv	0.31	0.83	0.44
2) Greenland Gyre, lower	18	0 Sv	-0.22	1.80	0.32
3) DW, East Greenland	19	0.3 Sv	0.54	0.26	0.52
4) Arctic, lower	20	0.1 Sv	-0.48	1.3	0.41
5) Færø-Shetland Channel	21	-1 Sv	-1.03	0.66	0.43
4) Barents Sea					
2) runoff	22	0.03 Sv	0.03	0.002	0.005
3) Arctic, upper	23	0 Sv	0.33	0.57	0.46
4) Arctic, lower	24	1.5 Sv	1.30	0.68	0.40
5) Air-Sea Interface, heat	25	70 W/m^2	25.2	4.65	6.43
6) Air-Sea Interface, salt	26	0 mm/yr	-3.75	59.5	125.2
5) Arctic, upper					
4) Bering Sea	27	0.8 Sv	0.46	3.85	0.28
5) Canadian Archipelago	28	-1.5 Sv	-1.59	0.13	0.61
6) Polar Water, EG	29	-1.5 Sv	-1.48	0.34	0.54
7) AAW, EG	30	-1.5 Sv	-1.54	0.86	0.54
8) IW, EG	31	0 Sv	0.17	0.75	0.5
9) runoff	32	0.1 Sv	0.1	0.004	0.005
10) Arctic, lower, vertical	33	0 m/s	2.1e-08	1.71e-07	1.7e-08
11) Air-Sea Interface, heat	34	0 W/m^2	8.5	1.4	0.8
12) Air-Sea Interface, salt	35	0 mm/yr	-7.5	112.2	50.6
6) Arctic, lower					
4) DW, EG	36	-1.0 Sv	-0.72	2.1	0.38
7) Polar Water, EG					
2) Greenland Gyre	37	0.1 Sv	0.03	0.29	0.53
3) Iceland Gyre, upper	38	0.1 Sv	-0.10	0.32	0.54

4) Denmark Strait	39	-1.5 Sv	-1.58	0.31	0.54
5) runoff	40	0 Sv	0	0.002	0.005
6) AAW, vertical	41	0 m/s	1.4e-07	6.2e-06	5.5e-07
7) Air-Sea Interface, heat	42	0 W/m^2	0.58	30.6	2.35
8) Air-Sea Interface, salt	43	0 mm/yr	-3.90	58.3	351.6
8) AAW, EG					
2) Greenland Gyre, upper	44	0 Sv	-0.17	0.23	0.54
3) Iceland Gyre, upper	45	0 Sv	-0.31	0.24	0.55
4) Denmark Strait	46	-2 Sv	-1.94	0.67	0.56
6) rAtW, vertical	47	0 m/s	-3.4e-07	2.3e-06	1.4e-06
9) rAtW, EG					
2) Greenland Gyre, upper	48	0 Sv	0.25	0.25	0.50
3) Iceland Sea, upper	49	0.1 Sv	0.22	0.24	0.51
4) Iceland Sea, lower	50	0.5 Sv	0.09	0.37	0.17
5) Denmark Strait	51	-1 Sv	-0.83	0.64	0.49
7) IW, vertical	52	0 m/s	1.4e-06	2.0e-06	1.0e-06
10) IW, EG					
2) Greenland Gyre, upper	53	-0.2 Sv	-0.17	0.35	0.50
3) Iceland Sea, lower	54	0.1 Sv	-0.24	0.70	0.47
5) DW, vertical	55	0 m/s	1.0e-08	6.9e-06	3.2e-08
11) DW, EG					
2) Greenland Gyre, lower	56	-0.1 Sv	-0.30	2.31	0.21
5) Iceland Sea, lower	57	0.1 Sv	0.48	1.23	0.42
12) Gr. Gyre, upper					
7) GG, lower, vertical	58	0 m/s	-3.6e-07	2.5e-06	1.2e-06
8) Air-Sea Interface, heat	59	70 W/m^2	27.4	22.1	32.0
9) Air-Sea Interface, salt	60	0 mm/yr	-3.8	58.0	305.9
14) Iceland Sea, upper					
6) Atlantic, Irminger	61	1 Sv	0.86	0.41	0.48
7) East of Iceland	62	-0.5 Sv	-0.69	0.44	0.53
8) IS, lower, vertical	63	0 m/s	1.1e-07	6.0e-07	1.4e-06
9) Air-Sea Interface, heat	64	70 W/m^2	48.3	34.8	41.3
10) Air-Sea Interface, salt	65	0 mm/yr	-3.75	58.7	276.1

outflow of 1.5 ± 0.8 Sv of Arctic Atlantic Water from the Arctic Ocean. There is a small contribution of this water from both of the gyres, giving a dense overflow of AAW in the Denmark Strait of 1.9 ± 0.7 Sv. The return Atlantic Water loses 0.2 ± 0.5 Sv to each of the gyres, resulting in 0.8± 0.6 Sv rAtW exiting in the Denmark Strait. The dense overflow in the Denmark Strait thus totals 2.8± 0.7 Sv. In the gyres there is production of Intermediate Water to support a 0.6± 0.8 Sv flow of Intermediate Water across the Iceland-Scotland Ridge. The bulk of the Deep Water flow through the Færø-Shetland Channel is formed in the Barents Sea. 0.7± 0.4 Sv of North Icelandic Winter Water is formed in the Iceland Sea. The total flow of dense water across the Iceland-Scotland Ridge thus becomes 2.3± 0.7 Sv.

As was anticipated from the initial imbalances, the heat balances in the surface boxes are modified; by altering the air-sea heat fluxes. The heat flux over the Greenland Sea is reduced to 27 ± 22 W/m^2, and the heat flux over the Iceland Sea is reduced to 48 ± 34 W/m^2, increasing the zonal heat flux gradient in the Nordic Sea. This is consistent with the atlases of figs. 4.4-4.6, which indicate a significantly higher heat flux over the North Atlantic Current than over the rest of the area. The solution for the heatflux over the North Atlantic Current is 68 ± 7.5 W/m^2. The heat flux over the Barents Sea is reduced to 25± 5 W/m^2, this probably indicates that the North Atlantic Current occupies a smaller fraction of the surface area of this large shelf sea, and that a smaller heat flux is more representative as an average value. In the Arctic Ocean the heat flux is raised from 0 W/m^2 to 9± 1 W/m^2. This result is consistent with Maykut (1978), who finds heat fluxes of O(10 W/m^2) through thick ice, and O(several hundred W/m^2) through leads. The heat flux over the East Greenland Current is 0 ± 31 W/m^2, which is a reasonable result as this region is normally ice-covered, and the current beneath is so swift that little exchange with the atmosphere is expected.

This solution - the standard model - does not significantly differ from the initial estimate, a finding that indicates that the direct transport estimates are consistent, not only internally, but also with the heat and salinity balances. And, even more importantly, the hypothesized circulation scheme of chapter 3 is consistent with the mass, heat and salt balances, and with the direct current estimates and with the knowledge of heat fluxes in the region.

The uncertainties are very large for parts of the scheme. For some parts of the total flow field the uncertainty is as large as the transport itself. Ideally one would want to include other types of data to constrain the model better, data that were not available to me during the development of this model. Note that for the solution elements where the core analysis already has provided an estimate of the direction of flow the sign of the total flow is not in question.

4.4 Unrealistic Scenarios

Although there are large uncertainties in the circulation scheme one must not be led to believe that just about any initial model would yield a possible solution. There are strong constraints in the system. In the following a few test cases will be described.

Swift et. al. (1980)'s hypothesis of formation of Denmark Strait Overflow Water in the Iceland Sea is tested with the model. In the paper they estimate a production rate of 0.6 Sv. Based on the above argument of sensitivity and uncertainties it is clear that the model will not be able to differentiate such a small production rate from zero. In fact, runs 22-7 and 22-8 (appendix) simulate such a situation. The (heavily quoted) conclusion of this paper state that "the component of the Denmark Strait overflow of greatest significance to the formation of NWABW, and hence the component influencing North Atlantic Deep Water, is an intermediate water of arctic origin ... This water is formed in

winter in the sea surface north of Iceland; some may form in the Greenland Sea north of Jan Mayen as well".

The test here will therefore be whether it is possible to form 2 Sv of AIW in the Iceland Sea. 2 Sv would correspond to 2/3 of the dense overflow in the Denmark Strait, and would therefore qualify as "the majority". In order to produce such an amount of dense water the model requires the heat flux over the Iceland Sea to exceed 150 W/m^2. There is certainly uncertainty in the heat fluxes in the region, but this is more than twice as high as the heat flux over the North Atlantic Current further east, and must be considered unrealistic. The surface area of the Iceland Sea is too small to successfully cool a significant amount of water. When the heat flux over the Iceland Sea is forced down to more realistic values, a significant inflow of Polar Water is induced to cool off the Atlantic Water. It has been shown, using tritium data (e.g. Doney, 1991), that significant amounts of Polar Water cannot enter the Iceland Sea. The above hypothesis - that the majority of the Denmark Strait overflow water is formed in the Iceland Sea, is therefore inconsistent with the model.

Another scenario that has been tested with the model is that a substantially smaller amount of Atlantic Water enters the Nordic Seas. A model was run with an initial estimate of the Atlantic inflow set to 3 Sv, instead of 7 Sv.

The model chooses an inflow of 3.5 Sv. The heat loss over the Norwegian Sea is much reduced, and over the Greenland Sea there is now a net heat gain. Only 2.5 Sv of dense water for the overflows is produced. This amount of dense water formation is unrealistically small: it corresponds to the estimates for either of the two straits alone. This scenario is therefore rejected.

Lastly, a model is run to test whether it is possible to send a substantial amount (compared to the amount formed in the Atlantic Domain) of dense water into the Iceland

Sea and the Greenland Sea, so that the flow in the Atlantic Domain cannot be treated as "flow in a channel". In this case 2 Sv was sent westward into the Iceland Sea, and 2 Sv westward into the Greenland Sea. The net annual heat loss rises to above 106 W/m^2 in the Greenland Sea, and to 130 W/m^2 in the Iceland Sea. In order to increase the heat loss in the gyres even further the model chooses to export water that originates outside the gyres (as return Atlantic Water), and this solution is regarded as unrealistic.

4.5 Discussion

In this chapter it has been confirmed that the circulation scheme that was constructed in chapter 3 is consistent with conservation statements for mass, heat and salt, and also with direct estimates of current transport where such exist, and with air-sea heat flux estimates. In particular, it is shown that forming the Arctic Atlantic Water in the Arctic is consistent with the model. Furthermore the majority of dense water is formed in the Atlantic Domain, not in the gyres.

It has been shown that it is unrealistic for the majority of the Denmark Strait Overflow Water to be formed in the Iceland Sea, as suggested by Swift et. al. (1980). However, the model cannot exclude the possibility that 0.6 Sv of DSOW is formed in the Iceland Sea (as was calculated by Swift et. al. 1980) or that 0.6 Sv of DSOW is formed in the Greenland Sea (as was calculated by Strass et. al., 1993). These production levels are within the uncertainty of the model. It is not surprising that the model - which is based on temperature, salinity and mass alone - cannot exclude the possibility of a (small) source in the Iceland Sea or the Greenland Gyre. If it were obvious from the temperature and salinity properties that the Denmark Strait Overflow Water were different from the AIW in the Iceland Sea then there probably would not be uncertainty about the source of the Denmark Strait Overflow Water. My hypothesis about a source in the Arctic Ocean

therefore goes beyond T and S and is backed up with an additional wide array of evidence.

The model would be more successful at testing different hypotheses if there were stronger observational control. Better knowledge of the air-sea heat and freshwater fluxes, and of the melting and formation of ice, would be extremely useful.

Chapter 5

Implications

5.1 Site of Dense Water Formation

As hypothesized in chapter 3, and tested in chapter 4, the Atlantic Domain is volumetrically by far the most important site of dense water formation north of the Greenland-Scotland Ridge. Production of dense water occurs in four boxes: the Atlantic Domain, the Barents Sea, the Greenland Sea, and the Iceland Sea. The production rates in the three latter boxes are roughly 1 Sverdrup, whereas the production rate in the Atlantic Domain is seven times larger. Production there does not conform with traditional notions of deep water formation: it is not a big gyre, with open ocean convection, and it is not a shelf. Rather, the formation of dense water in the Atlantic Domain can be thought of as cooling of water flowing as a current in a channel. Warm water enters near the Færø-Shetland Channel, interacts only negligibly with neighboring water masses along the way, but is continually cooled. The data are not detailed enough to resolve the exact process by which light water is transformed to dense water within the current. The existence of such a transformation process poses an interesting dynamical question: Is this water formed through the same type of convection which occurs in open ocean gyres or is another process responsible?

The water that enters the gyres have already become heavier in the Atlantic Domain. Atlantic Water enters the Iceland Sea south of Jan Mayen Island. Typical TS properties of the Atlantic Water at this latitude are 4 ^{0}C and 35.1. The temperatures and salinities of the water entering the Greenland Gyre are still lower, since this gyre lies further north. Thus the water that is converted into denser water in the gyres has already lost buoyancy in the Atlantic Domain.

The efficiency of the formation of water within the Atlantic Domain is increased by the presence of denser water beneath, through which the cooling does not penetrate. The extremely high heat loss over the North Atlantic Current is typical for a region where a current carries water poleward from its point of thermal equilibrium with the atmosphere (fig. 4.5) (Bunker, 1976), a prominent example being the Gulf Stream. But high heat loss alone is not a sufficient condition for efficient water mass formation; if the stratification is weak the heat loss may be distributed throughout the water column and the net density change will be small. But as the depth of the Atlantic Water itself is only 600-1000 m, the efficiency of the heat loss in removing buoyancy is magnified.

5.2 Freshening of the Atlantic Water

The development in TS-space of the Atlantic Water in the Norwegian Sea is characterized not only by a reduction of the temperature, but also by a decrease in salinity (changes in temperature dominate changes in the density). Although the atmospheric fluxes are able to explain the changes in θ, such is not the case for changes in salinity; explaining the reduction in salinity requires a net precipitation less evaporation of $\sim$ 1500 mm/year. The evaporation associated with the atmospheric cooling amounts to roughly 1000 mm/year. The precipitation is high, especially in the southern part of the domain, resulting in a change in sign of P-E through the Nordic Seas, with amplitudes north and south of this line being maximum 500 mm/year (according to all three atlases of net annual water flux; see figs. 4.6, 4.7 and 4.8). Even though precipitation is an unusually uncertain parameter, especially at Polar latitudes where the data coverage is most certainly fair-weather biased, it would be unrealistic and inconsistent with the atlases, to expect the precipitation to account for the additional 1500 mm/year needed to explain the freshening of the Atlantic Water. One can therefore assume that P-E has little influence

on the salinity budget in the Atlantic Domain, and therefore another source of fresh water must be sought.

It has been argued throughout this work that the exchange between the gyres and the Atlantic Water is minimal. Nevertheless one should examine whether it is possible to explain the freshening of the Atlantic Water by mixing with the gyres. A typical salinity for the upper layers of the gyres is 34.8, with a corresponding temperature around 0 ^{0}C. To decrease the salinity of the Atlantic Water from 35.3 to 35.0 (assuming a 7 Sv transport of Atlantic Water) requires an inflow of 10.5 Sv from the gyres, which would reduce the temperature of the Atlantic Water to 2.5 ^{0}C. This cooling would seriously change the heat budget, and one has to conclude that the freshwater source cannot be found in the Iceland and Greenland gyres.

The two remaining freshwater sources are: exchange with the Norwegian Coastal Current and melting of ice. Indications that either or both of these effects do influence the salinity budget in the Atlantic Domain will be examined in the following.

1. Norwegian Coastal Current: The Norwegian Coastal Current is 1-2 degrees colder than the Atlantic Water, with salinities around 33.0. Especially within the biological literature there are numerous indications of the interaction between the Atlantic Water and the Norwegian Coastal Current. Helland-Hansen and Nansen (1909) observed that the amount of coastal water in May was correlated with the amount of precipitation over southern Norway the previous winter, and also with the high catches of herring off northern Norway the following year. They suggested that entrainment of nutrient-rich Atlantic Water into the Norwegian Coastal Current may be expected due to the shear stress caused by the relative difference in velocity (although there are no indications that the velocities of the NCC actually are higher in summer (Skreslet (1981)).

Føyn and Rey (1981) considered 5 crossections of the Norwegian Coastal Current, one of their goals being to explain the relatively high nutrient levels in the surface layers of the coastal current waters throughout the production season. They conclude that the

source of the nutrients cannot be the fjords, or the Skagerak winter waters, but rather a more or less continuous inflow of nutrient-rich Atlantic Water from below.

Skreslet (1981) suggests that the westward extension of the Norwegian Coastal Current during summer enhances the potential mixing between the Atlantic Water and the Norwegian Coastal Current, due to the increased surface area, and thereby improving the conditions for primary production. He also notes that the large-scale storage of meltwater for hydroelectric power production has reduced the freshwater outflow to Norwegian coastal waters, and he suggests that there are indications of reduced overall biological production as a result.

Hence it is clear that the combination of freshwater outflow to the coastal currents and mixing with the Atlantic Water beneath, is of paramount importance for the biological production off Norway. But the influence of the Norwegian Coastal Current on the salinity of the Atlantic Water would only be a boundary effect if it weren't for the fact that the fresh waters of the Norwegian Coastal Current influence the entire Norwegian Sea; the Norwegian Coastal Current changes throughout the year; in winter it is narrow and deep (200 m), whereas in summer it is broader and shallower , corresponding to the outflow of continental meltwater which peaks in the late spring. Skreslet (1981) notes that although the lateral extent of the Norwegian Coastal Current during freshwater outflow usually refers to the seaward position of the 34 or 35 isohaline the freshwater from the Norwegian coast is transported beyond this limit, across the Atlantic Domain, and he suggests that the surface waters of the central Norwegian Sea, which are highly productive during summer, should be defined as a marginally stratified frontal zone of coastal water. This fresh water will be mixed downward as the wind and the cooling increases towards winter, hence contributing to a general reduction of the salinity, not just near the inshore edge of the domain, but in the entire Atlantic Water, as was observed and discussed in chapter 3. Since the salinity difference between the Norwegian Coastal Current and the Atlantic Water is large, whereas the temperature

difference is relatively small, this interaction, although it could be crucial to the salinity budget, has little influence on the heat or mass budget.

2. Ice melting: Although the ice export through the Fram Strait has been fairly well monitored (Wadhams, 1989; Vinje and Finnekåsa, 1986), little is known about the fate of this ice in the Nordic Seas, in particular: where does it melt? The Atlantic Water is the warmest in the region, so it is likely that any ice that enters the Atlantic Domain will melt (the Domain is permanently ice free). There are two paths by which ice may enter the Atlantic Domain: one is a direct path in the Fram Strait, and one is a more indirect path around the Greenland Gyre. Also in this case the heat budget would not be affected; melting enough ice to provide the necessary freshening only requires 12 W/m^2.

These two effects are suggested to be the agents by which the salinity of the Atlantic Water is reduced, although better data are needed to quantify their relative importance.

5.3 Residence Time

The detour through the Arctic Ocean implies a longer residence time for the freshest overflow waters in the Denmark Strait than would be the case if that water was formed in the Iceland Sea. Several authors have reported on an age of O(1-4 years) for the overflow waters (Swift et. al., 1980), (Smethie et. al. 1989).

At the same time the high helium values in the overflow waters imply a higher age. Doney (1991) found the tritium inventory of the North Atlantic to be increasing between 1972 and 1981, a finding he can only reconcile by invoking a delay in the Arctic. In his model the fresh Polar Water, with the high tritium values, enters the North Atlantic and participates in the subpolar gyre, reentering the Nordic Seas and being transformed into the overflow waters, thus entering the deep North Atlantic. Models of transient

tracers depend crucially on the circulation scheme chosen, and the mixing involved, the age calculations being biased towards the youngest water mass present. It would therefore be interesting to redo the calculations with the circulation scheme proposed here.

The return Atlantic Water - the part of the Denmark Strait overflows that doesn't enter the Arctic Ocean - will have a correspondingly younger age.

5.4 Oscillations in T and S, Connections with the North Atlantic

Observations indicate that the hydrographic properties of the deep North Atlantic are changing on decadal time scales. Brewer et. al (1983) found large-scale freshening (0.02 per mille) of the deep waters of the subpolar North Atlantic, by comparing data from the Erika Dan cruise of 1962 with data from the TTO/NAS expedition in 1981. Swift (1984) found that even between the GEOSECS expedition in 1972 and TTO/NAS there was a freshening of 0.02 per mille (and a cooling of 0.15 ^{0}C). These authors therefore suggest that the deep North Atlantic is sensitive to changes on time scales as short as 10 years.

Given the finding that the majority of the dense water formation within the Arctic Ocean and Nordic Seas occurs within the Atlantic Domain, one has an extra dataset for studying such changes in the western North Atlantic. As mentioned before, Weather Station Mike is positioned within the Atlantic Domain, towards the western edge (at 66 N, 2 E). Hydrological and meteorological variables have been monitored there for 45 years. The time series of temperature and salinity at Weather Station Mike is shown in fig. 3.17, and discussed in section 3.1. The recurrent oscillations in both temperature and salinity on a roughly 10 year time scale are prominent features of these time series.

Many authors have found indications that such oscillations are advective phenomena. Helland-Hansen and Nansen (1909) found a time lag of 2-3 years between anomalies in the Svinøy area (62 N, 5 E) and those observed in a section at 33.5 E in the Barents Sea. Jakhelln (1936), studying an area of the East Greenland Current between 72 N and 75 N notes: "It is evident ... that there are considerable variations of temperature and salinity in the Atlantic Water under the Polar Current. On account of the insufficiency of the material of observations at hand, it is not possible to give any details as to the nature of these observations. It must be pointed out that in 1931, and particularly in 1932, salinity as well as temperature are exceptionally high in the Atlantic Water, and that these conditions very probably correspond to the extraordinary conditions which were found by Helland-Hansen (1934) in the Atlantic Current off the western coast of Norway in 1928 and 1929. It appears that this extraordinary Atlantic Water has been present of the coast of East Greenland as early as 1931 ... Such extraordinary conditions are also found by Mosby off Spitsbergen in 1931, as mentioned by Helland-Hansen."

Blindheim and Loeng (1981) found a time lag of 2-3 years between a temperature and salinity maximum in the Rockall Channel around 1970 and a similar maximum near Bear Island. The fact that the oscillations at Weather Station Mike are in phase down to at least 300 m, with equally large amplitude at each depth led Gammelsrød et. al. (1984) to suggest that the signal was advected, rather than a local influence.

With the new circulation scheme there is the possibility of a fairly direct link to the deep North Atlantic. In particular the return Atlantic Water can carry the oscillations directly to the North Atlantic, as this water follows a direct path to the Denmark Strait (Jakhelln's observations in the East Greenland Current were obtained not far upstream of the Denmark Strait). The branch that enters the Arctic Ocean has a longer residence time, and is further modified in TS-space, so this signal may be somewhat more diluted (although the residence time scale is not longer than the time scale of the oscillations). It

is suggested, therefore, that the time series at Weather Station Mike may be quite valuable for studies of climatological change in the deep North Atlantic.

5.5 Seasonality

One might expect that that winter production of dense water would induce a seasonal signal in the circulation. Such a seasonal signal is not observed in the flow of dense water across the Greenland-Scotland Ridge. Several authors have sought to explain the dynamics of the dense overflows in terms of hydraulically controlled flow. If the reservoir of dense water is large, and the overflows are hydraulically controlled one could imagine that the seasonal signal would vanish. Here I have ignored the issue of whether the overflows are hydraulically controlled, and simply examined whether the formation process itself, within the North Atlantic Current upstream of the overflows, would induce a seasonal signal in the flow field. It will be shown that within the Atlantic Domain the net annual cooling dominates the seasonal fluctuations for time scales comparable with the residence time of the Atlantic Water within the domain, and that a seasonal signal therefore is not induced by the water mass formation.

The effect of the net annual atmospheric heat loss can be studied by comparing the heat content of a water volume near the Færø-Shetland Channel to that of a similar volume near the Fram Strait, since it is found, in chapters 3 and 4, that the Atlantic Water flows as if in a channel through the Atlantic Domain, essentially losing heat to the atmosphere. The boxes of chapter 4 may be used for this calculation. The box model does not contain depth information *per se*, only surface area and transports. To obtain a depth to apply to the heat content calculation one needs an independent estimate of the volume occupied by the Atlantic Water within the Atlantic Domain. This can be found by for instance considering Dietrich's atlas (1959), based on the IGY data from 1958. One finds $Vol_{ATLANTIC} = 6 \cdot 10^5 \pm 10^5$ km^3, which gives a depth of 400 m, given the area

estimate of $1.5 \cdot 10^6$ km^2 for the Norwegian Sea used in the box model (the values used in the box model are found in table 4.2).

The heat content H is given by:

$$H = \int \rho c_p T \, dz$$

With $\rho = 1.028 \cdot 10^{-3}$ kg/cm^3, $c_p = 953$ cal/kgK and 7 ^{0}C one gets, near the Færø-Shetland Channel:

$$H_{FSC} = 274 \pm 50 \text{ kcal/cm}^2$$

Near the Fram Strait the water is seldom warmer than 3 ^{0}C, and it is mostly around 2 ^{0}C. Using 2 ^{0}C the heat content near the Fram Strait becomes:

$$H_{Fram} = 78 \pm 50 \text{ kcal/cm}^2$$

The difference: $\Delta H = H_{FSC} - H_{Fram}$ has been lost by the Atlantic Water during the passage:

$$\Delta H = 196 \pm 50 \text{ kcal/cm}^2$$

The heat content relates to the atmospheric heat loss in the following way:

$$Q = \frac{DH}{Dt}$$

The residence time for the Atlantic Water in the Atlantic Domain can be calculated, given the throughflow transport estimate (chapter 4) and the volume occupied. One obtains:

$$\text{Time} = \frac{\text{Volume}}{\text{Tranport}} = \frac{6 \cdot 10^5 \text{ km}^3}{7 \cdot 10^6 \text{ m}^3/\text{s}} \approx 2\text{–}3 \text{ years}$$

This estimate of residence time is consistent with the observations of the time it takes for hydrographic anomalies to propagate through the Norwegian Sea, as discussed in the previous section.

The air-sea heat flux Q corresponding to this residence time, and the reduction in heat content ΔH, is given by:

$$Q = \frac{DH}{Dt} \approx 65 - 100 \text{ kcal/cm}^2 \text{ year} \approx 85 - 120 \text{ W/m}^2$$

This heat flux is, by implication, consistent with the findings of the box model (and therefore consistent with atlases of heat loss over the Nordic Seas). (The range is, nevertheless, somewhat on the high side, compared with the model (~ 70 W/m^2). The reason is partly that the Norwegian Sea box in the model occupies a larger volume than the Atlantic Domain containing the Atlantic Water. In addition, in the model some heat is used to melt ice).

It is concluded, therefore, that $\Delta H = 190 \pm 50$ kcal/cm^2 is a representative and consistent estimate of the heat loss of the Atlantic Water within the Atlantic Domain, and that this heat is lost over a 2-3 year time period.

The effect of the seasonal cycle of the atmospheric heat flux can be seen, qualitatively, e.g. near the Færø-Shetland Channel , where Tait (1957) shows several sections across the Atlantic inflow (fig. 5.1). A seasonal thermocline can be seen in the upper 100-200 m. Likewise, warm water can be seen in the surface layer during summer within the Atlantic Domain of the Norwegian Sea. But for most of the depth of the Atlantic Water the temperatures are fairly constant year around. Further insight into this effect can be gained by considering the situation at Weather Station Mike, positioned in the Atlantic Domain. The distribution of temperature at five different depths throughout the year, averaged over 34 years, is shown in fig. 5.2 (from Gammelsrød et. al., 1984). The downward propagation over time of the influence of summer heating is evident, with decreasing amplitude, similar to what was seen in a more qualitative manner in the sections. At 300 m the seasonal signal is practically negligible, so one can calculate seasonal variations in heat content at Station Mike. The results are shown in fig. 5.3. The amplitude of the seasonal signal is 20 kcal/cm^2, which is only roughly 10 % of the net heat loss for the column traveling from the Færø-Shetland Channel to the Fram Strait (190 kcal/cm^2). Assuming that the seasonal signal has a similar influence further north, towards the Fram Strait (as is indicated by Gorshkov (1983)) it is evident that the seasonal influence on the net heat loss from the Færø-Shetland Channel is negligible, and that the water will be uniformly dense when it arrives in the Fram Strait - short of a shallow seasonal thermocline - regardless of season. Support for this conclusion is found by plotting all the observations of Atlantic Water in the Fram Strait in a TS-diagram (fig. 3.36). Even for the summer cruises most of the Atlantic Water in the Fram Strait is dense enough to sink to the bottom of the North Atlantic.

The observed seasonal variations in heat content at Weather Station Mike can be compared to model predictions, using a one-dimensional model of oceanic heat content forced by atmospheric heat flux. Bunker's estimate of the atmospheric heat flux at

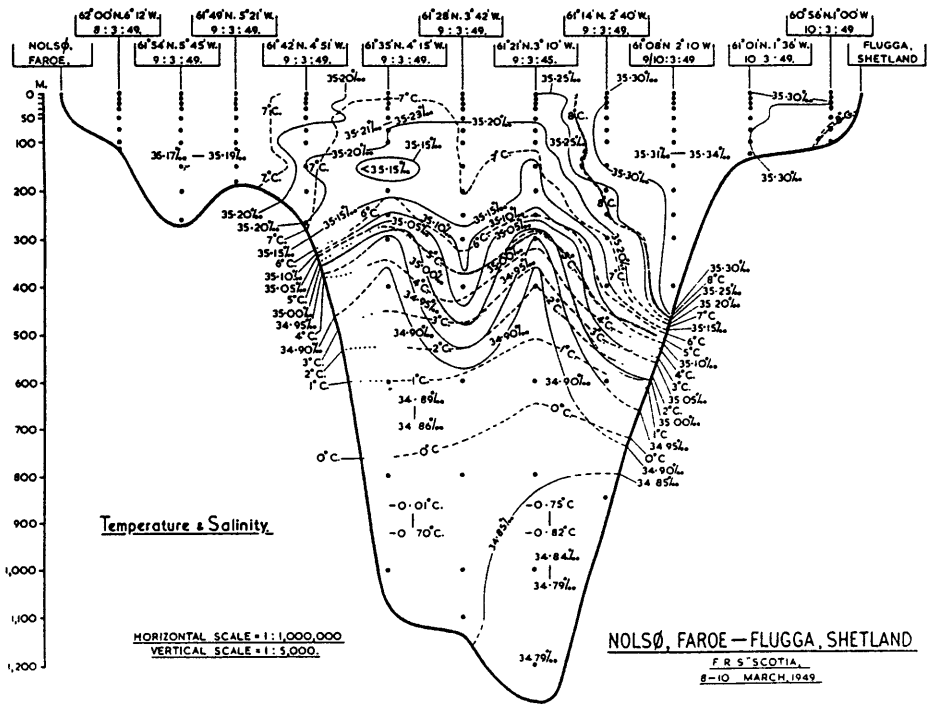

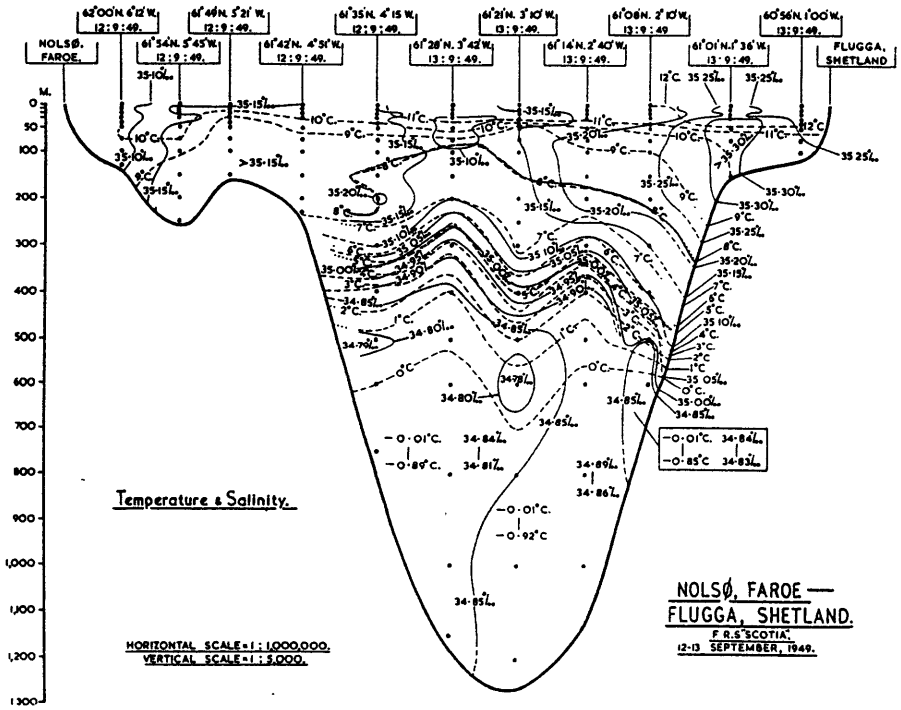

Fig. 5.1 T and S sections across the Atlantic Inflow (Tait, 1957)

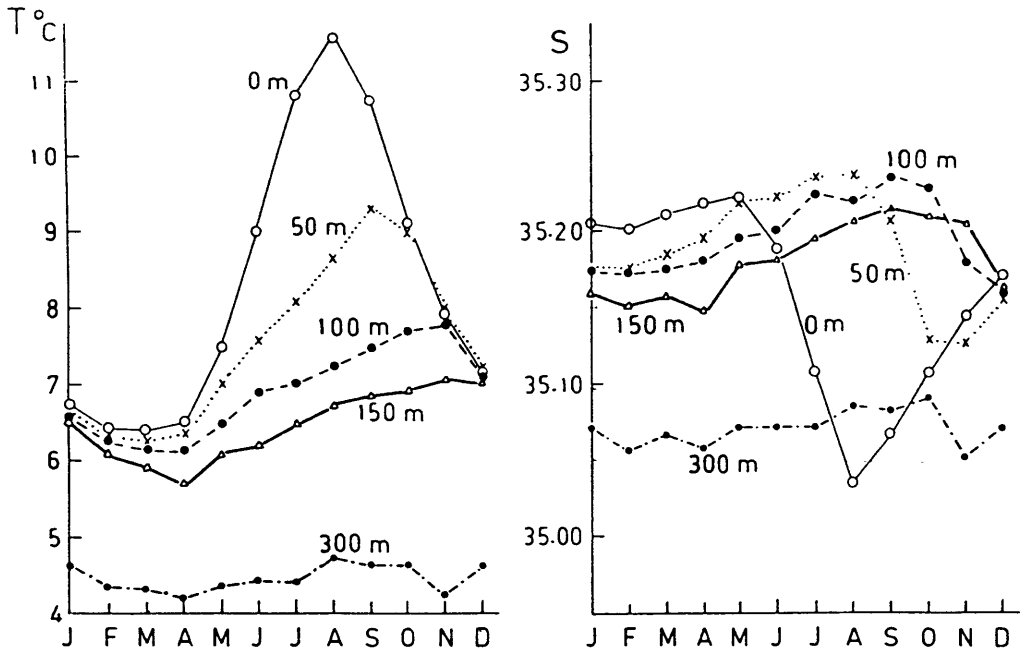

Fig. 5.2 Seasonal variations of T and S at Weather Station Mike.

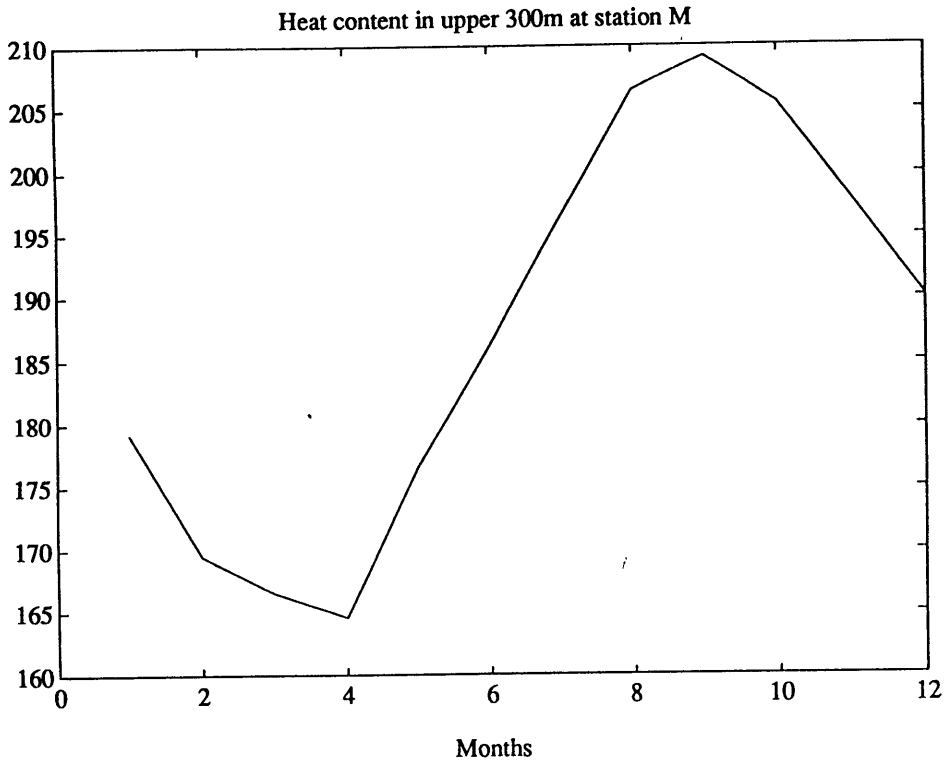

Fig. 5.3 Seasonal variations in heat content at Weather Station Mike.

Weather Station Mike is given in fig. 5.4, and Gorshkov's estimate in this general area is given in fig. 4.6. The heat flux can be parameterized as:

$$Q = 130\ (\pm 20)\ \cos(\omega t)\ \text{kcal/cm}^2\ \text{year}$$

The predicted changes in heat content due to this seasonal signal in the heat flux are given by:

$$H(t)=H(0) + \int Q dt$$

H(t) is plotted in fig. 5.5 with the observed heat content at Station Mike overlaid. The agreement between the two curves is very good, indicating that the seasonal signal in heat content at St. Mike is explainable by a local balance with the atmosphere alone. The accumulation of heat is greatest three months after the greatest surface heat input, ie. in September, as is typical for such a local balance.

The combined effect of the net annual heating and the seasonal oscillation in the heat flux on a volume of water flowing north can be parameterized as:

$$Q = 130\ (\pm 20)\ \cos(\omega t) - 60\ \text{kcal/cm}^2\ \text{year}$$

The predicted changes in heat content is the same as above: $H(t)=H(0) + \int Q dt$. The result is shown graphically in fig. 5.6 where the seasonal signal is seen to be a perturbation given the appropriate residence time.

The seasonal signal in the wind field in the Norwegian Sea, as discussed in chapter 2, reinforces the asymmetry of the winter cooling and the summer heating: the heating in the summer gets mixed down much less efficiently than the winter cooling.

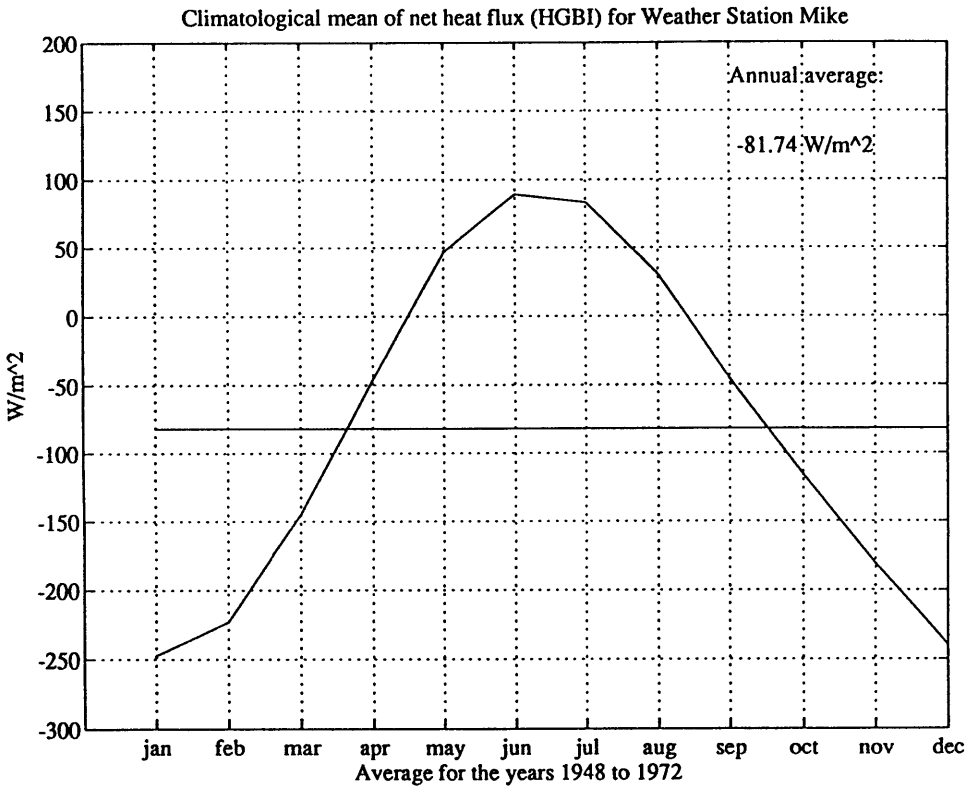

Fig. 5.4 Seasonal variations in atmospheric heat flux at station M (Bunker, 1976)

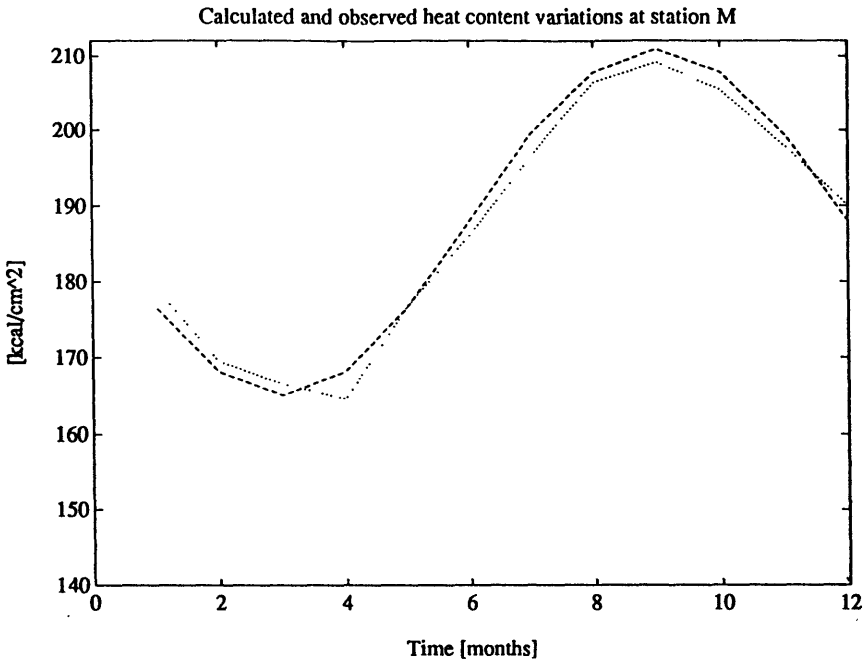

Fig. 5.5 Calculated and observed heat content at station M

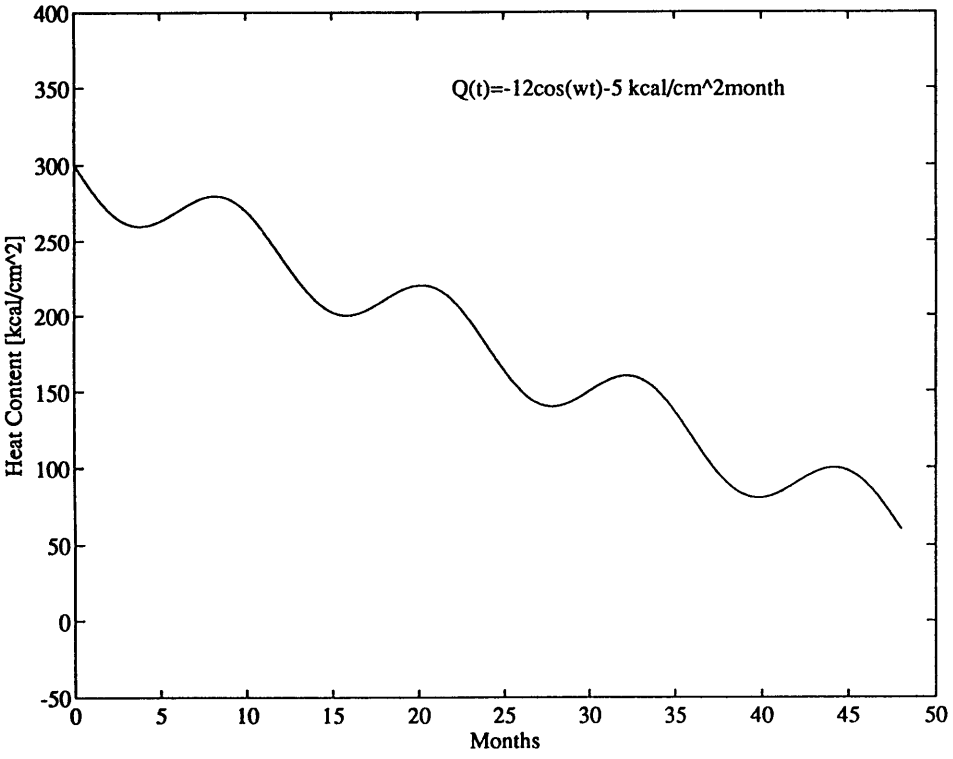

Fig. 5.6 Reduction of heat storage with a net cooling of 75 W/m^2

Thus it is found that due to the large net annual heat loss within the Atlantic Domain, and the relatively long residence time in this domain, the winter formation of water does not induce a seasonal signal in the flow field. Note that even if no water entered the Arctic Ocean, and it all recirculated in the Fram Strait, the above result would still hold. Formation of dense water within the Atlantic Domain does not induce a seasonal signal on the circulation.

Another seasonal signal within the domain is associated with that of the inflow of North Atlantic water. Not many long-term current meter measurements of the Atlantic Inflow to the Norwegian Sea exist. In Sept. 1984, four out of six 1-year moorings were recovered from the eastern slope of the Færø-Bank Channel, where the major inflow of Atlantic Water is expected to occur (Gould et. al. (1985)). Their transport estimates reveal a seasonal signal in the inflow: maximum inflow occurs in January / February (around 10 Sv), whereas minimum inflow occurs in July (around 5 Sv) (the data themselves are unfortunately confidential). Another current meter array was placed in the Færø-Bank Channel during 1986-1988 (Saunders, 1990). Three out of five moorings were recovered, with eight instruments. Of these, five were within the Atlantic Water, and two of these display a seasonal signal: the down-channel current component in late winter exceeding that in late summer by a factor of two. Also in the Bering Strait there are observations of a seasonal signal in the inflow; Coachman and Aagaard (1988) find a maximum inflow in June (1.1 Sv) and a minimum in February (0.5 Sv). The seasonal signal in the Bering Strait counteracts that in the Færø-Shetland Channel, so as to reduce the accumulation to a maximum excess of 4 Sv during winter, using the values from Gould et. al. (1985) for the Atlantic inflow.. Assume that the time-varying part of the inflow takes the form:

$$Tr=2\cos(\omega t)\ Sv,$$

where $\omega=2\pi/1$ year. The corresponding volume change within the Arctic Ocean / Nordic Seas become:

$$Vol=\int Trdt=(2/\omega)\sin(\omega t)$$

The amplitude of the volume change is 10^{13} m^3. Assuming that the excess water is distributed evenly in the Arctic Ocean and Nordic Seas - area = $11 \cdot 10^6$ km^2 - one gets a corresponding amplitude in sea level of 1 m, with the peak-to-peak amplitude being 2 m. Such a large summer vs. winter sea level change can probably not be permitted within the Arctic Ocean / Nordic Seas, unless it can be stored in the large ice sheet over the Arctic Ocean. More realistic numbers, e.g. from the coast of Norway, are 0.5 m for the peak-to-peak amplitude (fig. 5.7). So if the large seasonal variations measured by Gould et. al. (1985) are realistic, this excess must be transported out of the region within the same season, either through the dense or the shallow outflows.

It is reasonable to hypothesize that this seasonal signal would propagate through the system as a shallow - presumably winddriven - mode, exiting in the upper layer either east or west of Iceland. Unfortunately there do not, to my knowledge, exist long-term measurements of the shallow outflows from the Arctic Ocean and Nordic Seas. The rough ice-conditions are undoubtedly partly responsible.

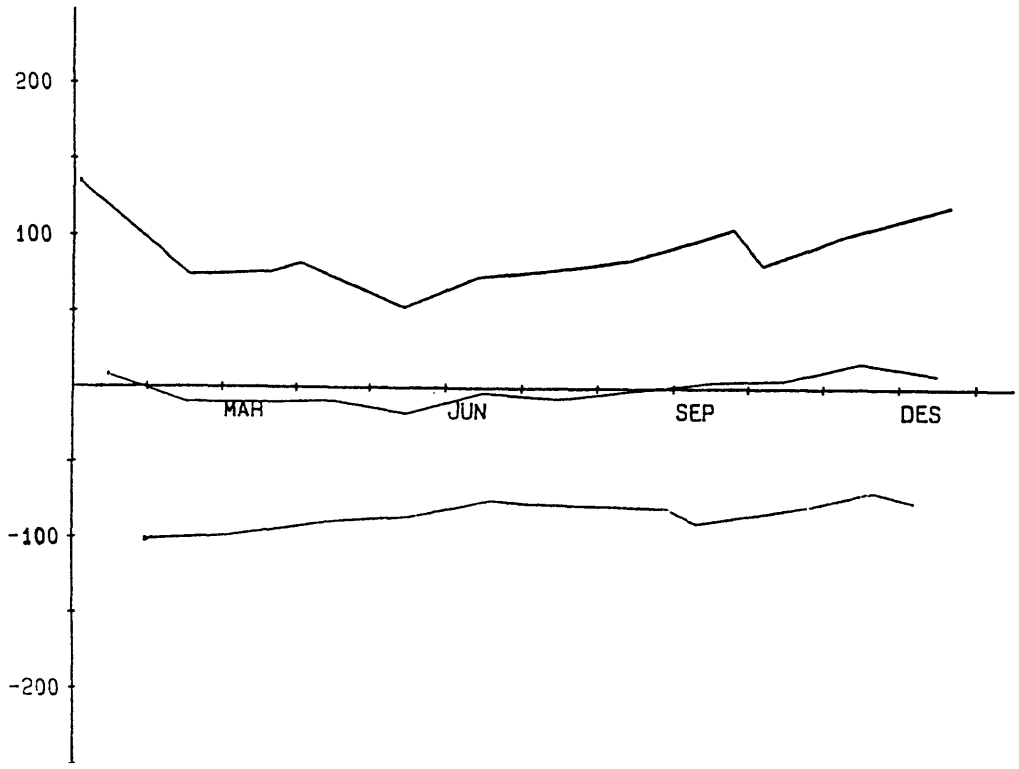

Fig. 5.7 Sea level variations off the coast of Bergen, Norway [cm] (middle line).

Chapter 6

Summary and Conclusions

Dense waters formed in the Nordic Seas and the Arctic Ocean spill over the Greenland-Scotland Ridge, and enter the world thermohaline circulation as the densest water both in the eastern and western North Atlantic. Thus the polar regions provide a direct link between the atmosphere and deep ocean, by means of deep water formation.

In this thesis it is suggested that contrary to the traditional view, the major buoyancy losses occur in the North Atlantic Current rather than in the gyre interiors of the Iceland and Greenland Seas. This conclusion is consistent with the watermasses, currents, and air-sea fluxes in the region, and with the observation that the overflows show little or no seasonal or interannual variability.

A new circulation scheme has been developed, with special emphasis on explaining the production of dense overflows to the North Atlantic. The North Atlantic Current flows northward in the Norwegian Sea towards the Arctic Ocean and the Barents Sea, east of the gyres, and brings warm water to unusually high latitudes. By the time the Atlantic Water subducts the Atlantic Water is generally as dense as the densest water in the North Atlantic, i. e. enough buoyancy is extracted to produce dense overflow waters for the Greenland-Scotland Ridge. The transformation is due to a large net annual heat loss over the North Atlantic Current, combined with a residence time of 2-3 years and a large surface area, giving surface heat loss time to act. The fact that the North Atlantic Current flows over even denser water limits the vertical extent over which the removal of buoyancy is distributed, and thus increases the efficiency of the atmospheric heat loss. It would be interesting to explore whether the dense water formation process within the current is

dynamically similar to the convection found in open ocean gyres, or whether another process is at work.

The cause of the freshening associated with the flow of the North Atlantic Current is unclear, but it was shown in chapter 5 that mixing with the Iceland and Greenland gyres cannot be the cause: the effects on the heat budget would be unrealistic. I have proposed that mixing with the Norwegian Coastal Current, and ice melt, are possible causes of the observed freshening of the North Atlantic Current. Neither of these processes would influence the mass or heat budget to a measurable degree.

As the North Atlantic Current continues north of the Lofoten Basin it splits into three branches; one entering the Barents Sea, one entering the Arctic Ocean, and the third recirculating in the Fram Strait, entering the East Greenland Current. The two latter branches eventually constitute the Denmark Strait Overflow.

The branch that enters the Arctic Ocean has its TS properties modified during its transit through the Arctic. As this water - the Arctic Atlantic Water - exits the Arctic Ocean in the western Fram Strait, beneath the Polar Water, it is fresher and colder then the directly recirculating Atlantic Water. It flows southwards, towards the Denmark Strait. The Arctic Atlantic Water has the properties that are generally associated with the Denmark Strait Overflow Water; low temperature and salinity, and matches the water found towards the bottom of the Irminger Basin in the North Atlantic. A main point in the support of an Arctic source of the Denmark Strait Overflow Water (DSOW), as opposed to a source in the Iceland Sea, as suggested by Swift et. al. (1980), is that the source in the Arctic has comparable properties to those of the DSOW. The waters of the Iceland Sea, the upper Arctic Intermediate Water, require modifications, especially in oxygen and helium, and also in temperature (more than is required for the AAW). The water masses available for mixing between the Iceland Sea and the Denmark Strait (Polar Water, return Atlantic Water, Irminger Sea Water) would not influence the properties in the right direction. To find this source in the Arctic it was important to realize that the areal coverage of any water mass in a

section is not the dynamically relevant parameter - the flux will depend on the flow field through the section. So although the water column in the Iceland Sea contains a higher percentage of "appropriate" water, the flux of this water will be higher in the East Greenland Current which is a swift current with a substantial barotropic component. It would be useful to obtain some more detailed sections of the East Greenland Current, extending all the way up the slope, to better sample the Arctic Atlantic Water. As it is intermediate in TS properties between the Polar Water and the return Atlantic Water it has not earlier been identified as a distinct water mass. The finding that this watermass is tagged by a high helium signal, although so far analyzed only for one station, is an indication that it will be possible to differentiate these three watermasses of the East Greenland Current.

The directly recirculating Atlantic Water - the return Atlantic Water - flows relatively unperturbed along the coast of Greenland towards the Denmark Strait along with the Arctic Atlantic Water. The return Atlantic Water is associated with a core of maximum temperature and salinity, found at roughly 300-500 m depth within the East Greenland Current. Since the return Atlantic Water is saltier than the bottom waters in the Irminger Basin it is generally thought that return Atlantic Water does not exit through the Denmark Strait, but I here propose that both return Atlantic Water and Arctic Atlantic Water exit the Denmark Strait. Since the Arctic Atlantic Water is colder, and therefore more compressible at high pressure, it will tend to sink deeper than the return Atlantic Water.

North of the Iceland-Scotland Ridge three dense water masses are available. Neither of these match the properties of the bottom water in the eastern North Atlantic. Thus some mixing must be invoked, contrary to the situation in the Denmark Strait.

The lightest of the dense water masses north of the Iceland-Scotland Ridge - the North Icelandic Winter Water - has been found by Stefansson (1962) to be formed in the Iceland Sea. Atlantic Water is brought into the Iceland Sea west of Iceland by the Irminger Current and is cooled off as it flows east with the East Icelandic Current, similar to the

cooling of the North Atlantic Current. As the East Icelandic Current enters the southern Norwegian Sea the water is denser than the Atlantic Water of the North Atlantic Current and is available as a dense overflow watermass north of the Iceland-Scotland Ridge.

The second dense watermass north of the Iceland-Scotland Ridge is the Intermediate Water. This water mass is found in a 100 m thin layer at $\sigma_0 \sim 28.0$. The data set analyzed in this thesis indicate that this water mass is remarkably widespread; it is found in the Norwegian Sea, in the Fram Strait, and along the slopes surrounding the Greenland Gyre. Although it is impossible to deduce the circulation of this shallow watermass, there can be no doubt that this water is formed in the Iceland and Greenland Gyres as suggested by Blindheim (1990); no other potential sources are available.

The densest water in the Færø-Shetland Channel is the lightest kind of Norwegian Sea Deep Water. Norwegian Sea Deep Water is generally thought to be formed from Greenland Sea Deep Water and Arctic Ocean Deep Water, where GSDW is formed in the Greenland Gyre and AODW is formed by brine rejection on the Arctic shelves. I propose that the source of the upper Norwegian Sea Deep Water is the branch of the North Atlantic Current that enters the Barents Sea. The strength of this branch is observed to be 1-2 Sv, which by mass conservation must continue into the Arctic Ocean. The heat loss over the North Atlantic Current in the Barents Sea is high, and it is likely that the Atlantic Water is transformed into denser water by the time it enters the Arctic Ocean, similar to the transformation of the North Atlantic Current within the Norwegian Sea. The water becomes fresher, similar to the freshening of the North Atlantic Current in the Norwegian Sea. This throughflow probably does not contribute to the densest water in the Arctic Ocean, but it is dense enough to contribute to the Færø-Shetland Channel overflow: Dense water from the Arctic Ocean enters the Nordic Seas through the western Fram Strait. It flows around the Greenland Basin and enters the Norwegian Sea without interacting much with the Greenland Gyre.

This concludes the description of the new circulation scheme. In chapter 4, an inverse box model was developed that shows that the new circulation scheme is consistent with conservation statements for mass, heat and salt, with direct current estimates, and with the knowledge of heat fluxes in the region.

Aside from the finding that the new scheme is more likely in terms of water mass properties, currents etc., one fundamental problem with the old circulation scheme lies with supplying a substantial overflow. There are indications that the production of dense water in the gyres is sensitive to the highly variable surface conditions, and that indeed the production tends to shut on and off. The reservoirs in the gyres are so small that they would be drained within ~ 5 years if they were to supply the overflows during a shutdown period. Likewise, there are indications that production of dense water through brine rejection on the Arctic shelves is not efficient enough to produce the necessary dense water.

The new circulation scheme is more consistent with these observations, and in particular it can maintain the persistent dense overflows across the Greenland-Scotland Ridge despite the variability of the gyres. One reason that the production of dense water within the North Atlantic Current is more stable than the vertical overturning in the gyres is that the density of the overflows is gained at a temperature well above freezing. The surface temperatures of the gyres, on the other hand, is closer to freezing. Therefore a freshwater anomaly in these two domains will have different consequences for vertical overturning; within the North Atlantic Current the freshening can be overcome by further cooling, whereas in the gyres the freshening cannot be overcome because freezing will occur. In fact the Norwegian Sea and large parts of the Barents Sea are observed to be ice-free year-round.

The observation of the lack of a significant seasonal signal associated with the dense overflows is consistent with the new circulation scheme: I have shown in chapter 5 that the winter formation of dense water within the North Atlantic Current does not induce a seasonal signal in the transport field of the dense water. The reason for this is that the net

annual cooling dominates the seasonal fluctuations in the atmospheric heat loss for time scales comparable with the residence time of the Atlantic Water within the domain.

6.1 The Iceland and Greenland Gyres

The focus of this work has been on the source of the dense overflows across the Greenland-Scotland Ridge. In this respect the importance of the Iceland and Greenland gyres is limited to the production of Intermediate Water. For processes occurring on a a much longer time scale (processes requiring much smaller production rates), e. g. maintaining the extreme bottom properties of the Greenland-Sea Deep Water, the Norwegian Sea Deep Water and the Arctic Ocean Deep Water, the gyres and the brine rejection on the Arctic shelves may be more important.

There are some questions that arise in conjunction with this finding. Why do these gyres exist? The topography of both basins is somewhat bowl shaped, and in general the vertical stability is low in this region, so it is possible that the wintertime cyclonic windfield easily can maintain a cyclonic circulation. Cyclonic circulation will induce doming of isopycnals, and thus enhance the likelihood of vertical overturning within the gyres. There is ample evidence (going back to the beginning of the century) that at least the Greenland Gyre must occasionally overturn all the way to the bottom; at all depth levels of the gyre the temperature, salinity and nutrients and lower - and the oxygen higher - than those of the surroundings. This difference can only be maintained from the surface.

Why then is so little water exported? It is possible that the exchange in and out of the gyre is reduced due to the existence of the front surrounding the gyre. Recent observations using neutrally buoyant floats in the Gulf Stream area suggest that water particles are most likely to remain on the side of the front where they originate (Bower and Lozier, subm. to JPO). One must hope that the process of cross-frontal exchange,

particularly in the conjunction with an open-ocean gyre, will be better understood in the future.

There is one water mass that does leave the gyres to a measurable degree: the Intermediate Water. The potential density of the Intermediate Water is close to 28.0. It is possible that this water is more likely to be produced than any other watermass, since the density of this water is found close to the surface in the gyres year-round.

6.2 Future Work

It is exciting that even in a region that historically is as well studied as the Nordic Seas it is possible to question - on a very basic level - *what* is happening. The new circulation scheme may be further developed as new data becomes available. Techniques are continually improving to acquire data from ice covered regions. More densely spaced hydrographic stations would in general be helpful; the Rossby radius is small and the currents are often concentrated over narrow slopes that are not well resolved with a typical station spacing of ~ 50 km. Then one would be able to take more advantage of geostrophic calculations. Obtaining a wide variety of data, including transient tracers, would be particularly important in this region where the temperature and salinity differences are small and the interannual variability is high. The deeper circulation could become better known with the aid of neutrally buoyant floats. The quantification of the circulation scheme, in terms of the box model, would benefit from a better knowledge of the atmospheric heat fluxes, both on an annual and seasonal time scale. A better quantitative understanding of the continental runoff and of the locations of ice melting and freezing would also be very helpful.

Appendix

To get a handle on the uncertainties I have considered the sensitivity to the initial model. One can easily find solutions that lie outside the range of the formal uncertainties (using the calculated σ^2), by changing the initial model (within realistic bounds). A set of examples are given in the following table:

Model runs with different initial conditions

Model Run	Comment on Initial Model	Comment on Result
22-1	Atlantic Inflow to Norwegian Sea reduced from 7 Sv to 6 Sv	The model accepts an inflow of 6 Sv. Heat flux over Norwegian Sea reduced from 68 W/m^2 to 58 W/m^2, over Greenland Sea from 23 W/m^2 to 13 W/m^2. Dense overflows reduced from 5.1 Sv to 4.5 Sv
22-2	Dense overflows reduced from 5.1 Sv to 4.1 Sv (0.5 Sv less AAW and 0.5 Sv less AW)	Model chooses to increase dense overflows to 4.8 Sv. Solution unchanged
22-3	Atlantic inflow to Barents Sea reduced from 1.5 Sv to 0.5 Sv	0.9 Sv flows into Barents Sea. Heat flux there is reduced from 25 W/m^2 to 14 W/m^2. Flow direction between upper Arctic Ocean and Barents Sea is reversed: 0.1 Sv flows into Barents Sea.
22-4	Increased production of Intermediate Water. In Greenland Sea increased from 0.4 Sv to 0.8 Sv; in Iceland Sea from 0.1 Sv to 0.7 Sv	Production rate increased only in the Iceland Sea. Heat flux over Iceland Sea increased from 45 W/m^2 to 52 W/m^2.
22-5	Inflow through Bering Strait reduced from 0.8 Sv to 0 Sv.	Model chooses an inflow of 0.3 Sv. Results practically unchanged.

22-6	Heat flux over Norwegian Sea reduced from 70 W/m^2 to 0 W/m^2.	Solution unchanged: heat flux equals 68 W/m^2.
22-7	Outflow of Arctic Atlantic Water from Arctic Ocean reduced from 1.5 Sv to 0 Sv	0.7 Sv of AAW is produced in the Arctic Ocean (down from 1.6 Sv). Additional amount from Greenland Sea (0.4 Sv) and from Iceland Sea (0.6 Sv) to make overflow of AAW in Denmark Strait 1.7 Sv (down from 2 Sv)
22-8	No Atlantic Water entering Arctic Ocean. No AAW produced in Arctic Ocean.	Model chooses to send 1.2 Sv of Atlantic Water into Arctic (down from 3.4 Sv). Heat flux over Norwegian Sea reduced to 60 W/m^2. 0.2 Sv AAW is produced in Arctic Ocean. Still production of 1.6 Sv of AAW for Denmark Strait: 0.6 Sv from Greenland Gyre, 0.8 Sv from the Iceland Sea.

In some cases the model is not sensitive to the changes, and the model remains unchanged, whereas in other cases the model is sensitive to changes in the initial model. One can vary the initial estimates within the *a priori* bounds and obtain perfectly sensible solutions that can not be told apart, based on our observational knowledge of the region.

Note in these examples that the effect of changing one initial estimate tends to diffuse quickly because each box has many interfaces through which it interacts with the surroundings, and any disturbance is distributed throughout these interfaces.

References:

Aagaard, K. and L. K. Coachman, 1968. The East Greenland Current North of Denmark Strait: Part 2. *Arctic*, **21**, 267-290.

Aagaard, K. and P. Greisman, 1975. Toward New Mass and Heat Budgets for the Arctic Ocean. *Journal of Geophysical Research*, **80**, (27), 3821-3827.

Aagaard, K. and S. Malmberg, 1978. Low-Frequency Characteristics of the Denmark Strait Overflow. *ICES CM*, (C:47), 1-22.

Aagaard, K., 1981. On the deep circulation in the Arctic Ocean. *Deep-Sea Res.*, **28A**, (3), 251-268.

Aagaard, K., C. Darnell, A. Foldvik and T. Tørresen, 1985a. Fram Strait Current Measurements 1984-1985. University of Bergen, Norway (Report no. 63) and University of Washington, Seattle, U.S.A (Report no. M85-9).

Aagaard, K., J. H. Swift and E. C. Carmack, 1985b. Thermohaline Circulation in the Arctic Mediterranean Seas. *Journal of Geophysical Research*, **90**, (C3), 4833-4846.

Aagaard, K., 1989. A synthesis of the Arctic Ocean circulation. *Rapp. P.-v. Reun. Cons. int. Explor. Mer.*, **188**, 11-22.

Aagaard, K and E. C. Carmack, 1989. The Role of Sea Ice and Other Fresh Water in the Arctic Circulation. *Journal of Geophysical Research*, **94**, (C10), 14485-14498.

Aken, H. J. v., Briem, E. Buch, S. S. Kristmannsson, S. Malmberg and S. Ober, 1992. Western Iceland Sea - Greenland Sea Project. Hafrannsoknastofnun Fjølrit, *30*.

Anderson, L. G., E. P. Jones, K. P. Koltermann, P. Schlosser, J. H. Swift and D. W. R. Wallace, 1989. The first oceanographic section across the Nansen Basin in the Arctic Ocean. *Deep-Sea Res.*, **36**, (3), 475-482.

Baumgartner, A. and E. Reichel, 1975. The World Water Balance. Amsterdam: Elsevier.

Blindheim, J., 1986. Arctic Intermediate Water in the Norwegian Sea. *ICES CM*, (C:14), 1-15.

Blindheim, J., 1989. Cascading of Barents Sea Bottom Water into the Norwegian Sea. *Rapp. P.-v. Reun. Cons. int. Explor. Mer*, **188**, 49-58.

Blindheim, J., 1990. Arctic Intermediate Water in the Norwegian Sea. *Deep-Sea Res.*, **37**, (9), 1475-1489.

Blindheim, J. and H. Loeng, 1981. On the Variability of Atlantic Influence in the Norwegian and Barents Seas. *FiskDir. Skr. Ser. HavUnders*, **17**, 161-189.

Bloom, G. L., 1961. Measurements of water transport and of temperature in the Eastern Bering Strait 1953-1958.

Bower, A. S. and M. S. Lozier, subm. 8/93. A closer look at particle exchange in the Gulf Stream. *Journal of Physical Oceanography.*

Brewer, P. G., W. S. Broecker, W. J. Jenkins, P. B. Rhines, C. G. Rooth, J. H. Swift, T. Takahashi and R. T. Williams, 1983. A Climatic Freshening of the Deep Atlantic North of 50^{0}N over the Past 20 years. *Science*, **222**, 1237-1239.

Bryan, F., 1986. High-latitude salinity effects and interhemispheric thermohaline circulations. *Nature*, **323**, 301-304.

Budyko, M. I., 1974. Climate and Life. New York: Academic Press.

Bunker, A. F., 1976. Computations of Surface Energy Flux and Annual Air-Sea Interaction Cycles of the North Atlantic Ocean. *Monthly Weather Report*, **104**, 1122-1140.

Carmack, E. and K. Aagaard, 1973. On the Deep Water of the Greenland Sea. *Deep-Sea Research*, **20**, 687-715.

Clarke, R. A., J. H. Swift, J. L. Reid and K. P. Koltermann, 1990. The Formation of Greenland Sea Deep Water: Double Diffusion of Deep Convection? *Deep-Sea Res.*, **37**, (9), 1385-1424.

Coachman, L. K. and C. A. Barnes, 1961. The contribution of Bering Sea water to the Arctic Ocean. *Arctic*, 147-161.

Coachman, L. K. and C. A. Barnes, 1963. The movement of Atlantic Water in the Arctic Ocean. *Arctic*, 8-16.

Coachman, L. K. and K. Aagaard, 1988. Transports Through Bering Strait: Annual and Interannual Variability. *Journal of Geophysical Research*, **93**, (C12), 15535-15539.

Collin, A. E., 1963. The waters of the Canadian Arctic Archipelago. In: *Proceedings of the Arctic Basin Symposium.* Arctic Institute of North America, Washington, D.C., 128-136.

Cooper, L. H. N., 1955. Deep water movements in the North Atlantic as a link between climatic changes around Iceland and biological productivity of the English Channel and Celtic Sea. *J. Mar. Res.*, **14**, 347-362.

Crease, J., 1965. The flow of Norwegian Sea Water through the Faroe Bank Channel. *Deep-Sea Res.*, **12**, 143-150.

Dickson, R. R., J. Meincke, S.-A. Malmberg and A. J. Lee, 1988. The "Great Salinity Anomaly" in the Northern North Atlantic 1968-1982. *Prog. Oceanog.*, **20**, 103-151.

Dickson, R. R., E. M. Gmitrowicz and A. J. Watson, 1990. Deep-water renewal in the northern North Atlantic. *Nature*, **344**, 848-850.

Dietrich, G., 1959. Atlas of the Hydrography of the Northern North Atlantic Ocean. Conseil International Pour L'Exploration de la Mer. Service Hydrographique,

Dietrich, G., 1967. The International "Overflow" Expedition (ICES) of the Iceland-Faroe Ridge, May-June 1960. *Rapp. P.-v. Reun. Cons. int. Explor. Mer.*, **157**, 268-274.

Doney, S. C., 1991. A Study of North Atlantic Ventilation Using Transient Tracers. PhD-thesis, Woods Hole Oceanographic Institution Massachusetts Institute of Technology Joint Program in Oceanography and Oceanographic Engineering.

Eggvin, J., 1961. Some Results of the Norwegian Hydrographical Onvestigations in the Norwegian Sea during the IGY. *Rapp. et. Proc.*, **149**, 212-218.

Foldvik, A., K. Aagaard and T. Tørresen, 1988. On the velocity field of the East Greenland Current. *Deep-Sea Res.*, **35**, (8), 1335-1354.

Furnes, G. K, B. Hackett and R. Sætre, 1986. Retroflection of Atlantic Water in the Norwegian Trench. *Deep-Sea Res.*, **33**, (2), 247-265.

Føyn, L. and F. Rey, 1981. Nutrient distribution along the Norwegian Coastal Current. In: *The Norwegian Coastal Current, vol. 2*, ed. R. Sætre and M. Mork, 629-639. Bergen: Reklametrykk A. S.

Gammelsrød, T. and A. Holm, 1984. Variations of temperature and salinity at Station M (660N 020E) since 1948. *Rapp. P.-v. Reun. Cons. int. Explor. Mer.*, **185**, 188-200.

Gill, A. E., 1982. Atmosphere-Ocean Dynamics. Vol. 30. International Geophysics Series, ed. W. L. Donn. Academic Press.

Gorshkov, S. E., 1983. Arctic Ocean. Vol. 3. World Ocean Atlas, New York, NY: Pergamon Press.

Gould, W. J., L. Loynes and J. Backhaus, 1985. Seasonality in Slope Current Transports N. W. of Shetland. *ICES CM*, (C:7), 1-13.

Grant, A. B., 1968. Atlas of Oceanographic Sections: Temperature-salinity-dissolved oxygen-silica, Davis Strait-Labrador Basin-Denmark Strait-Newfoundland Basin, 1965-1967. Atlantic Oceanographic Laboratory, Bedford Institute of Oceanography, Dartmouth, N.S., Canada, *Rep. A.O.L. 68-5*.

Hansen, B., and J. Meincke, 1979. Eddies and meanders in the Iceland-Faroe Ridge area. *Deep-Sea Res.*, **26A**, 1067-1082.

Hanzlick, D. J., 1983. The West Spitsbergen Current: transport, forcing and variability. PhD-thesis, University of Washington.

Harvey, J. G., 1961. Overflow of Cold Deep Water across the Iceland-Grenland Ridge. *Nature*, **189**, 911-913.

Helland-Hansen, B. and F. Nansen, 1909. The Norwegian Sea, its physical oceanography. Based on the Norwegian researches 1900-1904. *Report on Norwegian Fishery and Marine Investigations, Bergen*, **2**, (2).

Helland-Hansen, B., 1934. The Sognefjord section. Oceanographic observations in the northernmost part of the North Sea and the southern part of the Norwegian Sea. *James Johnstone Memorial Volume. Liverpool. University Press*, 257-274.

Hermann, F., 1959. Hydrographic observations in the Faroe Bank Channel and over the Iceland-Faroe Ridge, June 1959. *Cons. Int. Explor. Mer. Hydrographic Committee*, (118).

Hermann, F., 1967. The T-S diagram analysis of the water masses over the Iceland-Faroe Ridge and in the Faroe Bank Channel. *Rapp. P.-v. Reun. Cons. int. Explor. Mer.*, **157**, 139-149.

Hopkins, T. S., 1988. The GIN Sea. Review of physical oceanography and literature from 1972. Saclant Undersea Research Centre, *SR-124*.

Jakhelln, A., 1936. Oceanographic investigations in the East Greenland waters in the summer of 1930-1932. *Skrifter om Svalbard og Ishavet*, **67**.

Jónsson, S., 1989. The structure and forcing of the large- and mesoscale circulation in the Nordic Seas, with special reference to the Fram Strait. PhD-thesis, University of Bergen, Norway.

Koltermann, K. P. and H. Luthje, 1989. Hydrographischer Atlas der Gronland- und Nordlichen Norwegischen See. Deutsches Hydrographisches Institut, *2328*.

Kristmannsson, S. S., S.-A. Malmberg and J. Briem, 1987. Inflow of Warm Atlantic Water to the Sub-Arctic Iceland Sea. *ICES Symposium*, (26).

Lee, A. and D. Ellett, 1967. On the water masses in the Northwest Atlantic Ocean. *Deep-Sea Res.*, **14**, 183-190.

Maksimov, I. V., 1944. Determining the relative volume of the annual flow of Pacific water into the Arctic Ocean through Bering Strait. *Probl. Arktiki*, **2**, 51-58.

Malmberg, S., 1972. Annual and Seasonal Hydrographic Variations in the East Icelandic Current between Iceland and Jan Mayen. In: *Sea Ice Conference in Reykjavik, Iceland*, 42-54.

Malmberg, S.-A., H. G. Gade and H. E. Sweers, 1972. Current Velocities and Volume Transports in the East Greenland Current off Cape Nordenskjold in August-September 1965. In: *Sea Ice Conference in Reykjavik, Iceland*, 1-10.

Malmberg, S.-A., 1983. Hydrographic Investigations in the Iceland and Greenland Seas in late Winter 1971 - "Deep Water Project". *Jøkull*, **33**, 133-140.

Mann, C. R., 1969. Temperature and salinity characteristics of the Denmark Strait overflow. *Deep-Sea Res.*, Suppl. to **16**, 125-137.

Martin, S. and D. J. Cavalieri, 1989. Contributions of the Siberian Shelf Polynyas to the Arctic Ocean Intermediate and Deep Water. *Journal of Geophysical Research*, **94**, (C9), 12725-12738.

Maykut, 1978. Energy exchange over young sea ice in the central Arctic. *Journal of Geophysical Research*, **83**, 3646-3658.

McCartney, M. S., 1992. Recirculation components to the deep boundary current of the northern North Atlantic. *Prog. Oceanog.*, **29**, 283-383.

Menke, W., 1984. Geophysical Data Analysis: Discrete Inverse Theory. Vol. 45. International Geophysics Series, ed. R. and J. R. Holton Dmowska.

Metcalf, W. G., 1960. A note on the water movement in the Greenland-Norwegian Sea. *Deep-Sea Res.*, **7**, (3), 190-200.

Muench, R. D., 1971. The physical oceanography of the northern Baffin Bay region, Baffin Bay-N. Water Proj. Arctic Inst. of N. Amer., Montreal, Que, *Sci. Rep. 1.*

Nansen, F., 1906. Northern Waters. Captain Roald Amundsen's oceanographic observations in the Arctic Seas in 1901 with a discussion of the origin of the bottom waters in the Northern Seas. *Videnskabsselskabets Skrifter, Matematisk-Naturvidenskabelig Klasse*, **3**, (1).

Nansen, F., 1912. Das Bodenwasser und die Abkuhlung des Meeres. *Internationale Revue der Gesamten Hydrobiologie und Hydrographie*, **5**, (1), 1-42.

Ostlund, H. G. and C. Grall, 1993. Arctic Tritium: 1973-1991. Tritium Laboratory, Univ. Miami, *19.*

Parkinson, C. L., J. C. Comiso, H. J. Zwally, D. J. Cavalieri, P. Gloersen and W. J. Campbell, 1987. Arctic Sea Ice, 1973-1976: Satellite Passive-Microwave Observations. NASA, *SP-489.*

Peterson, W. H. and C. G. H. Rooth, 1976. Formation and exchange of deep water in the Greenland and Norwegian seas. *Deep-Sea Res.*, **23**, 273-283.

Quadfasel, D., B. Rudels and K. Kurz, 1988. Outflow of dense water from a Svalbard fjord into the Fram Strait. *Deep-Sea Res.*, **35**, (7), 1143-1150.

Rhein, M., 1991. Ventilation rates of the Greenland and Norwegian Seas derived from distributions of the chlorofluoromethanes F11 and F12. *Deep-Sea Res.*, **38**, (4), 485-503.

Rintoul, S. R., 1988. Mass, Heat and Nutrient Fluxes in the Atlantic Ocean Determined by Inverse Methods. PhD-thesis, Woods Hole Oceanographic Institution Massachusetts Institute of Technology Joint Program in Oceanography and Oceanographic Engineering.

Ross, C. K., 1975. Overflow 73, current measurements in Denmark Strait. *ICES CM*, (C:6), 1-13.

Ross, C. K., 1982. Overflow '73 - Denmark Strait: Volume 3 - Temperature, Salinity, and Sigma-t Sections. Bedford Institute of Oceanography, Nova Scotia, Canada, *Canadian Technical Report of Hydrography and Ocean Sciences 16.*

Ross, C. K., 1984. Temperature-salinity characteristics of the "overflow" water in Denmark Strait during "OVERFLOW '73". *Rapp. P.-v. Reun. Cons. int. Explor. Mer.*, **185**, 111-119.

Sælen, O. H., 1986. On the Exchange of Bottom Water between the Greenland and Norwegian Seas. In: *Nordic Perspectives on Oceanography*, 133-144. Geophysica 3. Gothenburg: Kugl. Vetenskaps- och Vitterhets-Samhallet.

Saunders, P. M., 1990. Cold Outflow from the Faroe Bank Channel. *Journal of Physical Oceanography*, **20**, 29-43.

Schlosser, P., G. Bonisch, M. Rhein and R. Bayer, 1991. Reduction of Deepwater Formation in the Greenland Sea During the 1980's: Evidence from Tracer Data. *Science*, **251**, 1054-1056.

Schlosser, P., D. Grabitz, R. Fairbanks and G. Bonisch, submitted. Arctic river-runoff: mean residence time on the shelves and in the halocline. *Deep-Sea Res.*

Schmitt, R. W., P. S. Bogden and C. E. Dorman, 1989. Evaporation Minus Precipitation and Density Fluxes for the North Atlantic. *Journal of Physical Oceanography*, **19**, (9), 1208-1221.

Sellmann, L., E. Fahrbach, G. Rohardt, V. H. Strass and B. v. Bodungen, 1992. Moored Instruments Oceanographic Data from the Greenland Sea 1987-1989. Alfred-Wegener-Institut fur Polar- und Meeresforschung, *AWI Berichte aus dem Fachbereich Physik 27.*

Skreslet, S., 1981. Informations and opinions on how freshwater outflow to the Norwegian Coastal Current influences biological production and recruitment to fish stocks in adjacent seas. In: *The Norwegian Coastal Current, vol. 2*, ed. R. Sætre and M. Mork, 712-748. Bergen: Reklametrykk A. S.

Smethie, W. M., Jr., D. W. Chapman, J. H. Swift and K. P. Koltermann, 1988. Chlorofluoromethanes in the Arctic mediterranean seas: evidence for formation of bottom water in the Eurasian Basin and deep-water exchange through Fram Strait. *Deep-Sea Res.*, **35**, (3), 347-369.

Smethie, Jr., W. M. and J. H. Swift, 1989. The Tritium:Krypton-85 Age of Denmark Strait Overflow Water and Gibbs Fracture Zone Water Just South of Denmark Strait. *Journal of Geophysical Research*, **94**, (C6), 8265-8275.

Steele, J. H., J. R. Barrett and L. V. Worthington, 1962. Deep Currents South of Iceland. *Deep-Sea Res.*, **9**, 465-474.

Stefansson, U., 1962. North Icelandic Waters. PhD-thesis, University of Copenhagen, Denmark.

Strass, V. H., E. Fahrbach, U. Schauer and L. Sellmann, 1993. Formation of Denmark Strait Overflow Water by Mixing in the East Greenland Current. *Journal of Geophysical Research*, **98**, (C4), 6907-6919.

Sverdrup, H. U., M. W. Johnson and R. H. Fleming, 1946. The Oceans: Their Physics, Chemistry and General Biology. Englewood Cliffs, New Jersey: Prentice-Hall.

Swift, J. H., K. Aagaard and S. Malmberg, 1980. The Contribution of the Denmark Strait Overflow to the Deep North Atlantic. *Deep-Sea Res.*, **27A**, 29-42.

Swift, J. H., K. Aagaard, 1981. Seasonal transitions and water mass formation in the Iceland and Greenland Seas. *Deep-Sea Res.*, **28A**, (10), 1107-1129.

Swift, J. H., 1984. A Recent θ-S Shift in the Deep Water of the Northern North Atlantic. In: *Climate Processes and Climate Sensitivity*, 39-47. Maurice Ewing Volume 5.

Swift, J. H. and K. P. Koltermann, 1988. The Origin of Norwegian Sea Deep Water. *Journal of Geophysical Research*, **93**, (C4), 3563-3569.

Tait, J. B., 1957. Hydrography of the Faroe-Shetland Channel 1927-1952. *Scottish Home department, Marine Research*, (2).

Tait, J. B., 1967. Introduction. *Rapp. P.-v. Reun. Cons. int. Explor. Mer.*, **157**.

Timofeyev, V. T., 1956. Annual water balance of the Arctic Ocean. *Priroda*, **7**, 89-91.

Timofeyev, V. T., 1963. Interaction of the Arctic Ocean waters with Atlantic and Pacific waters. *Okeanologiya*, **3**, 569-578.

Untersteiner, N., 1988. On the Ice and Heat Balance in the Fram Strait. *Journal of Geophysical Research*, **93**, (C1), 527-531.

Vinje, T. and Ø. Finnekåsa, 1986. The Ice Transport through the Fram Strait. *Norsk Polarinstitutt Skrifter*, **186**, 1-39.

Vowinckel, E. and S. Orvig, 1962. Water balance and heat flux of the Arctic Ocean. *Arctic*, **15**, 205-223.

Vowinckel, E. and S. Orvig, 1970. The Climate of the North Polar Basin. In: *Climates of the Polar Regions*, ed. S. Orvig, 129-225. 14. Elsevier.

Wadhams, P., 1989. Sea-ice thickness distribution in the Trans Polar Drift Stream. *Rapp. P.-v. Reun. Cons. int. Explor. Mer.*, **188**, 59-65.

Warren, B. A., 1981. Deep Circulation of the World Ocean. In: *Evolution of Physical Oceanography*, ed. B. A. and C. Wunsch Warren, 6-41. Cambridge, Massachusetts and London, England: The MIT Press.

Willebrand, J. and J. Meincke, 1980. Statistical analysis of fluctuations in the Iceland-Scotland frontal zone. *Deep-Sea Res.*, **27A**, 1047-1066.

Worthington, L. V., 1954. A preliminary note on the time scale in North Atlantic circulation. *Deep-Sea Res.*, **1**, 244-251.

Worthington, L. V., 1969. An attempt to measure the volume transport of Norwegian Sea overflow water through the Denmark Strait. *Deep-Sea Res.*, **16**, 421-432.

Worthington, L. V., 1970. The Norwegian Sea as a mediterranean basin. *Deep-Sea Res.*, **17**, 77-84.

Worthington, L. V. and W. R. Wright, 1970. North Atlantic Ocean Atlas of Potential Temperature and Salinity in the Deep Water Including Temperature, Salinity and Oxygen Profiles from the Erika Dan Cruise of 1962. *Woods Hole Oceanographic Institution Atlas Series 2*, 24 pp.

Worthington, L. V., 1982. North Atlantic circulation and water mass formation. *J. Mar. Res.*, suppl. to **40**, xiii-xxii.

Wunsch, C., 1978. The general circulation of the North Atlantic west of 50°W determined from inverse methods. *Reviews of Geophysics and Space Physics*, **16**, 583-620.

Wüst, G., 1935. Schichtung und Zirkulation des Atlantischen Ozeans. Das Bodenwasser und die Stratosphare. *Wissenschaftliche Ergebnisse der Deutschen Atlantischen Expedition 'Meteor' 1925-1927*, (Band 6), 1-288.